

INDC

INTERNATIONAL NUCLEAR DATA COMMITTEE

Evaluation of Nuclear Data for Pu-241
in Neutron Energy Range from 10^{-3} eV to 15 MeV

V.A. Konshin, G.V. Antsipov, E.Sh. Sukhovitskiy
L.A. Bakhanovich, A.B. Klepatskiy, G.B. Morogovskiy
Yu.V. Porodzinskiy

A.V. Lykov Institute of Thermal and Mass Exchange
Byelorussian SSR Academy of Sciences

Minsk 1979

Translated by the IAEA
January 1980

Evaluation of Nuclear Data for Pu-241
in Neutron Energy Range from 10^{-3} eV to 15 MeV

V.A. Konshin, G.V. Antsipov, E.Sh. Sukhovitskij
L.A. Bakhanovich, A.B. Klepatskij, G.B. Morogovskij
Yu.V. Porodzinskij

A.V. Lykov Institute of Thermal and Mass Exchange
Byelorussian SSR Academy of Sciences

Minsk 1979

Translated by the IAEA
January 1980

Abstract

The complete neutron reaction data evaluation for Pu-241 in the neutron energy range from 10^{-3} eV to 15 MeV is presented. The report describes the data analyses and theoretical model calculations performed to arrive at the complete set of nuclear data including all neutron reaction cross-sections, angular and energy distributions, and fission neutron and gamma-ray spectra. The final results are presented in ENDF/B format and as group constants.

Table of Content

		<u>Page</u>
Part 1	Analysis of experimental data below 1 eV	1
Part 2	Analysis of experimental data between 1 - 150 eV	47
Part 3	Cross-section evaluations in the 0.1 - 100 keV energy region	79
Part 4	Analysis of experimental data and cross- section calculations in the 0.1 and 15 MeV energy region	131
Part 5	Theoretical model calculations and evaluation of cross-sections, angular and energy distributions, fission spectra and secondary gamma ray spectra	179
Part 6	Representation of the complete Pu-241 evaluated nuclear data file in the ENDF/B format	219

Part 1

Analysis of Experimental Data Below 1 eV

EVALUATION OF NUCLEAR DATA FOR ^{241}Pu IN THE NEUTRON
ENERGY RANGE 10^{-3} eV-15 MeV

V.A. Kon'shin, G.V. Antsipov, E.Sh. Sukhovitskij, L.A. Bakhanovich
A.B. Klepatskij, G.B. Morogovskij, Yu.V. Porodzinskij
A.V. Lykov Institute of Thermal and Mass Exchange
Byelorussian SSR Academy of Sciences

ABSTRACT

The available experimental data on the ^{241}Pu cross-sections at energies below 1 eV are examined and analysed statistically and self-consistent evaluated constants are obtained. The cross-sections are parametrized by the use of a modified Adler-Adler formalism. Two negative resonances are introduced.

1. INTRODUCTION

In detailed studies of the best ways of developing nuclear power, careful attention has to be paid to the optimization of the physical and thermophysical parameters of fast reactors. The accurate prediction of these parameters depends on two factors: the precision of the methods used in the calculation and the accuracy of the nuclear data characterizing the interaction of neutrons with the nuclei.

It is of course still necessary to make further improvements in the accuracy of the nuclear data so that physicists will not in the future have to set up critical assemblies and models to simulate fast reactors.

One of the most important tasks is to achieve sufficiently accurate calculations of the breeding ratio of fast breeders since it is on the value of this parameter that the choice of the fuel composition and the approach to the reactor design depend. The breeding ratio is most strongly affected by the ^{238}U and ^{239}Pu capture cross-sections at energies below 100 keV, the ^{238}U inelastic scattering cross-section in the region

below 1 MeV and the value of $\bar{\nu}(^{239}\text{Pu})$. The evaluation of these quantities (currently the third version) through an analysis of all available experimental data and the use of theoretical models with carefully tested parameters is being carried out in the Physics of Elementary Processes Laboratory, Institute of Thermal and Mass Exchange (ITMO), Byelorussian SSR Academy of Sciences.

A knowledge of the ^{240}Pu , ^{241}Pu and ^{242}Pu neutron cross-sections is also becoming of increasing importance as a result of the fact that plutonium from thermal reactors containing ~ 20%-25% ^{240}Pu , 10%-15% ^{241}Pu and 5%-10% ^{242}Pu can be used in fast breeders. It may be noted that approximately equal contributions are made by the errors in the constants for ^{239}Pu and ^{238}U , the fission fragments and the isotopes ^{240}Pu and ^{241}Pu to the overall error in K_{eff} for the BN-1500 reactor.

Nuclear data for the higher transplutonium elements are required for calculating the build-up of these nuclei, for determining the changes in reactor characteristics during extended operation, for calculating the power of the internal neutron sources in a fast reactor resulting from the (α, n) -reaction in oxygen (^{242}Cm , ^{244}Cm and ^{238}Pu) and spontaneous fission (^{242}Cm , ^{244}Cm , ^{238}Pu , ^{242}Pu and ^{240}Pu) and also (and this may become most important) for studying problems of the transfer and reprocessing of irradiated fuel and the burial of high actinides. It is obviously impossible to obtain all this large quantity of experimental data in the near future, especially in view of the fact that the fabrication of properly shaped targets made from these nuclei is a very difficult process.

In the absence of experimental data for heavy nuclei, almost the only method of obtaining the nuclear constants is from theoretical evaluations with carefully tested parameters used in nuclear models. The development of methods of nuclear constant evaluation for heavy fissile nuclei and the use of these methods in the derivation of definite values for the nuclear constants to be included in a Soviet evaluated nuclear data library for fissile nuclei constitute the principal task of the Physics of Elementary Processes Laboratory (ITMO). This work, which forms an integral part of the All-Union programme for obtaining reliable nuclear data with guaranteed accuracy, is supervised by the Nuclear Data Commission and the Nuclear Data Centre of the USSR State Committee on the Utilization of Atomic Energy.

The present paper, which is issued in the form of a five-part ITMO preprint, contains the results of a nuclear data evaluation for ^{241}Pu carried out as part of the production of a complete file of nuclear constants for this isotope. The work on the evaluation of nuclear constants for ^{242}Pu is now complete. The results will be published, together with varied examples on the possible use of the theoretical models and achieved accuracies for the prediction of neutron cross-sections, in the form of a collection of ITMO papers.

Future work in the laboratory will deal with the evaluation of nuclear constants for the transplutonium elements (primarily ^{241}Am) within an international programme of co-ordinated studies under the aegis of the IAEA.

1.1. Possible reactions with the ^{241}Pu nucleus for energies up to 15 MeV

Table 1.1 shows the values of Q and the thresholds for the various neutron reactions with the ^{241}Pu nucleus. The value of the threshold (for negative Q) is given by the expression:

$$T = \frac{M_n + M_{241}}{M_{241}} \cdot (-Q) = 1.0042 (-Q), \quad (1.1)$$

where M_n is the mass of the neutron and M_{241} is the mass of the ^{241}Pu nucleus.

Table 1.1

Values of Q and thresholds for neutron reactions with the ^{241}Pu nucleus

Reactions	Values of Q, MeV	Threshold MeV
1	2	3
$^{241}\text{Pu}(n, 2n)^{240}\text{Pu}$	-5,241	5,263
$(n, 3n)^{239}\text{Pu}$	-11,775	11,824
$(n, 4n)^{238}\text{Pu}$	-17,430	17,503
$(n, \gamma)^{242}\text{Pu}$	6,301	-
$(n, p)^{241}\text{Np}$	-0,582	0,584
$(n, d)^{240}\text{Np}$	-4,332	4,350
$(n, t)^{239}\text{Np}$	-3,236	3,250
$(n, ^3\text{He})^{239}\text{U}$	-4,491	4,510
$(n, ^4\text{He})^{238}\text{U}$	11,233	-
$(n, np)^{240}\text{Np}$	-6,552	6,580
$(n, nd)^{239}\text{Np}$	-9,490	9,530

The first excited state of ^{241}Pu is at an energy of 40 keV. The ground state of the nucleus has a spin of $5/2^+$. The ^{241}Pu level scheme has been studied in detail up to energies of 1 MeV.

In nuclear reactors, ^{241}Pu is produced by successive neutron capture in ^{239}Pu and ^{240}Pu ; it is converted by beta-decay with a half-life of 15.02 ± 0.10 a into ^{241}Am [there is a small amount ($\approx 2.3 \times 10^{-3}\%$) of alpha-decay into ^{237}U].

2. NUCLEAR DATA FOR ^{241}Pu IN THE THERMAL ENERGY REGION (10^{-3} -1 eV)

2.1. ^{241}Pu constants at 2200 m/s

The ^{241}Pu constants at a thermal point (2200 m/s) have been evaluated by Hanna et al. [1]. The ^{241}Pu data were analysed separately from the constants for ^{233}U , ^{235}U and ^{239}Pu since they are inaccurate and cannot have any serious effect on the constants for the other three nuclei.

The least squares analysis was carried out on the following measurements:

σ_t and $\sigma_a(^{241}\text{Pu})$: Simpson et al. [2], Craig and Westcott [3], Smith [4] and Cabell [5];

$\sigma_f(^{241}\text{Pu})$: Watanabe and Simpson [6];

$\sigma_f(^{241}\text{Pu})/\sigma_f(^{235}\text{U})$: Leonard [7] and White [8];

$\sigma_f(^{241}\text{Pu})/\sigma_f(^{239}\text{Pu})$: Jaffly et al. [9], Raffle [10] and Bigham et al. [11];

$\eta(^{241}\text{Pu})$: Smith and Reeder [12]; $\eta(^{241}\text{Pu})/\eta(^{235}\text{U})$: Fast and Aber [13];

$\bar{\nu}(^{241}\text{Pu})/\bar{\nu}(^{235}\text{U})$: Sanders [14] and Colvin and Sowerby [15];

$\bar{\nu}(^{241}\text{Pu})/\bar{\nu}(^{239}\text{Pu})$: Kalashnikova et al. [16], Sanders [14], De Saussure and Silver [17], Jaffly and Lerner [18] and Boldeman and Dalton [19];

σ_γ and $\alpha(^{241}\text{Pu})$: Cabell [20].

As a result of their analysis, Hanna and Westcott recommend the following constants at 2200 m/s:

$$\begin{aligned} \sigma_a &= 1375.4 \pm 8.6 \text{ b}; \quad \sigma_f = 1007.3 \pm 7.2 \text{ b}; \quad \sigma_\gamma = 368.1 \pm 7.8 \text{ b}; \\ \alpha &= 0.3654 \pm 0.0090; \quad \eta = 2.149 \pm 0.014; \quad \bar{\nu}_t = 2.934 \pm 0.012; \\ \sigma_s (\text{bound at.}) &= 12.0 \pm 2.6 \text{ b and } \sigma_p = 12.0 \pm 2.2 \text{ b.} \end{aligned}$$

Since the evaluation by Hanna et al. [1], no new experimental data in the thermal region have appeared. However, it seems reasonable to combine the available ^{241}Pu data in an analysis together with results for ^{233}U , ^{235}U and ^{239}Pu . Lemmel et al. [21] carried out such an analysis of fissile nuclei cross-sections at thermal energies by the least squares method.

For ^{241}Pu , the same experimental data as in Hanna et al. were used except in the case of the g -factor-dependent fission cross-section ratios $^{241}\text{Pu}/^{235}\text{U}$ [8] and $^{241}\text{Pu}/^{239}\text{Pu}$ [9, 10], which were slightly changed within the limits of error. The thermal ^{241}Pu constants obtained at 2200 m/s have the following values: $\sigma_t = 1389 \pm 9$ and 1390 ± 9 b for metal and liquid samples, respectively; $\sigma_a = 1378.0 \pm 9.0$ b; $\sigma_f = 1015.0 \pm 7.0$ b; $\sigma_\gamma = 362.0 \pm 6.0$ b; $\alpha = 0.357 \pm 0.007$; $\eta = 2.155 \pm 0.010$; $\bar{\nu}_t = 2.924 \pm 0.010$; $\bar{\nu}_a = 0.0157 \pm 0.0015$; $\sigma_s = 10.8 \pm 2.6$ and 12.0 ± 2.6 b for metal and liquid samples, respectively; and $\nu_p(^{252}\text{Cf}) = 3.737 \pm 0.008$.

The experimental data for the thermal energy region were re-normalized to these values.

2.2. Experimental data for $\sigma_f(^{241}\text{Pu})$ in the thermal energy region (10^{-3} -1 eV)

The following experimental data are available for $\sigma_f(^{241}\text{Pu})$ in the thermal energy region: Watanabe [22], Watanabe and Simpson [6], Seppi [23], James [24], Adamchuk et al. [25], Seppi et al. [26], Raffle and Price [27] and White et al. [8]. These are old data, the most recent going back ten years.

1. Watanabe [22] measured $\sigma_f(^{241}\text{Pu})$ in the 0.01-0.5 eV range by a time-of-flight method. The data were normalized at the thermal point with an energy of 0.0253 eV to a value of 962 b. We ourselves have now renormalized the results to 1015 b. No detailed information on the measurement errors was given. The experimental results lie 2-3% above the evaluated curve in the region up to 0.1 eV and the discrepancies increase to 8-10% at 0.2 eV. The error assumed for the purpose of the evaluation was +5%. Watanabe's data [22] are given in Table 2.1, averaged over particular energy intervals.

Table 2.1

Experimental data of Watanabe [22] for $\sigma_f(^{241}\text{Pu})$

$E_n, \text{ eV}$	$\sigma_f, \text{ b}$	$E_n, \text{ eV}$	$\sigma_f, \text{ b}$	$E_n, \text{ eV}$	$\sigma_f, \text{ b}$	$E_n, \text{ eV}$	$\sigma_f, \text{ b}$
0,0072	1895,8	0,0255	1013,0	0,069	652,6	0,1567	748,9
0,0108	1502,9	0,0268	971,6	0,082	631,6	0,1707	821,1
0,0120	1379,0	0,0333	856,9	0,097	606,7	0,1841	953,2
0,0135	1302,6	0,0410	791,3	0,1148	618,9	0,1968	1067,9
0,0159	1186,4	0,049	730,4	0,1342	670,4	0,2135	1281,6
0,0188	1101,0	0,057	699,6	-	-	-	-

2. Watanabe and Simpson [6] measured $\sigma_f(^{241}\text{Pu})$ for energies of 0.02-100.0 eV by a time-of-flight method. The data were normalized to the fission cross-section at 6 eV, which the authors determined from the total cross-section of 436 ± 6 b at this energy by subtracting the calculated values of $\sigma_n(14 \pm 4$ b) and $\sigma_\gamma(14 \pm 7$ b). The value of $\sigma_f(^{241}\text{Pu})$ at 0.0253 eV obtained by the least squares method from the experimental points was 962 ± 38 b. These data were renormalized to $\sigma_f = 1015$ b at 0.0253 eV. We then averaged the values over the energy ranges. The errors given by Watanabe and Simpson [6] are 3.9% up to 0.24 eV and 4.0% above this energy. The original data are given in Table 2.2.

Table 2.2

Experimental data of Watanabe and Simpson [6] for $\sigma_f(^{241}\text{Pu})$

\bar{E}_f , eV	$\bar{\sigma}_f$, b	$\Delta\sigma_f$, b	\bar{E}_f , eV	$\bar{\sigma}_f$, b	$\Delta\sigma_f$, b
1	2	3	4	5	6
0,024	966,75	37,70	0,2597	1680,28	67,21
0,025	954,86	37,24	0,2645	1551,91	62,08
0,0265	926,17	36,12	0,2726	1466,29	58,65
0,0285	921,91	35,95	0,2857	1219,14	48,77
0,0305	893,06	34,83	0,3045	865,66	34,63
0,0325	856,65	33,41	0,3246	573,39	22,94
0,0355	851,84	33,22	0,3475	379,32	15,17
0,0390	838,61	32,71	0,3704	255,17	10,21
0,0445	790,50	30,83	0,3885	224,64	9,00
0,0505	739,80	28,85	0,4110	193,98	7,76
0,0560	707,13	27,58	0,4387	109,21	4,37
0,0640	679,09	26,48	0,4612	81,67	3,27
0,0745	649,19	25,32	0,4834	83,53	3,34
0,0855	630,02	24,57	0,5120	56,41	2,26
0,0945	599,91	23,40	0,5460	67,07	2,68
0,1043	611,31	23,84	0,5985	59,19	2,37
0,1190	621,16	24,22	0,6524	50,02	2,00
0,1412	671,38	26,18	0,6976	36,49	1,46
0,1650	784,24	30,58	0,7368	39,78	1,59
0,1865	975,47	38,04	0,7664	28,38	1,14
0,2068	1177,53	45,92	0,8028	38,78	1,55
0,2279	1174,68	45,81	0,8569	43,36	1,73
0,2460	1580,80	61,65	0,9053	31,60	1,26
0,2537	1600,70	64,00	0,9549	39,73	1,59

3. Seppi [23] determined $\sigma_f(^{241}\text{Pu})$ in the energy range 0.0257-0.874 eV by means of a crystal spectrometer. The renormalization coefficient at an energy of 0.0253 eV to the value $\sigma_f = 1015$ b is equal to 1.004. Unfortunately no detailed information is available about this experiment. The experimental data show only a small scatter and fit the shape of the evaluated curve well. The data have been used in the evaluation with an error of $\pm 3.5\%$. Seppi's results [23] are given in Table 2.3.

Table 2.3

Experimental data of Seppi [23] for σ_f (^{241}Pu)

E_f , eV	σ_f , b	E_f , eV	σ_f , b
1	2	3	4
0,0257	1002,0	0,212	1217,0
0,0281	962,4	0,219	1307,0
0,0309	923,8	0,224	1381,0
0,0342	864,1	0,231	1488,0
0,0381	820,0	0,240	1576,0
0,0429	783,4	0,248	1625,0
0,0486	744,7	0,257	1639,0
0,0556	708,4	0,267	1565,0
0,0643	679,3	0,281	1324,0
0,0713	661,1	0,292	1108,0
0,0775	640,7	0,304	892,7
0,0845	625,5	0,316	710,8
0,0925	621,9	0,329	565,2
0,105	613,4	0,344	437,4
0,114	605,3	0,359	314,9
0,128	621,9	0,375	231,9
0,136	642,0	0,392	183,8
0,146	668,2	0,411	140,7
0,155	708,2	0,431	108,6
0,161	736,9	0,452	90,3
0,164	740,7	0,484	69,1
0,169	766,8	0,509	56,1
0,172	800,6	0,537	43,8
0,177	828,9	0,567	40,5
0,181	876,1	0,600	39,1
0,186	907,9	0,636	39,3
0,190	936,5	0,675	40,7
0,196	1009,0	0,718	40,5
0,200	1075,0	0,765	34,1
0,207	1160,0	0,817	31,6
-	-	0,874	34,1

4. James [24] measured $\sigma_f(^{241}\text{Pu})$ for energies between 0.009 eV and 3 keV by a time-of-flight method. The neutron flux was determined with a BF_3 counter. The data were normalized at a thermal energy of 0.0253 eV to a value $\sigma_f = 1010$ b (normalization accuracy of $\pm 5.4\%$). We renormalized the results to $\sigma_f = 1015$ b. The total error in the experimental data is made up of the statistical error, the error in the energy determination resulting from the finite width of the time channel (1 μs) and the normalization error. The total error was equal to: 6.3% for 0.01-0.05 eV, 6.1% for 0.05-0.30 eV, 6.3% for 0.30-0.43 eV and 10% for 0.43-1.0 eV. James' experimental data [24] as averaged by us are shown in Table 2.4. There is generally satisfactory agreement with the shape of the evaluated curve although the points show a large scatter. A particularly poor description is given of the resonance peak at 0.26 eV.

Table 2.4

Experimental data of James [24] for $\sigma_f(^{241}\text{Pu})$

E, eV	$\bar{\sigma}_f, \text{b}$	$\Delta\sigma_f, \text{b}$	E, eV	$\bar{\sigma}_f, \text{b}$	$\Delta\sigma_f, \text{b}$
1	2	3	4	5	6
0,009	1647,2	103,77	0,090	583,5	36,0
0,010	1595,0	100,48	0,095	616,8	37,62
0,011	1486,0	93,62	0,100	590,1	36,00
0,012	1373,2	86,50	0,105	601,1	36,67
0,013	1364,5	85,96	0,11	634,6	38,71

Table 2.4 cont.

I	2	3	4	5	6
0,014	I3I3,0	82,72	0,115	621,3	37,90
0,015	I321,3	83,24	0,120	633,4	38,64
0,0164	I253,8	79,00	0,125	599,8	36,59
0,018	II45,1	72,14	0,135	650,7	39,69
0,0195	II54,0	72,70	0,150	683,0	41,66
0,021	I089,5	68,64	0,165	745,6	45,48
0,0225	I080,0	68,04	0,180	846,6	51,64
0,024	I041,8	65,63	0,195	954,8	58,24
0,0255	I035,1	65,21	0,205	I030,5	62,86
0,027	978,1	61,62	0,215	II86,0	72,35
0,0285	986,8	62,17	0,225	I262,0	76,98
0,031	936,4	59,00	0,235	I373,0	83,75
0,0335	821,0	51,72	0,244	I497,0	91,32
0,035	977,0	55,25	0,251	I467,0	89,49
0,037	828,4	52,20	0,255	I377,0	84,00
0,040	754,0	47,50	0,2574	I604,0	97,84
0,043	788,0	49,64	0,2602	I536,0	93,70
0,046	749,9	47,24	0,2631	I649,0	100,60
0,050	716,5	45,14	0,2690	I410,0	86,00
0,054	716,6	43,71	0,2749	I415,9	86,0
0,058	603,6	36,80	0,2780	I321,0	80,6
0,063	681,7	41,58	0,2811	I212,94	74,00
0,068	635,4	38,76	0,2843	II40,96	69,60
0,074	627,7	38,29	0,289	956,6	58,35
0,080	590,9	36,05	0,298	921,5	56,22
0,085	607,5	37,06	0,3046	861,24	54,26
0,310	604,6	38,09	0,5485	49,99	5,00
0,320	566,6	35,70	0,5662	58,61	5,90
0,327	482,4	30,39	0,5896	60,62	6,06
0,3312	390,7	24,61	0,6142	42,85	4,30
0,340	323,7	20,40	0,6352	46,03	4,60
0,3525	285,2	17,97	0,6805	47,85	4,80
0,3662	228,9	14,42	0,7049	39,29	3,93
0,381	174,1	11,00	0,7307	36,00	3,60
0,396	155,6	9,80	0,7580	33,39	3,34
0,425	I26,3	7,96	0,7868	27,79	2,78
0,43	88,34	5,57	0,8173	27,54	2,75
0,445	98,00	9,80	0,8495	34,66	3,47
0,4615	64,1	6,40	0,8838	34,24	3,42
0,482	61,89	6,19	0,9200	18,45	1,85
0,504	46,8	4,70	0,9488	17,58	1,76
0,528	50,0	5,00	0,9790	24,02	2,40

5. Adamchuk et al. [25] found the ^{241}Pu fission cross-section for monochromatic neutrons in the energy range 0.005-1000.0 eV using a mechanical chopper. They normalized their results to a value of 950 b at 0.0253 eV and we have renormalized them to 1015 b. The experimental data obtained by Adamchuk et al. are in satisfactory agreement with the results of other authors up to 0.3 eV but at higher energies they lie systematically above the evaluated curve and they give a poor description of the resonance peak. The data for 0.24-0.40 eV have therefore not been used in the analysis. The remaining results were taken with an error of $\pm 7\%$ for use in the evaluation. The experimental data of Adamchuk et al. [25] (Table 2.5) were averaged up to an energy of 0.143 eV.

Table 2.5

Experimental data of Adamchuk et al. [25]
for $\sigma_f(^{241}\text{Pu})$

E. eV	σ_f , b	E. eV	σ_f , b	E. eV	σ_f , b
1	2	3	4	5	6
0,0119	1262,5	0,106	611,0	0,351	567,0
0,0129	1216,7	0,119	603,5	0,367	393,0
0,0143	1241,0	0,133	630,0	0,384	260,0
0,0159	1178,3	0,143	654,0	0,402	258,0
0,0177	1127,7	0,152	697,0	0,421	166,0
0,0198	1094,0	0,168	709,0	0,442	117,0
0,0215	1072,5	0,171	745,0	0,464	75,4
0,0235	1070,5	0,181	843,0	0,489	99,0
0,0256	902,5	0,187	826,0	0,515	110,0
0,0283	879,5	0,193	991,0	0,543	50,0
0,0313	853,5	0,200	928,0	0,573	28,3
0,0349	828,0	0,206	1040,0	0,607	36,7
0,039	759,5	0,213	1088,0	0,643	60,9
0,0449	763,0	0,221	1194,0	0,682	52,0
0,049	756,0	0,229	1282,0	0,73	36,7
0,0525	715,0	0,237	1425,0	0,75	27,8
0,056	734,0	0,246	1603,0	0,77	80,3
0,060	662,5	0,255	1626,0	0,80	48,0
0,065	668,0	0,265	1678,0	0,83	17,1
0,070	665,5	0,275	1704,0	0,85	38,2
0,074	643,0	0,286	1466,0	0,88	61,7
0,070	608,0	0,297	1423,0	0,92	39,9
0,0825	610,0	0,309	1234,0	0,95	16,0
0,088	603,0	0,322	949,0	0,98	50,0
0,094	594,0	0,336	752,0	-	-

6. Seppi et al. [26] measured $\sigma_f(^{241}\text{Pu})$ in the range 0.00253-0.00473 eV. The details of this work are not available. The original data were normalized to a value of $\sigma_f = 541.0$ b at 0.1 eV. For the purposes of the present evaluation they have been renormalized to $\sigma_f = 626$ b at 0.1 eV. The experimental results of Seppi et al. [26] are shown in Table 2.6.

Table 2.6

Experimental data of Seppi et al., [26]

E_n, eV	σ_f, b
0,00253	2528,0 \pm 14,27
0,00269	2508,0 \pm 11,10
0,00286	2636,0 \pm 9,06
0,00305	2459,0 \pm 7,14
0,00326	2386,0 \pm 5,89
0,00346	2279,0 \pm 5,19
0,00375	2247,0 \pm 4,34
0,00404	2119,0 \pm 3,77
0,00436	2113,0 \pm 3,26
0,00473	2028,0 \pm 2,93

7. Raffle and Price [27] determined $\sigma_f(^{241}\text{Pu})$ in the 0.006-1.0 eV energy range. The results are identical to those published in Ref. [28]. For energies below 0.4 eV, the ^{241}Pu cross-section was measured relative to $\sigma_f(^{239}\text{Pu})$; at higher energies a ^{10}B sample was used as the standard. The measurements were made with a slow-neutron chopper below 0.1 eV, a single-crystal spectrometer for 0.05-1.0 eV and an electron accelerator at energies above 0.25 eV. The results were normalized to a fission cross-section value $\sigma_f(^{241}\text{Pu}) = 935 \pm 40$ b at 0.0253 eV and were renormalized by us to 1015.0 b. The measurements were used in the evaluation with the error taken as $\pm 8\%$ up to 0.1 eV and $\pm 6\%$ at higher energies.

The experimental values show a considerable scatter, especially near the resonance peak. The ^{241}Pu fission cross-sections measured in Refs [27, 28] are shown in Table 2.7.

Table 2.7

Experimental data of Richmond and Price
for $\sigma_f(^{241}\text{Pu})$

$E, \text{ eV}$	$\sigma_f, \text{ b}$	$\Delta\sigma_f, \text{ b}$	$E, \text{ eV}$	$\sigma_f, \text{ b}$	$\Delta\sigma_f, \text{ b}$
1	2	3	4	5	6
0,00615	1520,0	121,6	0,0730	588,0	47,0
0,00630	1540,0	123,2	0,0792	630,0	50,4
0,00775	1620,0	129,6	0,0794	652,0	52,2
0,00890	1470,0	117,6	0,0860	596,0	47,7
0,0101	1380,0	110,4	0,0935	545,0	43,6
0,0108	1485,0	118,8	0,0975	610,0	48,8
0,0117	1325,0	106,0	0,0995	579,0	46,3
0,0119	1370,0	109,6	0,101	632,0	37,9
0,0127	1240,0	99,2	0,127	564,0	33,8
0,0138	1225,0	98,0	0,146	716,0	43,0
0,015	1155,0	92,4	0,167	693,0	41,6
0,0165	1235,0	98,8	0,197	1058,0	63,5
0,0182	1075,0	86,0	0,202	933,0	56,0
0,0200	1120,0	89,6	0,213	1249,0	74,9
0,0221	1165,0	93,2	0,221	1314,0	78,8
0,0246	975,0	78,0	0,245	1588,0	95,3
0,0276	898,0	71,8	0,247	1517,0	91,0
0,0312	806,0	64,5	0,266	1385,0	83,1
0,0402	775,0	62,0	0,286	1453,0	87,2
0,0431	775,0	62,0	0,290	1349,0	80,9
0,0468	625,0	50,0	0,300	933,0	56,0
0,0550	665,0	53,2	0,318	520,0	31,2
0,0572	624,0	49,9	0,320	324,0	19,4
0,0630	714,0	57,1	0,341	377,0	22,6
0,0652	682,0	54,6	0,350	159,0	9,5
0,0675	638,0	51,0	0,395	192,0	11,5
0,0680	608,0	48,6	0,680	66,0	4,0

8. White et al. [8] measured the ratio $\sigma_f(^{241}\text{Pu})/\sigma_f(^{235}\text{U})$ in the energy range 0.016-0.55 eV. The monoenergetic neutrons were obtained by means of a crystal spectrometer. The total error in the measurement of the ratio was 2.7% and the greatest contributions came from the determination of the foil thickness (2%), non-uniformity of the beam (1%) and statistical errors (0.5-1.0%). The experimental data obtained by White et al. are given in Table 2.8.

Table 2.8

Experimental values of the ratio $\sigma_f(^{241}\text{Pu})/\sigma_f(^{235}\text{U})$ for energies of 0.016-0.545 eV

$E_n, \text{ eV}$	$\sigma_f(^{241}\text{Pu})/\sigma_f(^{235}\text{U})$	$\sigma_f(^{235}\text{U}), \text{ b}$	$\sigma_f(^{241}\text{Pu}), \text{ b}$
0,016	$1,681 \pm 0,044$	$7580,0 \pm 11,4$	$1274,1 \pm 38,2$
0,0253	$1,771 \pm 0,048$	$577,7 \pm 8,7$	$1023,1 \pm 31,5$
0,051	$1,876 \pm 0,050$	$380,0 \pm 5,70$	$712,9 \pm 21,8$
0,117	$2,719 \pm 0,070$	$225,0 \pm 3,4$	$611,8 \pm 18,2$
0,161	$3,960 \pm 0,100$	$182,5 \pm 2,7$	$722,7 \pm 21,2$
0,270	$8,230 \pm 0,300$	$190,1 \pm 2,8$	$1564,8 \pm 61,0$
0,545	$0,806 \pm 0,020$	$73,9 \pm 1,5$	$59,6 \pm 1,7$

2.3. Evaluation of $\sigma_f(^{241}\text{Pu})$ in the energy range 10^{-3} -1 eV

Figures 2.1-2.5 show the experimental values of $\sigma_f(^{241}\text{Pu})$ discussed above and the evaluated data. The evaluated curve was obtained by means of the PREDA program [29], which describes a set of experimental points by a polynomial of the appropriate order. The experimental points were taken with weights inversely proportional to the square of the errors indicated in the text.

The evaluated values of $\sigma_f(^{241}\text{Pu})$ are given below (see Table 2.15).

2.4. Experimental data for $\sigma_t(^{241}\text{Pu})$ in the energy range 10^{-4} -1 eV

The following experimental data on $\sigma_t(^{241}\text{Pu})$ are available in the energy range 10^{-3} -1 eV: Smith [4], Smith and Young [30], Simpson and Fluharty [31], Simpson and Schuman [32], Craig and Westcott [3] and Kolar and Carraro [33].

1. Young and Smith [4, 30] measured $\sigma_t(^{241}\text{Pu})$ for energies of 0.00051-0.09 eV by means of a crystal spectrometer and a fast neutron chopper (Tables 2.9 and 2.10). The sample was a metal foil with 99.3% ^{241}Pu enrichment. In order to obtain the absorption cross-section from the σ_t data derived by Young and Smith, we subtracted the value of the scattering cross-section, equal to 10.8 b. The Young and Smith measurements gave a total cross-section of 1389 ± 15 b at 0.0253 eV and there was therefore no need for renormalization.

The data obtained with the crystal spectrometer were systematically about 1% greater than those with the fast chopper in the region below 0.02 eV.

Table 2.9

Experimental data of Smith and Young [4, 30] obtained with a crystal spectrometer (taken from the graph)

E, eV	$\sigma_c \sqrt{E}, \text{b} \cdot (\text{eV})^{\frac{1}{2}}$	E, eV	$\sigma_c \sqrt{E}, \text{b} \cdot (\text{eV})^{\frac{1}{2}}$
1	2	3	4
0,00051	237,5	0,0055	238,0
0,00055	233,8	0,0054	234,5
0,00055	241,0	0,0056	235,7
0,00070	234,3	0,0063	236,9
0,00087	239,0	0,0065	235,0
0,0010	236,2	0,0079	233,2
0,0014	238,4	0,0085	235,8
0,0019	238,6	0,0094	232,7
0,0023	237,0	0,0095	237,5
0,0025	236,2	0,0100	232,8
0,0033	234,5	0,0125	231,2
0,0036	238,2	0,0127	228,0
0,0040	238,3	0,0145	229,0
0,0048	238,2	0,025	224,0
0,0049	235,9	0,040	223,0
		0,060	228,0

Table 2.10

Experimental data of Smith and Young [4, 30]
obtained with a fast chopper

E, eV	$6, \sqrt{E}, \text{b} \cdot (\text{eV})^{\frac{1}{2}}$	E, eV	$6, \sqrt{E}, \text{b} \cdot (\text{eV})^{\frac{1}{2}}$
1	2	3	4
0,0018	235,0	0,0053	232,8
0,0019	234,0	0,0060	232,8
0,0020	236,7	0,0062	232,0
0,0020	234,2	0,0070	232,0
0,0022	234,0	0,0076	231,8
0,0026	234,3	0,0082	232,2
0,0027	234,0	0,0110	229,5
0,0028	233,2	0,0115	232,0
0,00315	235,5	0,0118	229,3
0,0032	235,5	0,0140	228,0
0,0033	235,5	0,020	225,0
0,0036	235,6	0,030	225,0
0,0041	233,0	0,040	223,5
0,0044	234,4	0,050	224,3
0,0049	235,1	0,070	233,0
-	-	0,090	246,0

2. Simpson and Fluharty [31] determined $\sigma_t(^{241}\text{Pu})$ in the range 0.0105-0400 eV. Unfortunately, no detailed information is available about this experiment. The value of the cross-section $\sigma_t(^{241}\text{Pu})$ found by Simpson and Fluharty at 0.0253 eV was 1450 b (as derived by us from the experimental points by the least squares method). The renormalization factor is 0.958. In order to get σ_a from σ_t , we subtracted the value of the scattering cross-section (12 b).

The experimental data of Simpson and Fluharty given in Table 2.11 show a considerable scatter and give a poor description of the shape of the resonance.

Table 2.11

Experimental data of Simpson and Fluharty [31]

E_n, eV	σ_t, b	E_n, eV	σ_t, b	E_n, eV	σ_t, b	E_n, eV	σ_t, b
0,0105	2080,0	0,0465	1080,0	0,178	1330,0	0,280	1830,0
0,0111	1950,0	0,0520	1050,0	0,188	1390,0	0,289	1520,0
0,0137	2030,0	0,0578	940,0	0,197	1500,0	0,307	1200,0
0,0157	1860,0	0,0650	960,0	0,206	1630,0	0,326	960,0
0,0183	1680,0	0,0730	835,0	0,218	1830,0	0,348	630,0
0,0209	1580,0	0,0840	925,0	0,230	2000,0	0,372	450,0
0,0233	1430,0	0,0970	920,0	0,237	2050,0	0,400	300,0
0,0265	1430,0	0,1140	965,0	0,243	2100,0	0,428	170,0
0,0300	1460,0	0,135	950,0	0,252	2080,0	0,460	129,0
0,0348	1270,0	0,162	1200,0	0,260	2000,0	0,500	106,0
0,0408	1150,0	0,171	1260,0	0,268	1920,0	0,540	72,0

3. Simpson and Schuman [32] made reactor measurements of $\sigma_t(^{241}\text{Pu})$ with a fast chopper over the 0.0163-0.46 eV energy range. For recording, they used a system composed of a series of BF_3 proportional counters. The main sources of error below 0.5 eV were the statistical errors and uncertainties in the sample thickness and impurity content. The maximum error is observed to occur at the resonance peak and is equal to $\pm 5\%$.

At a thermal energy of 0.0253 eV, the total cross-section $\sigma_t(^{241}\text{Pu})$ is 1390 b, i.e. there is no need for renormalization. The scattering cross-section (12 b) was subtracted from σ_t to give σ_a . The experimental data of Simpson and Schuman show little scatter and form the basis of the evaluated curve.

The $\sigma_t(^{241}\text{Pu})$ data measured in Ref. [32] are given in Table 2.12.

Table 2.12

Results for $\sigma_t(^{241}\text{Pu})$ obtained by Simpson and Schuman [32]

$E, \text{ eV}$	$\bar{\sigma}_t, \text{ b}$	$E, \text{ eV}$	$\bar{\sigma}_t, \text{ b}$
1	2	3	4
0,0163	1752,57	0,0520	973,5
0,0170	1729,60	0,0566	938,23
0,0177	1705,17	0,0622	907,01
0,0186	1623,29	0,0681	875,68
0,0196	1584,43	0,0750	849,89
0,0205	1523,0	0,0829	825,07
0,0215	1474,75	0,0932	813,06
0,0229	1455,38	0,1061	811,67
0,0246	1419,14	0,1196	829,45
0,0260	1375,60	0,1347	872,40
0,0270	1327,80	0,1520	952,58
0,0280	1316,00	0,1729	1122,3
0,0290	1297,50	0,1965	1440,23
0,0300	1271,00	0,2208	1943,8
0,0310	1251,33	0,2390	2313,4
0,0320	1226,67	0,2456	2390,6
0,0330	1214,33	0,2525	2457,4
0,0340	1192,00	0,2597	2380,2
0,0350	1172,00	0,2672	2286,7

Table 2.12 (continued)

1	2	3	4
0,0365	1147,20	0,2750	2095,1
0,0384	1121,00	0,2918	1658,6
0,0401	1073,25	0,3147	1083,3
0,0424	1070,33	0,3409	657,76
0,0455	1032,83	0,3765	359,13
0,0485	1001,18	0,4100	238,51
-	-	0,4587	159,42

4. Craig and Westcott [3] measured $\sigma_t(^{241}\text{Pu})$ in the intervals 0.025-0.75 and 13.8-1000 eV, using samples with an 80% ^{241}Pu content. They quote the experimental and recommended data obtained after corrections had been made for the presence of other isotopes (^{238}Pu , ^{240}Pu and ^{241}Am).

The measurements used a time-of-flight method (base-line lengths of 5.66 and 16.32 m) with BF_3 counters as detectors. The value of $\sigma_a(^{241}\text{Pu})$ at 0.0253 eV was 1371 b, i.e. the renormalization coefficient is 1.005. The scattering cross-section $\sigma_n(^{241}\text{Pu})$ was taken as 12 b. The overall error in σ_t is made up of the statistical error and the error involved in normalizing the different experiments to a single curve. No allowance was made for the error resulting from the uncertainty in the corrections for the presence of other nuclei.

The experimental data of Craig and Westcott [3] were used as the basis of the evaluated curve (Table 2.13).

Table 2.13

Experimental data of Craig and Westcott [3] for $\sigma_t(^{241}\text{Pu})$

$E, \text{ eV}$	$\sigma_t, \text{ b}$	$E, \text{ eV}$	$\sigma_t, \text{ b}$
0,025	1391,0 \pm 30	0,24	2256 \pm 53
0,0253	1383,0 \pm 30	0,25	2352 \pm 55
0,030	1270 \pm 29	0,26	2349 \pm 55
0,040	1095 \pm 25	0,27	2236 \pm 54
0,050	988 \pm 23	0,28	1979 \pm 47
0,060	914 \pm 21	0,29	1694 \pm 41
0,070	862 \pm 20	0,30	1397 \pm 35
0,080	831 \pm 19	0,31	1164 \pm 29
0,090	807 \pm 19	0,32	955 \pm 24
0,100	800 \pm 19	0,33	787 \pm 19
0,110	805 \pm 19	0,34	655 \pm 16
0,12	814 \pm 19	0,35	545 \pm 14
0,13	843 \pm 20	0,36	447 \pm 11
0,14	879 \pm 21	0,37	383 \pm 10
0,15	930 \pm 22	0,38	337 \pm 9
0,16	988 \pm 23	0,39	288 \pm 8
0,17	1055 \pm 25	0,40	253 \pm 7
0,18	1167 \pm 28	0,45	155 \pm 5
0,19	1285 \pm 32	0,50	102 \pm 5
0,20	1447 \pm 36	0,55	82 \pm 4
0,21	1643 \pm 38	0,60	75 \pm 7
0,22	1868 \pm 42	0,65	70 \pm 7
0,23	2085 \pm 16	0,70	67 \pm 7
		0,75	66 \pm 8

5. Kolar and Carraro [33] used an electron linear accelerator to measure $\sigma_t(^{241}\text{Pu})$ by a time-of-flight method for the range 0.7-700 eV. The sample contained 94.66% ^{241}Pu . No correction was made for the contribution from the ^{240}Pu and ^{242}Pu resonances. To obtain σ_a from the σ_t results, the value of $\sigma_n(12 \pm 2 \text{ b})$ was subtracted. The Kolar and Carraro data are of little value for determining the detailed form of the curve below 1 eV because they are not corrected for the presence in the sample of ^{240}Pu , which has a strong resonance at 1.06 eV.

The experimental data of Kolar and Carraro [33] for energies below 1 eV are given in Table 2.14.

Table 2.14

Results for $\sigma_t(^{241}\text{Pu})$ obtained by Kolar and Carraro [33]

$\bar{E}_n, \text{ eV}$	$\bar{\sigma}_t, \text{ b}$	$\bar{E}_n, \text{ eV}$	$\bar{\sigma}_t, \text{ b}$
0,6839	74,94	0,8294	87,55
0,6960	79,13	0,8445	90,34
0,7095	75,99	0,8613	99,29
0,7205	81,46	0,8796	101,85
0,7319	82,80	0,8950	112,27
0,7445	80,95	0,9096	129,23
0,7550	82,11	0,9245	137,42
0,7679	78,89	0,9695	165,18
0,7813	77,71	0,9775	197,67
0,7962	80,36	0,9729	267,50
0,8125	83,96	0,9900	405,90

2.5. Evaluated $\sigma_a(^{241}\text{Pu})$ data below 1 eV

The evaluated $\sigma_a(^{241}\text{Pu})$ data obtained by means of the PREDA program [29] and the experimental data discussed above are shown in Figs 2.6-2.11. It can be seen that with the exception of the Simpson and Fluharty results, the various data are in satisfactory agreement with each other.

The evaluated values of $\sigma_a(^{241}\text{Pu})$ for energies below 1 eV are listed in Table 2.15. Also shown are the evaluated $\sigma_f(^{241}\text{Pu})$ and $\sigma_\gamma(^{241}\text{Pu})$ values obtained from the difference ($\sigma_a - \sigma_f$) and the α values derived from the evaluated σ_f and σ_a . The cross-section σ_γ and the ratio α are illustrated in Figs 2.12 and 2.13.

Table 2.15

Evaluated $\sigma_a, \sigma_f, \sigma_\gamma$ and α values for ^{241}Pu at thermal energies

$E, \text{ eV}$	$\sigma_a, \text{ b}$	$\sigma_f, \text{ b}$	$\sigma_\gamma = \sigma_a - \sigma_f, \text{ b}$	$\alpha = \frac{\sigma_\gamma}{\sigma_f}$
1	2	3	4	5
0,0001	23614,00	15680,20	7933,80	0,5050
0,0002	16692,80	11088,95	5603,85	0,5054
0,0004	11795,00	7842,70	3952,30	0,5039
0,0008	8329,80	5548,44	2781,36	0,5013
0,0010	7445,45	4963,70	2481,75	0,5000
0,0020	5247,42	3513,96	1733,46	0,4933
0,0030	4269,52	2872,42	1397,10	0,4864
0,0045	3468,14	2349,66	1118,48	0,4760
0,0065	2866,46	1959,58	906,88	0,4628
0,0085	2488,20	1717,56	770,64	0,4487

Table 2.15 (continued)

I	2	3	4	5
0,0105	2222,62	1548,96	673,66	0,4349
0,0145	1865,22	1324,00	541,22	0,4088
0,0200	1564,48	1134,63	429,85	0,3788
0,0250	1386,60	1020,85	365,75	0,3583
0,0253	1378,00	1015,00	363,00	0,3570
0,0300	1258,97	937,91	321,06	0,3423
0,035	1163,13	875,55	287,58	0,3285
0,040	1088,75	826,25	262,50	0,3177
0,045	1029,92	786,92	243,00	0,3088
0,050	982,08	754,90	227,18	0,3009
0,055	942,52	728,13	214,39	0,2944
0,060	909,17	706,07	203,10	0,2876
0,065	881,47	687,66	193,81	0,2818
0,070	858,21	671,95	186,26	0,2772
0,075	839,48	659,46	180,02	0,2730
0,080	823,96	648,81	175,15	0,2700
0,085	811,36	640,38	170,98	0,2670
0,090	802,00	633,50	168,50	0,2660
0,095	795,54	628,38	167,16	0,2660
0,100	793,10	626,13	166,97	0,2667
0,105	793,83	625,95	167,88	0,2682
0,110	796,29	626,63	169,66	0,2707
0,115	802,09	630,02	172,07	0,2731
0,120	808,12	633,56	174,56	0,2755
0,125	818,26	639,51	178,75	0,2795
0,130	830,11	646,39	183,72	0,2842

Table 2.15 (continued)

I	2	3	4	5
0,135	848,61	658,34	190,27	0,2890
0,140	868,87	671,35	197,52	0,2942
0,145	890,89	685,29	205,60	0,3000
0,150	916,17	702,04	214,13	0,3050
0,155	947,17	722,63	224,54	0,3107
0,160	981,00	744,88	236,12	0,3170
0,165	1020,20	770,55	249,65	0,3240
0,170	1061,82	798,26	263,56	0,3302
0,175	1106,78	827,81	278,97	0,3370
0,180	1156,26	860,03	296,23	0,3444
0,185	1218,71	902,08	316,63	0,3510
0,190	1282,64	944,44	338,20	0,3581
0,195	1365,53	999,65	365,88	0,3660
0,200	1457,47	1060,90	396,57	0,3738
0,205	1545,16	1118,23	426,93	0,3818
0,210	1650,38	1187,67	462,71	0,3896
0,215	1766,19	1263,09	503,10	0,3983
0,220	1881,71	1337,20	544,51	0,4072
0,225	1988,02	1402,58	585,44	0,4174
0,230	2099,04	1469,40	629,64	0,4285
0,235	2189,30	1521,97	667,33	0,4385
0,240	2265,85	1563,59	702,26	0,4491
0,245	2331,57	1598,06	733,51	0,4590
0,250	2368,31	1611,84	756,47	0,4693
0,255	2376,91	1606,42	770,49	0,4796
0,260	2359,50	1584,61	774,89	0,4890

Table 2.15 (continued)

I	2	3	4	5
0,265	2323,5I	1550,17	773,34	0,4989
0,270	2249,9I	1491,49	758,42	0,5085
0,275	2120,33	1395,87	724,46	0,5190
0,280	1984,3I	1297,79	686,52	0,5290
0,285	1831,96	1190,36	641,60	0,5390
0,290	1689,55	1090,03	599,52	0,5500
0,295	1537,36	985,49	551,87	0,5600
0,300	1405,82	896,00	509,82	0,5690
0,305	1262,07	800,30	461,77	0,5770
0,310	1138,70	718,42	421,28	0,5864
0,315	1020,5I	641,43	379,08	0,5910
0,320	931,05	583,36	347,69	0,5960
0,325	856,0I	535,0I	321,00	0,6000
0,330	781,6I	487,42	294,19	0,6036
0,335	704,92	438,82	266,10	0,6064
0,340	643,12	399,87	243,25	0,6083
0,345	586,60	364,34	222,26	0,6100
0,350	533,80	331,30	202,50	0,6112
0,355	486,73	301,97	184,76	0,6118
0,360	443,22	275,00	168,22	0,6117
0,365	410,65	254,87	155,78	0,6112
0,370	378,55	235,09	143,46	0,6102
0,375	351,86	218,69	133,17	0,6089
0,380	323,26	201,19	122,07	0,6067
0,385	304,96	190,17	114,79	0,6036
0,390	284,80	178,00	106,80	0,6000

Table 2.15 (continued)

I	2	3	4	5
0,395	266,83	167,25	99,58	0,5954
0,400	251,59	158,11	93,48	0,5912
0,405	238,50	150,38	88,12	0,5860
0,410	225,04	142,43	82,61	0,5800
0,415	212,85	135,14	77,71	0,5750
0,420	201,66	128,53	73,13	0,5690
0,425	191,58	122,50	69,08	0,5639
0,430	182,24	116,92	65,32	0,5587
0,435	173,70	111,85	61,85	0,5530
0,440	165,84	107,13	58,71	0,5480
0,445	158,47	102,70	55,77	0,5430
0,450	151,35	98,45	52,90	0,5373
0,46	138,45	90,66	47,79	0,527134
0,47	127,01	83,73	43,28	0,5169
0,48	116,45	77,22	39,23	0,5080
0,49	106,54	71,07	35,47	0,4991
0,50	98,33	65,90	32,43	0,4921
0,51	91,14	61,33	29,81	0,4861
0,52	85,16	57,53	27,63	0,4803
0,53	80,18	54,39	25,79	0,4742
0,54	75,54	51,43	24,11	0,4688
0,55	72,81	49,75	23,06	0,4635
0,56	70,34	48,24	22,10	0,4581
0,57	67,82	46,66	21,16	0,4535
0,58	65,99	45,55	20,44	0,4487
0,59	64,45	44,62	19,83	0,4444

Table 2.15 (continued)

I	2	3	4	5
0,60	63,22	43,89	19,33	0,4404
0,61	62,12	43,25	18,87	0,4363
0,62	61,16	42,70	18,46	0,4323
0,63	60,31	42,21	18,10	0,4288
0,64	59,48	41,73	17,75	0,4254
0,65	58,72	41,28	17,44	0,4225
0,66	57,99	40,85	17,14	0,4196
0,67	57,28	40,44	16,84	0,4164
0,68	56,63	40,06	16,57	0,4136
0,69	55,98	39,68	16,30	0,4108
0,70	55,38	39,33	16,05	0,4081
0,72	54,25	38,66	15,59	0,4033
0,74	53,13	37,99	15,14	0,3985
0,76	52,10	37,35	14,75	0,3949
0,78	51,10	36,73	14,37	0,3913
0,80	50,16	36,14	14,02	0,3879
0,82	49,26	35,57	13,69	0,3849
0,84	48,40	35,03	13,37	0,3817
0,86	47,58	34,51	13,07	0,3787
0,88	46,79	34,01	12,78	0,3758
0,90	46,02	33,52	12,50	0,3729
0,92	45,29	33,05	12,24	0,3703
0,94	44,57	32,59	11,98	0,3676
0,96	43,89	32,15	11,74	0,3652
0,98	43,23	31,72	11,51	0,3629
1,00	42,60	31,30	11,30	0,3610

2.6. Parametrization of the ^{241}Pu cross-sections in the thermal energy region (10^{-3} -1 eV)

For the parametrization of the cross-sections σ_t and σ_f , we used the evaluated data obtained above. We found it necessary to introduce two negative levels so as to get a good description of the cross-section variation below 0.1 eV. The first negative level ($E_r = -0.25$ eV, $\Gamma = 0.3$ eV) determines the general shape of the $\sigma(E)$ curve in the regions below 0.1 eV and between 0.5 and 1 eV; the second ($E_r = -0.01$ eV, $\Gamma = 0.01$ eV) serves to obtain an accurate description below 0.1 eV. The parameters of these levels are of significance only for curve adjustment purposes and cannot be given any physical interpretation. Their numerical values are quoted in the second part of this preprint.

An analysis of the $\sigma_t(E)$, $\sigma_f(E)$ and $\alpha(E)$ values obtained from the parameters leads to the conclusion that the experimental results for $\sigma_t(E)$ contain a systematic error in the region above 0.3 eV (and also possibly in the interval 0.2-0.3 eV). This error seems to be due to incorrect allowance for the effect of the ^{240}Pu impurity resonances above 1 eV. The σ_t , σ_f and α curves calculated from the final parameters are shown in Figs 2.1-2.11.

Seppi et al. (1958)
White et al. (1967)
Raffle and Price (1955)
Adamchuk et al. (1955)
James (1965)
Seppi (1958)
Watanabe and Simpson (1964)
Watanabe (1966)

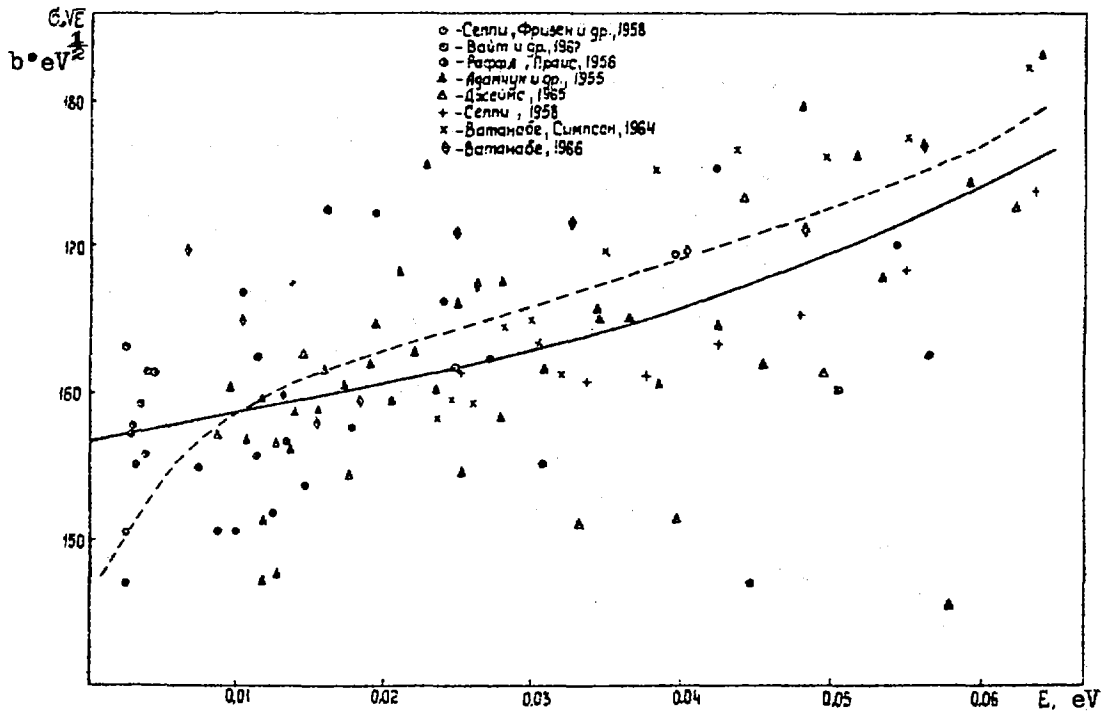


Fig. 2.1. Experimental and evaluated data for σ_f (^{241}Pu) in the region below 0.06 eV (--- calculation from the resonance parameters in Figs 2.1-2.5)

Watanabe (1966)
Watanabe and Simpson (1964)
Seppi (1958)
James (1965)
Adamchuk et al. (1955)
White et al. (1967)
Raffle and Price (1956)

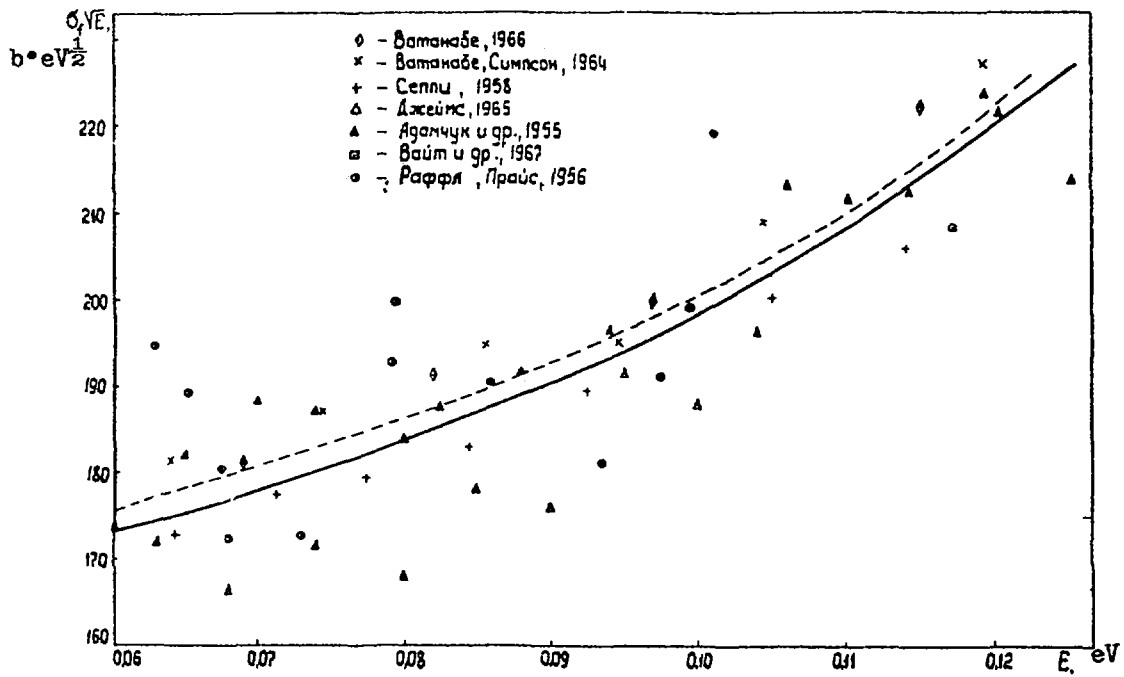


Fig. 2.2. Experimental and evaluated data for σ_f (^{241}Pu) in the range 0.06-0.12 eV

Watanabe (1966)
Watanabe and Simpson (1964)
Seppi (1958)
James (1965)
Adamchuk et al. (1955)
White et al. (1967)
Richmond and Price (1956)

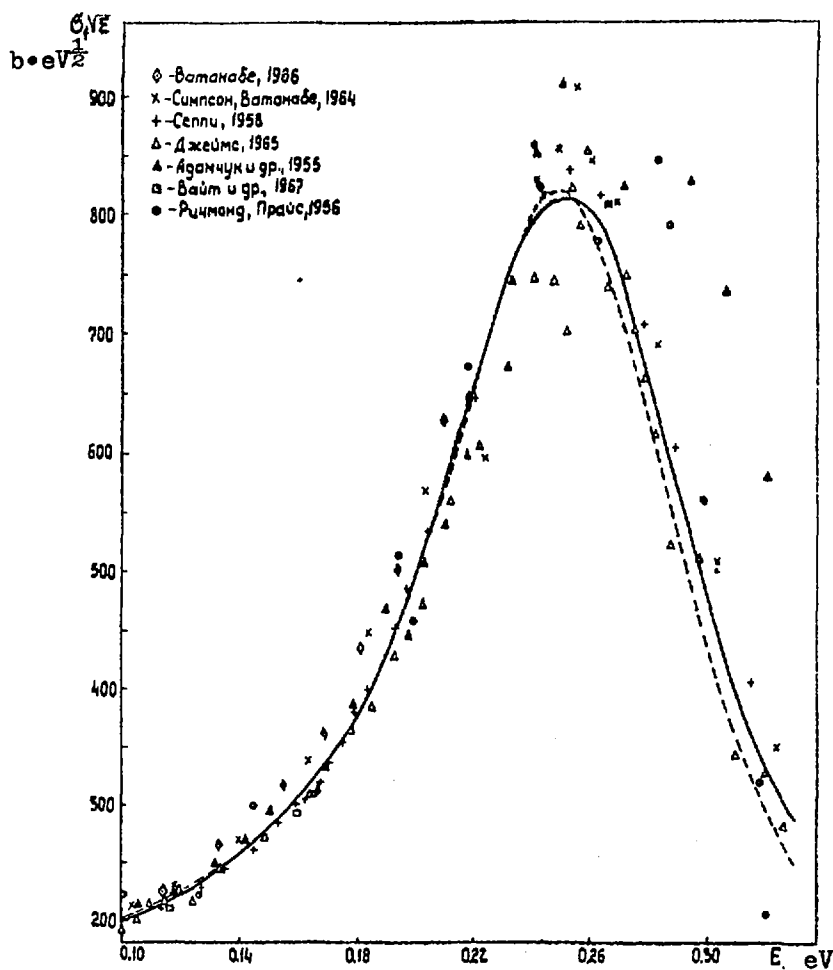


Fig. 2.3. Experimental and evaluated data for σ_f (^{241}Pu) in the range 0.1-0.3 eV

Watanabe and Simpson (1964)
Seppi (1958)
James (1965)
Adamchuk et al. (1955)
White et al. (1967)
Raffle and Price (1956)

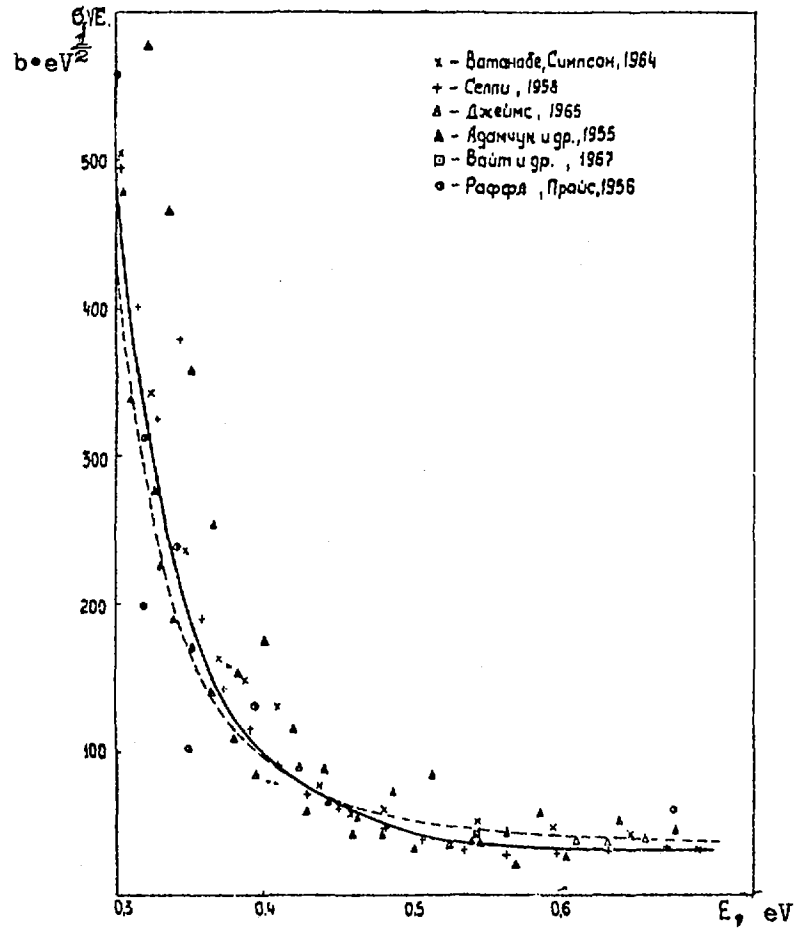


Fig. 2.4. Experimental and evaluated data
for σ_f (^{241}Pu) in the range
0.3-0.6 eV

Watanabe and Simpson (1964)
Seppi (1967)
James (1965)
Adamchuk et al. (1955)
Raffle and Price (1956)

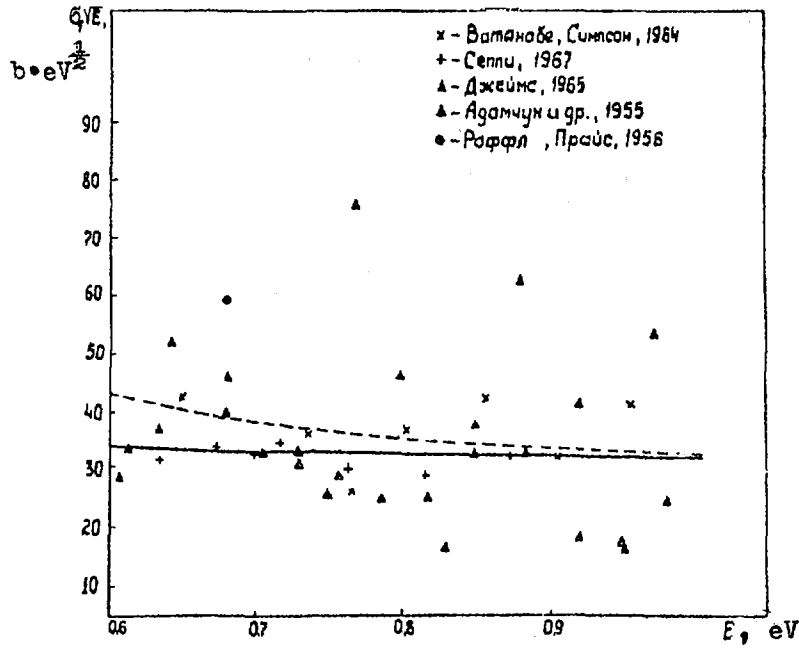


Fig. 2.5. Experimental and evaluated data
for σ_f (^{241}Pu) in the range
0.6-1.0 eV

Smith and Young (crystal spectrometer) (1969)
Smith and Young (fast chopper) (1969)
Simpson and Fluharty (1958)

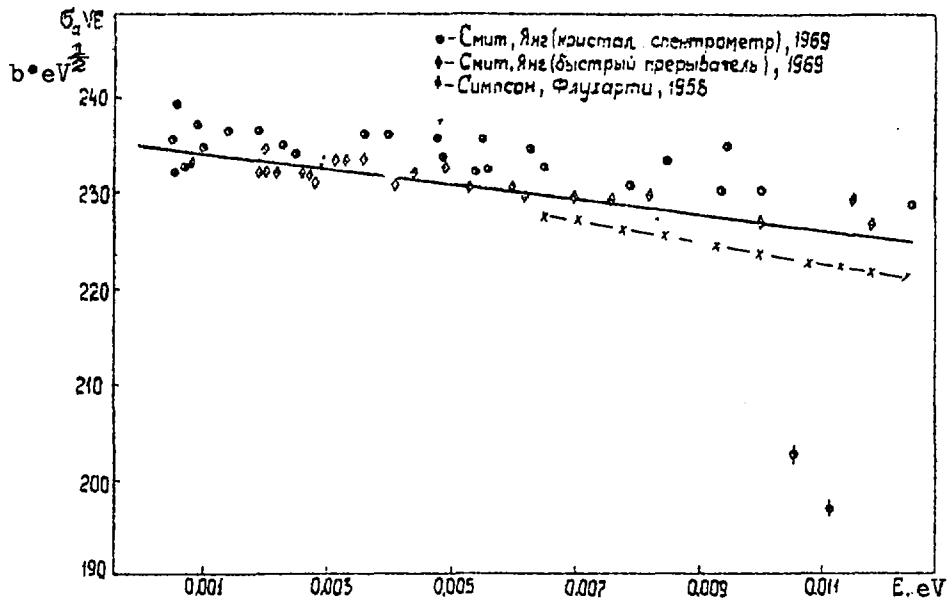


Fig. 2.6. Experimental and evaluated data for σ_a (^{241}Pu)
in the region below 0.012 eV
(—x—x— calculated from the resonance
parameters in Figs 2.6-2.11)

Simpson and Fluharty (1958)
Smith and Young (crystal spectrometer)
(1969)
Smith and Young (fast chopper) (1969)
Simpson and Schuman (1968)
Craig and Westcott (1968)

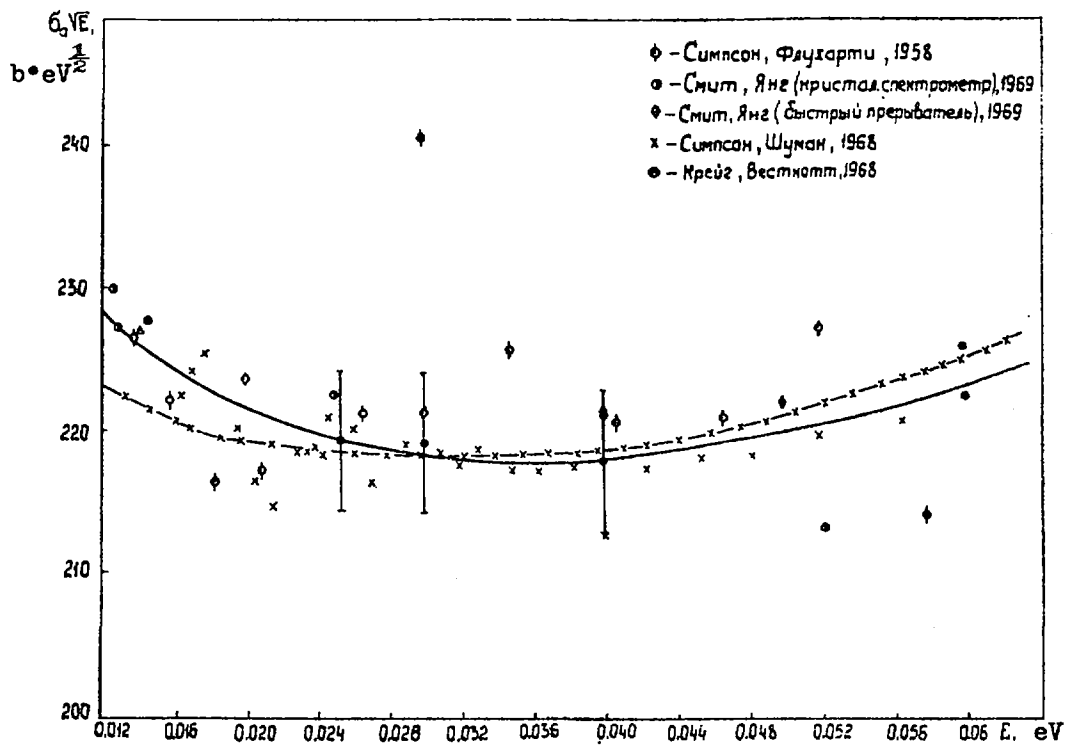


Fig. 2.7. Experimental and evaluated data for σ_a (^{241}Pu) in the range 0.012-0.06 eV

Smith and Young (fast chopper) (1969)
Simpson and Fluharty (1958)
Simpson and Schuman (1968)
Craig and Westcott (1968)

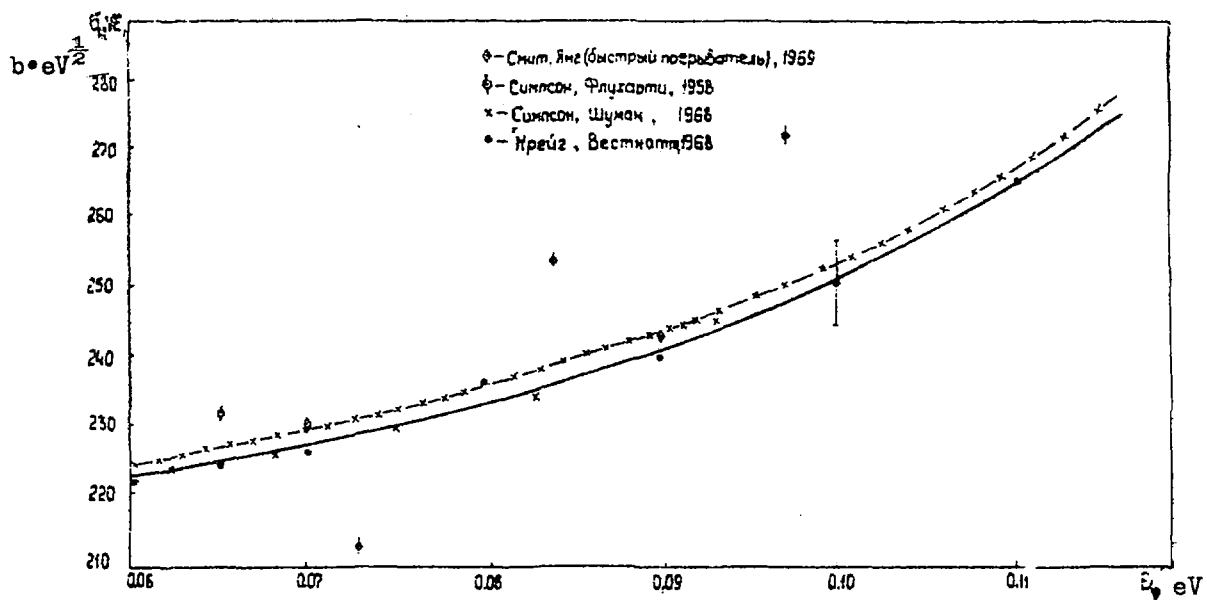


Fig. 2.8. Experimental and evaluated data for σ_a (^{241}Pu) in the range 0.06-0.12 eV

Simpson and Fluharty (1958)
Craig and Westcott (1968)
Simpson and Schuman (1968)

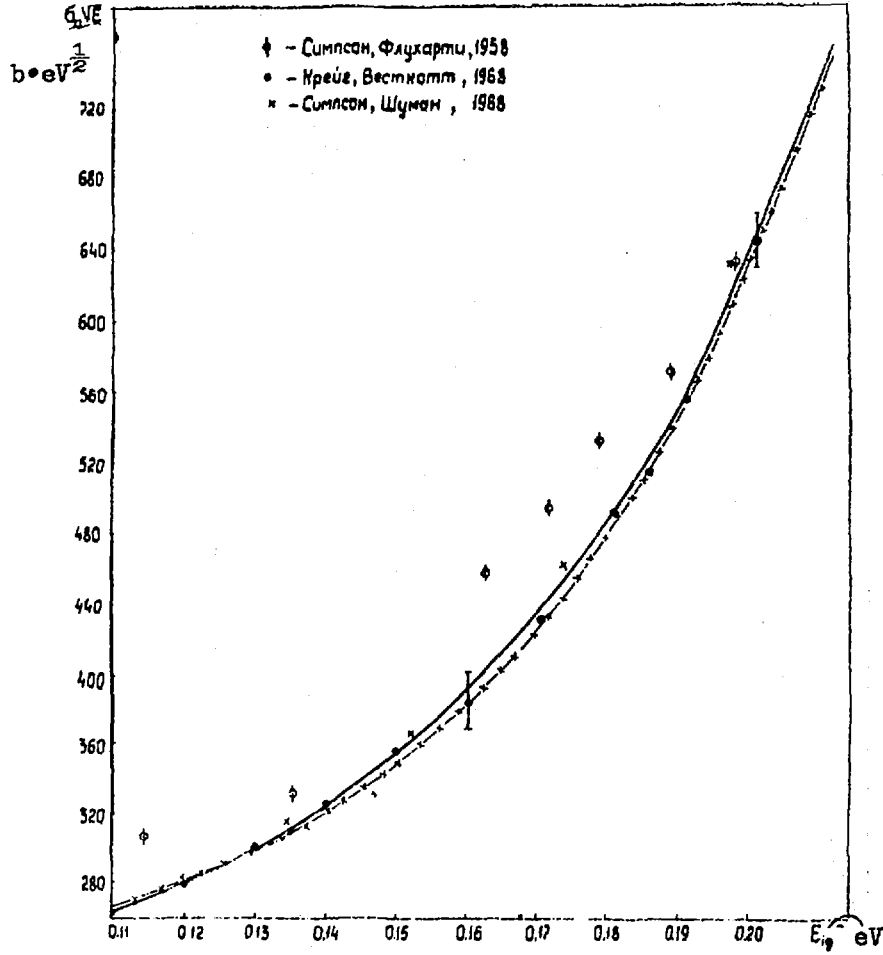


Fig. 2.9. Experimental and evaluated data for σ_a (^{241}Pu) in the range 0.11-0.2 eV

Simpson and Fluharty (1958)
Simpson and Schuman (1968)
Craig and Westcott (1968)

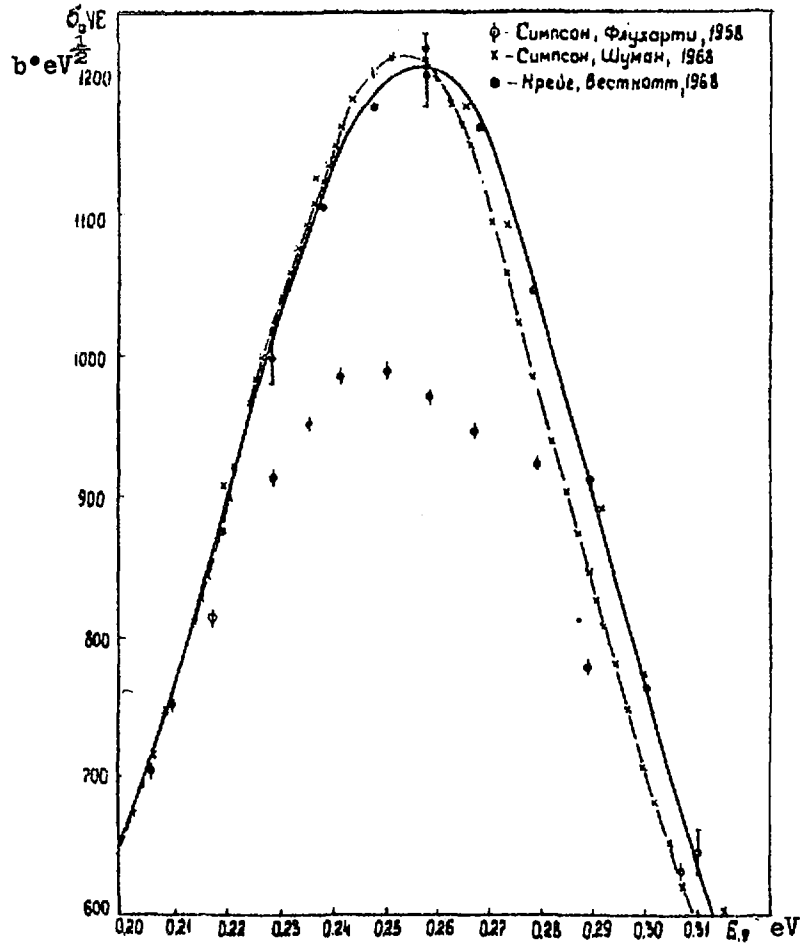


Fig. 2.10. Experimental and evaluated data
for σ_a (^{241}Pu) in the range
0.2-0.3 eV

Simpson and Fluharty (1958)
Simpson and Schuman (1968)
Kolar and Carraro (1971)
Craig and Westcott (1968)

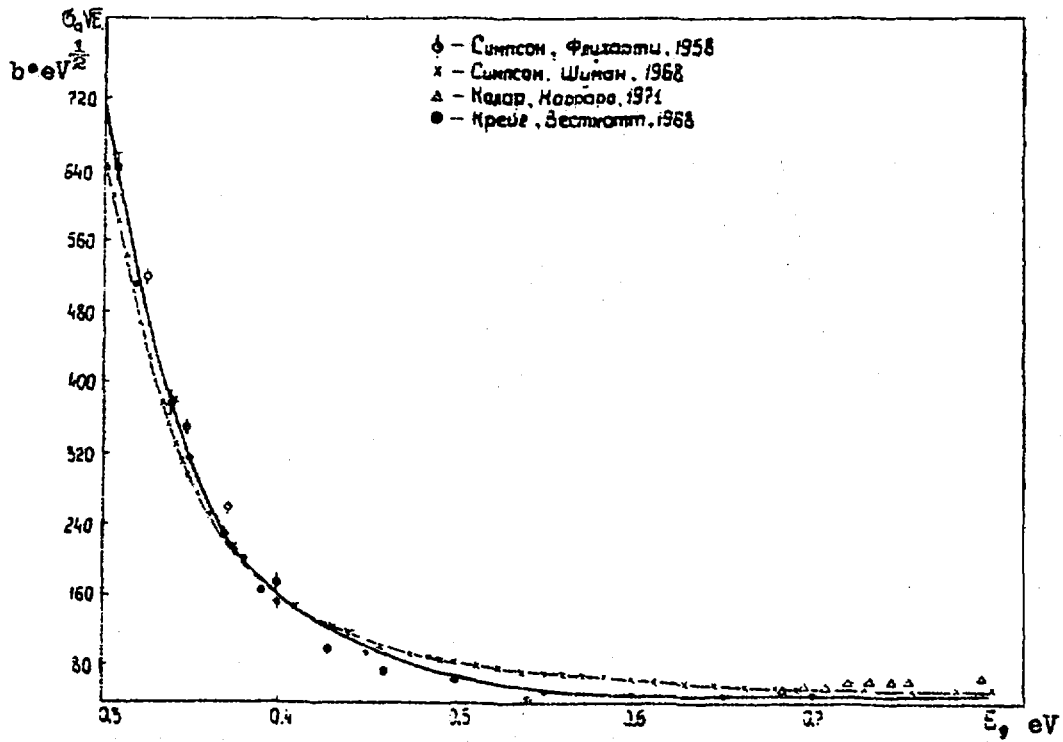


Fig. 2.11. Experimental and evaluated data for σ_a (^{241}Pu) in the range 0.3-0.8 eV

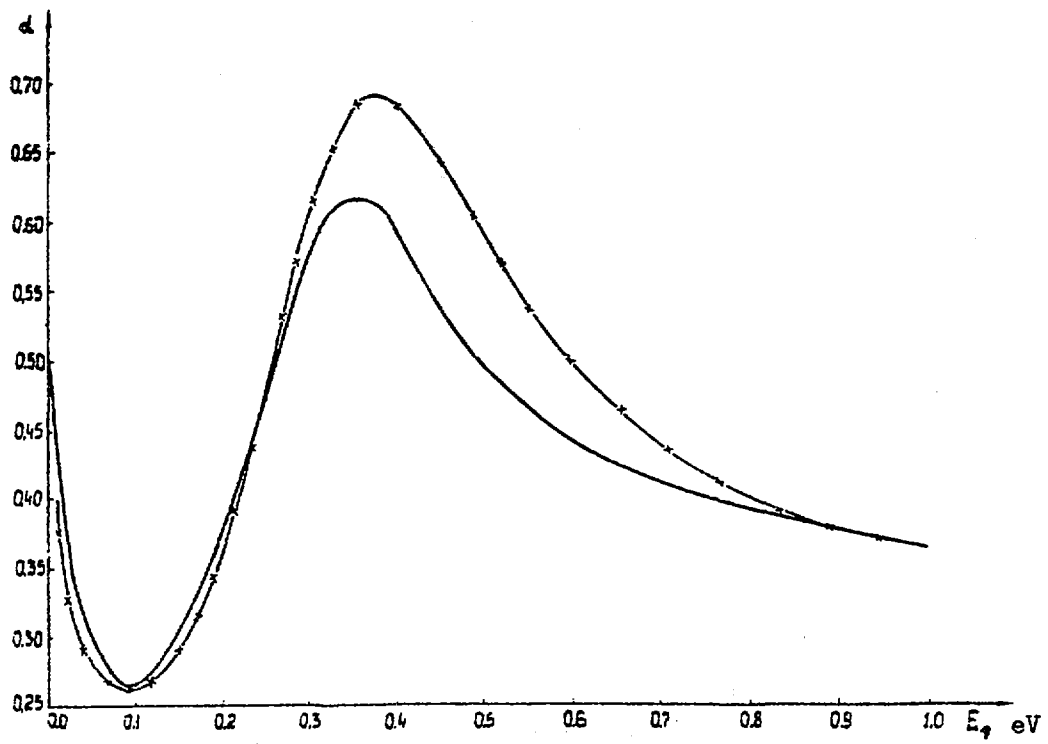


Fig. 2.12. Comparison of results for α : —x— calculated from resonance parameters; — calculated from evaluated cross-sections

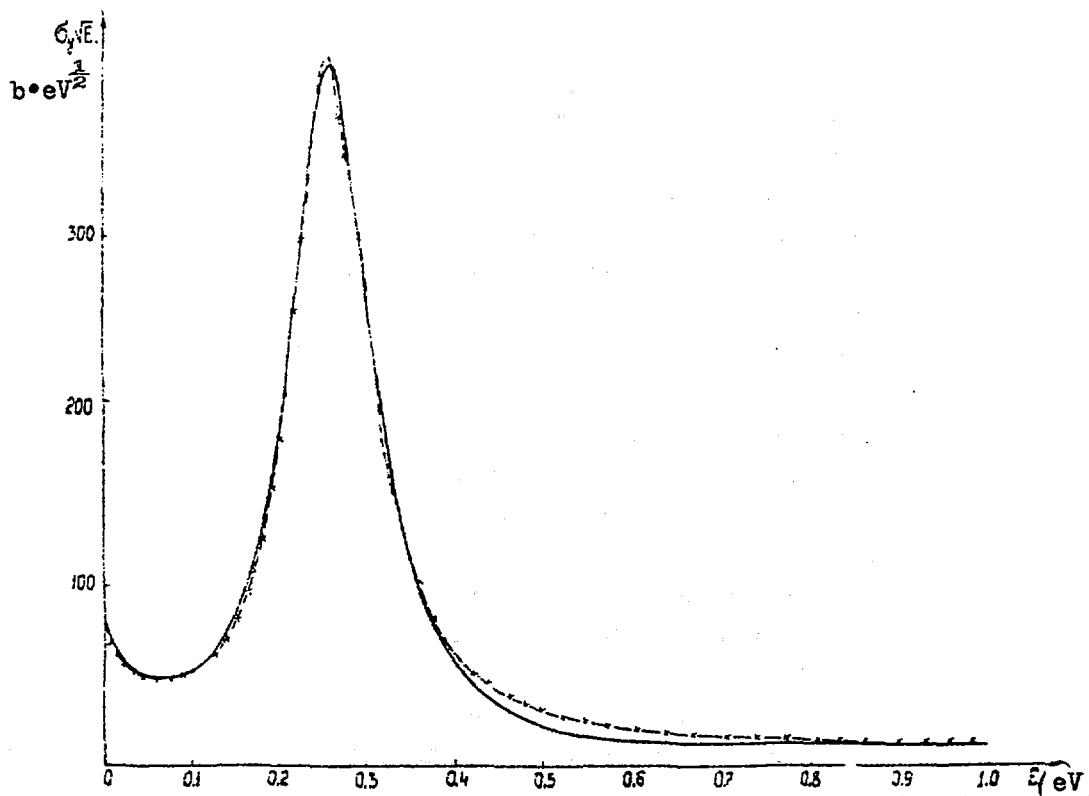


Fig. 2.13. ^{241}Pu capture cross-section σ_γ in the region below 1 eV: —x—x— calculated from resonance parameters; ——— difference between the evaluated cross-sections $\sigma_a - \sigma_f$.

REFERENCES

1. Hanna G.C., Westcott C.H., Lommel H.D., Leonard B.R., Jr., Story J.S., Attree P.M. - Atomic En.Review, v.7, 1969, 3p.
2. Simpson O.D., Marshall N.H., IDO-16679, 1961 and Simpson O.D., Schumann R.R. - Nucl.Sci.Eng., v.11, 1961, 111p.
3. Craig D.S., Westcott C.H., AECL-1948, 1964 and Can.J.Phys. v.42, 1968, 2384p.
4. Smith J.R., WASH - 1124, 1968, 64p. and WASH - 1093, 1968, 60p.
5. Cabell M.J. - UKAEA Rep. AERE - R 5674, 1968.
6. Watanabe T., Simpson O.D. - Phys.Rev., B, v.133, 1964, 390p. and IDO - 16995, 1964.
7. Leonard B.R., Jr. - ANL - 6122, 1959, 227p.
8. White P.H., Reichelt I.M.A., Warner G.F. - Proc.IAEA Conf on Nuclear Data. Paris, v.2, 1967, 29p.
9. Jaffly A.H., Studier M.H., Fields P.R., Bentley W.C. - ANL - 5397, 1955.
10. Raffle J.F. - First Intern.Conf.on Peaceful Uses Atomic Energy, v.4, 1956, 187p. and AERE - R - 2998, 1959.
11. Bigham C.B. et al. Second Intern.Conf.on Peaceful Uses of Atomic Energy, v.16, 1959, 125p.
12. Smith J.R., Reeder S.D. - Proc.of the Conf.on Neutron Cross-Sections and Technology, Washington, v.1, 1968, 589p. and WASH - 1093, 1968, 58p.
13. Fast E., Aber E.F. - IN - 1060, 1967.
14. Senders J.E. - J.Nucl.Energy, v.2, 1956, 247p. and Eselstaff P.A., Senders J.E. - First Intern.Conf.on Peaceful Uses of
15. Colvin D.W., Sowerby M.G. - Proc.Symp.on Physics and Chemistry of Fission, Salzburg, v.2, 1965, 25p.
16. Kalashnikova, V.I., et al., Peaceful Uses of Atomic Energy (Proc. Int. Conf. Geneva, 1955), Vol. 4, UN, New York (1956) 123.
17. De Saussure G., Silver B.G. - Nucl.Sci.Eng., v.5, 1959, 49p.
18. Jaffly A.H., Lerner J.L. - ANL-7625, 1969.
19. Boldeman J.W., Dalton A.W. - AAEC/E 172, 1967.
20. Cabell M.J. - UKAEA Rep.AERE - R5674, 1968 and IAEA Conf. on Nuclear Data for Reactors. Paris, v.2, 1967, 3p.

21. Lemmel H.D. - Proc.of the Conf.on Neutron Cross-Sections and Technology. Washington, v.1, 1975, 286p.
22. Watanabe T. - IN - 1012, 1966.
23. Seppi E.J. - Private Communication, 1958.
24. James G.D. - AERE - R - 4597, 1964 and Nucl.Phys., v.65; 1965, 353p.
25. Adamchuk, Yu.V. et al., Peaceful Uses of Atomic Energy (Proc. Int. Conf. Geneva, 1955), Vol. 4, UN, New York (1956) 259.
26. Seppi E.J., Friesen W.J., Leonard B.R. - HW-55879, 1958, 3p.
27. Raffle J.F., Price B.T. - First Intern.Conf.on Peaceful Uses of Atomic Energy, v.4, 1955, 225p.
28. Richmond R., Price B.T. - J.Nucl.Energy, v.2, 1956, 177p.
29. Antsipov, G.V., Kon'shin, V.A., Morogovskij, G.B., Byull. TsYaD, No. 10 (1972) 263.
30. Smith J.R., Young T.E. - WASH-1136, 1969, 43p.
31. Simpson F.B., Fluharty R.G. - Bull. Am.Phys.Soc., v.3,
32. Simpson O.D., Schuman R.P. - Nucl.Sci.Eng., v.11, 1961, 111p.
33. Kolar W., Carraro G. - Conf.on Neutron Cross-Sections and Technology, Knoxville, v.2, 1971, 707p.

Part 2

Analysis of Experimental Data Between

1 - 150 eV

Abstract

This preprint contains an analysis of the available experimental data on ^{241}Pu cross-sections in the energy range 1-150 eV. Selected series of experimental data are parameterized by means of a modified Adler-Adler formalism. The parameters obtained can be used for calculating both the detailed dependence of the cross-sections and the group constants. The mean resonance parameters needed to analyse data in the forbidden resonance region are calculated.

79-7974
Translated from Russian

A.V. Lykov Institute of Heat and Mass Transfer
Academy of Sciences of the Byelorussian SSR

EVALUATION OF NUCLEAR DATA FOR ^{241}Pu IN THE NEUTRON
ENERGY REGION FROM 10^{-3} eV TO 15 MeV

V.A. Kon'shin, G.V. Antsipov, E.Sh. Sukhovitskij,
L.A. Bakhanovich, A.B. Klepatskij,
G.B. Morogovskij and Yu.V. Porodzinskij

Preprint No. 3
Minsk, 1979

1. NUCLEAR REACTION CROSS-SECTIONS FOR ^{241}Pu IN THE RESONANCE ENERGY REGION

The nuclear reaction cross-sections for ^{241}Pu in the region up to 150 eV (the allowed resonance region) show a marked asymmetry resulting from interference between levels. The cross-sections in the energy region between resonances are not described well by the Breit-Wigner formula in its usual form, because $\langle D \rangle = 1.34$ eV, but $\langle \Gamma \rangle \approx 400$ meV, i.e. $\langle \Gamma \rangle / \langle D \rangle \approx 0.3$, therefore a multi-level analysis must be used to parameterize the cross-sections in the resonance energy region. It should also be noted that experimental data on ^{241}Pu are less reliable than analogous data on ^{235}U and ^{239}Pu , which makes the fitting procedure much more difficult.

We had at our disposal the following experimental data in the resonance energy region:

- (1) For σ_t - the data of Simpson and Schumann [1], Craig and Westcott [2], Kolar and Carraro [3], Pattenden et al. [4];
- (2) For σ_f - the data of Watanabe and Simpson [5], James [6], Simpson and Moore [7], Simpson et al. [8], Blons et al. [9], Migneco et al. [10], Weston and Todd [11], Leonard et al. [12];
- (3) For σ_n - the data of Sauter and Bowman [13].

No data were available for σ_γ .

1.1. Analysis of experimental data in the allowed resonance energy region

1.1.1. Experimental data on σ_t

Simpson and Schumann [1] measured σ_t in the range 0.2 eV-2 keV at room temperature, using a chopper and a reactor as the neutron source. The sample consisted of 81.3% ^{241}Pu , 7.74% ^{239}Pu , and 10.42% ^{240}Pu , therefore the data contain peaks due to impurities:

- At 3.95 and 5.4 eV - ^{241}Am ,
- At 2.7 eV - ^{242}Pu ,
- At 7.8, 10.8, 11.95, 15.5 and 17.9 eV and partly at 14.6 eV - ^{239}Pu .

To improve the resolution of the resonance peaks in the range 12-20 eV a flight distance of 45 m was used, and the region between resonances was measured with a path length of 16 m for better statistics. In the regions below 12 eV and above 20 eV the total cross-section σ_t was measured with a path length of 16 m. The analyser channel width was 32 μ s in the range 0.02-0.50 eV and 1 μ s in the range 1.5 eV-2 keV. No measurements of σ_t were performed in the range 0.5-1.5 eV because of the strong influence of the ^{240}Pu resonance at 1.06 eV.

The accuracy of the cross-section σ_t in the region below 0.5 eV is limited by the indeterminacy of the thickness and homogeneity of the sample, which is $\pm 5\%$ in the peak of the first resonance. In the region above 1.5 eV the accuracy is limited by statistical errors in the valleys between the resonances and the indeterminacy of the sample thickness and inhomogeneity in the resonance peaks. At energies above 20 eV identifying the resonances of ^{241}Pu becomes very difficult because of the numerous impurity resonances, the great width of the channel and the small path length (see above).

2. Craig and Westcott [2] measured the total cross-section of ^{241}Pu in the ranges 0.025-0.75 eV and 13.8-1000 eV, using a high-speed chopper. The sample consisted of 81.4% ^{241}Pu , 7.7% ^{239}Pu , 10.3% ^{240}Pu and 0.58% ^{242}Pu . In the range 0.025-0.75 eV the measurements were performed with flight distances of 5.87 and 16.32 m and an analyser channel width of 2 μ s. In the range 13.8-1000 eV the flight distance was 88.11 m and the analyser channel width was 1 μ s. The speed of rotation of the rotor was varied between 4200 and 6700 rev/min, and the resolution time was between 2.8 μ s at 14 eV and 1.8 μ s at 1000 eV.

The experimental data contain the following contributions from impurity resonances:

E, eV	Impurity resonance	E, eV	Impurity resonance
14,35	^{239}Pu	41,9	^{240}Pu
14,7	$^{239}\text{Pu}, \text{Am}$	44,6	^{239}Pu
	^{239}Pu	50,0	"-
15,6	<i>Am</i>	53,0	"-
15,7	"-	53,6	^{242}Pu
16,4	"-	59,5	^{239}Pu
16,8	"-	66,0	"-
17,6	^{239}Pu	67,0	^{240}Pu
18,4	<i>Am</i>	73,0	"-
20,5	^{240}Pu	75,5	^{239}Pu
22,25	^{239}Pu	86,0	"-
38,4	^{240}Pu	107,0	^{240}Pu
-	-	130,0	"-

3. Kolar and Carraro [3] measured σ_t in the energy range 0.2-700 eV on an electron linear accelerator at room temperature. The sample consisted of 25 g PuO_2 enriched to 94.66% ^{241}Pu (^{239}Pu : 0.87%, ^{240}Pu : 2.97%, ^{242}Pu : 1.5%). Two cycles of measurement were performed (Table 1.1).

The data show the following peaks (up to 100 eV) due to impurities in the sample:

1.06 eV - ^{240}Pu ; 2.7 eV - ^{242}Pu ; 7.85 eV - ^{239}Pu ;
 20.45 eV - ^{240}Pu ; 22.25 eV - ^{239}Pu ; 38.25 eV - ^{240}Pu ;
 41.35 eV - ^{239}Pu ; 41.65 eV - ^{240}Pu ; 44.5; 49.75; 52.7;
 59.02; 66.0 eV - ^{239}Pu ; 66.7, 72.7 eV - ^{240}Pu ; 74.9,
 86.0 eV - ^{239}Pu ; 90.5 eV - ^{240}Pu ; 90.8 eV - ^{239}Pu .

4. Pattenden et al. [4] measured the cross-section σ_t in the energy range 2.4-847.0 eV by the time-of-flight method. They give no detailed description of the experimental conditions, but information on the energy resolution and sample thickness is contained in the EXFOR system. The authors obtained eight sets of data in various energy ranges with a channel width of 0.25-1 μs and a sample thickness of 230-1700 b/atom.

1.1.2. Experimental data on σ_f

1. Watanabe and Simpson [5] measured σ_f in the energy range 0.02-100 eV by means of a high-speed neutron chopper, using a reactor as the source. The flight distance was 8.5 m.

Three series of measurements were performed:

0.023-92 eV at a resolution of 2.7 $\mu\text{s}/\text{m}$;

0.244-7.4 eV at a resolution of 0.72 $\mu\text{s}/\text{m}$;

1.47-106.6 eV at a resolution of 0.35 $\mu\text{s}/\text{m}$.

The experimental data were normalized to a value of $\sigma_f(^{241}\text{Pu})$ equal to 406 ± 10 b at an energy of 6 eV. This value was obtained from the measured total cross-section at 6 eV (434 ± 6 b) and the calculated values of σ_s (14 ± 4 b) and σ_γ (14 ± 7 b).

The value of σ_f obtained by the least squares method from the experimental points is equal to 962 ± 38 b at 0.0253 eV. Above 10 eV the resolution in this experiment deteriorates markedly and the data become useless for detailed analysis.

2. James [6] measured σ_f in the range 0.01 eV-3 keV by the time-of-flight method. Two experiments were conducted: the first involved a flight distance of 5 m and covered the energy range 0.0087-20 eV with a channel width of 1 μs ; the second, with a flight distance of 15 m and a channel width of 1 μs , covered the energy range 3 eV-3 keV.

The neutron spectrum was measured with a BF_3 counter. It was assumed that the cross-section of $^{10}\text{B}(n,\alpha)$ followed a $1/\sqrt{E}$ law. The sample used contained 97.33% ^{241}Pu and 1.44% ^{240}Pu .

The normalizing constant was determined from data measured with a path length of 5 m at an energy of 0.0253 eV (the cross-section σ_f was taken to equal 1010 b). Owing to the low statistical accuracy of data close to the thermal energy all the values of the cross-sections in the range 0.0253-0.05 eV were used for normalization. The statistical accuracy was $\pm 5.4\%$. For data obtained with a path length of 15 m the normalizing constant was determined by

calculating the area under the curve σ_f in the ranges 4-8, 8-16, and 16-32 eV and normalizing them to the results obtained with a path length of 5 m. The error in the normalization was $\pm 5.6\%$. Adding this to the 2% systematic error in determining the background gives a total error of $\pm 6\%$. This is the value given by James in the report in Ref. [6], although in the paper in [6] he changes the normalization error in the thermal point to $\pm 1\%$ without any explanation. In view of the scatter of the experimental data of James and of other authors we have retained our total error of $\pm 6\%$.

3. Simpson and Moore [7] measured $\sigma_f(^{241}\text{Pu})$ in the energy range 2-100 eV by the time-of-flight method on an electron linear accelerator. The neutron flux was measured with BF_3 counters, it being assumed that the cross-section of the $^{10}\text{B}(n,\alpha)$ reaction changes according to the $1/\sqrt{E}$ law. As in Ref. [5] the fission cross-section was normalized to a value of σ_f equal to 406 b in the resonance peak at 6 eV.

Two independent sets were normalized by calculating the integral fission cross-section in the region 8-100 eV. The entire region of energies (2-100 eV) was measured in two series with analyser channel widths of 0.5 and 0.25 μs and a path length of 10.56 m.

4. Simpson et al. [8] reported a measurement of $\sigma_f(^{241}\text{Pu})$ in the energy range 20 eV-2 keV utilizing an underground nuclear explosion, but no detailed information on the resolution function and the normalization of the experiment were available to us.

5. Blons et al. [9] measured $\sigma_f(^{241}\text{Pu})$ in the range 1 eV-30 keV on the linear accelerator at Saclay by the time-of-flight method with the sample cooled to 77 K. Two cycles of measurements were performed (Table 1.2). The data on the channel and pulse widths should be treated with caution, as the actual energy resolution of the experimental data does not correspond to that calculated on the basis of Table 1.2.

As the detector effectiveness is not known with sufficient accuracy, experimental data on σ_f must be normalized to absolute values.

Blons et al. [9] normalized their data to the value of the integral $\int_{20 \text{ eV}}^{70 \text{ eV}} \sigma_f(E) dE = 2367.5 \text{ b}\cdot\text{eV}$ evaluated by James in Ref. [14]. The error in the normalization was $\pm 3.4\%$.

The difficulties in determining the background in the energy range below 40 eV resulting from the low throughput of the boron filter were eliminated to a considerable extent for ^{241}Pu by using a shorter flight distance at low energies; the data on σ_f can therefore be used from 2 eV onwards. The experimental data were not corrected for the 0.87% ^{239}Pu impurity in the sample.

6. Migneco et al. [10] measured σ_f in the energy regions 2-2000 eV on an electron linear accelerator by the time-of-flight method. The measurements were performed in two series: (1) in the range 2-46.5 eV with an analyser channel width of 0.32 μs ; (2) in the range 46.5-2000 eV with a channel width of 0.04 μs . The flight distance in both cases was 30.617 m. The experimental data on σ_f were normalized to the resonance integral of fission $\int_{4.65 \text{ eV}}^{10 \text{ eV}} \sigma_f(E) \frac{dE}{E} = 193.6 \text{ b}$ obtained by Hennies [15]. The normalization between the low-energy and high-energy regions was carried out in the range 21.7-30.2 eV by calculating the fission integral in this range with a possible error of 2% introduced in the normalization. The data were not corrected for the 0.87% ^{239}Pu impurity in the sample.

7. Weston and Todd [11] describe measurements of σ_f and σ_α on an electron linear accelerator in the energy range 10 eV-250 keV, but only averaged numerical data in the range 10 eV-30 keV are given.

8. Leonard et al. [12] measured σ_f in the eV-region, but owing to the low resolution these data can be used only in the thermal energy region (up to 1 eV).

9. Wagemans and Deruytter [16] performed absolute measurements of the fission cross-section $\sigma_f(^{241}\text{Pu})$ on an electron linear accelerator in the energy range 0.01-50 eV with a direct normalization of σ_f at 2200 m/s to a value of $1015 \pm 7 \text{ b}$. The sample contained 93.432% ^{241}Pu . The number of fission events and the neutron flux were determined simultaneously by means of surface-barrier counters placed against the layers of ^{241}Pu and ^{10}B . As few experiments were conducted in the thermal energy region, Wagemans and Deruytter suggest renormalizing the experimental data to the fission integral from 12 to 20 eV, which is equal to $\int_{12 \text{ eV}}^{20 \text{ eV}} \sigma_f(E) dE = 1363 \pm 14 \text{ b}\cdot\text{eV}$.

10. Carlson et al. [17], using the time-of-flight method and an electron linear accelerator, measured the ratio of the fission cross-section $\sigma_f(^{241}\text{Pu})$ to the cross-section for the reaction $^6\text{Li}(n,\alpha)$ in the energy region from thermal to 70 keV. The fission chamber employed for this purpose was the same as was used by the authors of Ref. [17] to measure the ratio of the fission cross-section of ^{241}Pu to that of ^{235}U [18]. The sample contained 96.5% ^{241}Pu . The ^{241}Pu fission cross-section obtained was normalized to the value of 1015 b - the mean fission cross-section in the range 0.0203-0.0303 eV. Simultaneously with the measurements of the ratio of the fission cross-section $\sigma_f(^{241}\text{Pu})$ to the cross-section of the reaction $^6\text{Li}(n,\alpha)$, the fission cross-section $\sigma_f(^{235}\text{U})$ was measured in relation to the cross-section of $^6\text{Li}(n,\alpha)$ in the energy range 7.4 eV-70 keV; it was thus possible to determine the ratio of the ^{241}Pu to ^{235}U fission cross-sections. The largest components of the error in $\sigma_f(^{241}\text{Pu})$ are the indeterminacies in the normalization ($\pm 1.2\%$), in the measurement of the background and in the ^6Li cross-section ($\pm 3\%$ at 50 keV).

Unfortunately, the authors' measurement results are not averaged over the standard energy ranges. There is also a systematic difference between the data of Carlson et al. and the results of Wagemans and Deruytter, which, in spite of the identical normalization in the thermal region, are $\sim 5\%$ higher than the data of Ref. [17] in the energy range 9-44 eV, as can be seen from Table 1.3. This discrepancy exceeds the limit of the errors given by the authors. Experimental data on $\sigma_f(^{241}\text{Pu})$, especially less recent data, differ strongly from each other both in their absolute values and in their curve shapes. This may be due partly to the various normalizations, which are very different from each other and are often indirect, and partly to experimental difficulties (the high background in the experiment by Moore et al. [7], the low statistical accuracy in the experiment by James [6]). Wagemans and Deruytter [16] performed detailed measurements of the shape of the curve in the region below 50 eV, which enabled a comparison with other data to be made. It was found that the data of Moore et al. [7] fluctuate very strongly. The data of Simpson et al. [8], Adamchuk et al. [19]

and Watanabe et al. [5] differ sharply in curve shape from the data of Wagemans et al., and practically nothing is gained by renormalizing these data. They were therefore not used in the evaluation. The data of Blons [9] and Migneco et al. [10], on the other hand, agree quite well with those of Wagemans et al.

A general normalization to the fission integral from 12 to 20 eV, equal to 1363 b·eV [16], was carried out for the data of Blons, Migneco et al., James, Moore et al. (up to 50 eV), and Weston and Todd. For the remaining data the error in normalization plays a very insignificant part and the main sources of systematic error are not associated with the normalization. Experimental, renormalized and evaluated data on $\sigma_f(^{241}\text{Pu})$ are given in Tables 1.4 and 1.5.

The evaluated values of $\sigma_f(^{241}\text{Pu})$ were obtained as a weighted mean of the data of Wagemans et al., Carlson et al., Weston et al., the data of Migneco and Blons (the error of both sets of data was increased by 10% because there was no correction for ^{239}Pu impurities in the sample), the data of James (the weight of these data was reduced by 20% because of the low statistical accuracy), Moore et al. (the error in the region below 50 eV was increased by a factor of 1.5 because of the high background of the experiment; in the region above 50 eV the data were not used).

1.1.3. Experimental data on σ_n

Sauter and Bauman [13] measured the scattering cross-section in the energy range 2-32 eV on a linear accelerator by the time-of-flight method. The scattering cross-section to be measured was normalized to the cross-section of scattering on carbon. The sample contained 85.7% ^{241}Pu and was less than 0.01 cm thick. Although the sample was comparatively thin, it is necessary to introduce a correction for absorption of the incident neutron flux; this correction is particularly large in the resonance peaks, where the cross-section differs from the potential cross-section by a factor of 2-3. In the valleys between resonances this correction is ~10%. The correction for absorption was calculated analytically by the authors of Ref. [13].

Since the experimentally obtained areas under the resonances are small, analysis by the area method is possible only for three resonances: 13.38, 14.72 and 17.83 eV. The area under the scattering resonance being $2\pi^2 \chi^2 g \frac{\Gamma n^2}{\Gamma}$, we can use the $g\Gamma n$ and Γ obtained from other measurements to determine the g values for these three resonances. They are equal to 0.36, 0.58 and 0.41, respectively, i.e. the spins take the values $J = 2$ ($g = 0.417$) for the resonances 13.38 and 17.83 eV and $J = 3$ ($g = 0.583$) for the resonance 14.72 eV.

1.1.4. Experimental data used in the present evaluation

On the basis of the foregoing analysis of the available experimental data in the resonance energy region the following sets of data were selected for parameterization:

- (1) In the thermal region (up to 1 eV) the evaluated data obtained in the previous section were used;
- (2) For σ_t - Kolar and Carraro [3];
- (3) For σ_f - Blons et al. [9].

The remaining sets of experimental data were not used for the present analysis because their energy resolution is poorer than that of the sets selected, especially in the region above 10 eV, and also because their energy scales were found to be considerably shifted in relation to the scale chosen by us. The data in Ref. [13] on σ_n were not used for the reasons given in section 1.1.3.

1.2. Results of the parameterization of the ^{241}Pu cross-sections in the resonance energy region

The experimental data selected after a preliminary evaluation were used to obtain resonance parameters by the same formalism as was used in Ref. [20]. The only difference in the present work is that the dependence $1/\sqrt{E}$ was used instead of $1/E$ in the expression for the cross-section in terms of parameters so that the formula would take the generally accepted form

$$\sigma_i(E) = \frac{A}{\sqrt{E}} \sum_{i=1}^N (G_i^* \psi_i + H_i^* \chi_i), \quad (1.1)$$

where ψ_i and χ_i are Doppler functions of the i -th resonance;

A is a constant ($A \approx 2.6 \times 10^6$ b.eV);

r is the reaction in question.

The formalism used by us seems preferable in the case of ^{241}Pu to the Breit-Wigner formalism. In fact, if the number of resonances of a given spin is proportional to $2J + 1$, then in our case we have 46 resonances with 2^+ and 64 resonances with 3^+ . Using the evaluated data of Ref. [21] we obtain $\langle \Gamma \rangle^{2^+} / \langle D \rangle^{2^+} = 0.18$ and $\langle \Gamma \rangle^{3^+} / \langle D \rangle^{3^+} = 0.08$. Hence the (narrower) 3^+ resonances may be described with sufficient accuracy by the Breit-Wigner formalism without taking interference into account (it is known that the criterion of applicability of this formalism is that the condition $\langle \Gamma \rangle / \langle D \rangle \ll 1$ should be satisfied), but in the case of the 2^+ resonances it is necessary to take interference into account, and such resonances must constitute, from theoretical considerations, about 42% of all the resonances under discussion. These conclusions were confirmed by test calculations following the Breit-Wigner formalism in the resonance region of ^{241}Pu . Thus, the solution of the parameterization problem and the further evaluation of the parameters obtained are more conveniently performed in a formalism suitable for all the resonances in the region under consideration.

The parameterization was carried out taking into account the contribution to a given resonance of the ten neighbouring resonances (five each to the right and left, not counting the one underlying the energy point in which the cross-section is calculated). This was found to be sufficient for obtaining a satisfactory shape of the curve $\sigma(E)$.

The parameters G_t , H_t , G_f , H_f , and Γ obtained in processing the experimental data on $\sigma_t(E)$ and $\sigma_f(E)$ with due allowance for the corrections introduced (see below) and the parameters G_γ and H_γ obtained for the calculation of the averaged group constants are given in Table 1.6. Although no data on $\sigma_\gamma(E)$ and $\sigma_n(E)$ were available, i.e. the system was not closed, an attempt was made to obtain a consistent system of Breit-Wigner parameters analogous to that in Ref. [20]. Because of the missing experimental data (see above) spins were assigned to levels on the basis of their total width Γ in accordance with the generally accepted dependence of the level density on spin.

The parameters obtained in this way are given in Table 1.7. Note, however, that these parameters are tentative and should not be used in calculations of the detailed dependence of the cross-sections. We needed them to obtain tentative mean resonance parameters that could be used for calculations in the forbidden resonance region.

It should be borne in mind that some of the spins of the resonances in Table 1.7 may not correspond to reality, and a change in the spins of even an insignificant number of levels has a considerable effect on the widths $\langle \Gamma_f \rangle^{2+}$ and $\langle \Gamma_f \rangle^{3+}$. Thus, on the basis of the spin values we have assigned, we have $\langle \Gamma_f \rangle^{2+} = 741.46$ meV and $\langle \Gamma_f \rangle^{3+} = 84.52$ meV. But these values were obtained on the assumption that resonances with $\Gamma > 300$ ~~meV~~^m eV have a spin of 2^+ , the rest one of 3^+ . However, in reality, so strict a separation in the ^{241}Pu nucleus may also not exist, and besides, the generally accepted dependence of the level density on spin may not be fulfilled with absolute accuracy. All these anomalies cause the values obtained for the widths $\langle \Gamma_f \rangle^{2+}$ and $\langle \Gamma_f \rangle^{3+}$ to vary between wide limits. Thus, it is clear that the mean values of the fission widths for states 2^+ and 3^+ are strongly dependent on the assignment of spins to the resonances; therefore the quantities $\langle \Gamma_f \rangle^{2+}$ and $\langle \Gamma_f \rangle^{3+}$ obtained from Table 1.7 may be used only as a first approximation.

Let us consider the details of obtaining the parameters of negative levels. The necessity of introducing such levels follows from the shape of the curve $\sigma(E)$ in the energy range below 0.1 eV. A number of questions must be answered before these levels can be introduced:

- (1) What is the minimum number of negative levels required for a detailed description of the shape of $\sigma(E)$ in the thermal region?
- (2) Where are these levels located on the energy scale, and what is their total width Γ ?
- (3) How are the parameters of these levels calculated?

In the case of ^{241}Pu no outside information about the negative levels was available, and all the calculations were performed on the basis of evaluated experimental data in the thermal region. Initially it was assumed that there was one negative level with $E_r = -0.25$ eV and a total width $\Gamma = 0.30$ eV.

By varying the parameters G and H of this level (both for the total cross-section and for fission) and each time obtaining all the parameters of the first positive level, good agreement was achieved between the shape of the calculated curve $\sigma(E)$ and the corresponding evaluated data in the range above 0.05 eV. In order to correct the shape of the calculated curve in the range 0.01-0.05 eV it was necessary to introduce a second negative resonance with a sharply limited range of action: at 0.05 eV its contribution must be ~ 1 b. To this end, a resonance energy $E_2 = -0.01$ eV, a total width $\Gamma = 0.01$ eV and an interference $H = 0$ were assigned to a given level, and the values of the parameters G_t and G_f were calculated. The introduction of this resonance appreciably improved the agreement of the shapes of curves $\sigma_t(E)$ and $\sigma_f(E)$ with the evaluated data in the range 0.01-0.05 eV. The detailed shape of curves $\sigma_t(E)$ and $\sigma_f(E)$, calculated from the parameters obtained for the region 0.01-1.0 eV, is shown in Figs 2.1-2.11 of Part 1 of the present preprint.

It should be noted that the parameters G_f and H_f obtained on the basis of the detailed shape give sufficiently reliable averaged group fission cross-sections in the energy range 0.215-100 eV, whereas the averaged group total cross-sections calculated from the parameters G_t and H_t are systematically higher than the averaged group total cross-sections of the CNEN-RT/FI(73)15 library [22]. This is probably due to the fact that the experimental values of Kolar and Carraro [3], on which the parameterization was based, are somewhat on the high side because the impurities and background were not properly taken into account. In view of what was said above corrections were applied to the parameters G_t and H_t to reduce the energy dependence of the cross-sections and, accordingly, the averaged group total cross-sections. The parameters G_γ and H_γ were selected in such a way that when the averaged group cross-sections of capture were calculated a closed system of averaged group constants would be obtained, provided that the averaged group cross-sections of scattering were not necessarily very different from σ_p .

The parameters given in Table 1.6 give self-consistent averaged group cross-sections in all energy groups up to 100 eV except for the groups 0.465-1 eV and 1-2.13 eV, where the averaged group total cross-sections and radiative capture cross-sections are found to be higher. This may be due to the fact that the behaviour of the total cross-section in the ranges indicated is determined mainly by the parameters of the first and third resonances, which were obtained from the evaluated data in the thermal region. As a basis for the evaluation, data were taken from Ref. [2], the authors of which had made a correction for impurities of other isotopes, in particular for the resonance of ^{240}Pu at 1.06 eV. However, if this correction is not applied quite correctly, the averaged group total cross-sections and radiative capture cross-sections may be on the high side; this may possibly have occurred in our case. Since these groups do not contain resonances by means of whose parameters the situation could be corrected, the averaged group total cross-sections and the radiative capture cross-sections in these groups were calculated on the basis of the evaluated energy dependence of the cross-sections. The averaged group cross-sections are given in the conclusion.

1.3. Analysis of the resonance parameters obtained

On the basis of the parameters given above the following mean values were obtained in the allowed resonance region:

$$\begin{aligned}\langle D \rangle &= 1.34 \pm 0.10 \text{ eV} \\ \langle \Gamma \rangle &= 403.87 \pm 10.0 \text{ meV} \\ \langle \Gamma_f \rangle &= 352.9 \pm 35.0 \text{ meV} \\ \langle \Gamma_\gamma \rangle &= 43.0 \pm 5.0 \text{ meV}\end{aligned}$$

These mean resonance parameters agree closely with the data from Ref. [9].

The number of levels omitted was analysed both by the method proposed in Ref. [23] and by the least squares method; it was found that two levels were missing, i.e. the total number of levels in the region up to 150 eV is 112 (Fig. 1.1). The error in $\langle D \rangle$, determined according to the formula $\sigma^2 = 0.54 \frac{\langle D \rangle^2}{n}$, where n is the number of resonances, is ~ 0.1 .

Figure 1.2 shows a comparison of a Wigner distribution with a histogram of the distribution of the distances between levels. It can be seen from the diagram that there is a surplus of distances smaller than $\langle D \rangle$, but there are no grounds for speaking of a large number of levels having been omitted.

The errors in $\langle \Gamma \rangle$ and $\langle \Gamma_f \rangle$ were determined from the degree to which the curve $\sigma(E)$, calculated from the parameters, deviated from the corresponding experimental data. The values of the quantities agree on the whole with the data of other authors. The quantity $\langle \Gamma_\gamma \rangle$ was obtained only for physical values of the widths (47 of 110), which explains the large error in $\langle \Gamma_\gamma \rangle$, although the actual value of the quantity is close to that obtained by Kolar et al. [24].

The value of the strength function $S_o = \langle \Gamma_n^o \rangle / 2 \langle D \rangle$ calculated from the parameters given above was found to equal $(1.16 \pm 0.19) \times 10^{-4}$, which agrees well with the data of other authors [6, 9, 25-27].

Owing to the impossibility mentioned earlier of obtaining a self-consistent system of parameters, the data on the distributions $\Gamma_f / \langle \Gamma_f \rangle$, $\Gamma_n^o / \langle \Gamma_n^o \rangle$ and $\Gamma_\gamma / \langle \Gamma_\gamma \rangle$ are not given.

REFERENCES

1. Simpson O.D., Marshall H.H. IDO-16679, 1961 and Simpson O.D., Schumann R.R. Nucl. Sci. Eng., 1961, vol.11, p.111.
2. Craig D.S., Westcott C.H. AECL-1948, 1964 and Can. J. Phys., 1968, vol.42, p.2384.
3. Kolar W., Carraro G. Conf. on Neutron Cross-Sections and Technology, Knoxville, 1971, vol.2, p.707.
4. Pattenden N.T. et al. AERE-PR/NP-7, 1964, p.6 and AERE-PR/NH-6, 1964, p.10, BAPS, 1964, vol.11, p.178.
5. Watanabe T., Simpson O.D. Phys. Rev., B, 1964, vol.133, p.390 and IDO-16995, 1964.
6. James G.D. AERE-R-4597, 1964 and Nucl. Phys., 1965, vol.65, p.353.
7. Moore M.S. et al. Phys. Rev., B, 1964, vol.135, p.945.
8. Simpson O.D. et al. Conf. on Neutron Cross-Sections and Technology, 1966, vol.2, p.910 and IDO-17174, 1966.
9. Blons J. et al. Conf. on Neutron Cross-Sections and Technology, Knoxville, 1971, vol.2, p.836 and Nucl. Sci. Eng., 1973, vol.51, p.130.

10. Migneco E., Theobald J.P., Wastena J.A. IAEA Conf. on Nuclear Data, Helsinki, 1970, vol.1, p.437.
11. Weston L.W., Todd J.H. Nucl. Sci. Eng., 1978, vol.65, p.454.
12. Leonard B.R. HW-62727, 1959, p.19 and Proc. on the Conf. on the Physics of Breeding, 1959, p.227.
13. Sauter G.D., Bowman C.D. Phys. Rev., 1968, vol.174, p.1413.
14. James G.D. IAEA Conf. on Nuclear Data for Reactors, Helsinki, 1970, vol.1, p.267.
15. Hennies H.H. IAEA Conf. on Nuclear Data for Reactors, Paris, 1967, vol.2, p.333.
16. Wagemans C., Deruytter A. Nucl. Sci. Eng., 1976, vol.60, p.44.
17. Carlson G.W., Behrens J.W., Czirr J.B. Nucl. Sci. Eng., 1977, vol.63, p.149.
18. Behrens J.W., Carlson G.W. UCID-16878, 1975 and Proc. of the NEANDC/NEACRP Specialists Meeting on Fast Fission Cross-Section of ^{233}U , ^{235}U , ^{238}U and ^{239}Pu , June 28-30, 1976, p.47.
19. ADAMCHUK, Yu.V. et al., in Peaceful Uses of Atomic Energy (Proc. 1st Conf. Geneva, 1955) Vol. 4, United Nations (1956) 259.
20. ANTISIPOV, G.V. et al., in "Yadernye konstanty" (Nuclear constants) Vol. 20, part 2 (1975) p. 3.
21. Caner M., Yiftah S. IA-1276, 1973.
22. Menapace E., Motta M., Panini G.C. RT/FI(73)15, 1973.
23. KON'SHIN, V.A. et al., in "Yadernye konstanty" (Nuclear constants) Vol. 16 (1974) p. 329.
24. Kolar W., Theobald J.P., Wastena J.A. Conf. on Neutron Cross-Sections and Technology, Knoxville, 1971, vol.2, p.823.
25. Simpson O.D., Schuman R.P. Nucl. Sci. Eng., 1961, vol.11, p.111.
26. James G.D. AERE/MP-6, 1964.
27. Prince A. Proc. of the IAEA Conf. of Nuclear Data for Reactors, Helsinki, 1970, vol.2, p.825.

FIGURES

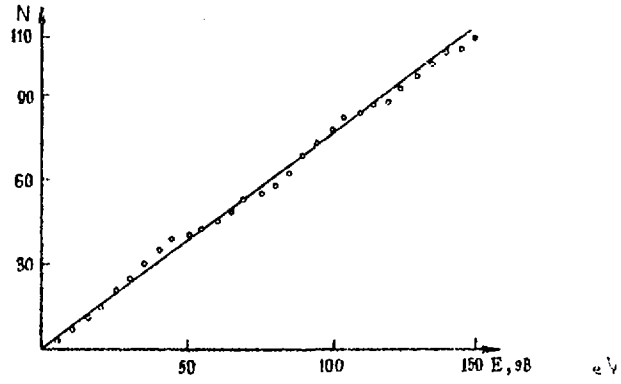


Fig. 1.1. Increasing sum of levels in the allowed resonance energy region (the straight line corresponds to $\langle D \rangle = 1.34$ eV).

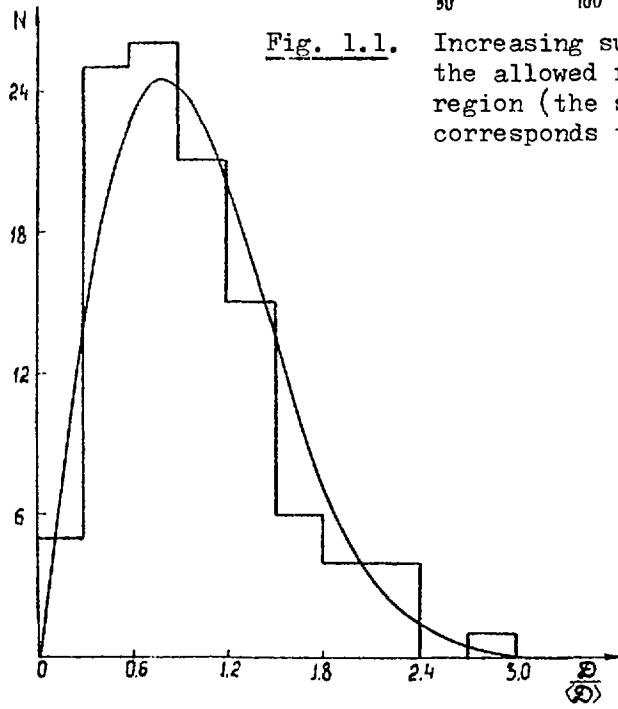


Fig. 1.2. Comparison of a Wigner distribution (smooth curve) with a histogram of the distribution of distances between levels.

TABLES

Table 1.1

Energy resolution in the Experiment of Kolar
and Carraro [3]

Cycle number	Energy range eV	Analyser channel width μ s	Bunch width μ s	Flight distance, m
	0,7 - 4,1	10,24	0,60	100,1
	4,1 - 10,5	2,56	to μ e	to μ e
I	10,5 - 21,0	1,28	"-	"-
	21,0 - 33,5	0,64	"-	"-
	33,5 - 82,0	0,32	"-	"-
	65,0 - 160,0	0,32	0,05	101,25
II	160,0 - 313,0	0,16	to μ e	to μ e
	313,0 - 730,0	0,08	"-	"-

Table 1.2

Energy resolution in the experiment by Blons et al. [9]

Cycle number	Energy range eV	Analyser channel width μ s	Bunch width μ s	Flight distance, m
I	1,6 - 14,0	0,18	0,05	10,69
	14,0 - 3500,0	0,1	to μ e	to μ e
II	11,6 - 18,0	0,4	"-	"-
	18,8 - 53,8	0,2	"-	50,07
	53,8 - 30000,0	0,1	"-	50,07

Table 1.3

Comparison of data on $\sigma_f(^{241}\text{Pu})$ normalized to $\sigma_f = 1015$ b at 2200 m/s
(Table taken from Ref. [17])

Energy region, eV	Carlson et al. [17]	Wagemans et al. [16]	James [6]
8 - 9	239,1 \pm 4,1	231,0	228,7 \pm 8,2
9 - 12	97,7 \pm 1,6	103,4	112,2 \pm 4,0
12 - 20	161,7 \pm 2,6	170,3 \pm 0,9	163,2 \pm 6,5
20 - 30	78,2 \pm 2,1	91,1	-
30 - 44	41,2 \pm 0,9	43,3	-

Table 1.4

Experimental, renormalized and evaluated values of $\sigma_f(^{241}\text{Pu})$ in the energy region 10 eV-30 keV (the renormalization was performed with respect to the fission integral from 12 to 20 eV, equal to 1363 b·eV [16])

Energy region, keV	Migneco et al. [10]		Blons [9]				James [6]				Moore et al. [7]				Wagemans et al. [16]	Carlson et al. [17]	Weston et al. [11]		Weighted mean σ_f^b			
	Experiment	Renormalization (x 1.026)	Experiment	Renormalization (x 1.0091)	Experiment	Renormalization (x 1.021)	Mean of renormalization	Experiment	Correction for $10B(n,\alpha)$	Renormalization (x 0.970)	Experiment	Renormalization (x 0.958)	Experiment	Renormalization (x 1.007)			Mean of both series	Experiment		Renormalization (x 0.968)		
	1	2	3	4	5	6	7	8	9	10	11	12	13	14	15	16	17	18	19	20	21	
0.01-0.02	346,82	150,61±2,00	-	-	145,86	148,94	148,94±6,4	152,74	152,74	149,53±10,0	156,60	150,02	148,0	149,04	149,53±22,0	149,47±1,7	-	151,69	150,14±1,95	147,56±2,07		
0.02-0.03	32,96	25,02±4,5	32,89	33,63	30,10	31,79	32,70±3,5	35,96	35,96	34,15±5,20	36,32	32,69	33,89	33,51	35,10±13,0	34,13±2,0	78,90±2,20	36,21	35,33±2,37	32,76±1,17		
0.03-0.04	46,30	37,70±2,5	46,77	47,19	46,37	47,35	47,26±2,0	46,44	46,44	45,46±3,00	47,23	45,25	50,32	50,67	47,06±7,0	47,43±1,0	-	45,27	45,77±1,81	47,60±1,17		
0.04-0.05	36,94	37,49±2,0	38,52	38,97	39,35	40,18	39,55±1,7	41,80	41,80	40,92±3,00	43,58	47,50	48,90	49,24	48,37±7,0	-	-	43,66	43,23±1,35	41,73±1,10		
0.05-0.06	16,90	17,24±0,9	15,43	15,97	16,45	16,80	16,20±0,7	19,26	19,26	18,06±1,30	-	-	-	-	-	-	-	17,07	17,30±0,57	17,33±0,11		
0.06-0.07	56,35	57,92±3,1	53,15	53,63	54,47	55,61	54,62±2,4	59,79*	-	-	-	-	-	-	-	-	-	58,65	59,07±1,67	57,07±1,17		
0.07-0.09	28,74	29,69±1,6	23,17	23,38	26,46	27,01	25,20±1,2	27,40	29,38	29,76±2,0	-	-	-	-	-	-	-	25,74	25,46±0,74	24,32±0,17		
0.09-0.09	63,55	70,33±1,8	66,24	66,84	64,89	66,25	66,55±2,8	83,67*	-	-	-	-	-	-	-	-	-	73,73	72,07±1,12	70,11±1,10		
0.09-0.10	27,79	28,42±1,5	24,00	24,22	25,71	26,25	25,24±1,2	33,03	32,85	32,20±3,50	-	-	-	-	-	-	-	27,37	26,81±1,78	26,85±1,17		
0.10-0.20	24,98	25,63±1,4	22,98	23,19	-	-	23,20±1,0	27,48	27,31	26,74±2,00	-	-	-	-	-	-	-	24,10±0,90	26,60	26,33±1,76	25,63±1,16	
0.20-0.30	26,09	26,76±1,45	24,71	24,93	27,00	27,57	26,25±1,1	28,93	29,75	28,15±2,00	-	-	-	-	-	-	-	28,90±0,77	28,87	28,52±1,83	27,62±1,17	
0.30-0.40	19,20	19,67±1,0	18,98	19,15	22,00	22,50	20,83±0,9	22,74	21,94	21,48±1,50	-	-	-	-	-	-	-	21,20±0,60	22,37	22,67±1,66	21,27±1,17	
0.40-0.50	14,73	15,16±0,8	17,45	17,61	18,82	19,22	17,42±0,8	20,60	20,39	19,36±1,50	-	-	-	-	-	-	-	18,20±0,85	19,32	19,32±0,85	18,54±1,17	
0.50-0.60	14,36	14,77±0,8	15,09	15,23	16,32	16,66	15,95±0,7	16,58	16,39	16,05±1,20	-	-	-	-	-	-	-	15,50±0,40	17,67	17,47±0,73	17,07±1,17	
0.60-0.70	9,37	10,24±0,6	10,21	10,30	11,24	11,48	10,89±0,5	11,56	11,42	11,18±0,80	-	-	-	-	-	-	-	-	-	12,46	12,74±0,30	12,76±1,17
0.70-0.80	9,55	9,30±0,5	9,64	9,73	10,42	10,64	10,19±0,4	11,02	10,88	10,65±0,70	-	-	-	-	-	-	-	11,00±0,40	11,87	11,71±0,34	11,48±1,17	
0.80-0.90	9,27	9,59±0,45	9,64	9,73	9,31	9,50	9,62±0,4	9,317	9,19	9,00±0,60	-	-	-	-	-	-	-	10,60±0,40	10,54	10,43±0,10	9,87±1,17	

* / High values obtained as a result of neutron scattering by the platinum backing and not used in the evaluation.

** / James's data were renormalized to $\sigma_f^{2200} = 1015$ b (coefficient 1.00495) and then to the fission integral from 12 to 20 eV (coefficient 0.984).

Table 1.4 (continued)

	1	2	3	4	5	6	7	8	9	10	11	12	13	14	15	16	17	18	19	20	21	
0,00-1,00	9,71	9,76±0,5	10,07	10,16	10,75	10,98	10,97±0,5	10,73	10,57	10,35±0,70	-	-	-	-	-	-	-	-	12,48	12,35±0,36	11,03±0,72	
1,0-2,0	7,64	7,84±0,4	8,76	8,94	9,34	8,52	8,67±0,4	9,327	9,16	8,97±0,70	-	-	-	-	-	-	-	8,99±0,25	9,86	9,76±0,43	8,85±0,24	
2,0-3,0	-	-	6,48	6,54	6,03	6,16	6,35±0,3	-	-	-	-	-	-	-	-	-	-	-	7,37	7,30±0,32	6,79±0,29	
3,0-4,0	-	-	6,13	6,19	-	-	6,19±0,3	-	-	-	-	-	-	-	-	-	-	-	6,53	6,46±0,28	6,33±0,27	
4,0-5,0	-	-	5,37	5,42	-	-	5,42±0,3	-	-	-	-	-	-	-	-	-	-	-	5,74	5,69±0,25	5,57±0,25	
5,0-6,0	-	-	4,34	4,38	-	-	4,38±0,2	-	-	-	-	-	-	-	-	-	-	-	5,06	5,01±0,22	4,67±0,20	
6,0-7,0	-	-	4,58	4,62	-	-	4,62±0,2	-	-	-	-	-	-	-	-	-	-	-	4,79	4,74±0,21	4,68±0,19	
7,0-8,0	-	-	4,01	4,05	-	-	4,05±0,2	-	-	-	-	-	-	-	-	-	-	-	4,13	4,09±0,18	4,07±0,18	
8,0-9,0	-	-	4,17	4,21	-	-	4,21±0,2	-	-	-	-	-	-	-	-	-	-	-	4,29	4,25±0,19	4,23±0,18	
9,0-10,0	-	-	3,71	3,74	-	-	3,74±0,2	-	-	-	-	-	-	-	-	-	-	-	3,86	3,82±0,17	3,79±0,17	
10,0-20,0	-	-	3,32	3,35	-	-	3,35±0,2	-	-	-	-	-	-	-	-	-	-	-	3,02±0,08	3,39	3,36±0,15	3,12±0,15
20,0-30,0	-	-	2,95	2,98	-	-	2,98±0,1	-	-	-	-	-	-	-	-	-	-	-	2,62±0,09	2,98	2,95±0,13	2,82±0,11

Table 1.5

Weighted mean data on σ_f , averaged over a smaller energy range in the region 0.1-3 keV

ΔE , keV	σ_f , b	ΔE , keV	σ_f , b
0,10 - 0,12	11,446	0,9 - 1,0	11,030
0,12 - 0,14	26,166	1,0 - 1,1	12,440
0,14 - 0,16	28,183	1,1 - 1,2	10,138
0,16 - 0,18	24,279	1,2 - 1,3	8,532
0,18 - 0,20	35,075	1,3 - 1,4	7,633
0,20 - 0,25	29,813	1,4 - 1,5	9,450
0,25 - 0,30	23,077	1,5 - 1,6	10,060
0,3 - 0,4	21,266	1,6 - 1,7	8,189
0,4 - 0,5	18,044	1,7 - 1,8	8,057
0,5 - 0,6	16,038	1,8 - 1,9	6,997
0,6 - 0,7	11,362	1,9 - 2,0	7,005
0,7 - 0,8	10,837	2,0 - 2,5	6,578
0,8 - 0,9	9,885	2,5 - 3,0	7,010

Table 1.6

Resonance parameters of ^{241}Pu

N	E_r , eV	Γ , eV	G_t	H_t	G_f	H_f	G_T	H_T
1	2	3	4	5	6	7	8	9
1	-0,25000+00	0,300000+00	0,697594-04	0,405487-04	0,465062-06	0,438284-04	0,692897-04	-0,327970-05
2	-0,10000-01	0,100000-01	0,665070-04	0,900000+00	-0,327508-04	0,000000+00	0,992515-04	0,000000+00
3	0,25300+00	0,100000+00	0,446056-03	-0,212141-04	0,232985-03	-0,281416-04	0,152899-03	0,881079-05
4	0,42800+01	0,690000-01	0,212666-02	-0,566759-04	0,109607-02	-0,353060-04	0,105116-02	-0,141659-04
5	0,45700+01	0,164000+00	0,400662-03	-0,536676-04	0,356556-03	-0,477597-04	0,974631-04	-0,766521-05
6	0,60000+01	0,129000+01	0,415135-03	0,186499-04	0,393765-03	0,196527-04	0,151293-04	0,106148-05
7	0,69300+01	0,129000+00	0,966821-03	0,570803-04	0,764107-03	0,606721-04	0,192832-03	0,312771-05
8	0,86200+01	0,950000-01	0,156766-02	-0,777821-04	0,100612-02	-0,329613-04	0,401629-03	-0,157949-04
9	0,95800+01	0,193000+00	0,105861-03	-0,950858-04	0,770485-04	-0,742824-04	0,174192-04	-0,114238-04
10	0,10010+02	0,102300+01	0,263457-03	-0,148508-04	0,262311-03	-0,265541-04	0,136876-04	0,163153-05
11	0,12790+02	0,273000+00	0,308710-03	0,566233-05	0,368590-03	-0,105935-04	0,206575-04	0,460094-05
12	0,13420+02	0,720000-01	0,468125-02	-0,204719-03	0,205930-02	0,102600-04	0,174446-02	-0,725093-04
13	0,14750+02	0,153000+00	0,458754-02	-0,339520-04	0,410443-02	0,238651-03	0,805169-03	-0,717039-04
14	0,16020+02	0,555000+00	0,299844-03	-0,567539-04	0,368232-03	-0,303538-04	0,207891-04	-0,116875-04
15	0,16670+02	0,225000+00	0,608705-03	-0,315047-04	0,596208-03	-0,146600-04	0,760788-04	-0,703958-05
16	0,17840+02	0,570000-01	0,567290-02	-0,155255-03	0,172503-02	0,198093-03	0,239791-02	-0,102819-03
17	0,18240+02	0,640000-01	0,391154-03	0,770063-04	0,516309-04	0,651861-05	0,205335-03	0,245235-04
18	0,20710+02	0,168000+00	0,355732-03	-0,283701-04	0,196537-03	-0,206852-04	0,686727-04	-0,305493-05
19	0,21930+02	0,104090+00	0,216163-03	0,133869-04	0,456659-04	0,700644-06	0,618606-04	0,340678-05
20	0,23000+02	0,342465+00	0,324250-03	-0,131971-04	0,287723-03	-0,192203-04	0,376927-04	0,118801-05
21	0,23690+02	0,457600+00	0,140803-03	0,452040-05	0,385221-04	0,148336-04	0,128321-04	-0,243118-05
22	0,24080+02	0,153641+00	0,987626-03	-0,170343-04	0,570872-03	-0,833598-04	0,163099-03	0,158996-04
23	0,24610+02	0,760000+00	0,861785-05	0,760286-05	0,326748-04	-0,125914-04	0,230390-06	0,512194-05
24	0,26420+02	0,313512+00	0,131725-02	-0,399133-04	0,114516-02	-0,483156-04	0,154697-03	0,118496-05
25	0,27620+02	0,135000+01	0,464298-07	0,371439-07	0,275117-05	0,220094-05	0,892633-09	-0,530103-06
26	0,28880+02	0,592827+00	0,650822-03	-0,264362-04	0,621282-03	-0,263698-04	0,457830-04	-0,526928-06
27	0,29420+02	0,234000+00	0,336821-03	0,160917-04	0,277900-03	0,373576-04	0,368618-04	-0,486447-05
28	0,31030+02	0,344898+00	0,645099-03	-0,265853-04	0,616875-03	-0,293946-04	0,784965-04	-0,434579-06
29	0,33300+02	0,220500+00	0,683615-04	-0,110037-04	0,780121-04	-0,120031-04	0,837482-06	-0,221090-06
30	0,33780+02	0,138000+00	0,171119-03	-0,266759-04	0,126406-03	-0,803068-05	0,317220-04	-0,584306-05
31	0,34900+02	0,224000+01	0,123141-03	-0,259903-03	0,122582-03	0,518783-05	0,252981-05	-0,897307-05

Table 1.6 (continued)

1	2	3	4	5	6	7	8	9
32	0,35000+02	0,880000-01	0,383786-03	-0,387254-04	0,120835-03	-0,675272-06	0,140846-03	-0,112490-04
33	0,36170+02	0,760000-01	0,125304-03	0,361438-04	0,670367-07	0,536293-07	0,541733-04	0,106444-04
34	0,37500+02	0,857000+00	0,302149-06	-0,241719-06	0,344030-05	0,275224-05	0,998040-08	-0,764593-06
35	0,38140+02	0,155000+00	0,370503-03	0,582621-06	0,131216-03	0,479809-05	0,785401-04	-0,103688-05
36	0,39350+02	0,310500+00	0,389248-03	-0,952660-04	0,386107-03	0,879485-05	0,399509-04	-0,303069-04
37	0,39890+02	0,153000+00	0,780895-03	-0,776546-04	0,472072-03	0,460554-04	0,167700-03	-0,345003-04
38	0,40900+02	0,140880+01	0,178205-03	-0,797641-05	0,135260-03	-0,382795-05	0,636405-05	-0,157985-05
39	0,42750+02	0,283755+00	0,127032-03	-0,476154-05	0,689429-04	0,155725-04	0,162021-04	-0,557358-05
40	0,43450+02	0,500000-01	0,533186-03	0,899279-04	0,158707-03	0,459445-04	0,222054-03	0,151538-04
41	0,46570+02	0,295000+00	0,358240-03	-0,483253-04	0,341819-03	0,314215-04	0,301262-04	-0,230486-04
42	0,48100+02	0,530612+00	0,873078-03	-0,419852-04	0,736174-03	0,504908-04	0,780657-04	-0,261860-04
43	0,50350+02	0,777000+00	0,136727-03	-0,346765-04	0,624516-04	0,448871-05	0,941827-05	-0,135978-04
44	0,52240+02	0,160000+00	0,147431-03	0,185744-04	0,823945-05	-0,467606-05	0,352270-04	0,814454-05
45	0,53370+02	0,593000+00	0,730558-04	0,108922-04	0,127782-03	-0,954177-05	0,405773-05	0,735182-05
46	0,55270+02	0,102000+01	0,228860-03	-0,102905-03	0,201957-03	0,476668-05	0,393682-05	-0,371117-04
47	0,60510+02	0,200000+00	0,144018-02	-0,014081-04	0,039703-03	0,186163-03	0,285244-03	-0,895157-04
48	0,62250+02	0,540816+00	0,604089-03	-0,429822-04	0,421426-03	0,649590-04	0,619457-04	-0,351756-04
49	0,63000+02	0,193500+01	0,157370-03	0,414296-04	0,434356-04	-0,227140-04	0,451022-05	0,216851-04
50	0,64540+02	0,620000-01	0,176581-03	0,114814-03	0,500856-04	-0,063597-05	0,762885-04	0,437785-04
51	0,65730+02	0,324000+00	0,107470-02	-0,126331-04	0,860669-03	-0,250456-05	0,187407-03	-0,372405-05
52	0,66620+02	0,173000+00	0,219040-02	0,198696-03	0,697449-03	-0,453000-04	0,501549-03	0,845133-04
53	0,67360+02	0,149000+00	0,110194-08	0,881557-09	0,593636-04	-0,444474-05	0,180284-09	0,136167-05
54	0,68270+02	0,526000-01	0,027418-03	0,592216-04	0,544659-03	0,630206-04	0,271811-03	0,175084-05
55	0,68240+02	0,464000-01	0,115115-02	-0,103483-03	0,431987-03	0,154439-04	0,461404-03	-0,415186-04
56	0,72250+02	0,267283+00	0,271533-03	0,263030-04	0,287638-03	-0,630607-05	0,392897-04	0,105827-04
57	0,73910+02	0,210000-01	0,105900-02	0,398753-03	0,449344-03	-0,277304-05	0,441696-03	0,138041-03
58	0,75860+02	0,608000-01	0,351468-02	-0,785852-04	0,257683-02	0,208327-03	0,950551-03	-0,752301-04
59	0,77140+02	0,534577-01	0,414762-02	0,875681-04	0,713501-03	-0,551794-04	0,191964-02	0,430933-04
60	0,77700+02	0,255000+01	0,102237-06	0,817303-07	0,628103-04	-0,205920-04	0,133658-08	0,476841-05
61	0,80210+02	0,640000-01	0,376566-02	-0,229117-03	0,221819-02	0,511228-04	0,105607-02	-0,921839-04
62	0,81460+02	0,126000+00	0,223918-02	0,195831-03	0,161543-02	0,764103-04	0,526415-03	0,466195-04
63	0,82070+02	0,100000+01	0,155886-03	-0,768293-04	0,271177-03	-0,689008-04	0,513302-05	-0,795910-05
64	0,83190+02	0,116000+00	0,258576-02	0,506206-04	0,132970-02	0,621071-04	0,843037-03	0,807274-06
65	0,85420+02	0,290000+00	0,190475-02	0,131251-03	0,832600-03	0,795882-04	0,191049-03	0,237636-04
66	0,85700+02	0,300000+00	0,438872-03	0,209114-03	0,519202-03	0,632703-04	0,184953-04	0,546249-04

Table 1.6 (continued)

1	2	3	4	5	6	7	8	9
67	0,86200+02	0,480000+00	0,103808-07	-0,830466-08	0,551009-04	-0,106210-04	0,711759-09	0,283033-05
68	0,87010+02	0,104163+00	0,328886-02	-0,440902-04	0,185348-02	0,135614-04	0,971955-03	-0,187327-04
69	0,87950+02	0,390000+00	0,278078-03	0,198785-04	0,288773-03	-0,720652-04	0,381326-04	0,260383-04
70	0,89200+02	0,800000+00	0,114401-03	-0,621064-04	0,186781-03	-0,190443-04	0,470632-05	-0,162389-04
71	0,90680+02	0,125000+00	0,625101-03	0,244183-03	0,357181-03	-0,880648-05	0,219547-03	0,985500-04
72	0,91350+02	0,480000+00	0,198511-09	0,158889-09	0,469357-04	-0,108555-04	0,363962-10	0,671558-05
73	0,91810+02	0,120000+00	0,413923-10	0,331138-10	0,540551-04	0,108021-04	0,216722-10	-0,668243-05
74	0,93880+02	0,296000+00	0,292053-04	0,772460-05	0,813586-04	0,496496-05	0,619920-05	0,406822-05
75	0,95360+02	0,142500+00	0,578667-04	0,462933-04	0,183910-03	-0,154933-04	0,255141-04	0,520016-04
76	0,96100+02	0,553528+00	0,632637-04	-0,200055-04	0,100982-03	-0,514288-05	0,100533-04	-0,151489-04
77	0,97500+02	0,593265+00	0,121181-06	-0,969449-07	0,111495-03	0,197803-04	0,179673-07	-0,123255-04
78	0,98370+02	0,194000+00	0,159836-02	-0,190166-03	0,150077-02	-0,203195-05	0,891638-03	-0,163823-03
79	0,99780+02	0,350000+00	0,331036-03	0,391633-04	0,289171-03	0,346001-04	0,135193-03	0,144796-04
80	0,10070+03	0,760000+00	0,214231-04	-0,171433-04	0,473687-04	-0,169287-04	0,321446-05	-0,786200-06
81	0,10152+03	0,142563+00	0,522765-03	0,342854-04	0,195972-03	0,539064-05	0,485225-03	0,344736-04
82	0,10240+03	0,452000+00	0,873348-04	-0,345141-04	0,740062-04	-0,126359-04	0,357948-04	-0,263778-04
83	0,10363+03	0,231000+00	0,369991-03	-0,448086-04	0,133231-03	-0,618362-05	0,211946-03	-0,160627-04
84	0,10754+03	0,143000+00	0,942809-04	-0,878585-04	0,561740-06	-0,449392-06	0,872431-04	-0,103815-03
85	0,10799+03	0,840000-01	0,752000-03	-0,122734-03	0,306008-03	-0,317958-04	0,900053-03	-0,108990-03
86	0,10917+03	0,470000+00	0,227149-03	0,141981-04	0,154513-03	-0,434876-05	0,898334-04	0,218886-04
87	0,11050+03	0,800000+00	0,233145-09	0,186517-09	0,387037-05	-0,309630-05	0,411476-10	0,260682-05
88	0,11324+03	0,400000-01	0,418356-03	-0,803893-04	0,301630-03	0,120910-04	0,607659-03	-0,128411-03
89	0,11540+03	0,240000+01	0,186045-06	-0,148835-06	0,376681-04	-0,301345-04	0,109450-07	0,251492-04
90	0,11725+03	0,360000+00	0,349932-03	-0,626411-04	0,469894-03	-0,364366-04	0,223020-03	-0,614557-04
91	0,12033+03	0,600000+00	0,752504-04	0,415883-04	0,732366-04	0,792839-05	0,247516-04	0,457405-04
92	0,12225+03	0,480000+00	0,548244-03	-0,131842-03	0,674020-03	-0,188378-04	0,225454-03	-0,150464-03
93	0,12338+03	0,947143-01	0,145608-02	0,856304-04	0,677111-03	0,158011-04	0,204033-02	0,945470-04
94	0,12408+03	0,459184+00	0,305507-05	0,244405-05	0,533105-04	0,167586-04	0,808030-06	-0,114343-04
95	0,12534+03	0,790000+00	0,211073-04	0,169359-04	0,199714-04	0,424974-05	0,595087-05	0,176785-04
96	0,12613+03	0,120000+00	0,844094-05	0,675264-05	0,626516-04	0,165352-04	0,610194-05	-0,578291-05
97	0,12793+03	0,705539+00	0,120225-06	-0,961901-07	0,116398-03	0,126104-04	0,206950-07	-0,110522-04
98	0,12858+03	0,450000-01	0,387588-02	-0,407464-03	0,203131-02	0,173376-03	0,458612-02	-0,670093-03
99	0,13008+03	0,585000+00	0,415500-08	-0,332401-08	0,204632-03	0,234198-04	0,674631-09	-0,209182-04
100	0,13080+03	0,480000-01	0,102250-01	-0,103243-02	0,371728-02	0,292249-03	0,820913-02	-0,128249-02

Table 1.6 (continued)

I	2	3	4	5	6	7	8	9
I01	0,13308+03	0,960000+00	0,405081-06	-0,324065-06	0,167991-03	0,120595-04	0,400791-07	-0,110303-04
I02	0,13374+03	0,661216-01	0,413667-02	-0,339313-03	0,140233-02	0,441613-04	0,430019-02	-0,375656-03
I03	0,13473+03	0,134935+01	0,926765-04	0,102829-04	0,740172-04	0,267072-04	0,106010-04	-0,136766-04
I04	0,13665+03	0,100000-01	0,447237-02	0,375030-03	0,131038-02	0,255192-03	0,491605-02	0,143163-03
I05	0,13838+03	0,301202+00	0,575755-03	-0,435516-04	0,390160-03	0,355176-04	0,295042-03	-0,748125-04
I06	0,14025+03	0,817160-01	0,312373-02	0,130135-03	0,153354-02	0,105617-03	0,238644-02	0,245190-04
I07	0,14133+03	0,307171+00	0,330666-03	-0,264533-03	0,624947-04	0,624765-05	0,103343-03	-0,685030-05
I08	0,14220+03	0,134773+00	0,458922-02	-0,356285-03	0,203241-02	0,113705-03	0,364611-02	-0,469990-03
I09	0,14514+03	0,885131-01	0,110193-03	-0,831513-04	0,267331-03	0,260932-04	0,953669-04	-0,114248-03
I10	0,14620+03	0,189763+00	0,160915-02	-0,671141-04	0,330844-03	0,247444-04	0,244891-03	-0,918585-04
I11	0,14700+03	0,240000+00	0,217067-05	-0,173651-05	0,774596-04	0,111541-04	0,620191-06	-0,129906-04
I12	0,14892+03	0,704673-01	0,122815-02	-0,200724-04	0,642199-03	0,520913-04	0,950391-03	-0,721637-04

Table 1.7

Breit-Wigner parameters obtained from the data of Table 1.6

N	E_r , eV	Γ , eV	Γ_n , eV	Γ_f , eV	Γ_s , eV	J
	2	3	4	5	5	7
3	0,25900+00	0,100000+00	0,389787-04	0,656895-01	0,242762-01	3
4	0,42300+01	0,690000-01	0,652455-03	0,285432-01	0,327178-01	3
5	0,45700+01	0,164000+00	0,304676-03	0,117142+00	0,465522-01	3
6	0,60000+01	0,123000+01	0,402761-02	0,122097+01	0,650000-01 ¹⁾	2
7	0,67300+01	0,123000+00	0,720052-03	0,734722-01	0,438017-01	3
8	0,96200+01	0,250000-01	0,958955-03	0,469311-01	0,471100-01	3
9	0,95800+01	0,193000+00	0,138688-03	0,127861+00	0,650000-01 ¹⁾	3
10	0,10010+02	0,102300+01	0,255969-02	0,955440+00	0,650000-01 ¹⁾	2
11	0,12730+02	0,273000+00	0,646252-03	0,241076+00	0,312775-01	3
12	0,12420+02	0,720000-01	0,264745-02	0,234142-01	0,453353-01	3
13	0,14750+02	0,153000+00	0,577925-02	0,101243+00	0,459771-01	3
14	0,16020+02	0,555000+00	0,199275-02	0,505790+00	0,472172-01	2
15	0,16670+02	0,225000+00	0,119899-02	0,162925+00	0,609062-01	3
16	0,17340+02	0,570000-01	0,292843-02	0,128124-01	0,412522-01	3
17	0,18240+02	0,640000-01	0,229243-03	0,624803-02	0,575227-01	3
18	0,20710+02	0,168000+00	0,524629-03	0,102405+00	0,650000-01 ¹⁾	3
19	0,21330+02	0,104030+00	0,211595-03	0,388784-01	0,650000-01 ¹⁾	3
20	0,23000+02	0,342465+00	0,149721-02	0,278918+00	0,627433-01	2
21	0,23680+02	0,457600+00	0,881483-03	0,391719+00	0,650000-01 ¹⁾	2
22	0,24080+02	0,153641+00	0,134388-02	0,906946-01	0,616026-01	3
23	0,24610+02	0,360000+00	0,115385-03	0,919895+00	0,400000-01 ²⁾	2
24	0,26420+02	0,313512+00	0,596781-02	0,250158+00	0,573364-01	2
25	0,27620+02	0,135000+01	0,926118-06	0,131000+01	0,400000-01 ²⁾	2
26	0,28850+02	0,592927+00	0,582224-02	0,521998+00	0,650000-01 ¹⁾	2
27	0,29420+02	0,234000+00	0,858482-03	0,177261+00	0,558510-01	3
28	0,31030+02	0,344898+00	0,384346-02	0,281753+00	0,593020-01	2
29	0,33300+02	0,220500+00	0,192677-03	0,214963+00	0,534383-02	3
30	0,33780+02	0,138000+00	0,304013-03	0,870874-01	0,506085-01	3
31	0,34900+02	0,224000+01	0,505333-02	0,216995+01	0,650000-01 ¹⁾	2
32	0,35000+02	0,890000-01	0,442580-03	0,236699-01	0,638976-01	3
33	0,26170+02	0,760000-01	0,126864-03	0,108731-01	0,650000-01 ¹⁾	3
34	0,37500+02	0,957000+00	0,491736-05	0,916995+00	0,400000-01 ²⁾	2
35	0,38140+02	0,155000+00	0,785596-03	0,892144-01	0,650000-01 ¹⁾	3
36	0,39350+02	0,310500+00	0,235112-02	0,263118+00	0,450312-01	2
37	0,39890+02	0,153000+00	0,167148-02	0,863285-01	0,650000-01 ¹⁾	3
38	0,40900+02	0,140880+01	0,472908-02	0,133907+01	0,650000-01 ¹⁾	2
39	0,42750+02	0,283755+00	0,499354-03	0,218256+00	0,650000-01 ¹⁾	3
40	0,43450+02	0,500000-01	0,369711-03	0,119663-01	0,376640-01	3
41	0,46570+02	0,295000+00	0,143084-02	0,245937+00	0,475826-01	3
42	0,49100+02	0,530612+00	0,892424-02	0,456688+00	0,650000-01 ¹⁾	2
43	0,50350+02	0,777000+00	0,201856-02	0,702281+00	0,650000-01 ¹⁾	2

Table 1.7 (continued)

1	2	3	4	5	6	7
44	0,52240+02	0,160000+00	0,326095-03	0,946739-01	0,650000-01 ¹⁾	3
45	0,59370+02	0,593000+00	0,986275-03	0,552114+00	0,400000-01 ²⁾	2
46	0,53270+02	0,102000+01	0,481230-02	0,993879+00	0,213086-01	2
47	0,60510+02	0,200000+00	0,444038-02	0,130560+00	0,650000-01 ¹⁾	3
48	0,62250+02	0,540816+00	0,715172-02	0,468664+00	0,650000-01 ¹⁾	2
49	0,63000+02	0,193500+01	0,670594-02	0,186329+01	0,650000-01 ¹⁾	2
50	0,64540+02	0,620000-01	0,174309-03	0,178736-01	0,439521-01	3
51	0,65730+02	0,324000+00	0,777982-02	0,251020+00	0,650000-01 ¹⁾	2
52	0,66620+02	0,173000+00	0,612966-02	0,101870+00	0,650000-01 ¹⁾	3
53	0,67360+02	0,149000+00	0,267062-08	0,109000+00	0,400000-01 ²⁾	3
54	0,68270+02	0,526000-01	0,907057-03	0,300918-01	0,286011-01	3
55	0,69240+02	0,464000-01	0,870831-03	0,150018-01	0,305173-01	3
56	0,72250+02	0,267289+00	0,119368-02	0,201095+00	0,650000-01 ¹⁾	3
57	0,73910+02	0,210000-01	0,369740-03	0,590941-02	0,147207-01	3
58	0,75960+02	0,609900-01	0,360131-02	0,295648-01	0,276359-01	3
59	0,77140+02	0,534577-01	0,376803-02	0,310755-02	0,415821-01	3
60	0,77700+02	0,255000+01	0,622827-05	0,250999+01	0,400000-01 ²⁾	2
61	0,80210+02	0,640000-01	0,412507-02	0,293343-01	0,305406-01	3
62	0,81460+02	0,126000+00	0,486663-02	0,707304-01	0,504030-01	3
63	0,82070+02	0,100000+01	0,378049-02	0,956220+00	0,400000-01 ²⁾	2
64	0,83190+02	0,116000+00	0,522949-02	0,464189-01	0,643526-01	3
65	0,85420+02	0,200000+00	0,355021-02	0,131450+00	0,650000-01 ¹⁾	3
66	0,95700+02	0,300000+00	0,232941-02	0,276158+00	0,215125-01	3
67	0,96200+02	0,480000+00	0,123780-06	0,440000+00	0,400000-01 ¹⁾	2
68	0,97010+02	0,104163+00	0,610717-02	0,456764-01	0,523794-01	3
69	0,97950+02	0,390000+00	0,272127-02	0,322279+00	0,650000-01 ¹⁾	2
70	0,99200+02	0,900000+00	0,231274-02	0,757687+00	0,400000-01 ²⁾	2
71	0,99680+02	0,125000+00	0,167430-02	0,593697-01	0,650000-01 ¹⁾	3
72	0,91350+02	0,480000+00	0,280185-08	0,440000+00	0,400000-01 ²⁾	2
73	0,91810+02	0,120000+00	0,104535-09	0,800000-01	0,400000-01 ²⁾	3
74	0,93880+02	0,296000+00	0,183774-03	0,255816+00	0,400000-01 ²⁾	3
75	0,95360+02	0,142500+00	0,176366-03	0,102323+00	0,400000-01 ²⁾	3
76	0,96100+02	0,553528+00	0,105560-02	0,512472+00	0,400000-01 ²⁾	2
77	0,97500+02	0,593265+00	0,218290-05	0,553263+00	0,400000-01 ²⁾	2
78	0,98370+02	0,174000+00	0,675499-02	0,122983+00	0,642621-01	3
79	0,99780+02	0,350000+00	0,355885-02	0,281441+00	0,650000-01 ¹⁾	2
80	0,10070+03	0,760000+00	0,465790-03	0,719534+00	0,400000-01 ²⁾	3
81	0,10152+03	0,142563+00	0,152869-02	0,760343-01	0,650000-01 ¹⁾	2
82	0,10240+03	0,452000+00	0,113850-02	0,385862+00	0,650000-01 ¹⁾	2
83	0,10363+03	0,231000+00	0,177124-02	0,164220+00	0,650000-01 ¹⁾	3
84	0,10754+03	0,143000+00	0,284626-03	0,777154-01	0,650000-01 ¹⁾	3
85	0,10799+03	0,840000-01	0,133634-02	0,332781-01	0,493856-01	3
86	0,10917+03	0,470000+00	0,317921-02	0,401821+00	0,650000-01 ¹⁾	2
87	0,11050+03	0,900000+00	0,622064-08	0,760000+00	0,400000-01 ²⁾	2

Table 1.7 (continued)

1	2	3	4	5	6	7
88	0,11324+03	0,400000-01	0,449979-03	0,165072-01	0,230438-01	3
89	0,11540+03	0,240000+01	0,169309-04	0,235978+01	0,400000-01 ²⁾	2
90	0,11725+03	0,360000+00	0,481495-02	0,290185+00	0,650000-01 ¹⁾	2
91	0,12033+03	0,600000+00	0,150376-02	0,537496+00	0,650000-01 ¹⁾	2
92	0,12225+03	0,480000+00	0,893591-02	0,406164+00	0,650000-01 ¹⁾	2
93	0,12333+03	0,747143-01	0,332221-02	0,301775-01	0,613145-01	3
94	0,12408+03	0,459184+00	0,474451-04	0,419137+00	0,400000-01 ²⁾	2
95	0,12534+03	0,700000+00	0,502236-03	0,634498+00	0,650000-01 ¹⁾	2
96	0,12613+03	0,120000+00	0,246706-04	0,799753-01	0,400000-01 ²⁾	3
97	0,12773+03	0,705539+00	0,291295-05	0,665536+00	0,400000-01 ²⁾	2
98	0,12858+03	0,450000-01	0,423917-02	0,161590-01	0,245518-01	3
99	0,13003+03	0,595000+00	0,658299-07	0,545000+00	0,400000-01 ²⁾	2
100	0,13080+03	0,480000-01	0,752076-02	0,157590-01	0,227202-01	3
101	0,13308+03	0,960000+00	0,106527-04	0,919989+00	0,400000-01 ²⁾	2
102	0,13374+03	0,661216-01	0,536522-02	0,202313-01	0,405245-01	3
103	0,13473+03	0,134935+01	0,344680-02	0,128090+01	0,650000-01 ¹⁾	2
104	0,13665+03	0,100000-01	0,889045-03	0,264073-02	0,647122-02	3
105	0,13838+03	0,301202+00	0,484421-02	0,231358+00	0,650000-01 ¹⁾	2
106	0,14025+03	0,817160-01	0,518221-02	0,401170-01	0,364168-01	3
107	0,14133+03	0,307171+00	0,289800-07	0,267171+00	0,400000-01 ²⁾	2
108	0,14220+03	0,134773+00	0,126458-01	0,596764-01	0,624503-01	3
109	0,14514+03	0,895171-01	0,201437-03	0,483117-01	0,400000-01 ²⁾	3
110	0,14620+03	0,199763+00	0,632944-02	0,118434+00	0,650000-01 ¹⁾	3
111	0,14700+03	0,240000+00	0,108280-04	0,199989+00	0,400000-01 ²⁾	3
112	0,14892+03	0,704673-01	0,181050-02	0,368473-01	0,318095-01	3

1/ For resonances at which Γ_Y is greater than 0.065 eV the value $\Gamma_Y = 0.065$ eV was taken.

2/ For resonances at which G_f is greater than G_t the value $\Gamma_Y = 0.040$ eV was taken.

UDK 539.173.4

ABSTRACT

NUCLEAR CONSTANTS, TOTAL CROSS-SECTION, FISSION CROSS-SECTION,
SCATTERING CROSS-SECTION, RESONANCE PARAMETERS

The available experimental data on the cross-sections of ^{241}Pu in the region 1-150 eV are reviewed. The cross-sections are parameterized and the mean resonance parameters obtained.

Tables: 7; Figures: 2; References: 27.

V.A. Kon'shin, G.V. Antsipov, E.Sh. Sukhovitskij, L.A. Bakhanovich,
A.B. Klepatskij, G.B. Morogovskij, Yu.V. Porodzinskij

EVALUATION OF NUCLEAR DATA FOR ^{241}Pu IN THE NEUTRON ENERGY REGION 10^{-3} eV-15 MeV

Part 3

Cross-Section Evaluations in the
0.1 - 100 keV Energy Region

ABSTRACT

The paper describes a method of calculating average cross-sections and average widths of fissionable nuclei processes in the region of unresolved resonances. Calculations are performed of all types of average cross-sections and widths for ^{241}Pu in the 0.1-100 keV region, and the evaluated cross-sections are given for the calculation of group constants.

79-7974
Translated from Russian

A.V. Lykov Institute of Heat and Mass Transfer,
Academy of Sciences of the Byelorussian SSR

EVALUATION OF NUCLEAR DATA FOR ^{241}Pu IN THE
NEUTRON ENERGY REGION FROM 10^{-3} TO 15 MeV

V.A. Kon'shin, G.V. Antsipov, E.Sh. Sukhovitskij,
L.A. Bakhanovich, A.B. Klepatskij,
G.B. Morogovskij and Yu.V. Porodzinskij

Preprint No. 4, Part 3

Minsk 1979

1. ^{241}Pu NUCLEAR DATA IN THE REGION OF UNRESOLVED RESONANCES

1.1. Introduction

The region of unresolved resonances of ^{241}Pu extends from 0.1 to 100 keV. As has been shown in the case ^{235}U [1], we can confine ourselves here to consideration of the contribution merely of s- and p-waves not only to the total interaction cross-section $\langle \sigma_t \rangle$ but also to the partial cross-sections. Because of the presence of excitation levels in this region it is necessary to take into account the neutron inelastic scattering reaction. Unlike the fissionable ^{235}U [1] and ^{239}Pu [2] nuclei considered earlier, in the case of ^{241}Pu there is much less experimental information on cross-sections in the region of unresolved resonances. For example, above 2 keV there are no data on σ_t . There are considerable discrepancies in the available data on σ_t in the region below 2 keV. This leads to complications in allowing for structure in cross-sections and in obtaining average p-wave parameters.

1.2. Calculation of average cross-sections

In order to obtain the expressions for the average cross-sections $\langle \sigma_{nx} \rangle$ we have to average $\sigma_{nx}(E)$ over the interval ΔE containing a sufficiently large number of resonances:

$$\langle \sigma_{nx} \rangle = \frac{1}{\Delta E} \int_{\Delta E} \sigma_{nx}(E) dE. \quad (1.1)$$

Assuming that $\sigma_{nx}(E)$ is described by the Breit-Wigner formula and taking into account the presence of potential scattering and its interference with resonance scattering, we obtain the following expressions:

$$\langle \sigma_f(x) \rangle = \frac{2\pi^2}{k^2} \sum_l \frac{g_f^2}{\langle D \rangle_l} \left\langle \frac{\Gamma_{nx} \Gamma_f(l)}{\Gamma_r} \right\rangle; \quad (1.2)$$

$$\langle \sigma_n \rangle = \sum_l \left[\frac{4\pi}{k^2} (2l+1) \sin^2 \psi_l (1 - \pi S_l E^{1/2} P_l) \right] + \frac{2\pi^2}{k^2} \sum_l \frac{g_f^2}{\langle D \rangle_l} \left\langle \frac{\Gamma_{nx}^2}{\Gamma_r} \right\rangle; \quad (1.3)$$

$$\langle \sigma_e \rangle = \sum_l \left[\frac{4\pi}{k^2} (2l+1) \sin^2 \psi_l + \frac{2\pi^2}{k^2} (2l+1) E^{1/2} S_l P_l \cos^2 \psi_l \right]. \quad (1.4)$$

Here, K is the neutron wave number:

$$K = 2,196771 \cdot 10^{-3} \left(\frac{AW}{A+1} \right) E^{1/2}; \quad (1.5)$$

where AW is the isotopic mass of the target nucleus equal to 238.986 for ^{241}Pu ; φ_ℓ is phase shift determined, in the case of the first two partial waves, by:

$$\varphi_0 = KR; \quad \varphi_1 = KR - \arctg(KR). \quad (1.6)$$

Here R is the scattering radius, which can be calculated from the potential scattering cross-section σ_p in the low-energy region where:

$$\sigma_p = 4\pi R^2. \quad (1.7)$$

The quantity g_j in (1.2) and (1.3) is a statistical factor, S_ℓ is the strength function, P_ℓ is barrier penetration.

$$P_0 = 1; \quad P_1 = (ka)^2 / [1 + (ka)^2], \quad (1.8)$$

where a is the radius of the scattering channel equal to the sum of the radii of the nucleus and the neutron:

$$a = r_0 A^{1/3} + 0,08 \text{ (} 10^{-12} \text{ cm)} \quad (1.9)$$

In the present work we used the value $r_0 = 0.123 \times 10^{-12}$ cm. The obtained value of a = 0.845439 $\times 10^{-12}$ cm.

In order to calculate the average values of $\langle \frac{\Gamma_{nr} \Gamma_{kr}}{\Gamma_r} \rangle$, we used the method described in Ref. [2], according to which

$$\left\langle \frac{\Gamma_{nr} \Gamma_{kr}}{\Gamma_r} \right\rangle = \frac{\langle \Gamma_n \rangle \langle \Gamma_r \rangle}{I_2 K_1 M_1} \sum_{l=1}^L \sum_{k=1}^K \sum_{m=1}^M \frac{f_{n,2,l} f_{r,2,l} \langle \Gamma_n \rangle \langle \Gamma_r \rangle}{f_{n,2,l} \langle \Gamma_n \rangle + f_{r,2,l} \langle \Gamma_r \rangle + f_{n,2,m} \langle \Gamma_n \rangle} \quad (1.10)$$

where I_r , K_r , M_r are the numbers of intervals for representation of the distributions of neutron, fission and inelastic widths, respectively; $f_{n,r,i}$, $f_{f,r,k}$, $f_{n',r,m}$ are the middle points of intervals ΔZ_i of integration over the corresponding parts of the distributions which are so chosen that when we substitute

$$\sum_{i=1}^N \int_{z_{i-1}}^{z_i} f P(f) df = \sum_{i=1}^N f_i \int_{z_{i-1}}^{z_i} P(f) df \quad (1.11)$$

the average value \bar{f} does not change:

$$\bar{f} = \frac{1}{N} \sum_{i=1}^N f_i. \quad (1.12)$$

The intervals ΔZ_i are chosen from the condition

$$\int_{z_{i-1}}^{z_i} P(f) df = \frac{1}{N}. \quad (1.13)$$

In the present work it was assumed that all the partial widths were governed by the χ^2 - distributions with different numbers of degrees of freedom. In order to represent the distributions, we used ten intervals for the number of degrees of freedom equal to 1 and 2 and 5 intervals for the number of degrees of freedom equal to 3 (channel 3 is for fission).

1.3. Average distance $\langle D \rangle_J$ between the levels of the compound nucleus

Because of the small amount of data on ^{241}Pu resonance spins in the region of low energies it is not possible to evaluate $\langle D \rangle_J$ for the s-wave by direct averaging. For example, in Ref. [3], out of 122 levels in the region up to 160 eV, spins are assigned to only 22 resonances. The separation of resonances according to spins, as performed in the present work, can apparently also not be regarded as sufficiently reliable although on the whole it reflects the true picture. Here we can obtain only $\langle D \rangle_{\text{obs.}}$, the average observed distance for two systems of resonances with $J = 2$ and 3. However, in order to obtain the spin dependence, we have to make use of theoretical concepts about the level density function of the nucleus.

A number of authors have obtained $\langle D \rangle_{\text{obs.}}$. From data in the region below 20 eV, where missing levels have not yet been observed, James [4] obtained the value of 1.3 ± 0.2 eV. Later, from the data in Ref. [6] for 43 resonances in the region up to 50.4 eV, Hennies [5] obtained $\langle D \rangle_{\text{obs.}} = 1.17$ eV. From an analysis of data on σ_t in the 12.8-50.2 eV region Kolar and Carraro [7] obtained $\langle D \rangle_{\text{obs.}} = 1.00 \pm 0.10$ eV. In this region they observed 39 resonances. However, according to their data, some of them belong to levels due to impurities. Thus, the resonances at energies 20.45, 38.28 and 41.67 eV belong to ^{240}Pu and those at 22.32, 41.37, 44.42 and 49.63 eV to ^{239}Pu , i.e. in the given region of energies we observe not 39 resonances of ^{241}Pu but only 32. In this case $\langle D \rangle_{\text{obs.}} = 1.21$ eV, which agrees with other data in this region [5].

Blons et al. [8] carried out an identification of the resonances in the region up to 160 eV, using data on σ_f and σ_t . They obtained three values of $\langle D \rangle_{\text{obs.}}$ for the different averaging intervals:

1.27 eV	0- 52 eV
1.23 eV	58-110 eV
1.48 eV	110-160 eV

An abrupt change in the slope of the curve of the cumulative sum of levels in the region of 55 eV is indicated also in Ref. [7]. It is interesting to note that in the 52-58 eV region no levels are observed. Blons et al. [8] note that even in the region below 110 eV there are missing levels due to overlap. Altogether 117 levels were observed in the 4-161 eV region.

$\langle D \rangle_{\text{obs.}}$ was analysed in the present work as well (see Part 2 of this preprint). The $\langle D \rangle_{\text{obs.}}$ value obtained in the region up to 150 eV is 1.34 ± 0.10 eV. It is in agreement with the value of Blons et al. [8] if their data are used in this energy region. In the region up to 150 eV 110 levels have been identified in all. Analysis of the missing levels performed by the method of Ref. [2] showed that in the region up to 150 eV not more than two resonances may be omitted. The change in the slope of

the curve of the cumulative sum of levels is apparently not due to the omission of levels but reflects the actual picture. This is indirectly confirmed by the fact that the change in the slope has no conventional systematic character. For this reason, in subsequent calculations the value used was $\langle D \rangle_{\text{obs.}} = 1.34 \pm 0.10$ eV.

To determine the spin dependence of $\langle D \rangle_J$, we used the model of non-interacting particles [9], which assumes that $\langle D \rangle_J$ is independent of parity. In deformed nuclei, such as ^{242}Pu , the dependence of $\langle D \rangle_J$ on parity can apparently be neglected [10]:

$$D(U, J) = \frac{24\sqrt{2} a^{3/4} U^{5/4} b^{-3} \cdot 10^6}{2J+1} \exp\left[2(aU)^{1/2} + \frac{(J+1/2)^2}{2b^2} \right]. \quad (1.14)$$

where a is the basic parameter of the level density theory and b the parameter of spin cut-off for which the following approximate dependence [9] was taken:

$$b^2 = 0.0889 (aU)^{1/2} A^{2/3}. \quad (1.15)$$

The effective energy of excitation of the compound nucleus U which takes account of residual interactions is

$$U = B_n - \Delta + E, \quad (1.16)$$

where B_n is the neutron binding energy, Δ the energy of pairing of nucleons in the nucleus with an even number of neutrons and protons.

The level density parameter a was obtained by numerical solution of the equation

$$\frac{1}{\langle D \rangle_{\text{obs.}}} = \frac{1}{2} \left(\frac{1}{\langle D \rangle_{J-1/2}} + \frac{1}{\langle D \rangle_{J+1/2}} \right). \quad (1.17)$$

The following values were taken for the calculation:

$$B_n = 6.301 \pm 0.024 \text{ MeV [11]}, \quad \Delta = 1.013 \pm 0.122 \text{ MeV.}$$

In obtaining the value of Δ we used the data of Ref. [11] on pairing energies, taking into account the corrections for differences in surfaces and Coulomb energies and the energy of symmetry of neighbouring nuclei which were suggested by Nemirovsky and Adamchuk [12].

The calculated value of parameter a was found to be equal to $26.90 \pm 0.90 \text{ MeV}^{-1}$. It agrees satisfactorily with the value calculated by Shubin [13], which is 27.62 MeV^{-1} . Baba and Baba [14] give parameters a for modifications of the level density expression of Lang and Le Couteur [15] (31.66 MeV^{-1}) and Ericson [16] (31.28 MeV^{-1}), which are somewhat higher than the value obtained by us. This difference is due, firstly, to the lower value of $\langle D \rangle_{\text{obs.}}$ (1.17 eV) and to the much smaller value of the energy of excitation of the compound nucleus (4.959 MeV against 5.283 MeV). By using the data of Ref. [14] on $\langle D \rangle_{\text{obs.}}$ and U , we can obtain some increase in our value of parameter a (to $\sim 28.7 \text{ MeV}^{-1}$). Secondly, the difference is due to the somewhat different forms of the expressions for level density.

Malyshev [9] obtained the value of parameter a as 27.6 MeV^{-1} . This agrees satisfactorily with the data of the present work because similar values were used:

$$\langle D \rangle_{\text{obs.}} = 1.25 \pm 0.20 \text{ eV and } U = 5.15 \text{ MeV.}$$

The calculated values of $\langle D \rangle_J$ for the s- and p-states in the low-energy region are given in Table 1.1.

We should here note the good agreement with the values of $\langle D \rangle_J$ for the s-wave obtained in the region of resolved resonances:

$$\langle D \rangle_{2^+} = 3.007 \text{ eV and } \langle D \rangle_{3^+} = 2.360 \text{ eV.}$$

Since the spins of the p-states do not differ greatly from those of the s-states and the basic level density parameter a is determined from $\langle D \rangle_{\text{obs.}}$, there is reason to hope that the model of non-interacting particles reproduces with sufficient reliability the spin dependence for the s- and p-states.

In calculating the average cross-sections in the region of unresolved resonances it is usually assumed that $\langle D \rangle_J$ is independent of incident neutron energy E . However, in spite of the condition $E \ll B_n - \Delta$, this effect is substantial and, according to (1.14), amounts to ~17% at 100 keV (Fig. 1.1). In what follows we shall consider the influence of the energy dependence $\langle D \rangle_J(E)$ on the calculated average cross-sections and the value of α .

1.4. Potential scattering cross-section σ_p

In order to calculate the average elastic scattering cross-section, we need to know the scattering radius R , which can be calculated from the value of σ_p in the low-energy region (1.7). σ_p was evaluated by Hanna et al. [17] during self-consistent analysis of data at the thermal point for a number of nuclei and was found to be 12.0 ± 2.2 b. The value of R is accordingly equal to 0.9772×10^{-12} cm.

In the present work we used the σ_p value recommended by Hanna et al. [17].

1.5. Strength functions S_0 and S_1

The strength function of the s-wave (S_0) was obtained by a number of authors. Simpson and Shuman [18] obtained $S_0 = (0.85 \pm 15) \times 10^{-4}$ from data on the average total cross-section $\langle \sigma_t \rangle$ in the keV region. From the resonance parameters obtained in the region up to 20 eV James [4] obtained $S_0 = (1.4 \pm 0.6) \times 10^{-4}$. Obviously, the low accuracy is due to the low resonance statistics. Prince [19] calculated S_0 and S_1 from the optical model of the nucleus with allowance for deformation. The values of S_0 and S_1 at 10 keV was found to be 1.31×10^{-4} and 2.30×10^{-4} , respectively.

From the data on resonance parameters in the 12-100 eV region Kolar and Carraro [7] obtained $S_0 = (1.25 \pm 0.35) \times 10^{-4}$. From the data on neutron widths in the region up to 160 keV Blons et al. [8] obtained $S_0 = (0.99 \pm 0.14) \times 10^{-4}$. It is this value which is taken in the atlas [3]. The evaluation of Kaner and Yiftah [20] takes $S_{0.2^+} = 1.54 \times 10^{-4}$, $S_{0.3^+} = 1.04 \times 10^{-4}$ and $S_1 = 2.73 \times 10^{-4}$. The value of S_1 was obtained

by fitting to $\langle \sigma_{nf} \rangle$ at 40 keV. In the ENDF/B-III data library the value of S_0 is variable and $S_1 = 2.5 \times 10^{-4}$. S_0 is evaluated in the present study as well from an analysis of the resolved resonance parameters obtained by simultaneous treatment of σ_t and σ_f data. The value of S_0 equals $(1.16 \pm 0.19) \times 10^{-4}$.

The available data on S_0 agree with one another within error limits (Table 1.2).

However, the uncertainties in S_0 are large. The high value of S_0 obtained in Ref. [4] from the resonance data in the region up to 20 eV is due to the fact that this region groups together levels with large reduced neutron widths, i.e. the slope of the curve of the cumulative sum of the reduced widths is greater here than in the entire region.

In the present work we have used the value of $S_0 = 1.16 \times 10^{-4}$ for calculations in the region of unresolved resonances. There are no data on S_1 except Prince's value obtained from the optical model. Unfortunately, for ^{241}Pu in the region of unresolved resonances there are practically no data on σ_t from which the necessary information on the strength functions could be derived. For S_1 in the present study we have taken the value of 2.0×10^{-4} , which is approximately the average for heavy actinide nuclei. It is obvious that the error in this value is not lower than 25%. This selection of strength functions should be confirmed by agreement with respect to the other measured average characteristics. This question will be discussed below.

1.6. Average neutron widths $\langle \Gamma_n \rangle_r$

The average neutron widths $\langle \Gamma_n \rangle_r$ can be calculated by the formula

$$\langle \Gamma_n \rangle_r = \langle \Gamma_n^0 \rangle_r P_t E^{1/2} v_r, \quad (1.18)$$

where v_r is the number of possible methods of obtaining the given state r .

The average reduced width

$$\langle \Gamma_n^0 \rangle_r = S_2 \langle D \rangle_r. \quad (1.19)$$

1.7. Average inelastic widths $\langle \Gamma_{n^{\ell}} \rangle_r$

In the region above 40 keV it is necessary to take into account the presence of the neutron inelastic scattering reaction. The partial inelastic widths $\langle \Gamma_{n^{\ell}} \rangle_r$ can be calculated by the formula

$$\langle \Gamma_{n^{\ell}} \rangle_r = \langle D \rangle_3 S_{\ell} \varepsilon^{1/2} P_{\ell}(\varepsilon) \mathcal{V}_{2\ell}^{\ell} , \quad (1.20)$$

where $\varepsilon = E - E_q$ is the energy of neutron with orbital moment ℓ^{ℓ} and E_q the excitation energy of the level.

The values of $v_{J, \ell^{\ell}}$ are determined in the same way as v_r in expression (1.18).

We shall confine ourselves to considering the excitation of only the first level (40 keV, $\frac{7}{2}^+$) since the contribution of the second level (92 keV, $\frac{9}{2}^+$) is small. In this case, the partial inelastic widths are written in the following manner

$$\begin{aligned} \langle \Gamma_{n^{\ell}} \rangle_{2^+}^0 &= 0; \\ \langle \Gamma_{n^{\ell}} \rangle_{3^+}^0 &= \langle \mathcal{D} \rangle_3 S_0 (E - E_1)^{1/2}; \\ \langle \Gamma_{n^{\ell}} \rangle_{1^-}^1 &= 0; \\ \langle \Gamma_{n^{\ell}} \rangle_{2^-}^1 &= \langle \mathcal{D} \rangle_2 S_1 (E - E_1)^{1/2} P_1(E - E_1); \\ \langle \Gamma_{n^{\ell}} \rangle_{3^-}^1 &= 2 \langle \mathcal{D} \rangle_3 S_1 (E - E_1)^{1/2} P_1(E - E_1); \\ \langle \Gamma_{n^{\ell}} \rangle_{4^-}^1 &= 2 \langle \mathcal{D} \rangle_4 S_1 (E - E_1)^{1/2} P_1(E - E_1); \end{aligned} \quad (1.21)$$

Here it was assumed that only the s- and p-waves contribute to the output as well as to the input channels.

1.8. Average radiation width $\langle \Gamma_{\gamma} \rangle$

The average radiation width $\langle \Gamma_{\gamma} \rangle$ is taken as constant for all channels and independent of the parity of the compound nucleus. This is related to the earlier assumption that $\langle D \rangle_r$ is independent of parity.

The average radiation width $\langle \Gamma_Y \rangle$ should be obtained from the data in the region of resolved resonances. By different methods of treatment of σ_t and σ_f data in the 12-30 eV region Kolar et al. [21] obtained $\langle \Gamma_Y \rangle = 47 \pm 6$ and 48 ± 7 MeV. The analysis performed in the present study gave $\langle \Gamma_Y \rangle = 43 \pm 5$ MeV.

It was obtained from the widths of only 47 out of 110 resonances in the region up to 150 eV. The accuracy of the widths Γ_Y for the remaining resonances is low because of the lack of experimental data on σ_Y .

In the present evaluation we took the value of $\langle \Gamma_Y \rangle = 43$ MeV.

1.9 Average fission widths $\langle \Gamma_f \rangle_r$

The average fission widths $\langle \Gamma_{fR} \rangle$ for s-states can in principle be obtained from data in the region of resolved resonances. In this way Sauter and Bowman [22] obtained $\langle \Gamma_f \rangle_{2^+}^0 = 0.510$ eV and $\langle \Gamma_f \rangle_{3^+}^0 = 0.190$ eV. Similar values were obtained in Ref. [23]: $\langle \Gamma_f \rangle_{2^+}^0 = 0.50$ eV and $\langle \Gamma_f \rangle_{3^+}^0 = 0.18$ eV. For both spin states in the 12-100 eV region Kolar et al. [21] obtained $\langle \Gamma_f \rangle = 0.253 \pm 0.042$ eV. They note that in the 12-30 eV region the average value $\langle \Gamma_f \rangle$ is only 0.190 eV. A somewhat higher value of $\langle \Gamma_f \rangle$ was obtained by Kaner and Yiftah [20]: 0.347 ± 0.034 eV. The values of $\langle \Gamma_f \rangle_{2^+}$ and $\langle \Gamma_f \rangle_{3^+}$ obtained by them are 0.567 ± 0.060 and 0.157 ± 0.015 eV, respectively. The value of $\langle \Gamma_f \rangle = 0.300$ eV was obtained by Blons et al. [8].

The analysis of data in the region of resolved resonances performed in the present study (see Part 2) gives the following results:

$$\langle \Gamma_f \rangle_{2^+} = 0.742 \text{ eV}, \quad \langle \Gamma_f \rangle_{3^+} = 0.0845 \text{ eV}, \quad \langle \Gamma_f \rangle = 0.353 \text{ eV} \quad \text{cf. JBL 1.3} := 0.:$$

It should be noted that, whereas the obtained value of $\langle \Gamma_f \rangle_{2^+}$ is much higher than the data of Refs [22, 23], the value of $\langle \Gamma_f \rangle_{3^+}$ is much lower. However, the value of $\langle \Gamma_f \rangle$ agrees comparatively satisfactorily with the results of Refs [8, 20]. All data on the average fission widths are given in Table 1.3.

The data from the region of resolved resonances are inadequate for a number of reasons: absence of data for the p-states; difficulty of identification of levels for the s-states; the possibility of substantial energy dependence of the average fission widths $\langle \Gamma_f \rangle_r(E)$ in the case of a number of channels. Besides, there is one more factor which restricts the use of the values of $\langle \Gamma_f \rangle_r$ for the s-states obtained in the region of resolved resonances. The fission cross-section exhibits a considerably wide structure (Fig. 1.2). Therefore the average fission widths obtained

in such a narrow energy interval will not necessarily show agreement in the whole region of unresolved resonances. This is demonstrated in Fig. 1.2, which compares the evaluated and calculated data on σ_f in the 0.1-10 keV region. Here the main contribution is made by the s-wave.

The calculation was performed with three sets of fission widths. The upper curve corresponds to $\langle \Gamma_f \rangle_{2^+} = 0.7404$ eV and $\langle \Gamma_f \rangle_{3^+} = 0.3383$ eV which enter into the evaluated set of parameters of the present study. The middle curve corresponds to widths $\langle \Gamma_f \rangle_{2^+} = 0.512$ eV and $\langle \Gamma_f \rangle_{3^+} = 0.189$ eV, which is in keeping with the values of Sauter and Bowman [22] and of Simpson et al. [23]. The lower curve corresponds to widths $\langle \Gamma_f \rangle_{2^+} = 0.7404$ eV and $\langle \Gamma_f \rangle_{3^+} = 0.0838$ eV, which approximately tally with the data obtained in the present study from the resolved resonance parameters. The other average parameters remained unchanged. As will be seen from the figure, neither of the lower curves, in general, ensure agreement throughout the energy region.

The difference between the average widths used has a still stronger influence on the value of $\langle \alpha \rangle$ (Fig. 1.3). Thus, the difference of ~14% for the cross-section $\langle \sigma_f \rangle$ between curves 1 and 3 corresponds to an ~75% change in $\langle \alpha \rangle$ at 100 eV. Of course, the difference in the fission cross-section $\langle \sigma_f \rangle$ can be made up by increasing the strength function S_0 , for which there are evidently no grounds. The criterion can be the experimental data on $\langle \alpha \rangle$, which is very sensitive to the fission parameters. Moreover, the value of $\langle \alpha \rangle$ depends little on S_0 (Fig. 1.4). The dependence of $\langle \sigma_f \rangle$ on S_0 is shown in Fig. 1.5.

It follows from the above that to obtain the average fission widths $\langle \Gamma_f \rangle_r$ the phenomenological approach is preferable as it would provide a means of correctly calculating $\langle \sigma_f \rangle$ for the entire energy region of unresolved resonances. The fission widths for the s-wave which are obtained with its help should not necessarily correspond to the values in the region of resolved resonances. This refers, first of all, to the width of the channel, which can be responsible for the possible intermediate structure in the fission cross-section.

It has now been shown that actinide nuclei have a double-humped fission barrier structure [24]. It is necessary to take this into account when the penetration of both peaks is much lower than unity, i.e. fission occurs in the deep sub-barrier region. Apart from the change in barrier penetration, which can be calculated by the Bohr-Hill-Wheller theory [25, 26] in the case of a single-humped barrier, we shall here observe a substantial departure of the distribution of fission widths from the usually assumed χ^2 -distribution

which is a consequence of the presence of states in the second minimum. We can however expect that for the calculation of the average cross-sections $\langle \sigma_f \rangle$ in the case of strongly fissionable nuclei with a negative fission threshold we can make fairly successful use of the conventional fission barrier concepts.

Analysis of the actual picture in the case of the ^{241}Pu nucleus with respect to the penetration of both peaks with the parameters of Ref. [27] shows that the s- and p-states are not sub-barrier for both peaks at the same time. For each state there are channels, the penetration of the second peak of which is equal to unity. In other words, the intermediate structure in the ^{241}Pu fission cross-section should be much less pronounced than in the case of the ^{239}Pu nucleus, the 1^+ state of which is sub-barrier for both peaks.

Thus, the fission barrier penetration can be represented as in Ref. [26] by:

$$P(E_{fk}, \hbar\omega_k) = \left\{ 1 + \exp\left[-\frac{2\pi}{\hbar\omega_k} (E - E_{fk})\right] \right\}^{-1} \quad (1.22)$$

where E_{fk} is the height of the k-th fission barrier and $\hbar\omega_k$ its curvature parameter.

The average fission width

$$\langle \Gamma_f \rangle_r = \frac{\langle D \rangle_r}{2\pi} \sum_k P(E_{fk}, \hbar\omega_k). \quad (1.23)$$

The fission barrier parameters E_{fk} , which were taken from Lynn [28] for the fission threshold value of 0.9 MeV, are given in Table 1.4. The barrier curvature parameters $\hbar\omega_k$ were taken to be identical and equal to 0.6 MeV^{-1} , which corresponds to the curvature parameter of the second peak of Ref. [27]. The average fission widths $\langle \Gamma_f \rangle_r$ at 100 eV obtained from them are given in Table 1.3 for comparison with $\langle \Gamma_f \rangle_r$ in the region below 100 eV.

1.10. Numbers of degrees of freedom of the χ^2 -distributions of partial widths

In the present work we used the ordinary assumption that $\langle \Gamma_f \rangle = \text{const}$, i.e. the radiation widths can be described by a χ^2 -distribution with an infinite number of degrees of freedom. This is in agreement with the analysis of resonance parameters in Ref. [21], where the value of $\nu_\gamma = 60 \pm 10$ was obtained for the 12-100 eV region.

The numbers of degrees of freedom ν_{nr} of the χ^2 -distributions of neutron widths were chosen as the number of methods of obtaining the given state r in the input channel. The numbers of the degrees of freedom $\nu_{n'r}$ of the χ^2 -distributions of inelastic widths were chosen similarly. The only difference was that in the latter case the output channel was considered.

The numbers of degrees of freedom ν_{fr} of the χ^2 -distributions of fission widths were determined as the number of open fission barriers. In the case where there were partially open barriers, the agreement of the calculated fission cross-section $\langle \sigma_{nf} \rangle$ with the evaluated one was also considered.

The values of ν_{nr} , $\nu_{n'r}$, ν_{fr} and ν_f obtained are given in Table 1.5. It should be noted that ν_{fr} for the s -states agree with the results of Ref. [21], where from an analysis of fission widths in the 12-100 eV region the value of $\nu_f = 2.8 \pm 0.4$ was obtained for both the spin states. The value of $\nu_f = 1$ was obtained in Ref. [29], but it does not agree with the conclusions of Ref. [21] and those of the present work.

1.11. Analysis of the results

The quality of the results obtained can be verified by comparing the calculated and experimental data on the average cross-sections and the value of $\langle \alpha \rangle$. For the region of unresolved resonances of ^{241}Pu (0.1-100 keV) we have highly contradictory data on $\langle \sigma_t \rangle$ (up to 2 keV), comparatively reliable data on $\langle \sigma_f \rangle$ and the preliminary results of Weston et al. [30] on $\langle \alpha \rangle$, which have however not been reviewed.

The available experimental and calculated values of the cross-section $\langle \sigma_t \rangle$ are compared in Fig. 1.6. As will be seen from the figure, the calculation does not, on the whole, contradict the available data [18, 31, 32]. The calculated cross-section $\langle \sigma_t \rangle$ and the different partial contributions are shown in Fig. 1.7. In the region up to 100 keV the predominant contribution to $\langle \sigma_t \rangle$ comes from the s -wave. Besides, in this region we can neglect the interference of the potential and resonance scattering for the p -wave. The contributions of the s - and p -waves to the cross-section for formation of a compound nucleus become comparable at ~ 80 keV.

The evaluated and calculated data on the fission cross-section $\langle \sigma_f \rangle$ are compared in Fig. 1.8. It will be seen from the figure that there is agreement in the whole energy region. Figure 1.9 gives the contributions of all channels of $\langle \sigma_f \rangle_r$. It is interesting to note that the average fission widths $\langle \Gamma_f \rangle_r$ decrease with energy (Fig. 1.10). This is a consequence of taking the energy dependence $\langle D \rangle_{J, \pi}(E)$ into account.

Figure 1.11 compares the calculated and experimental [30] data on $\langle \alpha \rangle$ (the continuous line represents the results of the present work). As will be seen, the agreement is satisfactory in the whole energy region.

The average resonance parameters obtained and the average cross-sections and their partial components calculated therefrom are given in Tables 1.6-1.15. In addition, the cross-sections $\langle \sigma_{n'} \rangle$ and $\langle \sigma_{\gamma} \rangle$ and their partial contributions are shown in Figs 1.12 and 1.13.

Thus, the above average resonance parameters agree both with the available data on average cross-sections and with the average parameters obtained in the present study in the region of resolved resonances. There is reason to hope that by using them it will be possible to take correct account of the effects of the detailed cross-section structure of the ^{241}Pu nucleus.

In considering the average resonance parameters the neutron inelastic scattering reaction is generally not taken into account in the region of unresolved resonances. In the case of the ^{241}Pu nucleus, the threshold of the (n, n') reaction is ~ 40 keV. The calculations show that the effect of competition of the (n, n') reaction on the cross-sections of the other processes is substantial although it is smaller than in the case of the ^{235}U and ^{239}Pu nuclei. Thus, it is $\sim 4\%$ at 100 keV for $\langle \sigma_f \rangle$ (Fig. 1.14), $\sim 10\%$ for $\langle \sigma_{\gamma} \rangle$ (Fig. 1.15) and $\sim 6\%$ for $\langle \alpha \rangle$ (Fig. 1.16).

As has been shown above (see formula 1.3), the average distance $\langle D \rangle_{J\pi}$ between levels exhibits a considerable energy dependence in the region of unresolved resonances. It is of interest to study the influence of this effect on the calculated cross-sections and α . Calculations have shown that at 100 keV, if the energy dependence of $\langle D \rangle_{J\pi}$ is neglected, $\langle \sigma_f \rangle$ increases by 1.1% and $\langle \sigma_{n'} \rangle$ by 2.1%, while $\langle \sigma_{\gamma} \rangle$ decreases by 15% (Fig. 1.17) and $\langle \alpha \rangle$ by 16% (Fig. 1.18). As was to be expected, allowance for this effect mainly affects $\langle \sigma_{\gamma} \rangle$.

Comparison of the results of the present work with other evaluations shows a considerable disagreement between the various evaluations of the capture cross-section $\langle \sigma_{\gamma} \rangle$ and consequently $\langle \alpha \rangle$. It is these values which are most sensitive to the average fission widths, as has been shown above.

Below we compare the results of the present study with the evaluations of Takano [35], Kaner and Yiftah [20] and the ENDF/B-III data (Tables 1.16-1.21). It will be seen from these tables that the differences in a number of cases are considerable. We should especially note the substantial difference in the average fission widths, which should affect the cross-sections. However, the description of $\langle \sigma_f \rangle$ is equally good in all the publications, i.e. this difference is offset by the higher values of the power functions in Refs [20, 35]. This leads to a change in $\langle \sigma_\gamma \rangle$ and consequently in $\langle \alpha \rangle$ since the values of $\langle \Gamma_\gamma \rangle$ are similar, except the value given by ENDF/B-III. Figure 1.19 compares the $\langle \sigma_\gamma \rangle$ data from the evaluation of Kaner and Yiftah [20], ENDF/B-III and the present study. The data of Takano [35] practically coincide with the results of Ref. [20]. The ENDF/B-III data are taken from Ref. [20]. The results of the present work lie considerably lower than those of Refs [20, 35] and agree satisfactorily with those of ENDF/B-III. It should be noted here that ENDF/B-III uses a much lower value of $\langle \Gamma_\gamma \rangle$ (0.030 eV).

A similar picture is observed also in the case of $\langle \alpha \rangle$ (Fig. 1.11). It will be seen from the figure that the calculation of the present study shows a better agreement with the experiment of Weston et al. [30], especially in the region above 3 keV. In order to refine the average parameters, we obviously need additional measurements of the total interaction cross-section $\langle \sigma_t \rangle$.

We should mention a few points about the evaluations of the other authors. Kaner and Yiftah [20] used $\sigma_p = 9.6$ b in the region of unresolved resonances but took the value of Hanna et al. [17] (12.0 b) in the region of resolved resonances. In Ref. [20] the average fission widths were determined from the data on resolved resonances. However, the statistics were very low (16 2^+ levels and 23 3^+ levels). The strength function S_0 was determined by fitting to $\langle \sigma_f \rangle$ in the 0.1-3 keV region, i.e. the strength function S_0 was correlated with the average fission widths of the s-wave.

In view of the agreement of the average resonance parameters obtained in the present study with the data in the region of resolved resonances and with the results on the average cross-sections it is hoped that these parameters will enable us to take into account with sufficient reliability the effects of the cross-section structure in the 0.1-100 keV region.

1.12. Evaluated ^{241}Pu data in the region of unresolved resonances

The average resonance parameters obtained above can be used for satisfactory description of data on $\langle\sigma_f\rangle$, $\langle\sigma_t\rangle$, and α in the 0.1-100 keV region. However, in determining the average parameters the present study did not take into account the structure in the cross-sections (it can be due to the finite number of resonances in the averaging interval or to the possible intermediate structure in the fission cross-section). This is due to the fact that detailed data are available only for σ_f , in which the structure can be caused by fluctuations of both neutron and fission widths. The analysis for ^{235}U [1] shows that they are quite strongly correlated. There are no detailed data on σ_t from which we could obtain the fluctuations in neutron widths in the region above 2 keV, while the data are very unreliable in the lower region. It is nevertheless desirable to take into account the structure in the cross-section $\langle\sigma_f\rangle$ observed in Fig. 1.8 in obtaining group constants. The average resonance parameters obtained are recommended for use only in the calculation of the resonance self-shielding coefficients and cross-sections $\langle\sigma_n\rangle$ and $\langle\sigma_{n'}\rangle$.

To calculate the group cross-sections, we assume a system of constants obtained in the following manner. The fission cross-section is evaluated from experiment. The elastic and inelastic scattering cross-sections are calculated from the average resonance parameters, ($\langle\sigma_{n'}\rangle$ is small and the competition of fission is considered to be fairly good on the whole; the cross-section $\langle\sigma_n\rangle$ using the compound nucleus is small in comparison with σ_p and competitive fission is considered, on the whole, to be sufficiently good). In order to obtain the evaluated cross-sections $\langle\sigma_\gamma\rangle$, we used the α data of Weston and Todd [30]. The accuracy of α data is 9% up to 30 keV and 10% above 30 keV. The total cross-section $\langle\sigma_t\rangle$ is determined as the sum of the partial cross-sections. The cross-sections so obtained are given in Table 1.22.

Table 1.1

Average distances $\langle D \rangle_J$ between the levels
of the ^{242}Pu compound nucleus in the
low-energy region

ℓ	r		$\langle D \rangle_{J, \pi}$, eV
	J	π	
0	2	+	$3,088 \pm 0,230$
0	3	+	$2,373 \pm 0,178$
I	I	-	$4,903 \pm 0,364$
I	2	-	$3,088 \pm 0,230$
I	3	-	$2,373 \pm 0,178$
I	4	-	$2,034 \pm 0,152$

Table 1.2

Data on strength functions S_0 and S_1 of ^{241}Pu

References	: Year :	$S_0 \cdot 10^4$: $S_1 \cdot 10^4$
Simpson and Shuman [18]	1961	$0,85 \pm 0,15$	-
James [4]	1964	$1,4 \pm 0,6$	-
Prince [19]	1970	1,31	2,30
Kolar and Carraro [7]	1971	$1,25 \pm 0,35$	-
Blons et al. [8]	1971	$0,99 \pm 0,14$	-
Present study	1979	$1,16 \pm 0,19$	$2,0 \pm 0,5$

Table 1.3

Average fission widths of the ^{241}Pu nucleus

r			References						
ℓ	J	π	Sauter & Bowman [22]	Simpson et al. [23]	Kolar et al. [21]	Kaner & Yiftah [20]	Blons et al. [8]	Present work, resolved resonances	Present work, unresolved resonances
0	2	+	0.510	0.50	-	0.567	-	0.742	0.7704
0	3	+	0.190	0.18	-	0.157	-	0.0845	0.3383
1	1	-	-	-	-	-	-	-	1.4642
1	2	-	-	-	-	-	-	-	0.6839
1	3	-	-	-	-	-	-	-	0.8975
1	4	-	-	-	-	-	-	-	0.4504
$\langle \Gamma_f \rangle$, eV			-	-	0.253	0.347	0.300	0.360	-

Table 1.4

Fission barrier parameters E_{fk} and $\hbar\omega_k$
for the ^{242}Pu compound nucleus

r			E_{fk}, MeV					$\hbar\omega_k, \text{MeV}^{-1}$
ℓ	J	π						
1	2	3	4					5
0	2	+	-0.8	<0.0	0.5	0.7	-	0.6
0	3	+	-0.2	0.5	-	-	-	0.6
1	1	-	-0.4	-0.2	0.8	-	-	0.6
1	2	-	-0.2	0.0	0.8	-	-	0.6
1	3	-	-0.4	-0.2	0.0	0.8	0.8	0.6
1	4	-	-0.2	0.0	0.8	0.8	-	0.6

Table 1.5

Numbers of degrees of freedom of the χ^2 -
distributions of partial widths

r			ν_{nR}	ν_{nR}	ν_{fR}	ν_f
ℓ	J	π				
0	2	+	1	-	2	∞
0	3	+	1	1	1	"
1	1	-	1	-	2	"
1	2	-	2	1	2	"
1	3	-	2	2	3	"
1	4	-	1	2	2	"

Table 1.6

Average distances $\langle D \rangle_{J\pi}$ between
compound nucleus levels

E, keV	$\langle D \rangle_{1-}$, eV	$\langle D \rangle_{2+}$, eV	$\langle D \rangle_{3+}$, eV	$\langle D \rangle_{4-}$, eV
1	2	3	4	5
0,10	4,9044	3,0891	2,3732	2,0341
0,15	4,9040	3,0888	2,3730	2,0339
0,2	4,9035	3,0885	2,3728	2,0337
0,3	4,9026	3,0879	2,3723	2,0334
0,4	4,9017	3,0873	2,3719	2,0330
0,5	4,9007	3,0868	2,3714	2,0326
0,6	4,8998	3,0862	2,3710	2,0322
0,7	4,8989	3,0856	2,3705	2,0318
0,8	4,8980	3,0850	2,3701	2,0314
0,9	4,8971	3,0844	2,3696	2,0310
1,0	4,8961	3,0839	2,3692	2,0307
1,5	4,8915	3,0810	2,3670	2,0287
2	4,8869	3,0781	2,3647	2,0268
3	4,8778	3,0723	2,3603	2,0230
4	4,8686	3,0665	2,3558	2,0191
5	4,8595	3,0607	2,3513	2,0153
6	4,8503	3,0549	2,3469	2,0115
7	4,8412	3,0492	2,3425	2,0076
8	4,8322	3,0435	2,3380	2,0038
9	4,8231	3,0377	2,3336	2,0000
10	4,8140	3,0320	2,3292	1,9962
15	4,7690	3,0036	2,3073	1,9774
20	4,7245	2,9755	2,2856	1,9587
30	4,6367	2,9200	2,2429	1,9219

Table 1.7

Average neutron widths $\langle \Gamma_n \rangle_r$

E, keV	$\langle \Gamma_n \rangle_2^o$, MeV	$\langle \Gamma_n \rangle_3^o$, MeV	$\langle \Gamma_n \rangle_1^f$, MeV	$\langle \Gamma_n \rangle_2^f$, MeV	$\langle \Gamma_n \rangle_3^f$, MeV	$\langle \Gamma_n \rangle_4^f$, MeV
I	2	3	4	5	6	7
0,10	3,5833	2,7529	0,0034	0,0042	0,0032	0,0014
0,15	4,3883	3,3713	0,0060	0,0078	0,0059	0,0026
0,2	5,0667	3,8925	0,0095	0,0119	0,0092	0,0039
0,3	6,2042	4,7664	0,0174	0,0219	0,0169	0,0072
0,4	7,1626	5,5028	0,0268	0,0338	0,0259	0,0111
0,5	8,0066	6,1511	0,0374	0,0471	0,0362	0,0155
0,6	8,7691	6,7369	0,0492	0,0619	0,0476	0,0204
0,7	9,4699	7,2754	0,0619	0,0780	0,0599	0,0257
0,8	10,1219	7,7762	0,0756	0,0953	0,0732	0,0314
0,9	10,7339	8,2464	0,0902	0,1136	0,0873	0,0374
1,0	11,3123	8,6908	0,1056	0,1330	0,1022	0,0438
1,5	13,8417	10,6339	0,1934	0,2437	0,1872	0,0802

Table 1.8

Average fission widths $\langle \Gamma_f \rangle_T$

E, keV	$\langle \Gamma_f \rangle_2^+$, eV	$\langle \Gamma_f \rangle_3^+$, eV	$\langle \Gamma_f \rangle_4^+$, eV	$\langle \Gamma_f \rangle_2^-$, eV	$\langle \Gamma_f \rangle_3^-$, eV	$\langle \Gamma_f \rangle_4^-$, eV
1	2	3	4	5	6	7
0.10	0,74041	0,33834	1,46416	0,68385	0,89754	0,45038
0.15	0,74041	0,33833	1,46406	0,68388	0,89753	0,45040
0.2	0,74040	0,33831	1,46397	0,68390	0,89751	0,45042
0.3	0,74039	0,33829	1,46379	0,68395	0,89749	0,45045
0.4	0,74039	0,33827	1,46361	0,68400	0,89746	0,45048
0.5	0,74038	0,33824	1,46342	0,68405	0,89744	0,45051
0.6	0,74037	0,33822	1,46324	0,68410	0,89741	0,45054
0.7	0,74036	0,33820	1,46306	0,68415	0,89738	0,45057
0.8	0,74036	0,33817	1,46287	0,68420	0,89736	0,45061
0.9	0,74035	0,33815	1,46269	0,68425	0,89733	0,45064
1.0	0,74034	0,33813	1,46250	0,68430	0,89730	0,45067
1.5	0,74030	0,33801	1,46158	0,68455	0,89717	0,45081
2	0,74026	0,33789	1,46066	0,68479	0,89703	0,45095
3	0,74018	0,33765	1,45817	0,68527	0,89675	0,45130
4	0,74010	0,33740	1,45696	0,68575	0,89647	0,45165
5	0,74001	0,33716	1,45511	0,68621	0,89618	0,45199
6	0,73992	0,33691	1,45324	0,68667	0,89589	0,45236
7	0,73983	0,33665	1,45138	0,68712	0,89559	0,45273
8	0,73974	0,33640	1,44950	0,68756	0,89528	0,45312
9	0,73965	0,33614	1,44762	0,68799	0,89497	0,45351
10	0,73955	0,33588	1,44574	0,68841	0,89465	0,45392
15	0,73902	0,33452	1,43625	0,69040	0,89298	0,45466
20	0,73843	0,33311	1,42665	0,69218	0,89116	0,45574
30	0,73701	0,33009	1,40715	0,69511	0,88708	0,45768

Table 1.9

Average inelastic widths $\langle \Gamma_{\kappa} \rangle_r$

E, keV	$\langle \Gamma_{\kappa} \rangle_{1^+}$, MeV	$\langle \Gamma_{\kappa} \rangle_{3^+}$, MeV	$\langle \Gamma_{\kappa} \rangle_{1^-}$	$\langle \Gamma_{\kappa} \rangle_{2^-}$, MeV	$\langle \Gamma_{\kappa} \rangle_{3^-}$, MeV	$\langle \Gamma_{\kappa} \rangle_{4^-}$, MeV
40	0,0	0,0	0,0	0,0	0,0	0,0
44	0,0	16,0262	0,0	0,4857	0,7460	0,6392
50	0,0	25,0548	0,0	1,8606	2,8579	2,4485
60	0,0	34,7717	0,0	4,9995	7,6786	6,5779
70	0,0	41,7926	0,0	8,7343	13,4141	11,4901
80	0,0	47,3589	0,0	12,8006	19,6577	16,8366
90	0,0	51,9632	0,0	17,0446	26,1734	22,4153
100	0,0	55,8641	0,0	21,3662	32,8074	28,0942

Table 1.10

Partial elastic scattering cross-sections using
the compound nucleus $\langle \sigma_n \rangle_r$

E, keV	$\langle \sigma_n \rangle_{2^+}, b$	$\langle \sigma_n \rangle_{3^+}, b$	$\langle \sigma_n \rangle_{1^-}, b$	$\langle \sigma_n \rangle_{2^-}, b$	$\langle \sigma_n \rangle_{3^-}, b$	$\langle \sigma_n \rangle_{4^-}, b$
1	2	3	4	5	6	7
0,10	0,5627	1,4349	$1,2 \cdot 10^{-7}$	$6,3 \cdot 10^{-7}$	$3,8 \cdot 10^{-7}$	$3,5 \cdot 10^{-7}$
0,15	0,5534	1,3990	$2,7 \cdot 10^{-7}$	$1,4 \cdot 10^{-6}$	$8,6 \cdot 10^{-7}$	$7,9 \cdot 10^{-7}$
0,2	0,5458	1,3706	$4,9 \cdot 10^{-7}$	$2,5 \cdot 10^{-6}$	$1,5 \cdot 10^{-6}$	$1,4 \cdot 10^{-6}$
0,3	0,5339	1,3261	$1,1 \cdot 10^{-6}$	$5,7 \cdot 10^{-6}$	$3,4 \cdot 10^{-6}$	$3,2 \cdot 10^{-6}$
0,4	0,5243	1,2914	$1,9 \cdot 10^{-6}$	$1,01 \cdot 10^{-5}$	$6,1 \cdot 10^{-6}$	$5,6 \cdot 10^{-6}$
0,5	0,5164	1,2627	$3,03 \cdot 10^{-6}$	$1,6 \cdot 10^{-5}$	$9,6 \cdot 10^{-6}$	$8,7 \cdot 10^{-6}$
0,6	0,5094	1,2381	$4,4 \cdot 10^{-6}$	$2,3 \cdot 10^{-5}$	$1,4 \cdot 10^{-5}$	$1,3 \cdot 10^{-5}$
0,7	0,5033	1,2166	$5,9 \cdot 10^{-6}$	$3,1 \cdot 10^{-5}$	$1,9 \cdot 10^{-5}$	$1,7 \cdot 10^{-5}$
0,8	0,4978	1,1974	$7,7 \cdot 10^{-6}$	$4,02 \cdot 10^{-5}$	$2,4 \cdot 10^{-5}$	$2,2 \cdot 10^{-5}$
0,9	0,4928	1,1801	$9,8 \cdot 10^{-6}$	$5,1 \cdot 10^{-5}$	$3,1 \cdot 10^{-5}$	$2,8 \cdot 10^{-5}$
1,0	0,4881	1,1643	$1,2 \cdot 10^{-5}$	$6,3 \cdot 10^{-5}$	$3,8 \cdot 10^{-5}$	$3,5 \cdot 10^{-5}$
1,5	0,4692	1,1010	$2,7 \cdot 10^{-5}$	0,0001	$8,5 \cdot 10^{-5}$	$7,8 \cdot 10^{-5}$
2	0,4547	1,0536	$4,8 \cdot 10^{-5}$	0,0002	0,0002	0,0001
3	0,4329	0,9847	0,0001	0,0005	0,0003	0,0003
4	0,4166	0,9345	0,0002	0,0009	0,0006	0,0005
5	0,40346	0,89508	0,0003	0,0015	0,0009	0,0008
6	0,39243	0,86268	0,0004	0,0021	0,0013	0,0012
7	0,38293	0,83522	0,0005	0,0028	0,0018	0,0016
8	0,37457	0,81143	0,0007	0,0036	0,0023	0,0020
9	0,36712	0,79048	0,0009	0,0045	0,0028	0,0025
10	0,36038	0,77178	0,0011	0,0054	0,0035	0,0031
15	0,33396	0,7005	0,0022	0,0111	0,0073	0,0065
20	0,31483	0,6508	0,0037	0,0181	0,0123	0,0107

Table 1.11

Partial fission cross-sections $\langle \sigma_f \rangle_r$

E, keV	$\langle \sigma_f \rangle_2^{\circ}, b$	$\langle \sigma_f \rangle_3^{\circ}, b$	$\langle \sigma_f \rangle_1^{\prime}, b$	$\langle \sigma_f \rangle_2^{\prime}, b$	$\langle \sigma_f \rangle_5^{\prime}, b$	$\langle \sigma_f \rangle_7^{\prime}, b$
1	2	3	4	5	6	7
0,10	16,7985	17,8270	0,0065	0,0201	0,0302	0,0171
0,15	13,6479	14,4592	0,0079	0,0246	0,0370	0,0209
0,2	11,7709	12,4536	0,0091	0,0284	0,0427	0,0242
0,3	9,5463	10,0776	0,0112	0,0348	0,0523	0,0296
0,4	8,2217	8,6637	0,0129	0,0402	0,0604	0,0342
0,5	7,3186	7,7004	0,0144	0,0449	0,0675	0,0382
0,6	6,6527	6,9903	0,0158	0,0491	0,0739	0,0418
0,7	6,1356	6,4392	0,0171	0,0530	0,0798	0,0452
0,8	5,7191	5,9956	0,0183	0,0567	0,0853	0,0483
0,9	5,3744	5,6286	0,0194	0,0601	0,0904	0,0512
1,0	5,0831	5,3185	0,0204	0,0633	0,0953	0,0539
1,5	4,0968	4,2699	0,0249	0,0774	0,1164	0,0659

Table 1.12

Partial neutron inelastic scattering cross-sections $\langle \sigma_n \rangle_r$

E, keV	$\langle \sigma_n \rangle_2^{\circ}, b$	$\langle \sigma_n \rangle_3^{\circ}, b$	$\langle \sigma_n \rangle_1^{\prime}, b$	$\langle \sigma_n \rangle_2^{\prime}, b$	$\langle \sigma_n \rangle_3^{\prime}, b$	$\langle \sigma_n \rangle_4^{\prime}, b$
40	0,0	0,0	0,0	0,0	0,0	0,0
44	0,0	0,0623	0,0	0,0005	0,0008	0,0009
50	0,0	0,0829	0,0	0,0019	0,0029	0,0034
60	0,0	0,0955	0,0	0,0052	0,0081	0,0091
70	0,0	0,0998	0,0	0,0088	0,0143	0,0155
80	0,0	0,1009	0,0	0,0125	0,0208	0,0221
90	0,0	0,0997	0,0	0,0196	0,0342	0,0347
100	0,0	0,1006	0,0	0,0161	0,0275	0,0285

Table 1.13

Partial neutron radiative capture cross-sections $\langle \sigma_\gamma \rangle_r$

E, keV	$\langle \sigma_\gamma \rangle_2^{\circ}, b$	$\langle \sigma_\gamma \rangle_3^{\circ}, b$	$\langle \sigma_\gamma \rangle_1^{\prime}, b$	$\langle \sigma_\gamma \rangle_2^{\prime}, b$	$\langle \sigma_\gamma \rangle_3^{\prime}, b$	$\langle \sigma_\gamma \rangle_4^{\prime}, b$
1	2	3	4	5	6	7
0,10	2,5746	8,6482	0,0006	0,0034	0,0027	0,0041
0,15	2,0763	6,9303	0,0007	0,0042	0,0033	0,0050
0,2	1,7799	5,9113	0,0008	0,0048	0,0038	0,0057
0,3	1,4297	4,7102	0,0010	0,0059	0,0046	0,0070
0,4	1,2218	3,9999	0,0012	0,0068	0,0054	0,0081
0,5	1,0805	3,5187	0,0013	0,0076	0,0060	0,0090
0,6	0,976E	3,6158	0,0014	0,0083	0,0066	0,0099
0,7	0,8961	2,8932	0,0015	0,0090	0,0071	0,0107
0,8	0,8315	2,6747	0,0016	0,0096	0,0076	0,0114
0,9	0,7781	2,4947	0,0017	0,0102	0,0080	0,0121

Table 1.14

Calculated reaction cross-sections using the
compound nucleus and the value of $\langle\alpha\rangle$

E, keV	$\langle\sigma_n\rangle$, b	$\langle\sigma_f\rangle$, b	$\langle\sigma_{in}\rangle$, b	$\langle\sigma_f\rangle$, b	$\langle\alpha\rangle$
1	2	3	4	5	6
0,10	1,9977	34,6994	0	11,2335	0,3237
0,15	1,9524	28,1976	0	9,0197	0,3199
0,2	1,9164	24,3290	0	7,7064	0,3168
0,3	1,8599	19,7519	0	6,1585	0,3118
0,4	1,8157	17,0331	0	5,2432	0,3078
0,5	1,7791	15,1840	0	4,6232	0,3045
0,6	1,7476	13,8237	0	4,1687	0,3016
0,7	1,7199	12,7699	0	3,8177	0,2990
0,8	1,6953	11,9232	0	3,5364	0,2966
0,9	1,6730	11,2240	0	3,3048	0,2944
1,0	1,6525	10,6345	0	3,1100	0,2924
1,5	1,5704	8,6514	0	2,4583	0,2841
2	1,5090	7,4871	0	2,0787	0,2776
3	1,4189	6,1344	0	1,6411	0,2675
4	1,3534	5,3506	0	1,3893	0,2597
5	1,3020	4,8302	0	1,2227	0,2531
6	1,2601	4,4562	0	1,1032	0,2476
7	1,2248	4,1731	0	1,0126	0,2426
8	1,1946	3,9505	0	0,9413	0,2383
9	1,1683	3,7708	0	0,8835	0,2343
10	1,1452	3,6223	0	0,8357	0,2307
15	1,0616	3,1499	0	0,6814	0,2163
20	1,0103	2,8973	0	0,5963	0,2058

Table 1.15

Calculated values of $\langle \sigma_t \rangle$ and its partial contributions

E, keV	$\langle \sigma_p \rangle_0, b$	$\langle \sigma_p \rangle_1, b$	$\langle \sigma_n \rangle_0, b$	$\langle \sigma_n \rangle_1, b$	$\langle \sigma_{int} \rangle_0, b$	$\langle \sigma_{int} \rangle_1, b$	$\langle \sigma_t \rangle, b$
1	2	3	4	5	6	7	8
0,10	11,998	$8 \cdot 10^{-7}$	47,846	0,0846	0,0437	$2 \cdot 10^{-12}$	59,885
0,15	11,997	$1,9 \cdot 10^{-6}$	39,066	0,1036	0,0535	$7 \cdot 10^{-12}$	51,113
0,2	11,996	$3,3 \cdot 10^{-6}$	33,832	0,1197	0,0618	$2 \cdot 10^{-11}$	45,866
0,3	11,994	$7,5 \cdot 10^{-6}$	27,624	0,1465	0,0757	$8 \cdot 10^{-11}$	39,689
0,4	11,993	$1,3 \cdot 10^{-5}$	23,923	0,1691	0,0874	$2 \cdot 10^{-10}$	35,997
0,5	11,991	$2,1 \cdot 10^{-5}$	21,397	0,1890	0,0977	$5 \cdot 10^{-10}$	33,479
0,6	11,989	$3,0 \cdot 10^{-5}$	19,533	0,2070	0,1070	$9 \cdot 10^{-10}$	31,622
0,7	11,987	$4,1 \cdot 10^{-5}$	18,084	0,2235	0,1156	$2 \cdot 10^{-9}$	30,179
0,8	11,985	$5,3 \cdot 10^{-5}$	16,916	0,2388	0,1235	$3 \cdot 10^{-9}$	29,017
0,9	11,983	$6,7 \cdot 10^{-5}$	15,949	0,2532	0,1310	$4 \cdot 10^{-9}$	28,054
1,0	11,982	$8,3 \cdot 10^{-5}$	15,130	0,2668	0,1381	$6 \cdot 10^{-9}$	27,241

Table 1.16

Potential scattering cross-sections σ_p and values of R for the ^{241}Pu nucleus used in the different evaluations

Value	Takano [35]	Kaner and Yiftah [20]	ENDF/B-III	Present Study
σ_p ,	8,7	9,6	10,9	12,0
R, fermi	8,30	8,74	9,83	9,77

Table 1.17

Average distances between the levels of the s- and p-states of ^{241}Pu according to the data of the different evaluations

r			$\langle D \rangle_{s,p}, \text{eV}$			
ℓ	J	π	Takano [35]	Kaner and Yiftah [20]	ENDF/B-III	Present Study
0	2	+	2,333	2,31	2,33	3,088
0	3	+	1,667	1,99	1,59	2,373
1	1	-	3,900	3,39	2,98	4,903
1	2	-	2,333	2,31	2,33	3,088
1	3	-	1,667	1,99	1,59	2,373
1	4	-	1,300	1,99	1,26	2,034
$\langle D \rangle_{\text{obs}}, \text{eV}$			0,97	1,07	0,83	1,34

Table 1.18

Strength functions and reduced neutron widths of ^{241}Pu
for the s- and p-states from the data
of the different evaluations

r			Takano	[35]	Kaner and Yiftah	ENDF/B-III		Present Study		
l	J	π	$S \cdot 10^{-4}$	$\langle \Gamma_n \rangle \cdot 10^3, \text{eV}$	$S \cdot 10^4$	$\langle \Gamma_n \rangle \cdot 10^3, \text{eV}$	$S \cdot 10^4$	$\langle \Gamma_n \rangle \cdot 10^3, \text{eV}$	$S \cdot 10^4$	$\langle \Gamma_n \rangle \cdot 10^3, \text{eV}$
0	2	+		0,3057	1,54	0,356	-	0,25-0,41		0,358
				1,31						1,16
0	3	+		0,2183	1,04	0,207	-	0,14-0,23		0,275
I	I	-	-	1,521		0,925		0,745		0,981
I	2	-	-	0,9099	2,73	0,631	2,5	0,582	2,0	0,618
I	3	-	-	0,6499		0,543		0,398		0,475
I	4	-	-	0,5070		0,543		0,440		0,407

Table 1.19

Average fission widths $\langle \Gamma_f \rangle_r$ from the data of the
different evaluations

r			$\langle \Gamma_f \rangle_r, \text{eV}$				
l	J	π	Takano	[35]	Kaner and Yiftah	[20]	Present Study
0	2	+		0,4445		0,567	0,7404
0	3	+		0,2464		0,157	0,3383
I	I	-		1,179		0,540	0,4642
I	2	-		0,4255		0,184	0,6839
I	3	-		0,5822		0,327	0,8975
I	4	-		0,2359		0,158	0,4504

Table 1.20

Average radiation widths $\langle \Gamma_i \rangle$ of ^{241}Pu from the data of the different evaluations

$\langle \Gamma_i \rangle, \text{eV}$			
Takano [35]	Kaner and Yiftah [20]	ENDF/B-III	Present Study
0,040	0,043	0,030	0,043

Table 1.21

Number of degrees of freedom of the χ^2 -distributions of the fission widths from the data of the different evaluations

r			$\nu_{f,r}$		
ℓ	J	π	Takano [35]	Kaner and Yiftah [20]	Present Study
0	2	+	3	2	2
0	3	+	2	1	1
I	1	-	3	2	2
I	2	-	3	1	2
I	3	-	3	2	3
I	4	-	3	1	2

Table 1.22

Evaluated data on $\langle \sigma_f \rangle$, $\langle \sigma_f \rangle$, $\langle \sigma_n \rangle$, $\langle \sigma_{n'} \rangle$
and on the value of α for ^{241}Pu in the
region of unresolved resonances

ΔE , keV	$\langle \sigma_f \rangle$, b	$\langle \sigma_f \rangle$, b	$\langle \sigma_n \rangle$, b	$\langle \sigma_{n'} \rangle$, b	α
1	2	3	4	5	6
0,1-0,2	25,031	6,708	13,895	0	0,268
0,2-0,3	26,462	6,986	13,812	0	0,264
0,3-0,4	21,266	6,720	13,748	0	0,316
0,4-0,5	18,044	6,315	13,696	0	0,350
0,5-0,6	16,038	5,094	13,651	0	0,317
0,6-0,7	11,362	4,022	13,610	0	0,354
0,7-0,8	10,837	2,850	13,573	0	0,263
0,8-0,9	9,885	2,728	13,541	0	0,276
0,9-1,0	11,030	2,890	13,511	0	0,262
1-2	8,851	2,629	13,373	0	0,297
2-3	6,794	1,732	13,196	0	0,255
3-4	6,334	1,545	13,064	0	0,244
4-5	5,574	1,371	12,955	0	0,246
5-6	4,665	1,209	12,860	0	0,259
6-7	4,677	1,015	12,778	0	0,217
7-8	4,072	1,173	12,703	0	0,288
8-9	4,231	0,977	12,643	0	0,231
9-10	3,786	0,761	12,570	0	0,201
10-20	3,124	0,762	12,284	0	0,244
20-30	2,816	0,611	11,908	0	0,217
30-40	2,610	0,452	11,627	0	0,173

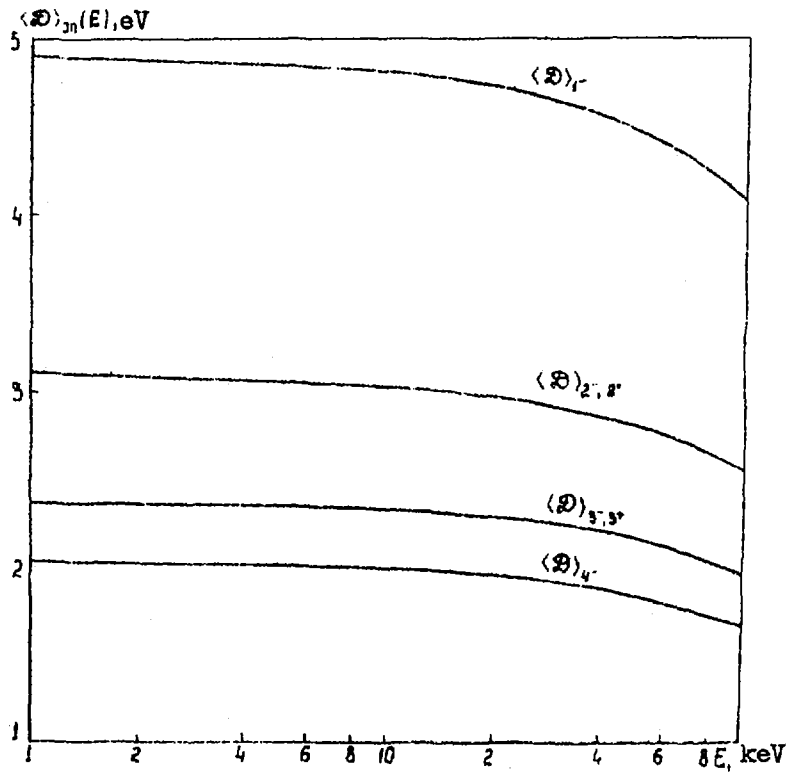


Fig. 1.1. Dependence of the average distances $\langle D \rangle_{j,n}$ between levels on the energy of incident neutrons.

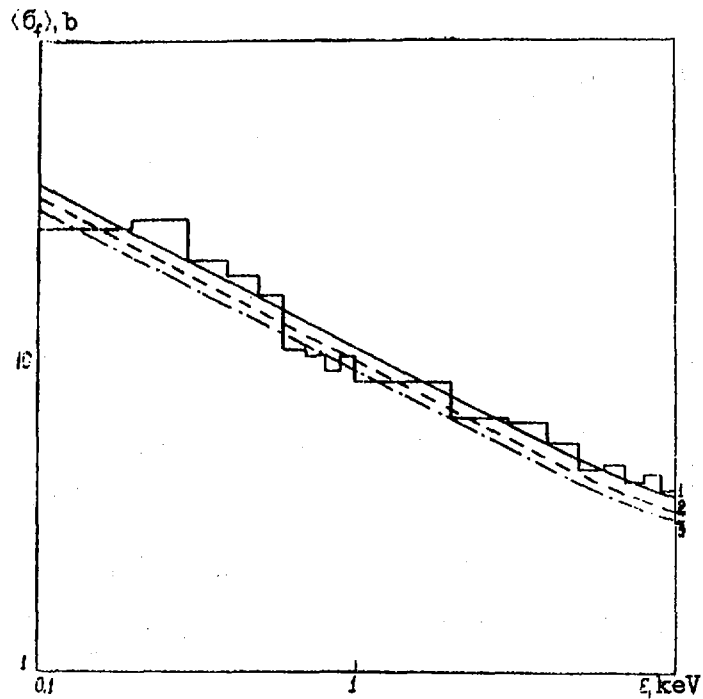


Fig. 1.2. Comparison of calculated and evaluated data on $\langle \sigma_f \rangle$ (^{241}Pu) in the 0.1-10 keV region:
— Evaluation; (1) calculation with $\langle \Gamma_f \rangle_{2^+} = 0.7404$ eV and $\langle \Gamma_f \rangle_{3^+} = 0.3383$ eV;
(2) calculation with $\langle \Gamma_f \rangle_{2^+} = 0.512$ eV and $\langle \Gamma_f \rangle_{3^+} = 0.189$ eV; (3) calculation with $\langle \Gamma_f \rangle_{2^+} = 0.7404$ eV and $\langle \Gamma_f \rangle_{3^+} = 0.0838$ eV.

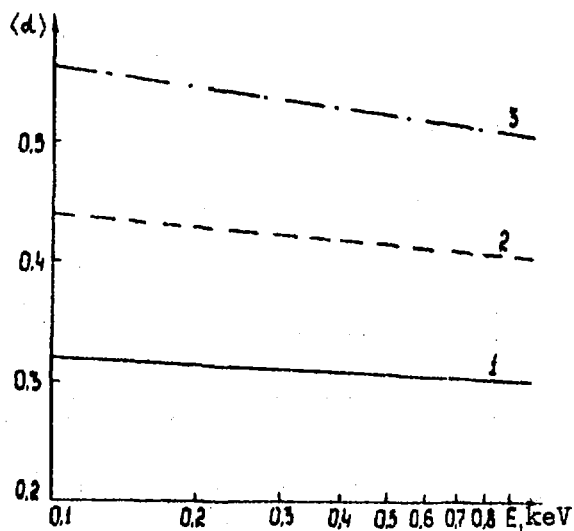


Fig. 1.3. Dependence of the value of $\langle d \rangle$ of ^{241}Pu on the average fission widths of the s-wave (notations are the same as in Fig. 1.2).

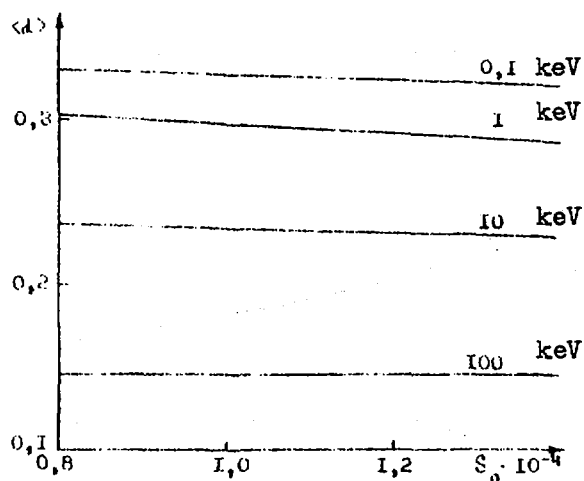


Fig. 1.4. Dependence of $\langle d \rangle$ of ^{241}Pu on the value of the strength function S_0 .

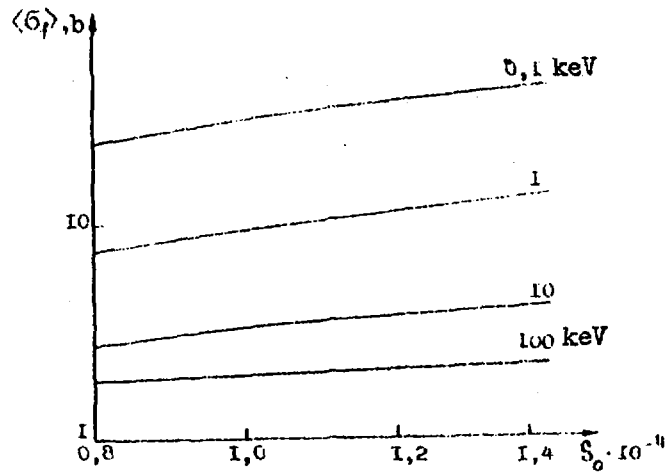


Fig. 1.5. Dependence of $\langle \sigma_f \rangle$ of ^{241}Pu on the value of the strength function S_0 .

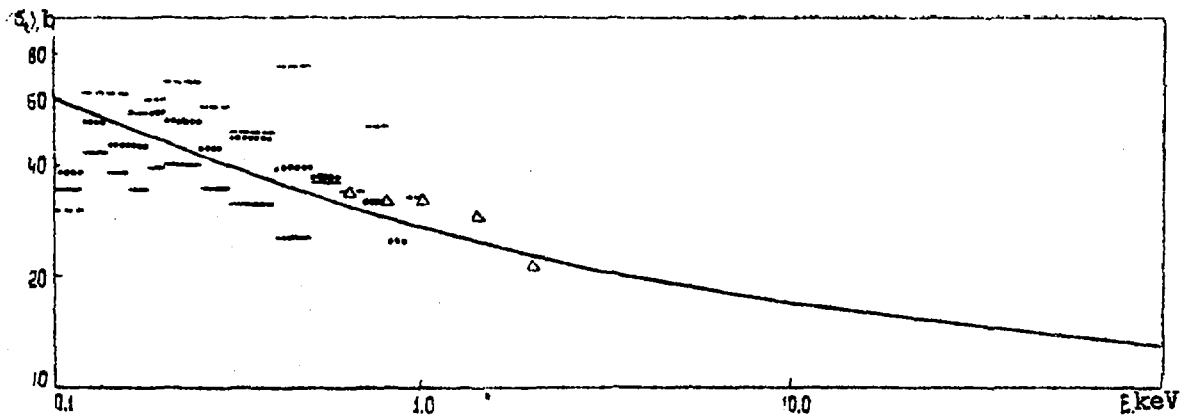


Fig. 1.6. Comparison of the calculated and experimental data on $\langle \sigma_f \rangle$:
— — calculation; Δ - Simpson et al. [18, 31]; - - - - Craig and Westcott [32]; ... - Pattenden et al. [34].

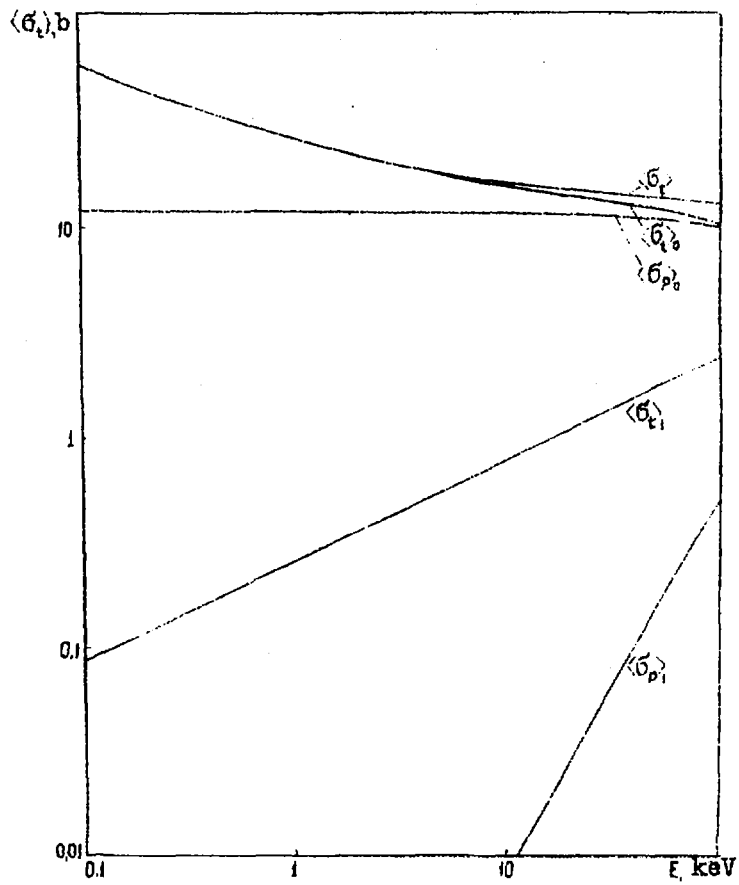


Fig. 1.7. Calculated cross-section $\langle \sigma_t \rangle$ and its components.

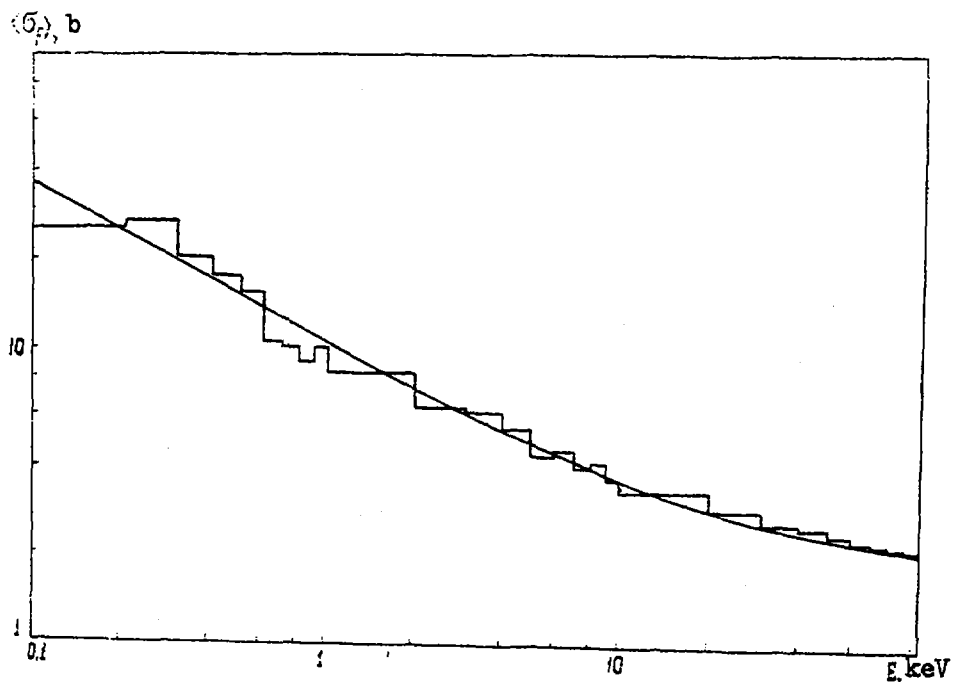


Fig. 1.8. Comparison of evaluated and calculated data on $\langle \sigma_p \rangle$ for ^{241}Pu .

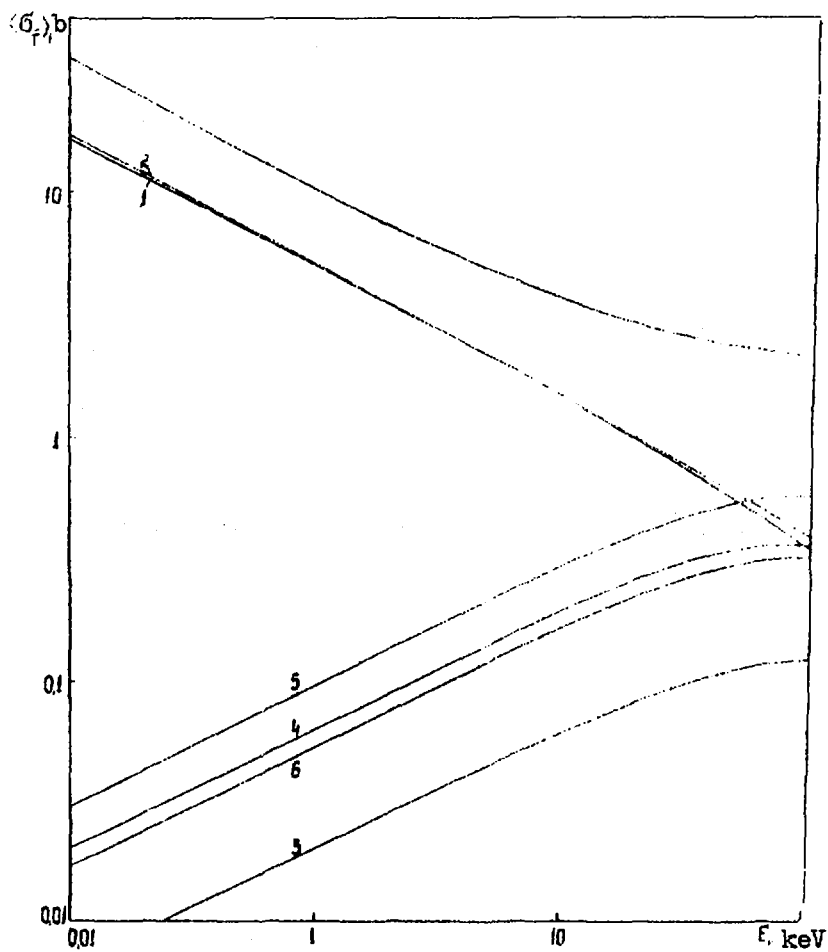


Fig. 1.9. Calculated cross-section $\langle \sigma_p \rangle$ and the different partial contributions: (1) contribution of channel (0.2+); (2) (0.3+); (3) (1.1-); (4) (1.2-); (5) (1.3-); (6) (1.4-).

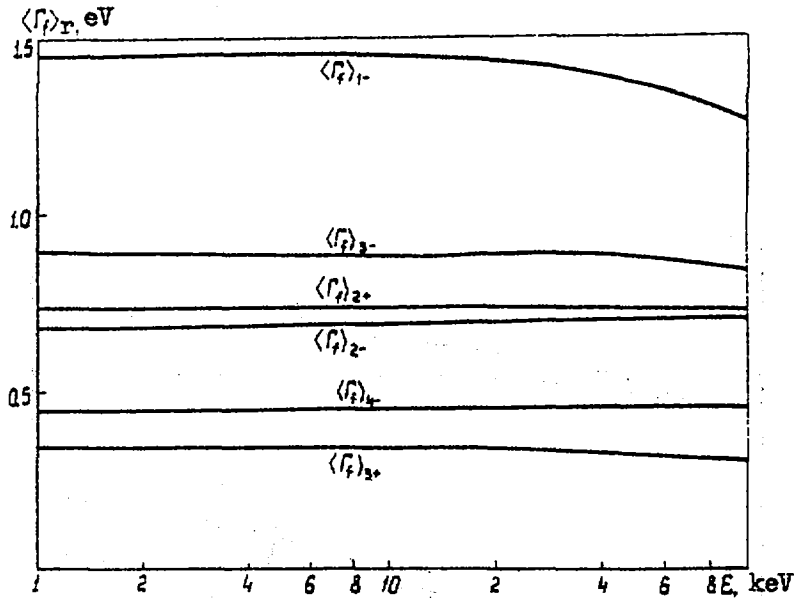


Fig. 1.10. Energy dependence of the average fission widths $\langle \Gamma \rangle_r$

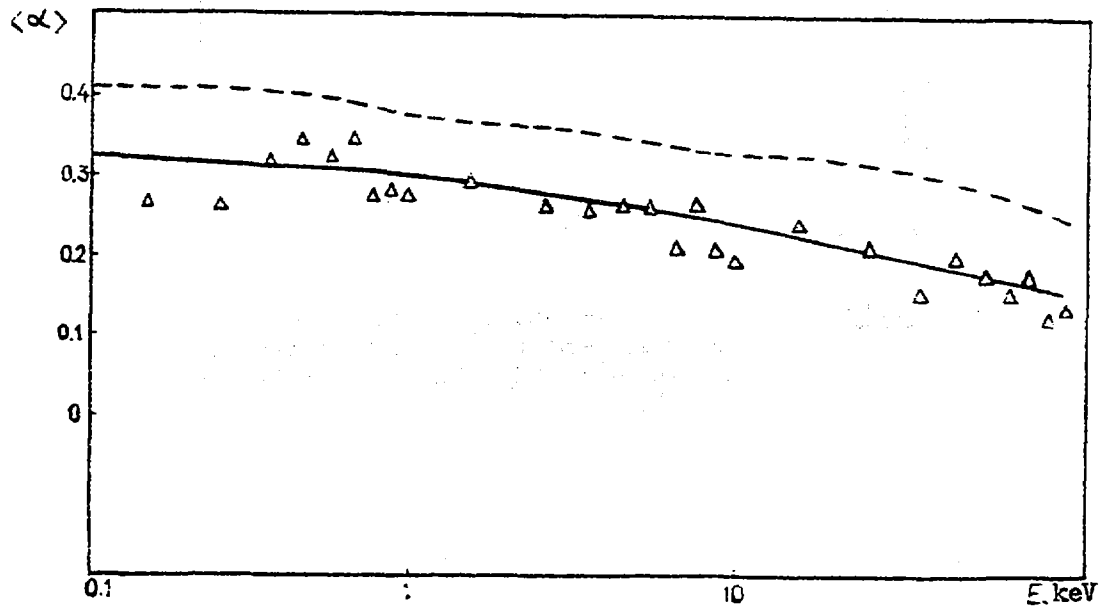


Fig. 1.11. Comparison of the calculated and experimental data of Weston and Todd [30] on $\langle \alpha \rangle$: — — data of the present study; --- — data of Kaner and Yiftah [20].

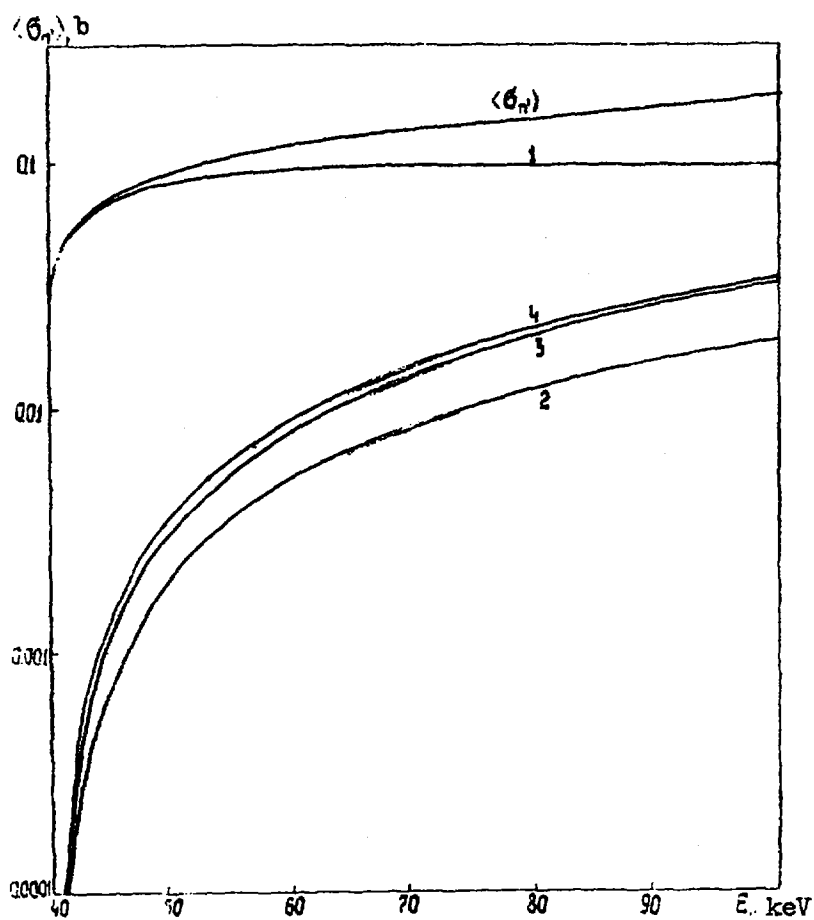


Fig. 1.12. Calculated cross-section $\langle \sigma_n \rangle$ and its partial components: (1) contribution of channel (0.3+); (2) (1.2-); (3) (1.3-); (4) (1.4-).

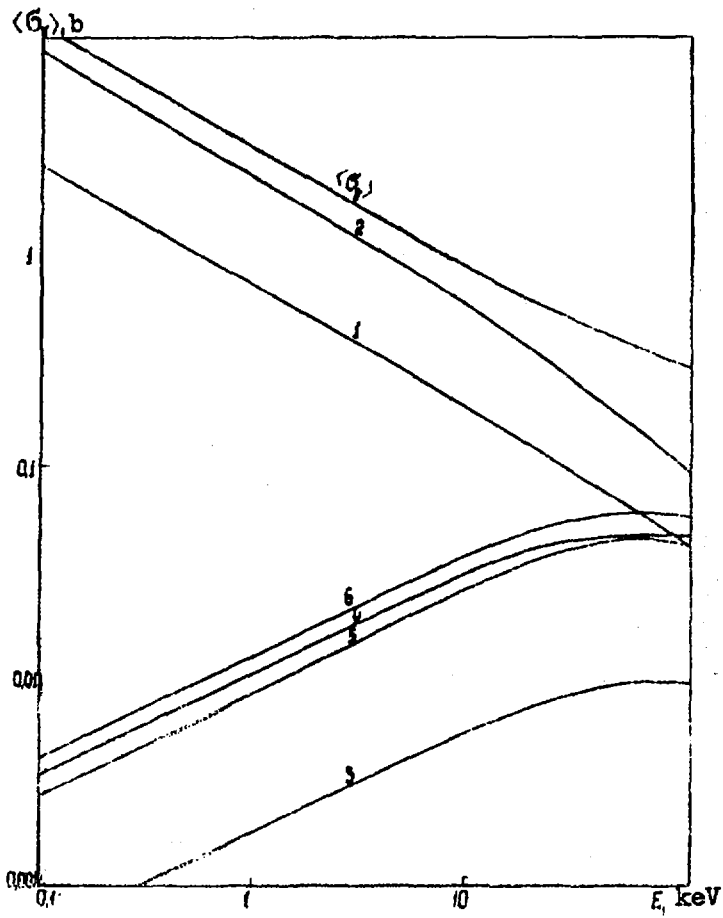


Fig. 1.13. Calculated cross-section $\langle \sigma_r \rangle$ and its partial components: (1) contribution of channel (0.2+); (2) (0.3+); (3) (1.1-); (4) (1.2-); (5) (1.3-); (6) (1.4-).

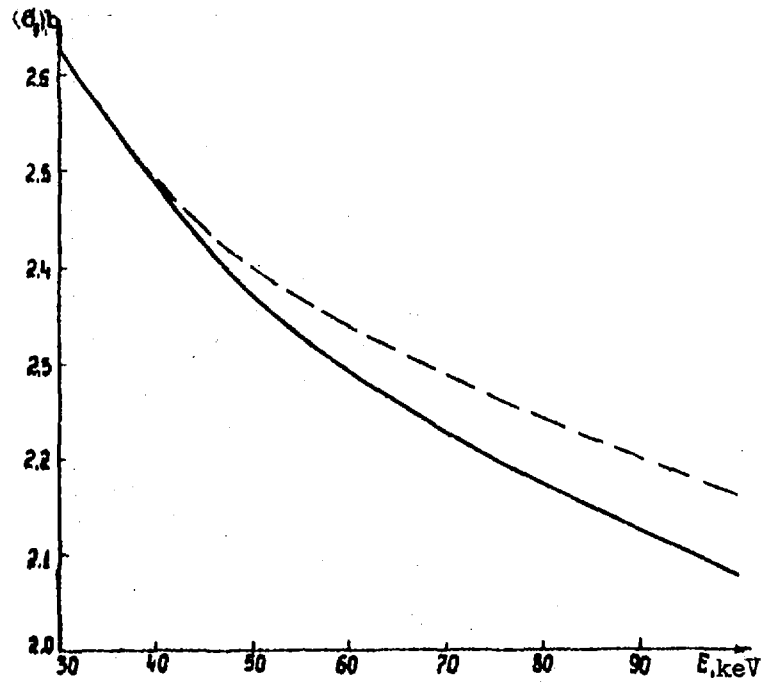


Fig. 1.14. Influence of the effect of competition of the (n,n') reaction on cross-section $\langle\sigma_p\rangle$:
— - with allowance for the (n,n') reaction;
--- - without allowance for it.

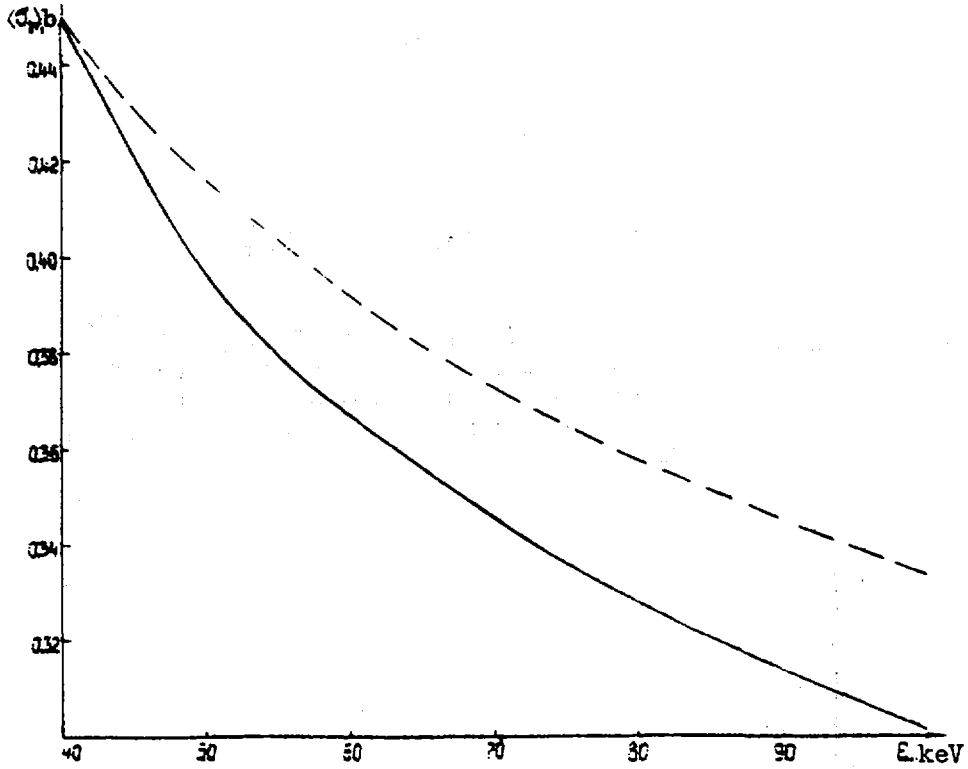


Fig. 1.15. Influence of the effect of competition of the (n,n') reaction on cross-section $\langle \sigma_T \rangle$: — - with allowance for the (n,n') reaction; --- - without allowance for it.

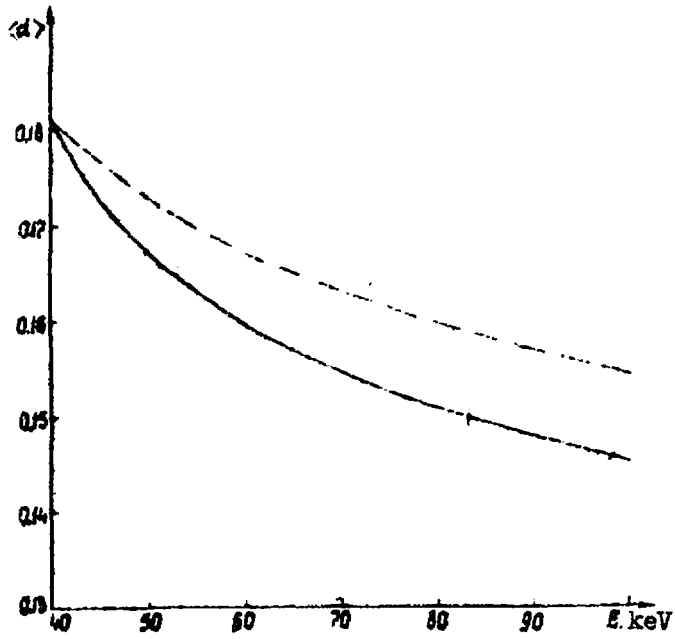


Fig. 1.16. Influence of the effect of competition of the (n, n') reaction on the value of $\langle \alpha \rangle$: — - with allowance for the (n, n') reaction; --- - without allowance for it.

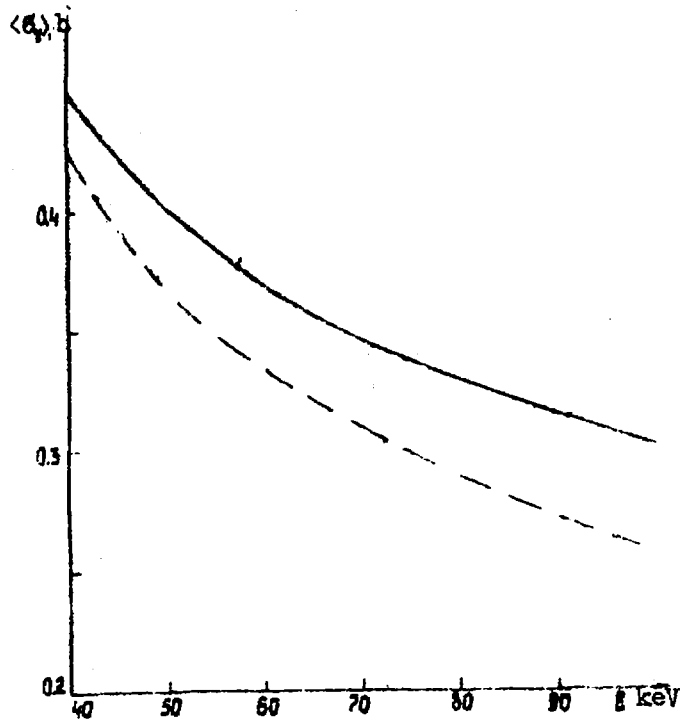


Fig. 1.17. Influence of allowance for the energy dependence $\langle \sigma_{\gamma, n}(E)$ on $\langle \sigma_p \rangle$: — - with allowance for dependence $\langle \sigma_{\gamma, n}(E)$; --- - without allowance for it.

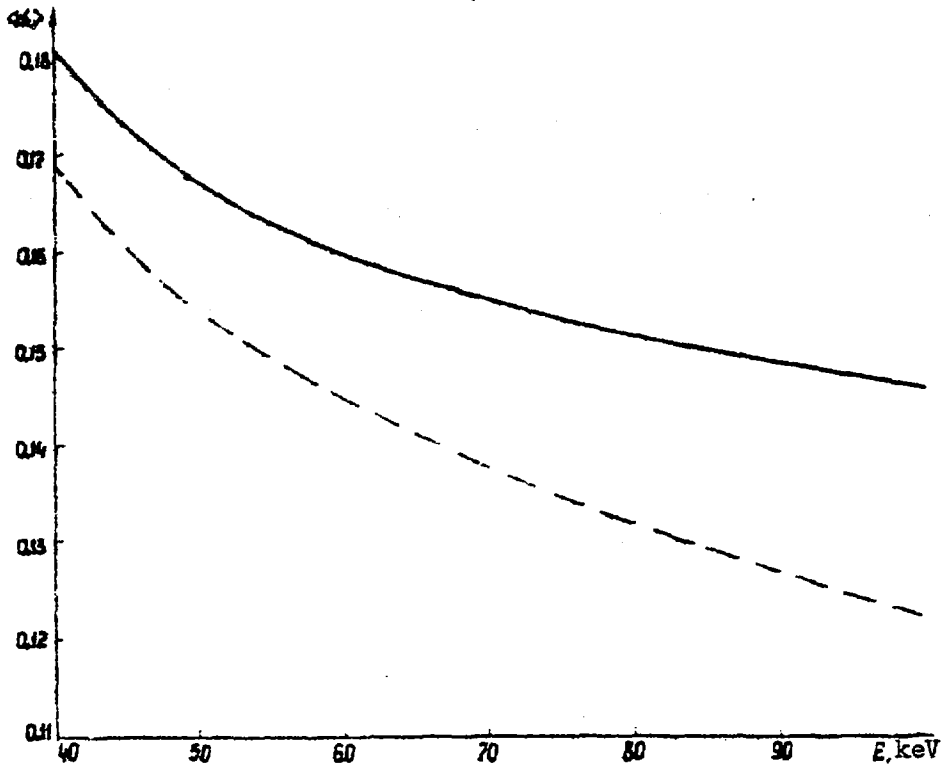


Fig. 1.18. Influence of allowance for the energy dependence $\langle D \rangle_{\alpha, \beta}(E)$ on $\langle d \rangle$: — - with allowance for dependence $\langle D \rangle_{\alpha, \beta}(E)$; --- - without allowance for it.

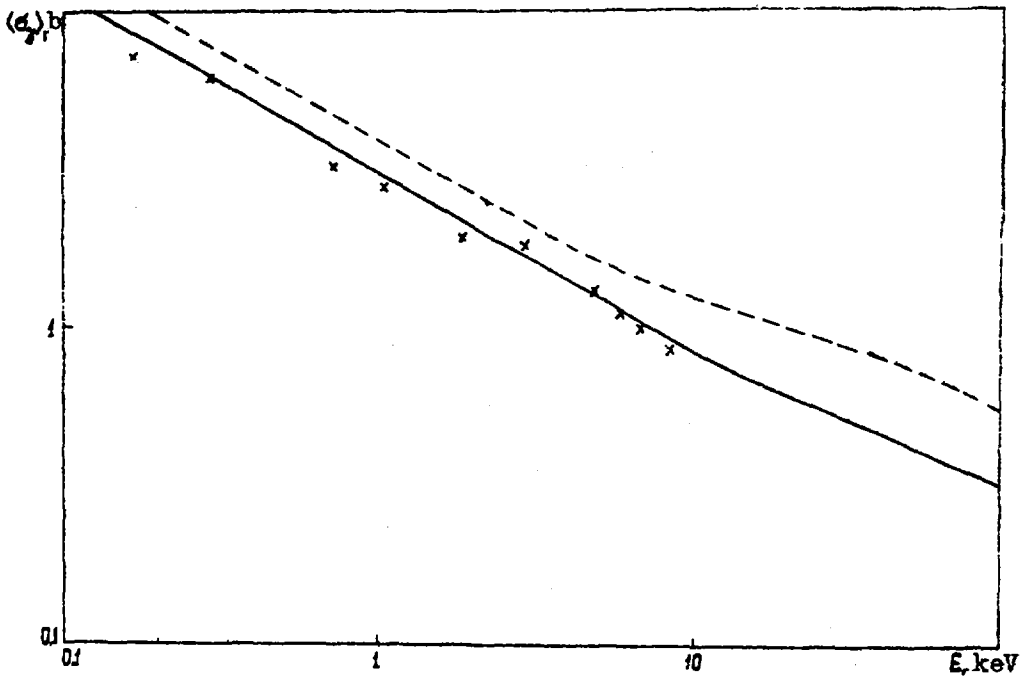


Fig. 1.19. Comparison of the data of the different evaluations of $\langle \sigma_T \rangle$: — - present study; --- - data of Kaner and Yiftah [20]; x - ENDF/B-III.

REFERENCES

- [1] ANTSIPOV, G.V. et al., Yadernye konstanty (Nuclear Constants), No. 20, part 2 (1975) 3.
- [2] KON'SHIN, V.A. et al., Yadernye konstanty (Nuclear Constants), No. 16, (1974) 329.
- [3] MUGHABGHAB, S.F., GARBER D.I., BNL-325, 3d Ed., Vol. 1 (1973).
- [4] JAMES, J.D., AERE/NP-6 (1964).
- [5] HENNIES, H.H., IAEA Conf. on Nuclear Data for Reactors, Helsinki (1970) Vol. 1, p. 267.
- [6] STEHN, J.R., et al., BNL-325, 2nd Ed., Suppl. 2 (1965).
- [7] KOLAR, W., CARRARO, G., Conf. on Neutron Cross-Sections and Technology, Knoxville (1971) Vol. 2, p. 707.
- [8] BLONS, J. et al., Conf. on Neutron Cross-Sections and Technology, Knoxville (1971) Vol. 2, p. 836 and J. Nucl. Phys., Vol. 39 (1962) Vol. 51, p. 130.
- [9] MALYSHEV, A.V., Plotnost' urovnej i struktura atomnykh yader (Level Density and the Structure of Atomic Nuclei), Atomizdat, Moscow (1969).
- [10] BLOKHIN, A.I., IGNATYUK, A.V., Trudy III Vsesoyuznoj konferentsii po nejtronnoj fizike (Proceedings of the Third All-Union Conference on Neutron Physics), Kiev, 3 (1976) 3.
- [11] KRAVTSOV, V.A., Massy atomov i ehnergii svyazi yader (Masses of Atoms and Binding Energies of Nuclei), Atomizdat, Moscow (1974).
- [12] NEMIROVSKY, P.E., ADAMCHUK, Yu.V., J. Nucl. Phys., Vol. 39 (1962) p. 551.
- [13] SHUBIN, Yu.N., Byulleten' TsYaD 4 (1967) 304.
- [14] BABA, H., BABA, S., IAERI-1183 (1969).
- [15] LANG, I.M.B., LE COUTEUR, K.I., Proc. Phys. Soc., A (1954) Vol. 67, p. 586.
- [16] ERICSON, I., Adv. in Phys. (1960) Vol. 9, p. 425.
- [17] HANNA, G.C. et al., Atomic En. Review (1969) Vol. 7, p. 3.
- [18] SIMPSON, O.D., SHUMAN, R.P., Nucl. Sci. Eng. (1961) Vol. 11, p. 111.
- [19] PRINCE, A., Proc. of the IAEA Conf. on Nuclear Data for Reactors, Helsinki (1970) Vol. 2, p. 825.

- [20] KANER, M., YIFTAH, S., IA-1276 (1973).
- [21] KOLAR, W., THEOBALD, J.P., WARTENA, J.A., Conf. on Neutron Cross-Sections and Technology, Knoxville (1971) Vol. 2, p. 823.
- [22] SAUTER, G.D., BOWMAN, C.D., Phys. Rev. (1968) Vol. 174, p. 1413.
- [23] SIMPSON, O.D. et al. Conf. on Neutron Cross-Section and Technology, Vol. 2 (1966) p. 910 and IDO-17174 (1966).
- [24] STRUTINSKY, V.M., Nucl. Phys., A (1967) Vol. 95, p. 420.
- [25] BOHR, N., WHELLER, J., Phys. Rev. (1939) Vol. 54, p. 426.
- [26] HILL, R., WHELLER, J., Phys. Rev. (1953) Vol. 89, p. 1102.
- [27] LYNN, J.E., AERE-R-7468 (1974)
- [28] LYNN, J.E., Theory of Neutron Resonance Reactions, Clarendon Press, Oxford (1968) p. 396.
- [29] BLONS, J. et al., Proc. of the Conf. on Nuclear Data for Reactors, Helsinki (1970) Vol. 1, p. 469.
- [30] WESTON, L.W., TODD, J.H., Nucl. Sci. Eng. (1978) Vol. 65, p. 454.
- [31] SIMPSON, F.B., FLUHARTY, R.G., Bull. Am. Phys. Soc. (1958) Vol. 3, p. 176.
- [32] CRAIG, D.S., WESTCOTT, C.H., AECL-194° (1964) and GAN, J., Phys., Vol. 42 (1968) p. 2384.
- [33] SMITH, J.R., YOUNG, T.E., WASH-1136 (1969) p. 43.
- [34] PATTENDEN, N.T. et al., AERE-PR/NP-7 (1964) p. 6 and AERE-PR/NP-6 (1964) p. 10, BAPS, Vol. 11 (1964) p. 178.
- [35] TAKANE, H.J. Nucl. Sci. and Technol. (1971) Vol. 8, p. 656.

Part 4

Analysis of Experimental Data and Cross-Section
Calculations in the 0.1 and 15 MeV Energy Region

Abstract

In this preprint the authors analyse the experimental data available on the cross-sections and the quantity ν for ^{241}Pu over the 0.1-15 MeV range. They calculate the cross-sections from various theoretical models and, on the basis of experimental data and the calculation results, evaluate the cross-sections σ_t , σ_{nx} , σ_f , σ_γ , σ_n and the quantity ν for ^{241}Pu over the energy range 0.1-15 Mev.

79-7974
Translated from Russian

A.V. Lykov Institute of Heat and Mass Transfer
Academy of Sciences of the Byelorussian SSR

EVALUATION OF NUCLEAR DATA FOR ^{241}Pu IN THE
NEUTRON ENERGY REGION FROM 10^{-3} TO 15 MeV

V.A. Kon'shin, G.V. Antsipov, E.Sh. Sukhovitskij,
L.A. Bakhanovich, A.B. Klepatskij,
G.B. Morogovskij and Yu.V. Porodzinskij

Preprint No. 5, Part 4
Minsk 1979

1. THE FISSION CROSS-SECTION $\sigma_f(^{241}\text{Pu})$ OVER THE ENERGY RANGE
1 keV-15 MeV

Most of the existing measurements of the ^{241}Pu fission cross-section are relative. There are only two measurements, made by Szabo et al. [1-3] and covering the region 35 keV-2.6 MeV, which are absolute. Hence the best curve for the ratio $\frac{\sigma_f(^{241}\text{Pu})}{\sigma_f(^{235}\text{U})}$ was first obtained with the aid of the PREDA program [4], after which the evaluated curve for the ratio was used to derive the cross-section $\sigma_f(^{241}\text{Pu})$, taking account of our evaluated curve for $\sigma_f(^{235}\text{U})$ [5]. This curve for $\sigma_f(^{241}\text{Pu})$ was then employed, together with the absolute ^{241}Pu fission cross-section measurements, to obtain the final evaluated curve for $\sigma_f(^{241}\text{Pu})$.

In the region below 20 keV the available data are "continuous" in terms of energy and were measured by the time-of-flight method. Above 20 keV the measurements are obtained only at a few energy points.

1.1 Experimental data on $\sigma_f(^{241}\text{Pu})$ and the ratio $\frac{\sigma_f(^{241}\text{Pu})}{\sigma_f(^{235}\text{U})}$

1. Szabo et al. [1] made absolute measurements of the cross-section $\sigma_f(^{241}\text{Pu})$ in the energy range 35-970 keV, using monoenergetic neutrons obtained in a Van de Graaff accelerator. The neutron flux was measured with a directional counter, the efficiency of which was determined in three ways: by the manganese bath method (with an accuracy of 1.8%), by the associated particle method using the reaction $\text{T}(p,n)^3\text{He}$, and by the proton recoil method.

The number of ^{241}Pu nuclei was measured in two ways:

- (1) By counting the alpha particles in a well-defined geometry (2% accuracy);
- (2) By counting the number of spontaneous fissions (3.5% accuracy).

The measurement data on the number of nuclei obtained by the two methods coincided only to within $\pm 7\%$. The final accuracy attained by the authors in measuring the ^{241}Pu mass is $\pm 3.5\%$. Corrections for neutron scatter in the fission chamber walls and target-holder were

introduced by the Monte Carlo calculation technique. The experimental data for $\sigma_f(^{241}\text{Pu})$ obtained by the absolute method and the data on $\sigma_f(^{235}\text{U})$ measured during the same research are shown in Table 1.1.

Table 1.1
Experimental data for $\sigma_f(^{241}\text{Pu})$ and $\sigma_f(^{235}\text{U})$
obtained by Szabo et al. [1]

E_n (keV)	$\sigma_f(^{241}\text{Pu})$ (barn)	$\sigma_f(^{235}\text{U})$ (barn) (obtained by extrapolation)	$\sigma_f(^{241}\text{Pu})/\sigma_f(^{235}\text{U})$		$\sigma_f(^{241}\text{Pu})$ (barn) (taking the correc- tion from Ref. [2] into account)
			without corrections	with correc- tion in Ref. [2]	
1	2	3	4	5	6
35±4	2,67±0,13	1,940±0,064	1,376	1,334±0,085	2,64±0,13
50±5	2,41±0,12	1,765±0,053	1,365	1,328±0,083	2,39±0,12
88±4	2,08±0,11	1,605±0,058	1,296	1,258±0,086	2,06±0,11
130±20	2,04±0,11	1,500±0,046	1,360	1,320±0,087	2,02±0,11
177±10	1,93±0,09	1,400±0,044	1,379	1,337±0,082	1,91±0,09
218±8	1,73±0,08	1,320±0,044	1,311	1,270±0,077	1,71±0,08
239±7	1,74±0,08	1,295±0,035	1,344	1,302±0,080	1,72±0,08
300±12	1,61±0,07	1,240±0,043	1,298	1,257±0,075	1,59±0,07
344±10	1,58±0,07	1,210±0,045	1,306	1,264±0,079	1,56±0,07
463±12	1,46±0,07	1,170±0,035	1,248	1,207±0,074	1,44±0,07
476±10	1,52±0,07	1,167±0,045	1,302	1,260±0,080	1,50±0,07
604±30	1,43±0,06	1,145±0,035	1,249	1,216±0,069	1,42±0,06
687±29	1,42±0,06	1,135±0,035	1,251	1,218±0,069	1,41±0,06
808±29	1,50±0,07	1,135±0,035	1,322	1,278±0,078	1,48±0,07
970±25	1,54±0,07	1,190±0,035	1,294	1,252±0,072	1,52±0,07

2. Szabo, Leroy and Marguette [2] made absolute measurements of $\sigma_f(^{241}\text{Pu})$ over the energy range 1.18-2.63 MeV, using the same method as applied in Ref. [1]. The number of ^{241}Pu nuclei was determined with an accuracy better than 1%. Some slight changes were made in the case of ^{235}U and ^{241}Pu , as compared with the previous work. Destructive analysis of ^{241}Pu showed that its mass was 1% higher than was assumed in Ref. [1] (728 ± 10 µg). Hence the cross-section $\sigma_f(^{241}\text{Pu})$ obtained in Ref. [1] should be multiplied by 0.99, and the cross-section $\sigma_f(^{235}\text{U})$ by 1.02.

The experimental data on $\sigma_f(^{241}\text{Pu})$ obtained by Szabo et al. [2] are shown in Table 1.2.

Table 1.2

Experimental data for $\sigma_f(^{241}\text{Pu})$ obtained by Szabo et al. [2]

E_n (MeV)	$\sigma_f(^{241}\text{Pu})$ (barn)	$\sigma_f(^{235}\text{U})$ (barn) (measured in Ref. [2])	$\frac{\sigma_f(^{241}\text{Pu})}{\sigma_f(^{235}\text{U})}$
1	2	3	4
1,180±0,025	1,620±0,045	1,195±0,030	1,356±0,055
1,470±0,022	1,690±0,050	1,235±0,030	1,368±0,053
1,7000±0,021	1,710±0,050	1,253±0,035	1,365±0,055
2,010±0,019	1,670±0,050	1,290±0,030	1,295±0,049
2,240±0,017	1,580±0,050	1,275±0,030	1,239±0,049
2,630±0,016	1,540±0,055	1,240±0,030	1,242±0,054

3. In Ref. [3] Szabo et al. gives the final values of $\sigma_f(^{241}\text{Pu})$, which include the correction for determination of the number of nuclei in the sample, as mentioned in Ref. [2] (the data on $\sigma_f(^{241}\text{Pu})$ in Ref. [1] should be multiplied by 0.99), as well as the correction for variation in the efficiency of the directional counter at energies higher than 800 keV (this chiefly concerns the data given in Ref. [2]). The latter correction stems from the fact that further experiments were conducted in Ref. [3] so as to be able to calibrate the directional counter more exactly in the MeV energy range. For this purpose, up to 2.2 MeV use was made of the associated particle method, which showed that below 0.8 MeV there was no need to alter the calibration values for the efficiency obtained earlier, but that above 0.8 MeV the newly obtained results were 1-2% higher than the previous ones. Consequently, the cross-sections given in Refs [1,2] should be increased by this value in the neutron energy region above 0.8 MeV.

The final cross-sections $\sigma_f(^{241}\text{Pu})$ and $\sigma_f(^{235}\text{U})$ and the ratio $\frac{\sigma_f(^{241}\text{Pu})}{\sigma_f(^{235}\text{U})}$ derived by Szabo et al. in Refs [1, 2] are shown in Table 1.3.

Table 1.3

Experimental data obtained by Szabo et al. [1, 2] for $\sigma_f(^{241}\text{Pu})$,
 $\frac{\sigma_f(^{235}\text{U})}{\sigma_f(^{241}\text{Pu})}$ and $\frac{\sigma_f(^{241}\text{Pu})}{\sigma_f(^{235}\text{U})}$ as altered in Ref. [3]

E_n (keV)	$\sigma_f(^{241}\text{Pu})$ (barn)	$\sigma_f(^{235}\text{U})$ (barn) (obtained by extrapolation)	$\frac{\sigma_f(^{241}\text{Pu})}{\sigma_f(^{235}\text{U})}$
1	2	3	4
35±4	2,64±0,13	1,940±0,064	1,361±0,085
50±5	2,39±0,12	1,765±0,053	1,354±0,085
88±4	2,06±0,11	1,605±0,058	1,283±0,087
130±20	2,02±0,11	1,500±0,055	1,347±0,087
177±10	1,91±0,09	1,390±0,044	1,374±0,082
218±8	1,71±0,08	1,320±0,044	1,295±0,080
239±7	1,72±0,08	1,290±0,034	1,333±0,080
300±12	1,59±0,07	1,240±0,043	1,282±0,080
344±10	1,56±0,07	1,215±0,045	1,284±0,080
463±12	1,44±0,07	1,175±0,035	1,226±0,076
476±10	1,50±0,07	1,170±0,045	1,282±0,082
604±30	1,42±0,06	1,145±0,035	1,240±0,070
687±29	1,41±0,06	1,135±0,035	1,242±0,070
808±29	1,49±0,07	1,135±0,035	1,313±0,078
970±25	1,52±0,07	1,180±0,035	1,288±0,075
1180±25	1,620±0,045	1,197±0,035	1,353±0,056
1470±22	1,707±0,050	1,240±0,035	1,377±0,055
1700±21	1,739±0,050	1,285±0,035	1,352±0,055
2010±19	1,700±0,050	1,325±0,035	1,283±0,049
2240±17	1,613±0,050	1,303±0,030	1,238±0,049
2630±16	1,569±0,055	1,268±0,030	1,237±0,053

4. Kappeler and Pflöschinger measured the ratio $\sigma_f(^{241}\text{Pu})/\sigma_f(^{235}\text{U})$ over the energy range 13.7-1133 keV and published their preliminary data in Ref. [6]; their final data, which differ from the preliminary figures by 8% on account of an error in the layer thickness, were published in Ref. [7]. To measure the ratio they used two gas scintillation chambers and applied the time-of-flight method. As the neutron source they employed the $^7\text{Li}(p,n)^7\text{Be}$ reaction. The measurement errors contain the following components: determination of the number of ^{241}Pu nuclei (1.8%); losses through absorption by the sample (1.0%); correction for background

from the reaction $n, \gamma(0.4\%)$, and asymmetry in the neutron flux (0.8%). The overall systematic error in measurement was $\pm 2.6\%$. The statistical errors are 1.2-2.7%. The experimental data obtained by Käppeler and Pfletschinger are shown in Table 1.4.

Table 1.4

Experimental data obtained by Käppeler and Pfletschinger [7]
for the ratio $\sigma_f(^{241}\text{Pu})/\sigma_f(^{235}\text{U})$

E_n (keV)	$\frac{\sigma_f(^{241}\text{Pu})}{\sigma_f(^{235}\text{U})}$	Statistical error (%)	E_n (keV)	$\frac{\sigma_f(^{241}\text{Pu})}{\sigma_f(^{235}\text{U})}$	Statistical error (%)
1	2	3	4	5	6
13,7	$1,252 \pm 0,050^*$	3,0	125,2	$1,373 \pm 0,040$	1,4
15,7	$1,277 \pm 0,048$	2,7	137,3 ± 14	$1,353 \pm 0,041$	1,5
17,6 ± 2	$1,318 \pm 0,047$	2,5	151,1	$1,337 \pm 0,041$	1,6
19,5	$1,205 \pm 0,043$	2,4	166,9	$1,360 \pm 0,042$	1,7
21,5	$1,306 \pm 0,045$	2,3	192 ± 16	$1,382 \pm 0,044$	1,8
23,9	$1,222 \pm 0,039$	1,8	230 ± 19	$1,360 \pm 0,040$	1,4
26,8 ± 3	$1,343 \pm 0,042$	1,7	273 ± 20	$1,396 \pm 0,042$	1,5
29,7	$1,258 \pm 0,038$	1,6	324 ± 29	$1,380 \pm 0,044$	1,9
32,5	$1,243 \pm 0,039$	1,7	388 ± 18	$1,261 \pm 0,039$	1,7
35,4 ± 4	$1,241 \pm 0,038$	1,6	436 ± 22	$1,257 \pm 0,039$	1,6
38,9	$1,279 \pm 0,038$	1,5	486 ± 25	$1,315 \pm 0,039$	1,4
42,7	$1,290 \pm 0,038$	1,4	535 ± 32	$1,305 \pm 0,036$	0,9
46,7	$1,280 \pm 0,037$	1,3	584 ± 23	$1,265 \pm 0,038$	1,1
51,7 ± 5	$1,241 \pm 0,036$	1,3	633 ± 29	$1,320 \pm 0,039$	1,5
56,9	$1,238 \pm 0,036$	1,3	678 ± 33	$1,287 \pm 0,037$	1,3
63,2	$1,225 \pm 0,036$	1,2	740 ± 31	$1,353 \pm 0,043$	1,8
69,8	$1,305 \pm 0,038$	1,3	790 ± 38	$1,320 \pm 0,043$	-
77,4	$1,314 \pm 0,038$	1,3	870 ± 32	$1,320 \pm 0,041$	-
84,6	$1,306 \pm 0,038$	1,4	945 ± 40	$1,229 \pm 0,038$	-
93,6	$1,312 \pm 0,038$	1,2	1035 ± 40	$1,263 \pm 0,042$	-
103,8 ± 10	$1,338 \pm 0,038$	1,2	1133 ± 49	$1,267 \pm 0,042$	-
113,5	$1,345 \pm 0,039$	1,3	-	-	-

*/ The total error is obtained by mean square addition of the statistical and systematic (2.6%) errors.

5. White et al. [8] measured $\sigma_f(^{241}\text{Pu})/\sigma_f(^{235}\text{U})$ at neutron energies of 40, 67, 127, 312 and 505 keV, using a double ionization chamber. The thickness of the ^{241}Pu layer was determined by alpha radiation analysis, direct weighing and calorimetry. The accuracy attained in determining the layer thickness was $\pm 2.0\%$. Other sources of error are statistical errors (1.0%); the scattering correction (0.1%); foil thickness correction (0.5-1.0%); extrapolation of the fragment spectrum to zero shift (0.2-0.5%); and the variation in neutron flux along the foil (0.1%). The total error in measuring the ratio is $\pm 2.5\%$.

The numerical data are given in Table 1.5.

Table 1.5

The ratio $\frac{\sigma_f(^{241}\text{Pu})}{\sigma_f(^{235}\text{U})}$ as measured by White et al. [8]

E_n (keV)	$\frac{\sigma_f(^{241}\text{Pu})}{\sigma_f(^{235}\text{U})}$	$\sigma_f(^{235}\text{U})$ (barn) (measured in Ref. [9])
40 \pm 10	1,310 \pm 0,033	2,10 \pm 0,06
67 \pm 10	1,330 \pm 0,033	1,79 \pm 0,05
127 \pm 7	1,360 \pm 0,034	1,54 \pm 0,04
312 \pm 7	1,300 \pm 0,032	1,30 \pm 0,03
505 \pm 10	1,260 \pm 0,031	1,17 \pm 0,03

6. White and Warner [10] measured $\sigma_f(^{241}\text{Pu})/\sigma_f(^{235}\text{U})$ at neutron energies of 1.0, 2.25, 5.4 and 14.1 MeV, using the sandwich technique. The total measurement error is $\pm 2.0\%$ and consists of the error due to the correction for determination of the total counting rate, uncertainty in determining the number of nuclei in the fissile materials, and the counting statistics. The measured ratios $\sigma_f(^{241}\text{Pu})/\sigma_f(^{235}\text{U})$ are shown in Table 1.6.

Table 1.6

The ratio $\sigma_f(^{241}\text{Pu})/\sigma_f(^{235}\text{U})$ obtained by White et al. [10]

E_n (MeV)	$\sigma_f(^{241}\text{Pu})/\sigma_f(^{235}\text{U})$
1,00	1,356 \pm 0,027
2,25	1,325 \pm 0,026
5,40	1,290 \pm 0,026
14,10	1,119 \pm 0,022

7. Smith et al. [11] measured the ratio $\sigma_f(^{241}\text{Pu})/\sigma_f(^{235}\text{U})$ in the 0.12-21.0 MeV range, using a spherical ionization chamber and two layers of ^{241}Pu and ^{235}U positioned one behind the other. The nuclear masses were determined with an accuracy of $\pm 3\%$. Other sources of error were uncertainties in the corrections for impurities in the plutonium sample, self-absorption and so forth, which amounted to $\pm 2\%$. The overall accuracy attained in determining the ratio was $\pm 5\%$. Table 1.7 shows the measured values of the ratio $\sigma_f(^{241}\text{Pu})/\sigma_f(^{235}\text{U})$.

Table 1.7

The ratio $\sigma_f(^{241}\text{Pu})/\sigma_f(^{235}\text{U})$ as obtained by Smith et al. [11]

E_n (MeV)	$\sigma_f(^{241}\text{Pu})/\sigma_f(^{235}\text{U})$ ($\pm 5\%$)
1	2
0,12 \pm 0,03	1,39 \pm 0,07
0,155 \pm 0,035	1,31 \pm 0,07
0,27 \pm 0,03	1,40 \pm 0,07
0,40 \pm 0,06	1,40 \pm 0,07
0,43 \pm 0,10	1,26 \pm 0,06
0,528 \pm 0,094	1,40 \pm 0,07
0,75 \pm 0,31	1,39 \pm 0,07
1,00 \pm 0,23	1,39 \pm 0,07
1,50 \pm 0,20	1,43 \pm 0,07
2,01 \pm 0,15	1,37 \pm 0,07
2,45 \pm 0,15	1,33 \pm 0,07
3,01 \pm 0,13	1,29 \pm 0,06
3,50 \pm 0,12	1,31 \pm 0,06
4,00 \pm 0,11	1,33 \pm 0,06
4,49 \pm 0,10	1,31 \pm 0,06

Table 1.7 cont.

I	2
5,00 \pm 0,24	1,40 \pm 0,07
5,43 \pm 0,34	1,43 \pm 0,07
6,02 \pm 0,28	1,38 \pm 0,07
6,30 \pm 0,08	1,38 \pm 0,07
6,52 \pm 0,25	1,32 \pm 0,07
6,54 \pm 0,08	1,35 \pm 0,07
7,00 \pm 0,23	1,28 \pm 0,06
7,42 \pm 0,21	1,25 \pm 0,06
8,01 \pm 0,19	1,26 \pm 0,06
8,22 \pm 0,06	1,26 \pm 0,06
8,53 \pm 0,06	1,27 \pm 0,06
12,4 \pm 0,3	1,21 \pm 0,06
14,4 \pm 0,6	1,18 \pm 0,06
17,0 \pm 0,5	1,15 \pm 0,06
18,0 \pm 0,4	1,16 \pm 0,06
19,0 \pm 0,3	1,17 \pm 0,06
20,0 \pm 0,25	1,17 \pm 0,06
21,0 \pm 0,20	1,21 \pm 0,06

8. Perkin et al. [12] measured $\sigma_f(^{241}\text{Pu})$ with an Sb-Be source in absolute terms. The source neutron yield was measured with a manganese bath ($\pm 0.6\%$ accuracy), and an oil bath ($\pm 2.0\%$ accuracy), as well as by comparing these results with a ^{240}Pu source calibrated with a boron prism ($\pm 1.5\%$ accuracy). The number of ^{241}Pu nuclei was determined to within an accuracy of $\pm 2.0\%$. The ^{241}Pu fission cross-section obtained is 2.83 ± 0.21 barn between 24 and 26 keV. The ratio $\sigma_f(^{241}\text{Pu})/\sigma_f(^{235}\text{U})$ is 1.31 ± 0.12 , if the $\sigma_f(^{235}\text{U})$ cross-section is taken as 2.16 ± 0.10 barn at 24-26 keV.

9. Butler and Sjoblom [13] measured the ratio $\sigma_f(^{241}\text{Pu})/\sigma_f(^{235}\text{U})$ over the energy range 0.02-1.80 MeV, using a gas scintillation counter with the layers pressed together, and also employing $^7\text{Li}(p,n)$ as the neutron source.

The measurement error for this ratio is composed of the error in determining the mass of the sample ($\sim 2\%$), the uncertainty in the correction for the number of fissions producing pulses invisible against

the alpha particle background (~5%); the uncertainty in the background (~5% below 150 keV), and the statistical errors (~1% above 150 keV and ~3% below 150 keV). The authors cite data only for $\sigma_f(^{241}\text{Pu})$ and do not give the experimentally measured ratios, which sharply reduces the value of their work. For normalization purposes Butler et al. used data obtained by Allen and Henkal [14] and data published in the BNL-325 report [15]. The cross-section $\sigma_f(^{241}\text{Pu})$ obtained in this way is shown in Table 1.8.

Table 1.8

The fission cross-section $\sigma_f(^{241}\text{Pu})$ measured by Butler et al. [13]

E_n (keV)	$\sigma_f(^{241}\text{Pu})$ (barn) [13]	$\sigma_f(^{235}\text{U})$ (barn) (used in Ref. [13])	$\frac{\sigma_f(^{241}\text{Pu})}{\sigma_f(^{235}\text{U})}$
1	2	3	4
20	4,80	2,94	1,63±0,15
40	4,30	2,46	1,75±0,16
60	3,50	2,16	1,62±0,15
80	3,10	2,07	1,50±0,14
100	2,90	1,88	1,54±0,14
130	2,60	1,67	1,56±0,14
160	2,27	1,58	1,44±0,13
200	2,09	1,49	1,40±0,10
250	1,94	1,40	1,38±0,10
300	1,83	1,34	1,36±0,10
400	1,70	1,28	1,33±0,10
500	1,62	1,24	1,31±0,09
600	1,59	1,20	1,33±0,10
700	1,56	1,19	1,33±0,10
800	1,59	1,18	1,35±0,10
900	1,60	1,19	1,34±0,10
1000	1,61	1,22	1,32±0,10
1100	1,62	1,27	1,28±0,09
1200	1,67	1,28	1,30±0,09
1300	1,74	1,28	1,36±0,10
1400	1,77	1,29	1,37±0,10
1500	1,78	1,30	1,37±0,10
1600	1,78	1,31	1,36±0,10
1700	1,79	1,31	1,37±0,10
1800	1,79	1,32	1,36±0,10

10. Kazarinova et al. [16] made absolute measurements of the cross-section $\sigma_f(^{241}\text{Pu})$ at 14.6 MeV, determining the neutron flux from the reaction $T(d,n)^4\text{He}$ by counting the alpha particles, and also measured it with respect to ^{238}U at 2.5 MeV by means of a double fission chamber. The ^{238}U fission cross-section was taken as equal to 0.58 barn at 2.5 MeV [15]. The values obtained by the authors for $\sigma_f(^{241}\text{Pu})$ are 1.2 ± 0.2 barn at 2.5 MeV and 2.05 ± 0.10 barn at 14.6 MeV. The ratios $\sigma_f(^{241}\text{Pu})/\sigma_f(^{235}\text{U})$ calculated from the measured values of $\sigma_f(^{241}\text{Pu})$ and $\sigma_f(^{235}\text{U})$, equal to 1.246 barn at 2.5 MeV and 2.181 barn at 14.6 MeV, are: 0.963 ± 0.160 and 0.940 ± 0.066 at 2.5 and 14.6 MeV, respectively. They are substantially lower than the results of other measurements.

11. Behrens and Carlson [17] recently reported measurement of $\sigma_f(^{241}\text{Pu})$ relative to $\sigma_f(^{235}\text{U})$ over the range 0.001-30.0 MeV by means of the threshold method. Use was made of the time-of-flight method in a linear electron accelerator, fission ionization chambers with more than 90% efficiency being used as the detectors. The recording efficiency over the whole of the measured energy region varied by not more than 0.75%. In the threshold method use was made of two fission chambers: one contained a mixture of the two isotopes studied, while the other had layers of one single pure isotope. The method makes it possible to eliminate, or at least substantially to reduce, errors inherent in other methods. The authors measured the ratio $\frac{\sigma_f(^{238}\text{U})}{\sigma_f(^{241}\text{Pu})}$ which proved equal to 0.3484 ± 0.0055 between 1.75 and 4.00 MeV, and $\frac{\sigma_f(^{238}\text{U})}{\sigma_f(^{235}\text{U})} = 0.4422 \pm 0.0039$ over the same energy range, which gives a normalized value of 1.269 ± 0.023 for $\frac{\sigma_f(^{241}\text{Pu})}{\sigma_f(^{235}\text{U})}$ over the range 1.75-4.00 MeV. Measurement of the ratio $\frac{\sigma_f(^{241}\text{Pu})}{\sigma_f(^{235}\text{U})}$ in the thermal energy region yields 1.772 ± 0.044 , which is 1.8% higher than Lemmel's evaluation [18] i.e. 1.740 ± 0.013 .

Behrens and Carlson's data are shown in Table 1.9 for 1, 2.25, 5.4 and 14.1 MeV, and in Figs 1.1-1.3 which indicate other authors' experimental data for the energy range 0.1-30.0 MeV.

Table 1.9

Experimental data obtained by Behrens and Carlson [17]

E_n (MeV)	$\frac{\sigma_f(^{241}\text{Pu})}{\sigma_f(^{235}\text{U})}$
1,0	1,291 \pm 0,027
2,25	1,262 \pm 0,027
5,40	1,273 \pm 0,035
14,10	1,070 \pm 0,038

12. Fursov et al. [19] reported measurement of the ratio $\frac{\sigma_f(^{241}\text{Pu})}{\sigma_f(^{235}\text{U})}$ over the energy range 0.024-7.4 MeV using an electrostatic accelerator. The ratio was measured in two stages: during the first stage an ionization chamber was used to study the energy dependence of the ratio, while at the second stage the authors made absolute measurements of the ratio by means of the glass detector technique in a reactor thermal column. The total error in the ratio measurement was 1.9%, though it increased to 2.2-2.4% at the boundaries of the neutron energy range studied. The total error in the resultant data was made up of the error in determination of the number of fissile nuclei (1.35%) [the main contribution to this error component (1.13%) was made by uncertainty in the neutron spectrum temperature ($\pm 11^\circ\text{C}$)]; missing out of glass detectors (0.4%); the correction for the angular anisotropy of fission (0.3%); statistical error in fast neutron measurements (0.5%); fission of the minority isotopes (0.22%); scattered neutron background (0.3%); neutron background of the experimental laboratory (0.24%); background due to neutrons accompanying the (p,n) reaction (0.22%) and inelastic scattering (0.20%). The total error obtained by the glass procedure amounted to 1.65%. To this was added the error in the energy dependence of the fission cross-section ratios (0.5-1.8%) and the error involved in normalizing the energy dependence curve to the reference values (0.25%).

The experimental data obtained by Fursov et al. are shown in Tables 1.10 and 1.11.

Table 1.10

The ratio $\frac{\sigma_f(^{241}\text{Pu})}{\sigma_f(^{235}\text{U})}$ obtained by Fursov et al. [19]
using the glass detector method

E_n (MeV)	$\frac{\sigma_f(^{241}\text{Pu})}{\sigma_f(^{235}\text{U})}$	E_n (MeV)	$\frac{\sigma_f(^{241}\text{Pu})}{\sigma_f(^{235}\text{U})}$
1	2	3	4
0,127±0,020	1,344±1,66%	3,000±0,084	1,2930±1,65%
0,320±0,040	1,3439±1,64%	4,000±0,146	1,2957±1,95%
0,500±0,034	1,3103±1,61%	5,000±0,126	1,3010±1,67%
1,000±0,031	1,3038±1,70%	6,000±0,142	1,3452±1,69%
1,500±0,054	1,4011±1,73%	7,000±0,173	1,2385±1,74%
2,250±0,072	1,3024±1,64%	-	-

13. Carlson et al. [20] measured $\sigma_f(^{241}\text{Pu})$ relative to the $^6\text{Li}(n,\alpha)$ cross-section over the range from thermal energies up to 70 keV. They measured $\sigma_f(^{235}\text{U})$ at the same time, which makes it possible to derive the ratio $\frac{\sigma_f(^{241}\text{Pu})}{\sigma_f(^{235}\text{U})}$ from the data obtained in the experiment. Carlson's experimental data are shown in Table 1.10a. The data for the ratio σ_f between 20 and 60 keV tally up to an accuracy better than 2% with Fursov's data [17] at some of the energy points.

Table 1.10a

Experimental data obtained by Carlson et al. [20]
for the ratio $\frac{\sigma_f(^{241}\text{Pu})}{\sigma_f(^{235}\text{U})}$

E_n (keV)	$\sigma_f(^{241}\text{Pu})$ (barn)	$\sigma_f(^{235}\text{U})$ (barn)	$\frac{\sigma_f(^{241}\text{Pu})}{\sigma_f(^{235}\text{U})}$
1 - 2	3,22 ± 0,25	6,966 ± 0,130	1,210 ± 0,044
10 - 20	3,02 ± 0,09	2,315 ± 0,044	1,3045 ± 0,043
20 - 30	2,62 ± 0,07	2,07 ± 0,04	1,3035 ± 0,052
40 - 50	2,28 ± 0,08	1,72 ± 0,06	1,326 ± 0,065
50 - 60	2,75 ± 0,07	1,69 ± 0,06	1,272 ± 0,065
60 - 70	2,11 ± 0,07	1,69 ± 0,06	1,249 ± 0,065

Table 1.11

Fission cross-section ratio for $^{241}\text{Pu}/^{235}\text{U}$ obtained by
Fursov et al. [19], using an ionization chamber

E_n (MeV)	$\sigma_f(^{241}\text{Pu})/\sigma_f(^{235}\text{U})$	E_n (MeV)	$\sigma_f(^{241}\text{Pu})/\sigma_f(^{235}\text{U})$	E_n (MeV)	$\sigma_f(^{241}\text{Pu})/\sigma_f(^{235}\text{U})$
1	2	3	4	5	6
0,024±0,012	1,2967±2,42%	0,860±0,031	1,3570±1,83%	2,800±0,079	1,2869±1,82%
0,040±0,014	1,3060±2,22%	0,900±0,031	1,3368±1,83%	2,900±0,082	1,2858±1,82%
0,050±0,017	1,2961±2,19%	0,950±0,031	1,3137±1,83%	3,000±0,084	1,2858±1,84%
0,080±0,021	1,3298±2,16%	1,000±0,031	1,3015±1,82%	3,100±0,086	1,2810±1,82%
0,100±0,025	1,3463±2,12%	1,050±0,034	1,2964±1,83%	3,200±0,088	1,2783±1,82%
0,115±0,026	1,3562±1,95%	1,100±0,037	1,3007±1,82%	3,300±0,091	1,2753±1,84%
0,127±0,020	1,3597±1,83%	1,150±0,040	1,3183±1,82%	3,400±0,093	1,2794±1,84%
0,150±0,020	1,3634±1,81%	1,200±0,042	1,3317±1,82%	3,600±0,192	1,2829±1,89%
0,180±0,020	1,3597±1,96%	1,250±0,044	1,3603±1,82%	3,800±0,182	1,2855±1,97%
0,210±0,019	1,3568±1,91%	1,300±0,045	1,3782±1,82%	4,000±0,146	1,2900±1,90%
0,240±0,018	1,3787±1,82%	1,350±0,046	1,3942±1,83%	4,200±0,141	1,2927±1,90%
0,270±0,018	1,3827±1,85%	1,400±0,047	1,4056±1,82%	4,400±0,132	1,2886±1,92%
0,300±0,018	1,3597±1,84%	1,450±0,048	1,3990±1,84%	4,600±0,131	1,2951±1,90%
0,320±0,040	1,3562±1,82%	1,500±0,049	1,3988±1,81%	4,800±0,125	1,2949±1,91%
0,350±0,038	1,3391±1,82%	1,600±0,060	1,3977±1,81%	5,000±0,126	1,3012±1,91%
0,380±0,037	1,3306±1,84%	1,700±0,061	1,3793±1,84%	5,200±0,129	1,3044±1,90%
0,420±0,036	1,3205±1,85%	1,800±0,063	1,3712±1,81%	5,400±0,131	1,3175±1,89%
0,460±0,035	1,4179±1,83%	1,900±0,066	1,3618±1,81%	5,600±0,135	1,3285±1,90%
0,500±0,034	1,3253±1,83%	2,000±0,068	1,3371±1,81%	5,800±0,138	1,3300±1,83%
0,540±0,033	1,3215±1,87%	2,100±0,070	1,3245±1,81%	6,000±0,142	1,3274±1,94%
0,580±0,033	1,3157±1,83%	2,200±0,071	1,3073±1,83%	6,200±0,147	1,3189±1,91%
0,620±0,032	1,3253±1,94%	2,250±0,072	1,3063±1,81%	6,400±0,152	1,2906±1,93%
0,660±0,032	1,3197±1,84%	2,300±0,073	1,3105±1,81%	6,600±0,160	1,2559±1,95%
0,700±0,032	1,3180±1,85%	2,400±0,074	1,2886±1,84%	6,800±0,167	1,2361±2,01%
0,740±0,032	1,3306±1,82%	2,500±0,075	1,2937±1,83%	7,000±0,173	1,2209±2,05%
0,780±0,031	1,3525±1,82%	2,600±0,077	1,2895±1,82%	7,200±0,178	1,1990±2,11%
0,820±0,031	1,3570±1,83%	2,700±0,078	1,2914±1,82%	7,400±0,183	1,1864±2,16%

1.2 Evaluated values of the ratio $\sigma_f(^{241}\text{Pu})/\sigma_f(^{235}\text{U})$ and $\sigma_f(^{241}\text{Pu})$

Figures 1.1-1.3 plot the experimental values of the ratio $\sigma_f(^{241}\text{Pu})/\sigma_f(^{235}\text{U})$ over the energy range 1 keV-20 MeV. It is clear from these diagrams that up to 30 keV there is a certain discrepancy - though admittedly it lies within the limits of the experimental errors - between the results of the continuous measurements (Blons's data [21]) and measurements at certain points between 10 and 30 keV. Käppeler's data are approximately 5% below those of Blons.

The data recently obtained by Fursov et al. [19] and Behrens et al. [17] for the fission cross-section ratio between 0.1 and 10 MeV show a clear-cut structure, i.e. a rise at 0.25, 0.75, 1.45 and 5.5 MeV and a drop at 0.45, 1.0, 3.5 and 9.0 MeV. Fursov's data also show this structure and tally to within 1% with Behrens's data up to 1 MeV. Szabo's data for this energy region are systematically ~5% lower than the data in Refs [17, 19]. Above 1 MeV there is a systematic difference between the data obtained by Fursov et al. and Behrens et al., especially marked between 3 and 5 MeV (~5%). Behrens's data for 1, 2.25 and 14.1 MeV are 5% lower than those obtained by White and Warner.

The evaluated curve was based on the most accurate data for the ratios obtained by Fursov, Behrens and Käppeler, as well as those of White, which as a whole agree to within 3-5%. Above 5 MeV the errors in Fursov's data may sharply increase and it seems therefore preferable to use those of Behrens et al.

The error in the evaluated ratio curve was determined by mean-square addition of the systematic error, which was taken as ~2%, and the statistical error determined from the spread of the experimental points used for the evaluation. The overall error in the fission cross-section ratio curve is ~2.5-5%.

The evaluated data for $\sigma_f(^{241}\text{Pu})/\sigma_f(^{235}\text{U})$, $\sigma_f(^{241}\text{Pu})$ and $\sigma_f(^{235}\text{U})$ are shown in Table 1.12. As the fission cross-section $\sigma_f(^{235}\text{U})$ use was made of our latest evaluated data, while the cross-section $\sigma_f(^{239}\text{Pu})$ over the range 0.1-2.0 MeV was obtained with allowance for the absolute measurements made by Szabo et al.

A comparison of the evaluated $\sigma_f(^{241}\text{Pu})$ data with the results obtained by Kaner and Yiftah (Figs 1.4-1.5) shows satisfactory agreement.

Table 1.12

Evaluations of $\sigma_f(^{235}\text{U})$, $\sigma_f(^{241}\text{Pu})/\sigma_f(^{235}\text{U})$ and $\sigma_f(^{241}\text{Pu})$ over the energy range 1 keV-20 MeV

E_n (keV)	$\sigma_f(^{235}\text{U})$ (barn)	$\sigma_f(^{241}\text{Pu})/\sigma_f(^{235}\text{U})$	$\sigma_f(^{241}\text{Pu})$ (barn)
1	2	3	4
1 - 2	7,10±0,22	1,246±0,060*	9,85±0,26
2 - 3	5,27±0,20	1,288±0,075*	6,79±0,29
3 - 4	4,73±0,15	1,338±0,070*	6,33±0,27
4 - 5	4,15±0,14	1,392±0,074*	5,57±0,25
5 - 6	3,70±0,15	1,262±0,077*	4,67±0,20
6 - 7	3,31±0,12	1,414±0,070*	4,68±0,19
7 - 8	3,26±0,11	1,248±0,071*	4,07±0,18
8 - 9	2,70±0,10	1,454±0,071*	4,23±0,18
9 -10	2,03±0,11	1,251±0,071*	3,79±0,17
10 - 20	2,44±0,09	1,278±0,062*	3,12±0,16
20 - 30	2,10±0,08	1,363±0,033*	2,82±0,17
30 - 40	2,00±0,06	1,305±0,033	2,610±0,105
40 - 50	1,915±0,057	1,310±0,032	2,503±0,100
50 - 60	1,823±0,055	1,285±0,031	2,343±0,093
60 - 70	1,749±0,052	1,295±0,035	2,265±0,098
70 - 80	1,677±0,050	1,325±0,030	2,222±0,094
80 - 90	1,617±0,049	1,336±0,032	2,160±0,091
90 -100	1,575±0,047	1,348±0,033	2,123±0,092
100	1,555±0,047	1,348±0,040	2,096±0,090
120	1,522±0,046	1,360±0,040	2,070±0,088
140	1,478±0,044	1,368±0,040	2,022±0,086
160	1,433±0,043	1,374±0,040	1,976±0,084
180	1,399±0,042	1,378±0,040	1,928±0,082
200	1,366±0,041	1,380±0,040	1,885±0,080
220	1,336±0,040	1,381±0,040	1,845±0,080
240	1,311±0,040	1,382±0,035	1,812±0,075
260	1,289±0,039	1,381±0,030	1,780±0,070
280	1,270±0,038	1,377±0,030	1,749±0,070
300	1,250±0,038	1,369±0,030	1,710±0,070

*/

The data were not obtained by direct measurement

Table 1.12 cont.

1	2	3	4
0,320	1,233±0,037	1,353±0,032	1,668±0,070
0,340	1,221±0,037	1,342±0,035	1,639±0,072
0,360	1,215±0,036	1,330±0,038	1,616±0,072
0,380	1,214±0,036	1,322±0,035	1,605±0,065
0,400	1,212±0,036	1,316±0,035	1,595±0,065
0,420	1,206±0,036	1,312±0,035	1,582±0,063
0,440	1,196±0,036	1,310±0,035	1,567±0,063
0,460	1,196±0,036	1,309±0,035	1,552±0,063
0,480	1,176±0,035	1,308±0,035	1,538±0,063
0,500	1,166±0,035	1,308±0,035	1,525±0,060
0,550	1,146±0,034	1,310±0,033	1,501±0,059
0,600	1,128±0,034	1,314±0,033	1,432±0,058
0,650	1,113±0,034	1,320±0,033	1,469±0,057
0,700	1,105±0,033	1,330±0,032	1,470±0,057
0,750	1,104±0,033	1,340±0,032	1,479±0,057
0,800	1,117±0,034	1,350±0,032	1,503±0,057
0,850	1,144±0,034	1,352±0,033	1,547±0,057
0,900	1,180±0,035	1,320±0,033	1,558±0,058
0,950	1,204±0,036	1,295±0,033	1,559±0,060
1,00	1,215±0,036	1,296±0,033	1,563±0,060
1,10	1,220±0,037	1,294±0,032	1,579±0,060
1,20	1,226±0,037	1,332±0,033	1,633±0,063
1,40	1,239±0,037	1,370±0,034	1,722±0,069
1,60	1,258±0,038	1,382±0,034	1,739±0,069
1,80	1,276±0,038	1,344±0,033	1,715±0,060
2,00	1,284±0,038	1,313±0,033	1,685±0,060
2,20	1,278±0,038	1,293±0,033	1,652±0,060
2,40	1,259±0,038	1,276±0,037	1,605±0,060
2,60	1,237±0,037	1,265±0,037	1,565±0,060
2,80	1,221±0,037	1,259±0,037	1,536±0,061
3,00	1,205±0,036	1,254±0,037	1,511±0,060
3,20	1,195±0,036	1,252±0,037	1,497±0,060
3,40	1,183±0,035	1,252±0,038	1,481±0,060

Table 1.12 cont.

1	2	3	4
3,60	1,171±0,035	1,253±0,038	1,467±0,060
3,80	1,159±0,035	1,255±0,038	1,455±0,060
4,00	1,147±0,034	1,257±0,038	1,442±0,060
4,50	1,117±0,034	1,264±0,038	1,412±0,060
5,00	1,087±0,033	1,275±0,037	1,386±0,060
5,50	1,052±0,032	1,298±0,040	1,355±0,060
6,00	1,139±0,034	1,292±0,040	1,472±0,062
6,50	1,386±0,042	1,230±0,045	1,705±0,082
7,00	1,600±0,048	1,164±0,045	1,862±0,094
7,50	1,755±0,053	1,130±0,045	1,983±0,099
8,00	1,820±0,055	1,105±0,045	2,011±0,100
8,50	1,824±0,055	1,094±0,045	1,995±0,100
9,00	1,812±0,054	1,098±0,045	1,990±0,100
9,50	1,800±0,054	1,120±0,045	2,016±0,100
10,00	1,796±0,054	1,150±0,045	2,054±0,100
10,50	1,776±0,053	1,193±0,050	2,119±0,105
11,00	1,770±0,053	1,197±0,050	2,119±0,105
11,50	1,769±0,053	1,187±0,050	2,100±0,105
12,00	1,769±0,053	1,167±0,050	2,063±0,104
13,00	1,922±0,058	1,121±0,050	2,155±0,114
14,00	2,063±0,062	1,075±0,050	2,218±0,123
15,00	2,108±0,063	1,037±0,050	2,186±0,124
16,00	2,087±0,063	1,005±0,050	2,097±0,120
17,00	2,032±0,061	0,930±0,050	2,012±0,120
18,00	1,977±0,059	0,985±0,050	1,947±0,120
19,00	1,956±0,059	0,985±0,050	1,927±0,120
20,00	2,015±0,060	0,989±0,050	1,993±0,120

2. EVALUATION OF THE TOTAL INTERACTION CROSS-SECTION σ_t , INELASTIC INTERACTION CROSS-SECTION σ_{nx} , AND ELASTIC SCATTERING CROSS-SECTION σ_n (^{241}Pu) IN THE ENERGY RANGE 0.1-15 MeV

There are no measurements at all for the cross-sections σ_t , σ_{nx} and σ_n for the ^{241}Pu nucleus over the energy range 0.1-15.0 MeV. To obtain such data it is necessary to use either the optical model or the data for the neighbouring ^{239}Pu nucleus, for which experiments have been carried out. Use of the optical model will be discussed below when we consider inelastic neutron scattering. We would only point out that the potentials used by different investigators do not provide agreement on the strength functions that is satisfactory from the standpoint of the evaluation, hence use was made of the data for the ^{239}Pu nucleus instead. The reason for this is the only slight difference in the masses of the nuclei, plus the fact that they have close strength functions S_0 and S_1 in the low-energy region. The evaluation was based on data obtained by us in Ref. [23], which gave a smooth fit to the calculation results in the unresolved resonance region.

The evaluated data for σ_t , σ_{nx} , σ_n are plotted in Fig. 2.1 and given in Table 2.1 (to facilitate use the Table also shows the cross-sections for all the possible reactions). The accuracy of the evaluated data is 10%, but this figure is somewhat arbitrary and based on the accuracy of the ^{239}Pu data.

Figs 2.2-2.4 show a comparison with the results of other evaluations (Kaner and Yiftah [22] and Prince [24]).

Table 2.1

Evaluated ²⁴¹Pu cross-section data for the energy range 0.1-15 MeV

E (MeV)	σ_t (barn)	σ_n (barn)	σ_{nx} (barn)	σ_f (barn)	σ_γ (barn)	σ_{n^*} (barn)	σ_{n2n} (barn)	σ_{n3n} (barn)
1	2	3	4	5	6	7	8	9
0.10	13,097	10,5090	2,588	2,096	0,3010	0,1910	-	-
0.12	12,682	10,1240	2,558	2,070	0,2570	0,2310	-	-
0.14	12,290	9,7910	2,509	2,022	0,2220	0,2650	-	-
0.16	11,919	9,4400	2,477	1,976	0,1970	0,3060	-	-
0.18	11,591	9,1400	2,451	1,928	0,1760	0,3470	-	-
0.20	11,303	8,8620	2,441	1,885	0,1580	0,3920	-	-
0.22	11,042	8,6020	2,440	1,845	0,1430	0,4520	-	-
0.24	10,804	8,3600	2,444	1,812	0,1300	0,5020	-	-
0.26	10,564	8,1340	2,450	1,780	0,1180	0,5520	-	-
0.28	10,360	7,9990	2,461	1,749	0,1090	0,6030	-	-
0.30	10,162	7,6880	2,474	1,710	0,1040	0,6600	-	-
0.32	9,985	7,4990	2,486	1,668	0,1010	0,7170	-	-
0.34	9,827	7,3120	2,509	1,639	0,0990	0,7710	-	-
0.36	9,688	7,1320	2,536	1,610	0,0980	0,8220	-	-
0.38	9,547	6,9770	2,574	1,605	0,0970	0,8720	-	-
0.40	9,410	6,7950	2,607	1,595	0,0960	0,9160	-	-
0.42	9,270	6,6310	2,627	1,582	0,0950	0,9500	-	-
0.44	9,155	6,5080	2,647	1,567	0,0945	0,9855	-	-
0.46	9,035	6,3720	2,663	1,552	0,0940	1,0170	-	-
0.48	8,921	6,2760	2,695	1,538	0,0940	1,0530	-	-
0.50	8,811	6,1780	2,701	1,525	0,0940	1,0820	-	-
0.55	8,545	5,7980	2,747	1,507	0,0942	1,1518	-	-
0.60	8,267	5,4870	2,772	1,482	0,0950	1,1950	-	-
0.65	8,024	5,2180	2,705	1,469	0,0960	1,2400	-	-
0.70	7,846	4,9860	2,360	1,470	0,0990	1,2920	-	-
0.75	7,678	4,7590	2,310	1,478	0,0990	1,3410	-	-
0.80	7,554	4,5640	2,320	1,508	0,1000	1,3820	-	-
0.85	7,468	4,4080	2,368	1,547	0,1005	1,4205	-	-
0.90	7,370	4,2528	2,318	1,558	0,1010	1,4582	-	-
0.95	7,300	4,1320	2,168	1,559	0,1010	1,5080	-	-
1.00	7,205	4,0330	2,172	1,563	0,1010	1,5080	-	-
1.1	7,092	3,8720	2,220	1,579	0,0991	1,5419	-	-
1.2	7,064	3,7710	2,293	1,633	0,0960	1,5640	-	-
1.4	7,143	3,6690	2,474	1,722	0,0890	1,6630	-	-
1.6	7,250	3,6740	2,576	1,739	0,0790	1,7580	-	-
1.8	7,361	3,7310	2,630	1,715	0,0660	1,8490	-	-

Table 2.1 cont.

I	2	3	4	5	6	7	8	9
2,0	7,456	3,7960	3,660	1,685	0,0500	1,9250	-	-
2,2	7,587	3,7530	3,634	1,652	0,0350	1,9470	-	-
2,4	7,696	4,1000	3,586	1,605	0,0260	1,9550	-	-
2,5	7,788	4,2440	3,544	1,565	0,0190	1,9600	-	-
2,8	7,984	4,3730	3,511	1,536	0,0130	1,9620	-	-
3,0	7,965	4,4960	3,469	1,511	0,0100	1,9490	-	-
3,2	8,051	4,5390	3,452	1,497	0,0088	1,9462	-	-
3,4	8,119	4,6827	3,4353	1,481	0,0080	1,9463	-	-
3,6	8,166	4,7450	3,421	1,467	0,0076	1,9464	-	-
3,8	8,196	4,7730	3,413	1,455	0,0072	1,9508	-	-
4,0	8,198	4,7900	3,403	1,442	0,0070	1,9540	-	-
4,5	8,028	4,6750	3,354	1,412	0,0066	1,9354	-	-
5,0	7,937	4,5390	3,298	1,396	0,0064	1,9056	-	-
5,5	7,562	4,3390	3,231	1,355	0,0063	1,8397	0,0300	-
6,0	7,263	4,0910	3,272	1,472	0,0062	0,7738	0,8200	-
6,5	7,218	3,9460	3,372	1,705	0,0062	0,6758	0,9950	-
7,0	6,864	3,6160	3,248	1,862	0,0061	0,3593	1,0200	-
7,5	6,705	3,4230	3,282	1,783	0,0060	0,278	1,0150	-
8,0	6,518	3,2700	3,248	2,011	0,0058	0,2277	1,0035	-
8,5	6,250	3,1530	3,137	1,775	0,0056	0,1331	1,0033	-
9,0	6,243	3,0740	3,169	1,990	0,0054	0,1710	1,0026	-
9,5	6,170	3,0230	3,147	2,016	0,0052	0,1520	0,7738	-
10,0	6,060	2,9390	3,077	2,054	0,0050	0,1350	0,8330	-
10,5	5,978	2,8620	3,036	2,119	0,0048	0,1205	0,7917	-
11,0	5,942	2,8650	2,994	2,119	0,0045	0,1095	0,7510	-
11,5	5,878	2,9700	2,908	2,100	0,0043	0,1010	0,7027	-
12,0	5,817	2,9700	2,849	2,063	0,0041	0,0920	0,6799	0,010
12,5	5,810	3,0000	2,810	2,093	0,0039	0,0850	0,5772	0,050
13,0	5,842	3,0560	2,796	2,155	0,0037	0,0900	0,4273	0,120
13,5	5,895	3,1120	2,776	2,192	0,0036	0,0768	0,3436	0,160
14,0	5,976	3,1800	2,736	2,218	0,0034	0,0740	0,2626	0,178
14,5	5,953	3,2500	2,703	2,204	0,0033	0,0710	0,2347	0,190
15,0	5,973	3,2340	2,689	2,136	0,0032	0,0708	0,2340	0,195

3. ENERGY DEPENDENCE OF $\bar{\nu}$ (^{241}Pu)

3.1 Experimental data on $\bar{\nu}_p$ (^{241}Pu)

There are three sets of experimental data on $\bar{\nu}_p$ (^{241}Pu), of which two (the Conde and Frehaut measurements) are direct.

1. Conde et al. [25] measured $\bar{\nu}$ at 5 energy points (between 0.5 and 14.8 MeV). As the fission detector they used a large liquid scintillator, and the neutron energy was determined from the time of flight. The contribution made by spontaneous fission to the experimental values of $\bar{\nu}$ was 10-15%. The experimental values of $\bar{\nu}$ (^{241}Pu) measured by Conde et al. are shown in Table 3.1. They have been renormalized to the up-to-date value of $\bar{\nu}_p$ (^{252}Cf) [18].

Table 3.1

Experimental data on the energy dependence of $\bar{\nu}_p$ (^{241}Pu) obtained by Conde et al. [25]

E_n (MeV)	$\bar{\nu}_{\text{exp}}$	Standard	$\frac{\bar{\nu}_p}{\bar{\nu}_p^{252}\text{Cf}}$ renormalized to $\bar{\nu}_p^{252}\text{Cf} = 3.737$	$\bar{\nu}_t = \bar{\nu}_p + \bar{\nu}_\alpha$
0,52±0,02	2,89±0,11		2,87±0,11	2,88±0,11
2,71±0,01	3,37±0,11	$\bar{\nu}_p^{252}\text{Cf} =$	3,35±0,11	3,36±0,11
4,19±0,02	3,50±0,10	= 3,764	3,47±0,10	3,49±0,10
5,88±0,12	3,84±0,12		3,81±0,12	3,83±0,12
14,80±0,20	5,02±0,14		4,98±0,14	5,00±0,14

2. D'yachenko et al. [26] determined the energy dependence of $\bar{\nu}_p$ (^{241}Pu) on the basis of the fission energy balance, with incorporation of experimental data for the mass and kinetic energy fragment distributions over the range 0-2.8 MeV at intervals of 150-200 keV, and also at $E_n = 5$ MeV. The main difficulty in determining the energy dependence of $\bar{\nu}$ by this method is to arrive at the quantity α contained in the energy dependence equation

$$\bar{\nu}(E) = \bar{\nu}_0 + \alpha(E - \Delta E_k) + \Delta \bar{\nu}_j$$

where E is the energy of neutrons causing nuclear fission:

$\bar{\nu}_0$ is the mean number of prompt neutrons during thermal-neutron-induced fission of ^{241}Pu ;

ΔE_k is the variation in the fragment kinetic energy proper, unassociated with variation in fission yield;

$\Delta \bar{\nu}_j$ is the variation in the number of prompt neutrons due only to the difference in the fission yields for neutrons with energy E and for thermal neutrons.

The accuracy attained in determining α is 20% and corresponds to an error of 0-1.5% in determining $\bar{\nu}$, given a neutron energy variation between 0 and 2 MeV. The experimental results obtained in Ref. [26] are shown in Table 3.2.

Table 3.2

Results obtained by D'yachenko et al. [26] for the energy dependence of $\bar{\nu}_p$ (^{241}Pu)

E_n (MeV)	$\bar{\nu}^*$ obtained in Ref. [26]	$\bar{\nu}_p$ renormalized to $\bar{\nu}_p^{\text{renn}} = 2.908 \pm 0.010$
1	2	3
0,28	2,975 \pm 0,015	2,962 \pm 0,018
0,40	2,974 \pm 0,015	2,961 \pm 0,018
0,55	3,008 \pm 0,017	2,995 \pm 0,020
0,70	3,031 \pm 0,022	3,018 \pm 0,024
0,85	3,031 \pm 0,022	3,018 \pm 0,024
1,00	3,047 \pm 0,026	3,034 \pm 0,028
1,33	3,092 \pm 0,032	3,079 \pm 0,033
1,54	3,126 \pm 0,038	3,113 \pm 0,039
1,74	3,139 \pm 0,040	3,126 \pm 0,041
1,94	3,195 \pm 0,048	3,182 \pm 0,049
2,15	3,201 \pm 0,050	3,188 \pm 0,051
2,36	3,250 \pm 0,056	3,237 \pm 0,057
2,56	3,250 \pm 0,056	3,237 \pm 0,057
2,74	3,305 \pm 0,065	3,292 \pm 0,066
5,00	3,660 \pm 0,115	3,647 \pm 0,115

*/ The value of $\bar{\nu}$ was taken as 2.921 for thermal-neutron-induced fission of ^{241}Pu .

The errors indicated in Table 3.2 include the error in the measurement of the kinetic energy of the fragments (± 100 keV) and the error involved in determining α (20%).

The experimental data obtained by Conde et al. and D'yachenko et al. are shown in Fig. 3.1. The value of $\bar{\nu}_p(^{241}\text{Pu})$ at a thermal neutron energy of 0.0253 eV was taken as 2.908 ± 0.009 ; $\bar{\nu}_t = 2.924 \pm 0.010$.

3. Frehaut et al. [27] measured the energy dependence of $\bar{\nu}_p(^{241}\text{Pu})$ over the energy range 1.5-15.0 MeV. The measurements were based on the use of a fission chamber located at the centre of a large liquid scintillator (80 cm in diameter) containing Gd. The neutron source was a Van de Graaff accelerator and the fission events were identified by coincidence of the signals from the fission chamber (fission fragment recording) and from the photomultiplier. The fission chamber contained 10 mg of ^{241}Pu (97%), which was applied to 16 aluminium discs in such a way that the thickness of the coating was of the order of 1 mg/cm^2 . The chamber also contained a layer of ^{252}Cf for normalizing the $\bar{\nu}_p$ measurements. Experimental data on $\bar{\nu}_p$ were corrected for background (0.2-0.3% maximum correction) and for losses due to the dead time of the detector (0.15-0.20%). The authors analysed the sources of systematic errors: the presence of impurities (0.05%); anisotropy of the fission fragments (0.2%); fission losses in the layer (0.1%); fission induced by scattered neutrons (0.2%); delayed gamma rays (0.1%); the difference between the energy spectrum for fast fission neutrons and ^{252}Cf (0.05-0.26%), and other effects (0.05%).

Table 3.3 shows the measurement data obtained by Frehaut et al. [27] with the errors cited by the authors, together with the values of $\bar{\nu}_p$ renormalized to $\bar{\nu}_p(^{252}\text{Cf}) = 3.737$.

Table 3.3

Data obtained by Frehaut et al. [27] for $\bar{\nu}_p$ (^{241}Pu)

E_n (MeV)	$\bar{\nu}_p$	$\bar{\nu}_p$ renormalized	$\Delta \bar{\nu}_p$
1	2	3	4
1,87	3,160	3,164	0,053
2,45	3,209	3,213	0,054
2,98	3,322	3,326	0,028
3,50	3,322	3,336	0,033
4,03	3,474	3,479	0,042
5,06	3,631	3,636	0,073
6,97	3,951	3,956	0,067
7,48	3,967	3,972	0,038
7,99	4,055	4,060	0,030
8,49	4,127	4,133	0,028
9,00	4,249	4,255	0,038
9,49	4,252	4,256	0,034
9,98	4,372	4,378	0,030
10,47	4,449	4,455	0,030
10,96	4,528	4,534	0,031
11,44	4,605	4,611	0,041
11,93	4,658	4,664	0,033
12,41	4,744	4,750	0,032
12,88	4,827	4,833	0,040
13,36	4,873	4,880	0,034
13,84	4,999	5,006	0,043
14,31	5,089	5,096	0,051
14,79	5,112	5,119	0,058

3.2 Evaluation of $\bar{\nu}_p(E)$ and $\bar{\nu}_t(E)$ for ^{241}Pu

When evaluating the energy dependence of the mean number of neutrons per fission use was made of all the experimental data, which were renormalized for the evaluation to the thermal values

$\bar{\nu}_p = 2.908 \pm 0.009$ and $\bar{\nu}_t = 2.924 \pm 0.010$ obtained by Lemmel [18].

All the $\bar{\nu}_p$ data were processed by the method of least squares and the following energy dependences were obtained:

$$\bar{\nu}_p(E) = 2.9094 + 0.13445 E + 0.0011429 E^2 \quad (3.1)$$

without inclusion of the thermal point, and

$$\bar{\nu}_p(E) = 2.9086 + 0.13471 E + 0.0011248 E^2 \quad (3.2)$$

with inclusion of the thermal point.

The discrepancy between the curves (3.1) and (3.2) is less than 0.1% over the entire energy range, which is less than the experimental errors, i.e. both relationships can be regarded as equivalent. Relationship (3.2) was used to obtain the evaluated data. Taking into account that $\bar{\nu}_\alpha = 0.0157$, we get the following expression for the total $\bar{\nu}_t(^{241}\text{Pu})$:

$$\bar{\nu}_t(E) = 2.9243 + 0.13471 E + 0.0011248 E^2 \quad (3.3)$$

The evaluated data for $\bar{\nu}_p$ and $\bar{\nu}_t$ are shown in Table 3.4 and in Fig. 3.1.

Table 3.4

Evaluated data on $\bar{\nu}_p(^{241}\text{Pu})$ up to energies of 15 MeV

E (MeV)	$\bar{\nu}_p(^{241}\text{Pu})$	E (MeV)	$\bar{\nu}_p(^{241}\text{Pu})$	E (MeV)	$\bar{\nu}_p(^{241}\text{Pu})$
$2,53 \cdot 10^{-8}$	2,90870	1,0	3,04448	6,5	3,83178
$1,0 \cdot 10^{-2}$	2,90999	1,5	3,113240	7,0	3,90673
$2,0 \cdot 10^{-2}$	2,91134	2,0	3,18256	7,5	3,98224
$4,0 \cdot 10^{-2}$	2,91404	2,5	3,25245	8,0	4,05832
$6,0 \cdot 10^{-2}$	2,91673	3,0	3,32289	9,0	4,21215
$8,0 \cdot 10^{-2}$	2,91943	3,5	3,39389	10,0	4,36824
$1,0 \cdot 10^{-1}$	2,92213	4,0	3,46548	11,0	4,52657
$2,0 \cdot 10^{-1}$	2,93563	4,5	3,53760	12,0	4,68715
$4,0 \cdot 10^{-1}$	2,96271	5,0	3,61030	13,0	4,84999
$6,0 \cdot 10^{-1}$	2,98987	5,5	3,68358	14,0	5,01507
$8,0 \cdot 10^{-1}$	3,01713	6,0	3,75740	15,0	5,1824

4. RADIATIVE CAPTURE CROSS-SECTION $\sigma_{\gamma}({}^{241}\text{Pu})$ IN THE ENERGY RANGE 0.1-15 MeV

There are virtually no experimental data available for the cross-section $\sigma_{\gamma}({}^{241}\text{Pu})$ over the energy range 0.1-15.0 MeV. There have only been measurements by Weston and Todd [28] of the quantity a up to energies of 0.25 MeV. Hence the evaluation of $\sigma_{\gamma}({}^{241}\text{Pu})$ was based on calculations made with theoretical models. At neutron energies below 5 MeV the main interaction mechanism is the formation of the compound nucleus. So it is possible to calculate the cross-sections σ_{γ} from a statistical model for these energies.

The basic expressions and parameters of the Hauser, Feshbach and Moldauer statistical model [29, 30] used to calculate radiative capture cross-sections are given in Part 5 of the Preprint. Here we will merely consider the "effective" penetration factor (?) $T_{\gamma J \pi}(E)$ for radiative neutron capture. This "effective" penetration factor was calculated with allowance for the possibility of cascade gamma radiation.

The penetration factor for a single gamma transition $T_{\gamma J \pi}(E, \epsilon_{\gamma})$ with the emission of gamma quanta with energy ϵ_{γ} from the excited state with energy $E + B_n$, total angular momentum J , and parity π was taken in the following form:

$$T_{\gamma J \pi}(E, \epsilon_{\gamma}) = \frac{2\pi \langle \Gamma_{\gamma} \rangle_{J \pi}(E, \epsilon_{\gamma})}{\langle D \rangle_{J \pi}(E + B_n)} = 2\pi \cdot f(E, \epsilon_{\gamma}) \quad (4.1)$$

The total "effective" penetration factor for radiative capture can be obtained by summing over all possible gamma transitions. If we take into account dipole gamma transitions alone, then

$$T_{\gamma J \pi}(E) = 2\pi \int_0^{E+B_n} d\epsilon_{\gamma} \sum_{J_k=|J-1|}^{J+1} f(E, \epsilon_{\gamma}) \rho(E + B_n - \epsilon_{\gamma}, J_k). \quad (4.2)$$

where $\rho(E + B_n - \epsilon_{\gamma}, J_k)$ is the level density of the compound nucleus for the excitation energy $E + B_n - \epsilon_{\gamma}$ and spin J_k .

The dependence of the level density on parity was not taken into account since for deformed nuclei such as the ${}^{242}\text{Pu}$ nucleus it can clearly be disregarded [31]. For the level density $\rho(U, J)$ use was made of the expression for the non-interacting particle model [32], the optimized parameters of which are described in Part 3 of the Preprint.

The spectral factor $f(E, \varepsilon_\gamma)$ can be taken in the form proposed by Weisskopf in Ref. [33]: $f(E, \varepsilon_\gamma) \approx C_\gamma \cdot \varepsilon_\gamma^{2l+1}$, or in the form that follows from experimental dependence of the cross-section for the (photo-nuclear) reaction, inverse of radiative capture, in Ref. [34].

$$f(E, \varepsilon_\gamma) = \frac{8}{3} \frac{NZ}{A} \frac{e^2}{\hbar c} \frac{1.4}{m_e c^2} \frac{\Gamma_c \varepsilon_\gamma^l}{(\varepsilon_\gamma^2 - E_c^2)^2 + (\Gamma_c \varepsilon_\gamma)^2} \quad (4.3)$$

For heavy deformed nuclei it is demonstrated that the best agreement with the experimental data on the photonuclear reaction cross-section is found when the dependence is used in the form of two Lorentz lines [35], i.e. when the spectral factor can be represented in the following form:

$$f(E, \varepsilon_\gamma) = \frac{8}{3} \frac{NZ}{A} \frac{e^2}{\hbar c} \frac{1.4}{m_e c^2} \sum_{i=1}^2 \frac{i}{3} \frac{\Gamma_{iG} \varepsilon_\gamma^l}{(\varepsilon_\gamma^2 - E_{iG}^2)^2 + (\Gamma_{iG} \varepsilon_\gamma)^2} \quad (4.4)$$

In the present calculations use was made of Eq. (4.4), since it is expected to give a truer description of the energy dependence of the radiation width. The parameters of the giant resonance Γ_{iG} and E_{iG} for the ^{242}Pu nucleus were not determined experimentally, but they can be selected as mean values for close-lying nuclei [36]:

$$\begin{array}{ll} E_{1G} = 11 \text{ MeV} & \Gamma_{1G} = 2.9 \text{ MeV} \\ E_{2G} = 14 \text{ MeV} & \Gamma_{2G} = 4.5 \text{ MeV} \end{array}$$

followed by normalization of the theoretical radiation widths $\Gamma_{\gamma J\pi}$ to the evaluated $\langle \Gamma_\gamma \rangle$ in the resolved resonance region.

When calculating $T_{\gamma J\pi}(E)$ it is essential in principle to take into account the existence of a discrete spectrum for the ^{242}Pu nucleus levels in the lower excitation energy region. This leads to variation in the lower limit for integration in Eq. (4.2) and to the appearance of an additional term taking into account the gamma transitions from the continuous to the discrete spectrum. But the calculations given show that the contribution made by the discrete spectrum to the radiation width is considerably less than the accuracy with which it was determined, and it was not taken into account in subsequent calculations.

The expressions given above are valid for a case in which the emission of gamma quanta is the only way of removal of the residual excitation of the compound nucleus after emission of the first gamma quantum.

In actual fact, though, when the first gamma quantum has been emitted there is a possibility of de-excitation through neutron emission and fission. Neutron escape is possible whenever the excitation energy after the first gamma quantum is greater than the neutron detachment energy, i.e. $E - \epsilon_\gamma > 0$. It was assumed in the calculations that if the excitation energy is greater than the neutron binding energy after emission of the first gamma quantum, further discharge proceeds either by neutron emission or by fission, i.e. that the contribution by these gamma transitions to the radiative capture width is zero. The correctness of this assumption is governed by the fact that the radiative capture cross-section is much smaller than the compound nucleus formation cross-section even at energies of 0.1 MeV. It is important to take this effect into account when calculating the penetration factor for radiative capture in the case of neutron energies greater than the mean gamma quantum energy of the first cascade (~ 1 MeV). For example, calculation shows that for ^{242}Pu consideration of this effect at a neutron energy of 0.5 MeV reduces $\langle \Gamma_\gamma \rangle$ by only $\sim 0.5\%$.

Let us now deal in greater detail with consideration of the competition between the $(n, \gamma f)$ reaction and the radiative capture process when the excitation energy of the nucleus is smaller than the neutron binding energy after emission of the first gamma quantum. Competition is possible when $E - E_f > \bar{E}_\gamma$, where E_f is the fission threshold energy measured from the binding energy, i.e. for nuclei with a fairly low fission threshold (^{239}Pu : $E_f \approx -1.6$ MeV; ^{241}Pu : $E_f \approx -1.2$ MeV; ^{233}U : $E_f \approx -1.5$ MeV), and it is possible even for thermal neutron energies. In order to take this effect into account the spectral factor should be multiplied by $\frac{T_\gamma(E - \epsilon_\gamma)_{Jk\pi}}{T_\gamma(E - \epsilon_\gamma)_{Jk\pi} + T_{fJk\pi}(E - \epsilon_\gamma)}$ where $T_{fJk\pi}(E - \epsilon_\gamma)$ is the effective penetration factor for fission at the excitation energy $E - \epsilon_\gamma + B_n$.

The parity of the fission channel is the opposite of the parity of the compound nucleus, since in our assumptions the fission process is preceded by the emission of a gamma quantum. The fission penetration factors were calculated from the Bohr, Hill and Wheeler channel theory [37, 38], the main expressions of which are given in Part 3 of the Preprint. The parameters for the transition states of the fissioning nucleus are shown in Part 5 of the Preprint.

Let us discuss the results of taking the processes $(n, \gamma f)$ and $(n, \gamma n^0)$ into consideration when calculating the cross-section widths for the reactions (n, γ) and (n, F) . Since the fission penetration factors are functions of such channel characteristics as spin and parity, consideration of the competition of the $(n, \gamma f)$ process leads to the dependence of the mean radiation widths on parity and to an even greater dependence on spin. The results of calculating the mean radiation widths of ^{241}Pu for a number of states without consideration of the processes $(n, \gamma f)$ and $(n, \gamma n^0)$ are shown in Tables 4.1 and 4.2.

Table 4.1

Mean radiation widths $\langle \Gamma_Y \rangle$ of ^{241}Pu calculated with and without consideration of the processes $(n, \gamma f)$ in the case of incident neutrons with 1 keV energy

Spin and parity of the state of compound nucleus, J^π	$\langle \Gamma_Y \rangle$ (MeV) with consideration of the process $(n, \gamma f)$	$\langle \Gamma_Y \rangle$ (MeV) without consideration of the process $(n, \gamma f)$
1	2	3
2+	42,43	43,53
3+	43,44	42,59
1 ⁻	37,30	44,18
2 ⁻	40,49	43,53
3 ⁻	35,02	42,59
4 ⁻	37,87	41,38
1 ⁺	44,76	44,18
4 ⁺	40,57	41,38
0 ⁺	40,67	44,51
0 ⁻	48,40	44,51

Table 4.2

Mean radiation widths $\langle \Gamma_\gamma \rangle$ of ^{241}Pu calculated with and without consideration of the processes $(n, \gamma f)$ and $(n, \gamma n')$ in the case of incident neutrons with an energy of 1.5 MeV

Spin and parity of the state of the compound nucleus, J^π	$\langle \Gamma_\gamma \rangle$ (MeV) with consideration of the processes $(n, \gamma n')$ and $(n, \gamma f)$	$\langle \Gamma_\gamma \rangle$ (MeV) without consideration of the processes $(n, \gamma n')$ and $(n, \gamma f)$
0^+	30,78	81,09
0^-	69,61	81,09
1^+	46,40	80,65
1^-	35,66	80,65
2^+	57,90	79,78
2^-	39,29	79,78
3^+	43,56	78,50
3^-	25,66	78,50
4^+	57,22	76,65
4^-	32,71	76,65

The given widths were normalized to the mean radiation width $\langle \Gamma_\gamma \rangle = 0.043$ eV obtained from data in the resolved resonance region (Part 2 of the Preprint).

Consideration of the processes $(n, \gamma f)$ and $(n, \gamma n')$ results likewise in a change in the energy dependence of the mean radiation widths (Fig. 4.1). For example, at 1.5 MeV allowance for the processes mentioned brings about a decrease in $\langle \Gamma_\gamma \rangle$ for the 3^+ and 3^- channels by a factor of approximately 1.8 and 3, respectively. This leads, of course, to a substantial change in the energy dependence of the calculated radiative capture cross-section $\langle \sigma_\gamma \rangle$ (Fig. 4.2). For example, at 3 MeV the calculation data differ by a factor of 7. The cross-sections $\sigma_\gamma(^{241}\text{Pu})$ shown in Fig. 4.2 were normalized to the compound nucleus formation cross-section, evaluated in this work.

In the low-energy region, where the $(n, \gamma x)$ process cross-section is large, the $(n, \gamma f)$ cross-section may turn out to be substantial, and has to be taken into account when calculating the section $\langle \sigma_F \rangle$.

Calculation data for the widths of the processes $\Gamma_{\gamma f}$ for channels 2^+ and 3^+ can be compared with the experimental values $\Gamma_{\gamma f}^{2^+} \approx 7$ MeV and $\Gamma_{\gamma f}^{3^+} \approx 2$ MeV [39]. The results of the calculation with the Lorentz dependence of the spectral factor $\Gamma_{\gamma f}^{2^+} = 4.95$ MeV and $\Gamma_{\gamma f}^{3^+} = 2.91$ MeV agree better with the experimental data than those calculated on the basis of the Weisskopf concept $\Gamma_{\gamma f}^{2^+} = 10.44$ MeV, $\Gamma_{\gamma f}^{3^+} = 6.62$ MeV.

It is interesting to compare the calculations of the $(n, \gamma f)$ process widths, for ^{239}Pu with the experimentally-measured width difference for channels 0^+ and 1^+ [40]: $|\langle \Gamma_{\gamma f} \rangle_{0^+} - \langle \Gamma_{\gamma f} \rangle_{1^+}| < 4$ MeV. Our calculation using the Weisskopf expressions for the spectral factor gives the following values: $\langle \Gamma_{\gamma f} \rangle_{0^+} = 20.2$ MeV; $\langle \Gamma_{\gamma f} \rangle_{1^+} = 10.5$ MeV. The use of Eq. (4.4) yields $\langle \Gamma_{\gamma f} \rangle_{0^+} = 10.1$ MeV and $\langle \Gamma_{\gamma f} \rangle_{1^+} = 4.9$ MeV, which tallies far better with the experimentally-measured difference for these values [40].

Furthermore, the calculation data on $\langle \Gamma_{\gamma f} \rangle_{1^+}$ agree with the measured value 4.1 ± 0.9 MeV [41]. This may indicate that it is preferable to use the spectral factor $f(E, \epsilon_{\gamma})$ in the form of the Lorentz dependence.

Calculation data for the mean radiation widths with allowance for competition by the processes $(n, \gamma f)$ and $(n, \gamma n')$ were used in the statistical model calculations up to energies of 5 MeV. The calculation data were then renormalized in order to take into account the difference between the evaluated data and the data based on the optical model for the compound nucleus formation cross-section (see Part 5 of the Preprint).

At higher energies the main contribution to the radiative capture cross-section σ_{γ} is made by collective and direct mechanisms. Theoretical model calculations in this region for fissile nuclei have not so far been made. Hence when evaluating the cross-section σ_{γ} use was made here of experimental data on the ^{238}U nucleus [42-44].

The evaluated data for the cross-section $\sigma_{\gamma}(^{241}\text{Pu})$ for energies 0.1-15 MeV are shown in Table 4.3 and in Fig. 4.3.

Table 4.3

Evaluated data on the cross-section σ_{γ} (^{241}Pu) for energies of 0.1-15 MeV

E (MeV)	σ_{γ} (barn)	E (MeV)	σ_{γ} (barn)	E (MeV)	σ_{γ} (barn)
1	2	3	4	5	6
0,10	0,317	0,65	0,096	4,0	0,0070
0,12	0,262	0,70	0,098	4,5	0,0066
0,14	0,222	0,75	0,099	5,0	0,0064
0,16	0,197	0,80	0,100	5,5	0,00637
0,18	0,176	0,85	0,1005	6,0	0,0062
0,20	0,158	0,90	0,101	6,5	0,0062
0,22	0,143	0,95	0,101	7,0	0,0061
0,24	0,130	1,00	0,101	7,5	0,0060
0,26	0,118	1,1	0,0991	8,0	0,0058
0,28	0,109	1,2	0,096	8,5	0,0056
0,30	0,104	1,4	0,098	9,0	0,0054
0,32	0,101	1,6	0,079	9,5	0,0052
0,34	0,099	1,8	0,066	10,0	0,0050
0,36	0,098	2,0	0,050	10,5	0,0048
0,38	0,097	2,2	0,035	11,0	0,0045
0,40	0,096	2,4	0,026	11,5	0,0043
0,42	0,095	2,6	0,019	12,0	0,0041
0,44	0,0945	2,8	0,013	12,5	0,0039
0,46	0,0940	3,0	0,010	13,0	0,0037
0,48	0,0940	3,2	0,0088	13,5	0,0036
0,50	0,0940	3,4	0,0080	14,0	0,0034
0,55	0,0942	3,6	0,0076	14,5	0,0033
0,60	0,0950	3,8	0,0072	15,0	0,0032

It is of interest to compare the present σ_{γ} data with the results of other evaluations. A comparison with Kaner and Yiftah's data [22] and those of Prince [24] is shown in Fig. 4.3. As can be seen, over the region 0.1-1 MeV our data lie below the values obtained in Refs [22, 24], the data of Kaner and Yiftah being considerably higher. Over the region 1-15 MeV our data are far below those of Prince and tally better with Kaner and Yiftah's [22].

Szabo et al. (1970)
Käppeler et al. (1973)
White et al. (1965)
Fursov et al. (1977) (chamber)
Perkin et al. (1965)
Butler et al. (1961)
Evaluated data from time-of-flight measurements

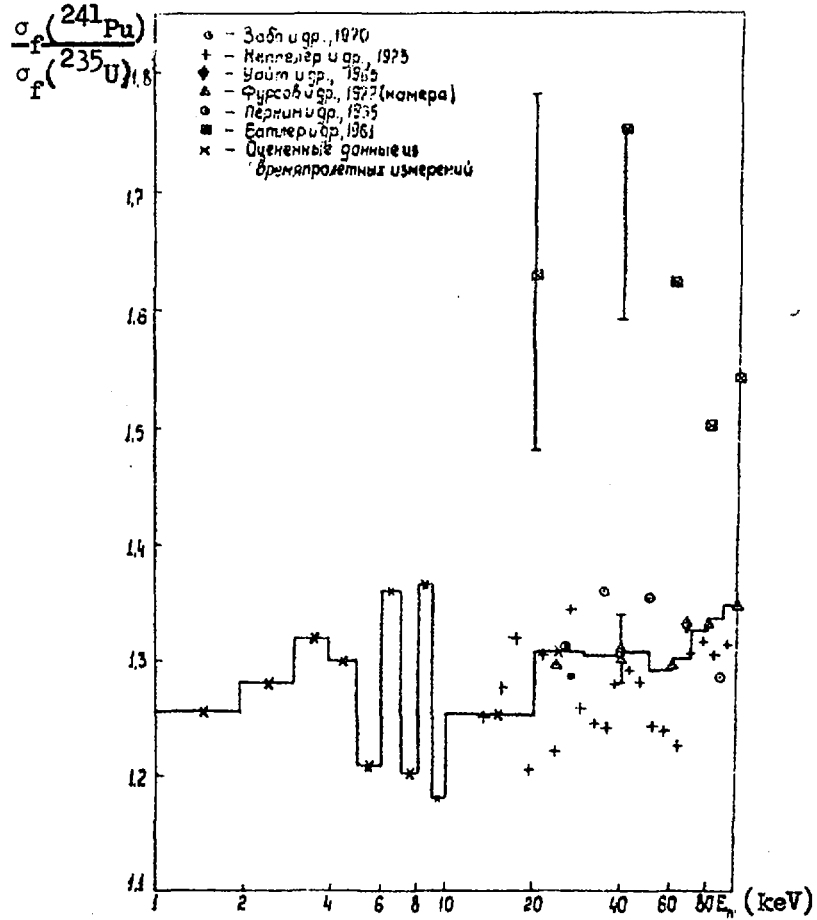


Fig. 1.1. Evaluated and experimental data on the ratio $\sigma_f(^{241}\text{Pu})/\sigma_f(^{235}\text{U})$ over the energy range 1-100 keV

Käppeler et al. (1973)
Behrens and Carlson (1975)
White et al. (1965)
Fursov et al. (1977) (chamber)
Fursov et al. (1977) (glass)
Butler et al. (1961)
Smith et al. (1962)
White and Warner (1967)
Szabo et al. (1970)
Szabo et al. (1973)

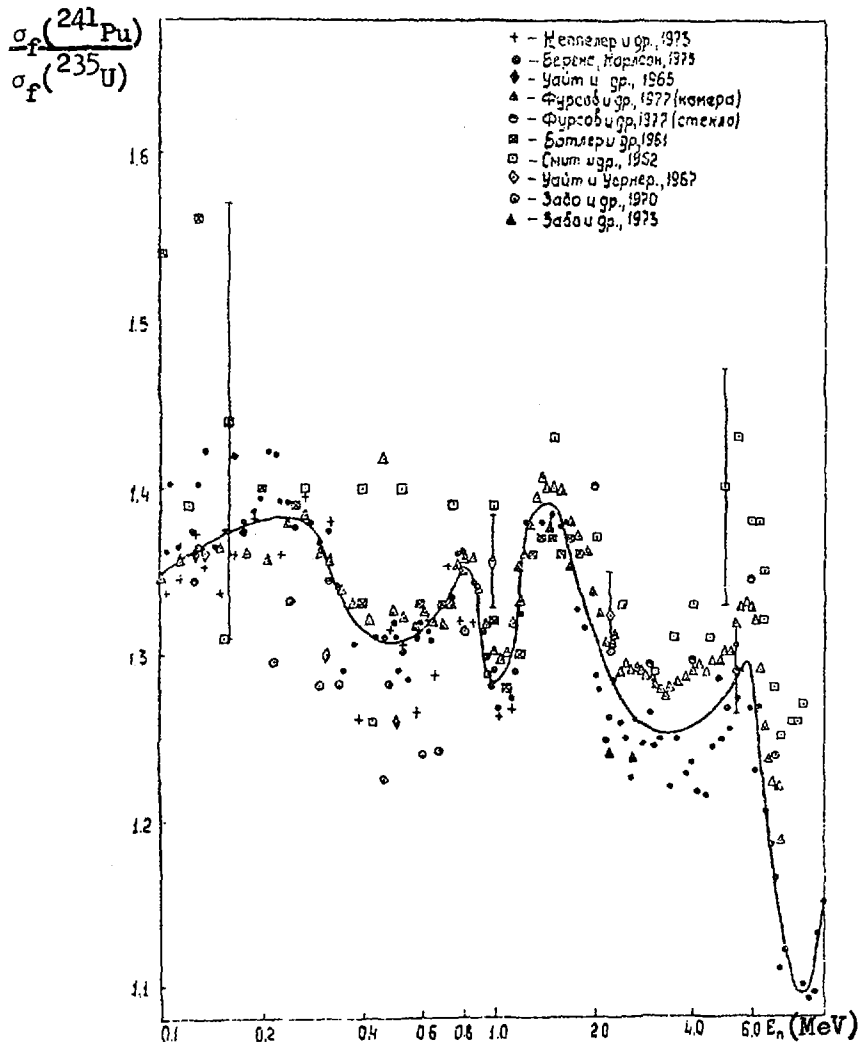


Fig. 1.2. Evaluated and experimental data for the ratio $\sigma_f(^{241}\text{Pu})/\sigma_f(^{235}\text{U})$ in the energy range 0.1-10 MeV

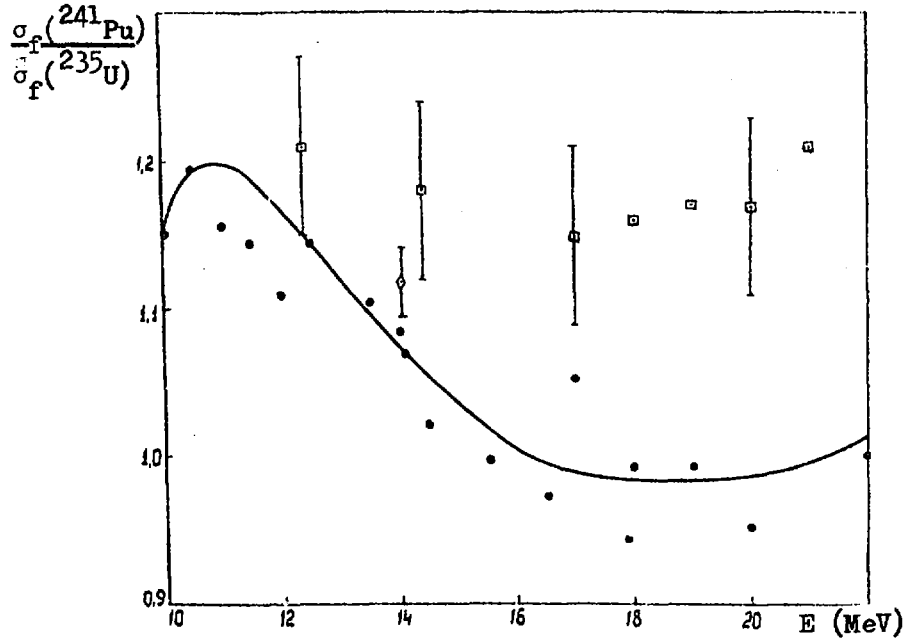


Fig. 1.3. Evaluated and experimental data on the ratio $\sigma_f(^{241}\text{Pu})/\sigma_f(^{235}\text{U})$ over the energy range 10-22 MeV

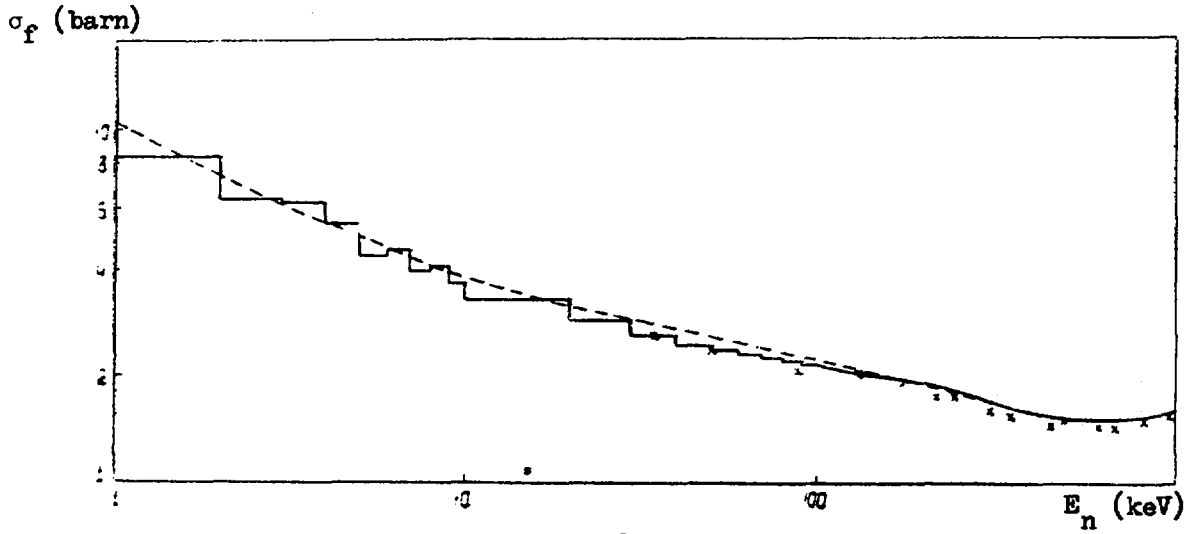


Fig. 1.4. Evaluated data for $\sigma_f(^{241}\text{Pu})$ over the energy range 1-1000 keV (the solid curve shows the present work and the broken line represents data obtained by Kaner et al. [22]; x - Szabo's absolute measurements [3])

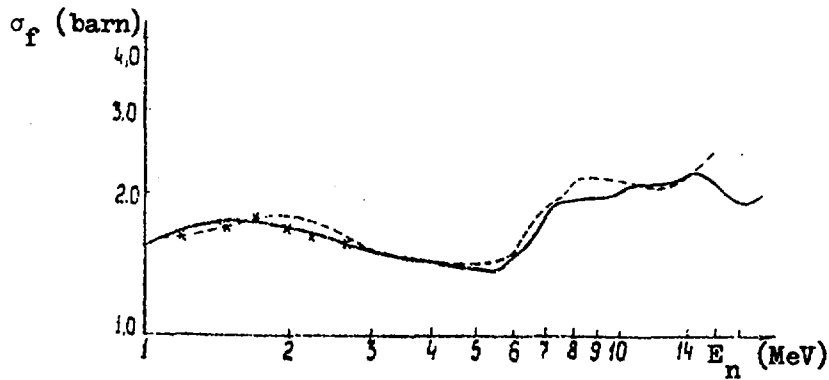


Fig. 1.5. Evaluated data for $\sigma_f(^{241}\text{Pu})$ over the energy range 1-20 MeV (the curves refer to the same work as in Fig. 1.4.)

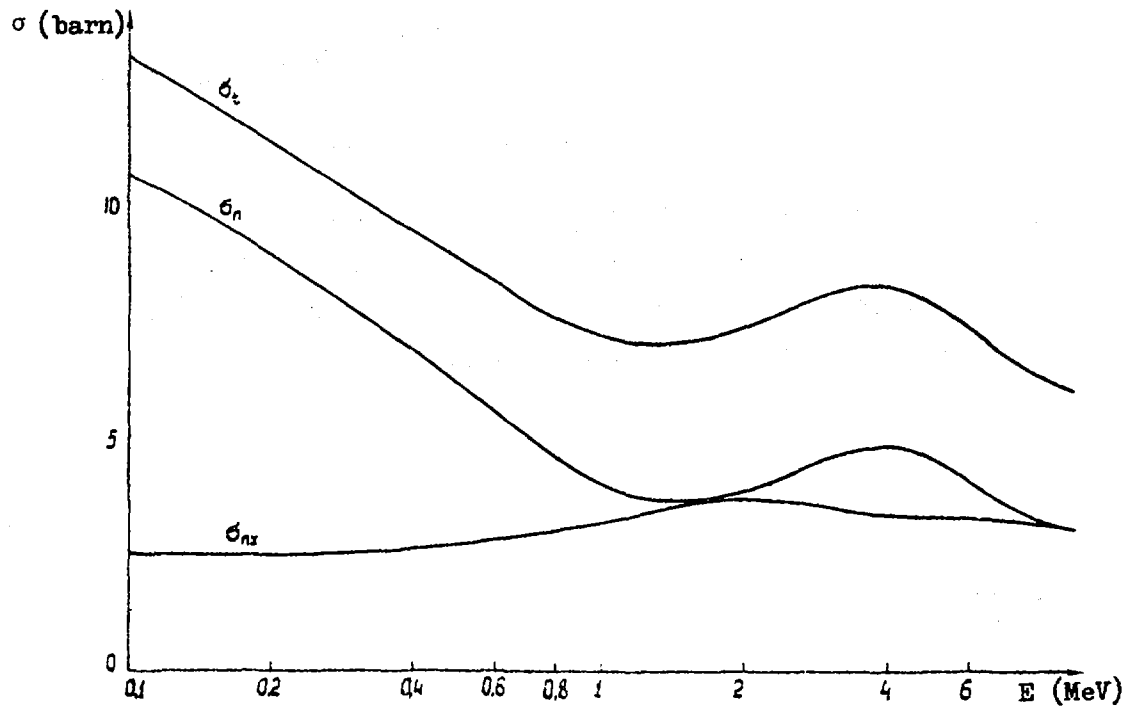


Fig. 2.1. Evaluated cross-sections σ_t , σ_n and σ_{nx} (^{241}Pu)

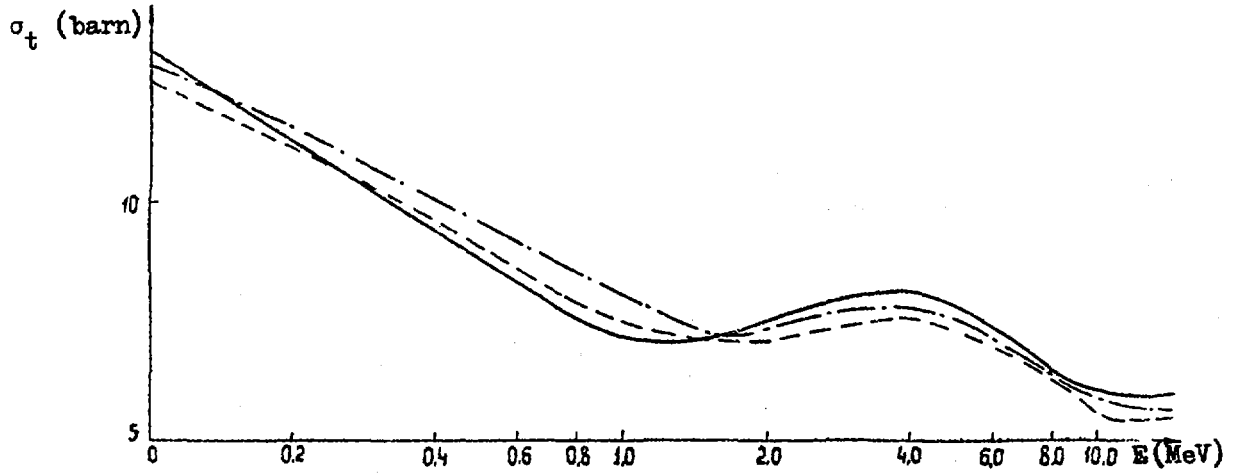


Fig. 2.2. Comparative data on $\sigma_n(^{241}\text{Pu})$; — data from the present work; - - - data obtained by Kaner and Yiftah [22]; - · - · - data obtained by Prince [24]

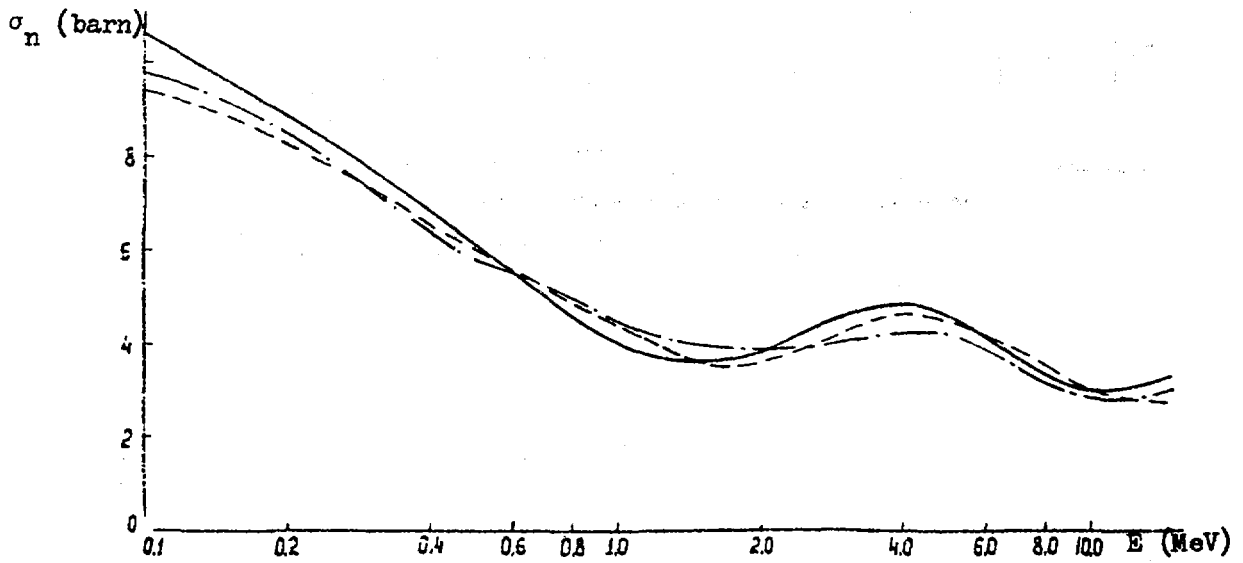


Fig. 2.3. Comparative data on $\sigma_n(^{241}\text{Pu})$; — data from the present work; - - - data obtained by Kaner and Yiftah [22]; - · - · - data obtained by Prince [24]

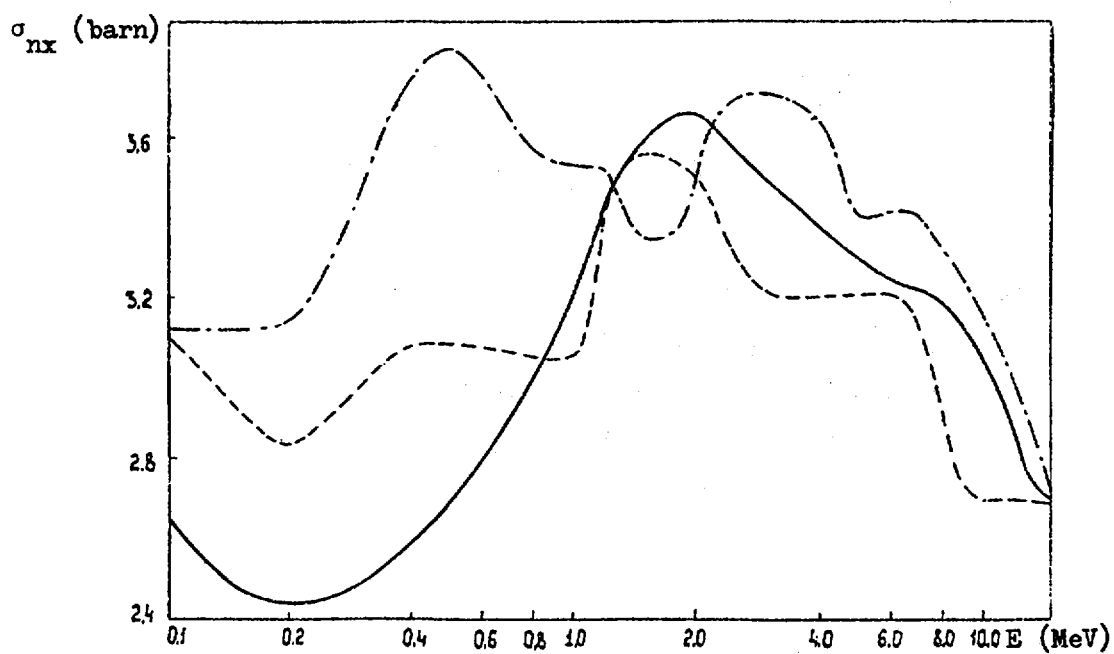


Fig. 2.4. Comparative data on $\sigma_{nx}({}^{241}\text{Pu})$; — data from the present work; - - - data obtained by Kaner and Yiftah [22]; - · - · data obtained by Prince [24]

Fréhaut et al. (1974)
Conde et al. (1968)
D'yachenko et al. (1974)
Heat point

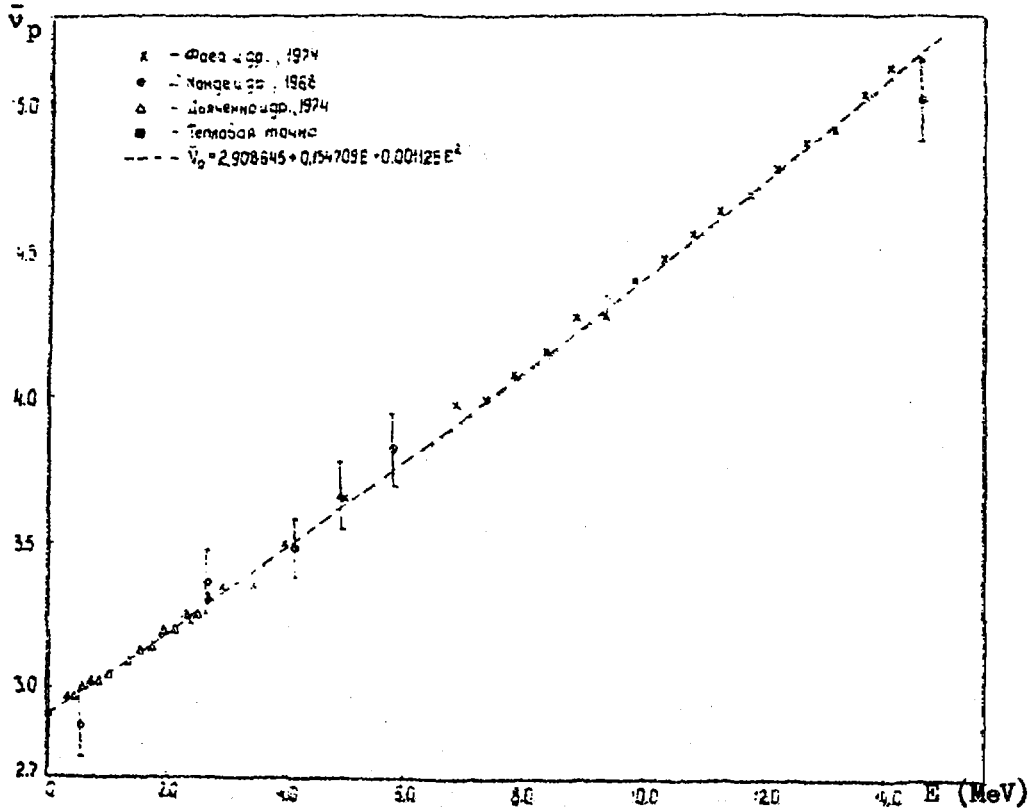


Fig. 3.1. Evaluated and experimental data on $\bar{\nu}_p$ (^{241}Pu) up to energies of 15 MeV

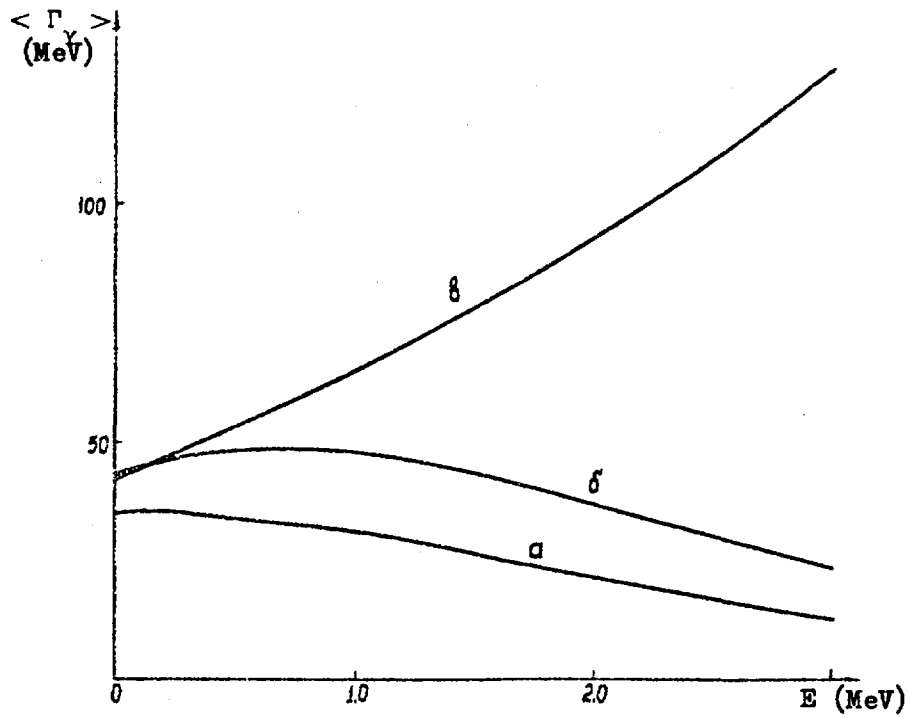


Fig. 4.1. Energy dependence of mean radiation widths $\langle \Gamma_Y \rangle$:
(a) width of channel 3^- with allowance for the processes $(n, \gamma n^*)$ and $(n, \gamma f)$; (b) width of channel 3^+ with allowance for the processes $(n, \gamma n^*)$ and $(n, \gamma f)$; (c) width of channel 3^+ without allowance for the processes $(n, \gamma n^*)$ and $(n, \gamma f)$

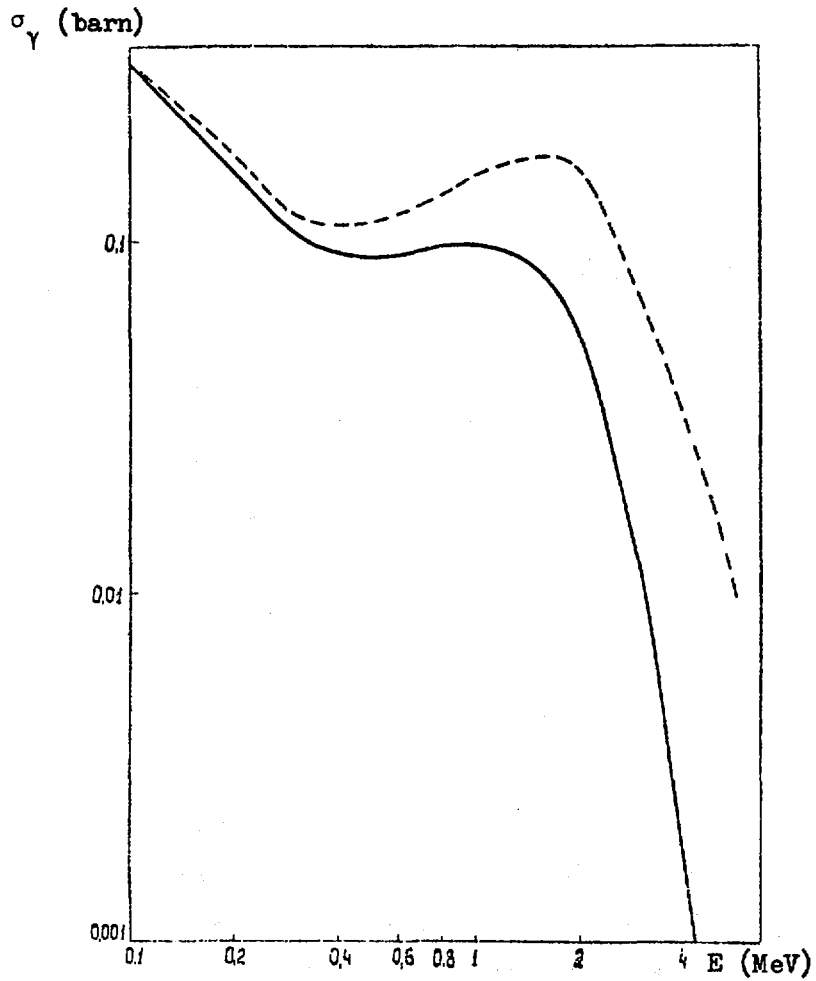


Fig. 4.2. Theoretical values of $\sigma_\gamma(^{241}\text{Pu})$ for energies of 0.1-5.0 MeV: ——— with allowance for the processes $(n, \gamma n')$ and $(n, \gamma f)$; - - - - without allowance for the processes $(n, \gamma n')$ and $(n, \gamma f)$

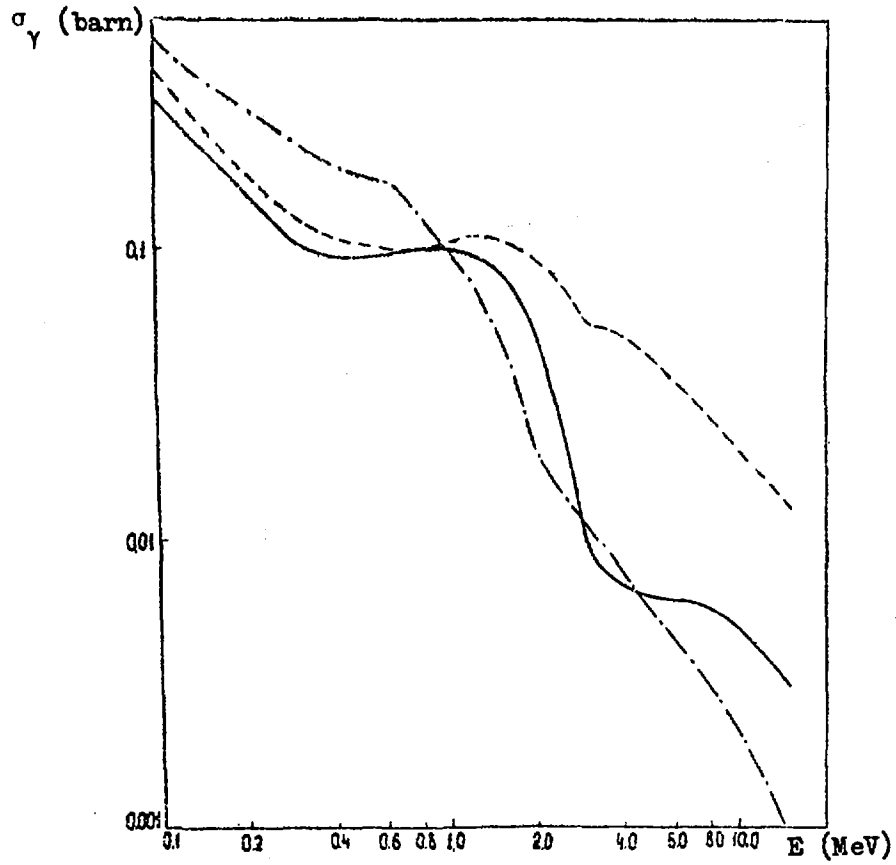


Fig. 4.3. Evaluated data on $\sigma_\gamma(^{241}\text{Pu})$ over the energy range 0.1-15 MeV:
—— the present work;
----- Prince's data [24];
- · - · - Kaner and Yiftah's data [22]

REFERENCES

1. Szabo I. et al. Proc. of the Conf. of Neutron Standards and Flux Normalization, AEC Symposium, Ser.23, 1970, p.257.
2. Szabo I., Leroy J.L., Marguette J.P. Third All-Union Conf. on Neutron Physics. Kiev, v.3, 1974, p.27.
3. Szabo I., Marguette J.P. Proc. of the NEANDC/NEACRP Specialists Meeting on Fast Fission Cross-Sections of ^{233}U , ^{235}U , ^{238}U and ^{239}Pu , June 28-30, 1976, p.208.
4. Antsipov, G.V., Kon'shin, V.A., Morogovskij, G.B., Byull. Inf. Tsentra Yad. Dannym, No. 10 (1972) 263.
5. Antsipov, G.V. et al., Yad. Konst. 20 2 (1975) 3.
6. Kappeler F., Pflutschinger E. IAEA Conf. on Nuclear Data for Reactors, v.2, 1970, p.77.
7. Kappeler F., Pflutschinger E. Nucl. Sci. Eng., v.51, 1973, p.124.
8. White P.H., Hodgkinson J.G., Wall G.J. Proc. of Symposium on Physics and Chemistry of Fission, Salzburg, v.1, 1965, p.329.
9. White P.H. J. Nucl. Energy, v.19, 1965, p.325.
10. White P.H., Warner G.F. J. Nucl. Energy, v.21, 1967, p.673.
11. Smith H.L., Smith R.K., Henkel R.L. Phys. Rev., v.125, 1962, p. 1329.
12. Perkin J.L. et al. J. Nucl. Energy, v.19, 1965, p.423.
13. Butler D.K., Sjoblom R.K. Phys. Rev., v.124, 1961, p.1129.
14. Allen D.W., Henkel R.L. Progress in Nuclear Energy, v.2, 1958, p.23.
15. Hughes D.J., Schwartz R.B. ENL-325, 2nd ed., 1958.
16. Kazarinova, M.N. et al., At. Ehnerg. 8 (1960) 139.
17. Behrens J.W., Carlson G.W. UCID-16078, 1975 and Proc. of the NEANDC/NEACRP Specialist Meeting on Fast Fission Cross-Sections of ^{233}U , ^{235}U , ^{238}U and ^{239}Pu , June 28-30, 1976, p.47.
18. Lemmel H.D. Proc. of the Conf. on Neutron Cross-Sections and Technology, Washington, v.1, 1975, p.286.
19. Fursov, B.I., Kupriyanov, V.M., Smirenkin, G.N., Proc. III All-Union Conf. Neut. Phys., Kiev 6 3.
20. Carlson G.W., Behrens J.W., Czirr J.B. Nucl. Sci. Eng., v.63, 1977, p.149.
21. Blons J. et al. Conf. on Neutron Cross-Sections and Technology, Knoxville, v.2, 1971, p.836 and Nucl. Sci. Eng., v.51, 1973, p.130.
22. Kaner M., Yiftah S. IA-1276, 1973.
23. Kon'shin, V.A. et al., Yad. Konst, 16 (1974) 329.
24. Prince A. Proc. of the IAEA Conf. on Nuclear Data for Reactors, Helsinki, v.2, 1970, p.825.
25. Conde H., Hansen J., Holmberg M. J. Nucl. Energy, v.22, 1968, p.53.

26. D'yachenko, N.P., et al., *At. Ehnerg.* 36 4 (1974).
27. Frehaut J. et al. CEA-R-4626, 1974.
28. Weston L.W., Todd J.H. *Nucl. Sci. Eng.*, v.65, 1978, p.454.
29. Hauser W., Feshbach H. *Phys. Rev.*, v.87, 1952, p.366.
30. Moldauer P.A. *Phys. Rev.*, B, v.135, 1964, p.642.
31. Blokhin, A.I., Ignatyuk, A.V., *Proc III All-Union Conf. Neut. Phys., Kiev* 3 (1976) 3.
32. Mal'shev, A.V., *Plotnost' urovnej i struktura atomnykh yader (Level density and structure of atomic nuclei)*, Moscow, Atomizdat (1969).
33. Blatt, J., Weisskopf, V., *Teoreticheskaya jadernaya fizika (Theoretical nuclear physics)*, Moscow, For. Lit. Press (1954).
34. Levinger, J., *Fotoyadernye reaktsii (Photomuclear reactions)*, Moscow, For. Lit. Press (1962).
35. Veyesiere A. et al. *Nucl. Phys.*, A, v.199, 1973, p.45.
36. Lynn J.E. AERE-R-7468, 1974.
37. Bohr N., Wheller J. *Phys. Rev.*, v.54, 1939, p.426.
38. Hill R., Wheller J. *Phys. Rev.*, v.89, 1953, p.1102.
39. Simon, J., Frehaut, J., *Proc. III All-Union Conf. Neut. Phys., Kiev* 5 (1976) 337.
40. Zen Chan Bom, Panteleev, U., *Tyan San Khak, Izv. Akad. Nauk USSR, Ser. Fiz.* 37 (1973) 82.
41. Ryabov J. et al. *Nucl. Phys.*, A, v.216, 1973, p.325.
42. Sarry J.E., Buncel J., White P.H. *J. Nucl. Energy*, v.18, 1964, p.481.
43. Perkin J.L., O'Conna L.P., Coleman R.F. *Proc. Phys. Soc.*, v.72, 1958, p.505.
44. Stavisskij, Yu. Ya. et al., *Radiatsionnyj zakhvat bystrykh nejtronov (Radiative capture of fast neutrons)*, Moscow, Atomizdat (1970).

Part 5

Theoretical Model Calculations and Evaluation of
Cross-Sections, Angular and Energy Distributions
Fission Spectra and Secondary Gamma Ray Spectra

Abstract

Methods of calculating the cross-sections $\sigma_{n,n}$, $\sigma_{n,2n}$, $\sigma_{n,3n}$ with the aid of a statistical model and a pre-equilibrium decay model are described. The results of evaluation of these cross-sections, the angular and energy distributions of neutrons, the fission spectra and the secondary gamma ray spectra of ^{241}Pu are presented. Group constants for ^{241}Pu were also obtained.

79-7974
Translated from Russian

Academy of Sciences of the Byelorussian SSR
A.V. Lykov Institute of Heat and Mass Transfer

V.A. Kon'shin, G.V. Antsipov, E.Sh. Sukhovitskij, L.A. Bakhanovich,
A.B. Klepatskij, G.B. Morogovskij, Yu.V. Porodzinskij

EVALUATION OF NUCLEAR DATA FOR ^{241}Pu IN THE
 10^{-3} eV-15 MeV NEUTRON ENERGY RANGE

Part 5

Preprint No. 6

Minsk 1979

1. CROSS-SECTION FOR NEUTRON INELASTIC SCATTERING BY ^{241}Pu

1.1. Introduction

No experimental data exist on the cross-section for neutron inelastic scattering by ^{241}Pu . Therefore, to perform evaluations of the cross-section $\sigma_n(E)$, it is necessary to use the results of theoretical calculations in the range of discrete and continuous spectra of levels, the results of calculations of the first level excitation cross-section based on mean resonance parameters, and data on the cross-sections of other competing processes.

1.2. Discrete and continuous spectra of the levels of the ^{241}Pu nucleus

The level scheme of the ^{241}Pu nucleus is dealt with most thoroughly in a paper by Elze and Huizenga [1] who used the reactions $^{242}\text{Pu}(d,t)^{241}\text{Pu}$ and $^{242}\text{Pu}(^3\text{He},\alpha)^{241}\text{Pu}$ for this purpose. They established 27 levels in the range up to 2 MeV. However, it is clear that above 1 MeV the number of omitted levels rises sharply, and so, when studying the discrete spectrum, it is advisable not to go beyond the range up to 1 MeV. The data in Ref. [1] agree with the latest data of Baranov and Shatinskij [2]. A large number of excitation levels was also recorded in an earlier paper by Braid et al. [3], but the identification of these was tentative; therefore, the newer level scheme from Ref. [1] has been used as a basis in our calculations. A spin and parity of $1/2^+$ has been assigned to the level 753 keV on the basis of Ref. [3]. The scheme used in the calculations which contains 27 levels is presented in Table 1.1.

Table 1.1

Scheme of levels of the ^{241}Pu nucleus used in the calculations

Number of level	E_q , keV	J^π	Number of level	E_q , keV	J^π
1	2	3	4	5	6
0	0	$5/2^+$	14	378	$13/2^+$
1	40	$7/2^+$	15	444	$11/2^-$
2	92	$9/2^+$	16	499	$13/2^+$
3	163	$1/2^+$	17	568	$15/2^-$
4	167	$11/2^+$	18	753	$1/2^+$
5	169	$3/2^+$	19	809	$3/2^+$
6	172	$7/2^+$	20	835	$5/2^+$
7	230	$9/2^+$	21	875	$7/2^+$
8	235	$5/2^+$	22	931	$9/2^+$
9	235.1	$13/2^+$	23	967	$1/2^-$
10	244	$7/2^+$	24	994	$11/2^+$
11	296	$11/2^+$	25	1009	$3/2^-$
12	334	$9/2^+$	26	1009	$5/2^-$
13	361	$11/2^+$	-	-	-

A representation of the continuous density of target nucleus levels was used in the higher excitation energy range. For the continuous density of levels in this study we used an expression obtained in the non-interacting particle model [4] with the following parameters: pairing energy $\Delta = 1.013$ MeV (calculated from data in Ref. [5] with allowance for the corrections proposed by Nemirovskij and Adamchuk [6]), density parameter $a = 27.44 \text{ MeV}^{-1}$ (obtained by fitting to $\langle D \rangle_{\text{obsv}} = 13.5 \text{ eV}$ ^{240}Pu in the resolved resonance range [7]). In the present paper, the level density was assumed to be independent of parity in accordance with the conclusion of Ref. [8].

1.3. Calculation of the excitation cross-sections of discrete and continuous level spectra

The calculation of the cross-section $\sigma_{n,}(E)$ in the range up to 5 MeV was performed on the basis of the statistical model, as compound nucleus formation is the principal mechanism in this energy range. Above this range, it becomes necessary to take into account the competition of the processes (n,n'x). It is also necessary to take into account the fact that Bohr's assumption regarding compound nucleus formation [9] is not entirely correct for the higher energies. A proportion of the neutrons is emitted from the nucleus until statistical equilibrium is established in it. This question is examined in greater detail in Section 2.

Calculation of the excitation cross-sections of the discrete levels was carried out according to the Hauser-Feshbach formalism [10], generalized to the case of competition between the fission and radiative capture processes and which also allows for the effect of fluctuation of both neutron and fission widths:

$$\sigma_{n,}(E, E_{q'}) = \frac{\pi}{k^2} \frac{1}{2(2i+1)} \sum_{l,j} T_{lj}(E) \sum_J (2J+1) \frac{\sum_{l',j'} T_{l'j'}(E - \frac{A+1}{A} E_{q'}) S_{\alpha\alpha'}}{T_{\text{comp}} + \sum_{l',j'} T_{l'j'}(E - \frac{A+1}{A} E_{q'})} \quad (1.1)$$

where K is the neutron wave number;

i is the spin of the ground state of the target nucleus;

l, j are the orbital and total moments of an incident neutron;

l', j' are the orbital and total moments of an escaping neutron;

J is the spin of the compound nucleus;

$T_{l,j}(E)$ is the neutron transparency of the target nucleus.

The summation in Eq. (1.1) is performed for all channels which satisfy the laws of conservation of energy, parity and total moment. The coefficient $(A + 1)/A$ in the transparencies for the exit channels takes account of the fact that part of the neutron energy is converted into nuclear recoil energy. The quantity $S_{\alpha\alpha'}$ in expression (1.1) allows for the effect of fluctuation of both the neutron and fission widths, and is described as follows.

$$S_{\alpha\alpha'} = \left(\sum_{\alpha'} T_{\alpha'} \right) \int_0^{\infty} \frac{(t + \frac{2}{\nu_{\alpha'}} \delta_{\alpha\alpha'}) e^{-\langle \tau \rangle t}}{(t + \frac{2}{\nu_{\alpha}} T_{\alpha} t) (t + \frac{2}{\nu_{\alpha'}} T_{\alpha'} t) \prod_{\alpha''} (t + \frac{2}{\nu_{\alpha''}} T_{\alpha''} t)} dt \quad (1.2)$$

It is assumed that all partial widths are subject to χ^2 -distributions with numbers of degrees of freedom ν , so that $\nu_n = 1$ for neutron channels and $\nu_\gamma = \infty$ for radiative capture. The choice of the number of degrees of freedom ν_f of the distribution law for the partial fission widths will be considered below.

The value T_{comp} in Eq. (1.1) takes into account the competition of non-neutron decay channels and includes the transparencies corresponding to radiative capture and fission:

$$T_{\text{comp}} = T_{\gamma J\pi} \left(\frac{A}{A+1} E + S_n \right) + T_{f J\pi} \left(\frac{A}{A+1} E + S_n \right) \quad (1.3)$$

Here $\frac{A}{A+1} E + S_n$ is the compound nucleus excitation energy. The quantity $T_{\gamma J\pi}$ is considered in more detail in Part 4 of the present preprint.

The "effective" transparency $T_{f J\pi}$ for fission was calculated on the basis of the Bohr-Hill-Wheeler model [11,12] with allowance for the discrete and continuous spectra of the transient states of a fissile nucleus [13]:

$$T_{f J\pi} = \sum_K P(E_{fk}, \hbar\omega_k) + \int_{E_{f0}}^{\infty} dE \rho_f(\epsilon, J, \pi) P(E_{f0} + \epsilon, \hbar\omega) \quad (1.4)$$

where

$$P(E_{fk}, \hbar\omega_k) = \frac{1}{1 + \exp\left[-\frac{2\pi(E - E_{fk})}{\hbar\omega_k}\right]} \quad (1.5)$$

and

$$\rho_f(\epsilon, J, \pi) = (2J+1) e^{-(J+1/2)\sigma} C_f \theta_f \quad (1.6)$$

Here E_{fk} is the energy of the known transient states;

$\hbar\omega_k$ is the curvature parameter of the fission barrier;

σ , C_f , θ_f are the continuous density parameters of the transient states of the fissile nucleus.

In accordance with calculations in the unresolved resonance range, the fission threshold was taken as 1.2 MeV, and the curvature parameter $\hbar\omega$, which is identical for all transient states, was taken as 0.6 MeV. The energies of the transient states were selected in accordance with Ref. [14] and are given in Table 1.2.

Table 1.2.

Scheme of transient fission states of the compound nucleus ^{242}Pu

Excess energy above threshold, MeV	Spins and parities of the states
0,1	$0^+, 2^+, 4^+, \dots$
0,5	$1^-, 3^-, 5^-, \dots$
0,7	$2^+, 3^+, 4^+, \dots$
0,9	$1^-, 2^-, 3^-, \dots$
1,2	$2^-, 3^-, 4^-, \dots$
1,4	$1^+, 2^+, 3^+, \dots$
1,6	$0^+, 2^+, 4^+, \dots$
1,6	$4^+, 5^+, 6^+, \dots$
1,7	$1^-, 2^-, 3^-, \dots$
1,7	$3^-, 4^-, 5^-, \dots$

The density parameters of the transient states, taken from Ref. [13], are: $\sigma = 5.7$, $C_f = 0.02135 \text{ MeV}^{-1}$, $\theta_f = 0.3005 \text{ MeV}$. The value of E_f was taken as 1.8 MeV.

The numbers of degrees of freedom ν_f of the distribution law for the fission widths necessary for calculating the coefficient $S_{\alpha\alpha}$, (1.2) were selected as follows:

$$\nu_{fj\pi} = T_{fj\pi} / \max[\rho(E, \hbar\omega)] \quad (1.7)$$

where $\max[\rho(E, \hbar\omega)]$ is the maximum possible fission transparency for the channel $\{J, \Pi\}$.

This approach does not restrict the values ν_f to whole numbers only. In the excitation energy region corresponding to the continuous target nucleus excitation spectrum, it is possible to disregard the effect of fluctuation of the partial widths because of the large number of channels. The cross-sections are written as follows:

$$\sigma_{n'}(E) = \sum_{q'} \sigma_{n'}(E, E_{q'}) + \sigma_{n', \text{cont}}(E) \quad (1.8)$$

where σ_n , $\text{cont}(E)$ is the excitation cross-section of the continuous spectrum:

$$\sigma_{n, \text{cont}}(E) = \frac{\pi}{k^2} \frac{1}{2(2i+1)} \sum_{l_j} T_{l_j}(E) \sum_J (2J+1) \frac{\alpha(E, J)}{\sum_{l_j} T_{l_j}(E - \frac{A+1}{A} E_{q'}) + d(E, J)} \quad (1.9)$$

Here

$$\alpha(E, J) = \sum_{l_j} \int_{E_{q', \text{max}}}^{\frac{A+1}{A} E} \rho(l, E') T_{l_j}(E - \frac{A+1}{A} E') dE', \quad (1.10)$$

where $E_{q', \text{max}}$ is the energy at which the continuous spectrum begins, which in the present calculation is 1.025 MeV. In this case the cross-section $\sigma_n(E, E_{q'})$ is calculated in a similar fashion to Eq. (1.1) with $S_{\alpha\alpha} = 1$ and an additional term $\alpha(E, J)$ to take account of the competition in the continuous spectrum.

In the case of the continuous spectrum of target nucleus levels, fission competition was allowed for by introducing the "effective" transparencies:

$$T_{f, \text{eff}}(E) = (2J+1) T_f(E), \quad (1.11)$$

where $T_f(E)$ was determined by fitting the fission cross-section σ_f calculated on the basis of a unified formalism to that evaluated from experiment. The contribution of the process $(n, \gamma f)$ was taken into account in calculating the fission cross-section.

The optical potential of the target nucleus must be known in order to calculate the neutron transparencies. As data on σ_t and $\sigma_n(\theta)$ normally used to determine the parameters of the potential do not exist in this case, the choice of the potential has to be based on the classification of neighbouring nuclei which have been investigated more thoroughly. Some information can also be obtained by comparing the strength functions for s- and p-waves, obtained by calculations based on the optical model and an analysis of the data in the resolved and unresolved resonance range.

For calculating the neutron transparencies here we used the potential:

$$V(r) = -V_r f(r) - i W_{\text{im}} [\alpha f(r) + (1-\alpha) g(r)] - V_{s0} \left(\frac{\hbar}{\mu r c} \right)^2 \frac{d}{dr} \left(\frac{f(r)}{\delta} \right), \quad (1.12)$$

$$f(r) = \left[1 + \exp\left(\frac{r-R}{\alpha}\right) \right]^{-1}, \quad (1.13)$$

$$g(r) = \exp\left[-\left(\frac{r-R}{\delta}\right)^2\right], \quad (1.14)$$

$$R = r_0 A^{1/3}, \quad (1.15)$$

with the following parameters taken from Ref. [15]:

$V_r = 42.915 - 0.833 E$ (MeV), $W_{im} = 6.204 - 0.12 E$ (MeV), $a = 0.47$ fm, $b = 1.00$ fm, $d = 0.1781$ and $r_0 = 1.32$ fm. This potential was chosen to describe the cross-sections of ^{238}U . In our case the strength functions, calculated from the optical model at an energy of 10 keV, are: $S_0 = 0.734 \times 10^{-4}$, $S_1 = 2.507 \times 10^{-4}$. Comparison of these with the evaluated values $S_0 = (1.16 \pm 0.19) \times 10^{-4}$ and $S_1 = (2.0 \pm 0.5) \times 10^{-4}$ shows that the calculation based on the optical model gives a lower value for S_0 . This is a common phenomenon, and is caused by the use of a spherical potential for non-spherical nuclei.

Let us compare the cross-sections σ_t and σ_n obtained using the optical potential (1.12) with the data evaluated in the present paper. Fig. 1 shows a comparison of the calculated σ_t with the evaluation in the region up to 4 MeV which is the most important for calculations of the cross-sections for processes involving the formation of a compound nucleus. As can be seen from the figure, the calculated cross-section is a little lower than the evaluated one; the discrepancy, however, does not exceed the assumed error of the evaluated data. Figure 1.2 presents a comparison of the data on σ_n and also shows the calculated contributions of potential and compound scattering. In general, there is good agreement on σ_n except in the low-energy region. Figure 1.3 compares data on the cross-section for compound nucleus formation. Here the contribution of elastic scattering by the compound nucleus, calculated on the basis of the statistical model (Fig. 1.2), is added to the evaluated cross-section σ_{nx} . It can be seen from the figure that the discrepancies are significant in the region above 1 MeV. This indicates the need to renormalize the cross-sections calculated from the statistical model as well as the cross-section σ_f in the region above 1 MeV used for making adjustments to allow for fission competition.

The formalism described above for calculating the cross-sections for reactions involving compound nucleus formation was used within the framework of the MOST computer program, written in Fortran. The results of the calculations performed with this program using the initial data given above provided the basis for the evaluation.

1.4. Evaluated data on σ_n , (^{241}Pu) and their accuracy

As mentioned above, in order to obtain evaluated values for the cross-sections calculated with the statistical model, it is necessary to renormalize the result of the calculation to take into account the difference between the calculated and evaluated cross-sections for inelastic interactions which is caused by the error in the optical potential:

$$\bar{\sigma}_{n^{\prime}eval} = \bar{\sigma}_{n^{\prime}calc} \frac{\bar{\sigma}_{n^{\prime}eval} - \bar{\sigma}_{f^{\prime}eval}}{\bar{\sigma}_{n^{\prime}calc} + \bar{\sigma}_{f^{\prime}calc}}, \quad (1.16)$$

$$\bar{\sigma}_{n^{\prime}eval}(E_{q^{\prime}}) = \bar{\sigma}_{n^{\prime}calc}(E_{q^{\prime}}) \frac{\bar{\sigma}_{n^{\prime}eval}}{\bar{\sigma}_{n^{\prime}calc}}, \quad (1.17)$$

$$\bar{\sigma}_{j^{\prime}eval} = \bar{\sigma}_{j^{\prime}calc} \frac{\bar{\sigma}_{n^{\prime}eval} - \bar{\sigma}_{f^{\prime}eval}}{\bar{\sigma}_{n^{\prime}calc} + \bar{\sigma}_{f^{\prime}calc}} \quad (1.18)$$

Data given in Part 4 of the preprint were used for this normalization.

Evaluated data on the excitation cross-sections for discrete $\sigma_{n^{\prime}}(E_{q^{\prime}})$ and continuous ($\sigma_{n^{\prime} cont}$) spectra are given in Table 1.3 and Fig. 1.4.

The evaluated cross-sections $\sigma_{n^{\prime}}$ in the energy region above 5 MeV are based on the results of calculation of (n,n^{\prime}) reaction cross-sections with allowance for the competition of many-particle processes and for the possibility of neutrons being emitted from the nucleus until equilibrium is established. The method and results of the calculations are set out in detail in section 2. The evaluated cross-sections $\sigma_{n^{\prime}}$ in the region above 5 MeV are presented in Table 2.1 of Part 4 of the preprint.

Comparison of the results of the present paper with the evaluations of other authors (Fig. 1.5) shows that the data presented here are in fairly good agreement with the evaluation of Kaner and Yiftah [16]. Prince's data [17] are systematically higher.

Table 1.3

Cross-sections for neutron inelastic scattering by ^{241}Pu in the energy range up to 5 MeV

E, MeV	E_p , MeV																	σ_n, b
	0,040	0,092	0,163	0,167	0,169	0,172	0,230	0,235	0,2351	0,244	0,296	0,334	0,361	0,378	0,444	0,499	0,566	
0,10	0,1852	0,0058	0,0	0,0	0,0	0,0	0,0	0,0	0,0	0,0	0,0	0,0	0,0	0,0	0,0	0,0	0,0	0,191
0,12	0,2042	0,0266	0,0	0,0	0,0	0,0	0,0	0,0	0,0	0,0	0,0	0,0	0,0	0,0	0,0	0,0	0,0	0,231
0,14	0,2183	0,0467	0,0	0,0	0,0	0,0	0,0	0,0	0,0	0,0	0,0	0,0	0,0	0,0	0,0	0,0	0,0	0,265
0,16	0,2396	0,0664	0,0	0,0	0,0	0,0	0,0	0,0	0,0	0,0	0,0	0,0	0,0	0,0	0,0	0,0	0,0	0,306
0,18	0,2355	0,0768	0,0068	0,0027	0,0119	0,0133	0,0	0,0	0,0	0,0	0,0	0,0	0,0	0,0	0,0	0,0	0,0	0,347
0,20	0,2262	0,0826	0,0155	0,0075	0,0299	0,0363	0,0	0,0	0,0	0,0	0,0	0,0	0,0	0,0	0,0	0,0	0,0	0,398
0,22	0,2240	0,0886	0,0235	0,0120	0,0465	0,0574	0,0	0,0	0,0	0,0	0,0	0,0	0,0	0,0	0,0	0,0	0,0	0,452
0,24	0,2190	0,0922	0,0299	0,0159	0,0598	0,0742	0,0034	0,0076	0,0	0,0	0,0	0,0	0,0	0,0	0,0	0,0	0,0	0,502
0,26	0,2056	0,0909	0,0337	0,0183	0,0680	0,0841	0,0118	0,0261	0,0002	0,0133	0,0	0,0	0,0	0,0	0,0	0,0	0,0	0,552
0,28	0,1971	0,0905	0,0370	0,0203	0,0749	0,0925	0,0202	0,0425	0,0004	0,0276	0,0	0,0	0,0	0,0	0,0	0,0	0,0	0,603
0,30	0,1939	0,0918	0,0405	0,0224	0,0820	0,1011	0,0281	0,0577	0,0007	0,0414	0,0004	0,0	0,0	0,0	0,0	0,0	0,0	0,660
0,32	0,1928	0,0936	0,0437	0,0243	0,0887	0,1090	0,0354	0,0715	0,0011	0,0541	0,0028	0,0	0,0	0,0	0,0	0,0	0,0	0,717
0,34	0,1924	0,0954	0,0468	0,0262	0,0947	0,1159	0,0419	0,0839	0,0015	0,0655	0,0055	0,0013	0,0	0,0	0,0	0,0	0,0	0,771
0,36	0,1916	0,0968	0,0495	0,0277	0,1000	0,1217	0,0476	0,0946	0,0020	0,0755	0,0082	0,0068	0,0	0,0	0,0	0,0	0,0	0,822
0,38	0,1913	0,0981	0,0520	0,0292	0,1049	0,1269	0,0526	0,1043	0,0025	0,0844	0,0103	0,0132	0,0018	0,0	0,0	0,0	0,0	0,872
0,40	0,1906	0,0991	0,0543	0,0305	0,1090	0,1311	0,0569	0,1124	0,0030	0,0920	0,0132	0,0196	0,0041	0,0002	0,0	0,0	0,0	0,916
0,42	0,1889	0,0994	0,0559	0,0315	0,1120	0,1338	0,0604	0,1188	0,0035	0,0981	0,0153	0,0255	0,0064	0,0005	0,0	0,0	0,0	0,950
0,44	0,1882	0,1003	0,0577	0,0327	0,1152	0,1368	0,0637	0,1249	0,0041	0,1038	0,0173	0,0311	0,0088	0,0009	0,0	0,0	0,0	0,9855
0,46	0,1876	0,1010	0,0592	0,0337	0,1178	0,1394	0,0667	0,1301	0,0046	0,1086	0,0191	0,0361	0,0110	0,0013	0,0008	0,0	0,0	1,017
0,48	0,1880	0,1024	0,0610	0,0351	0,1210	0,1424	0,0698	0,1355	0,0053	0,1136	0,0210	0,0410	0,0132	0,0018	0,0019	0,0	0,0	1,053
0,50	0,1878	0,1034	0,0623	0,0363	0,1233	0,1446	0,0724	0,1397	0,0060	0,1176	0,0227	0,0453	0,0152	0,0024	0,0030	0,0	0,0	1,082
0,55	0,1881	0,1065	0,0656	0,0395	0,1287	0,1496	0,0785	0,1488	0,0078	0,1263	0,0268	0,0548	0,0200	0,0039	0,0061	0,0008	0,0	1,1516
0,60	0,1860	0,1080	0,0672	0,0422	0,1310	0,1515	0,0826	0,1532	0,0097	0,1311	0,0302	0,0618	0,0240	0,0055	0,0089	0,0021	0,0	1,195
0,65	0,1852	0,1105	0,0689	0,0454	0,1333	0,1535	0,0868	0,1571	0,0118	0,1354	0,0337	0,0680	0,0279	0,0072	0,0116	0,0037	0,0	1,240
0,70	0,1861	0,1142	0,0708	0,0491	0,1362	0,1566	0,0914	0,1611	0,0142	0,1399	0,0375	0,0740	0,0318	0,0093	0,0142	0,0055	0,0001	1,292

(continued on page 12)

E, MeV	E _g , MeV															
	0,040	0,092	0,163	0,167	0,169	0,172	0,230	0,235	0,2351	0,244	0,296	0,334	0,361	0,378	0,444	0,499
0,75	0,1872	0,1179	0,0724	0,0531	0,1383	0,1592	0,0959	0,1641	0,0168	0,1437	0,0413	0,0794	0,0358	0,0114	0,0167	0,0075
0,80	0,1870	0,1208	0,0730	0,0568	0,1387	0,1602	0,0994	0,1651	0,0194	0,1458	0,0449	0,0838	0,0394	0,0137	0,0189	0,0095
0,85	0,1849	0,1226	0,0725	0,0600	0,1372	0,1597	0,1019	0,1638	0,0220	0,1460	0,0481	0,0870	0,0426	0,0159	0,0208	0,0115
0,90	0,1809	0,1229	0,0711	0,0626	0,1339	0,1570	0,1030	0,1602	0,0243	0,1443	0,0508	0,0888	0,0453	0,0179	0,0224	0,0134
0,95	0,1779	0,1237	0,0701	0,0652	0,1314	0,1552	0,1044	0,1576	0,0267	0,1432	0,0534	0,0908	0,0480	0,0201	0,0239	0,0153
1,0	0,1691	0,1201	0,0669	0,0655	0,1249	0,1482	0,1061	0,1496	0,0281	0,1373	0,0541	0,0893	0,0489	0,0214	0,0245	0,0167
1,1	0,1566	0,1116	0,0660	0,0616	0,1207	0,1385	0,0957	0,1422	0,0273	0,1288	0,0514	0,0844	0,0467	0,0211	0,0252	0,0167
1,2	0,1414	0,1045	0,0591	0,0608	0,1078	0,1260	0,0907	0,1276	0,0288	0,1178	0,0516	0,0806	0,0472	0,0228	0,0258	0,0184
1,4	0,1147	0,0895	0,0479	0,0564	0,0867	0,1041	0,0795	0,1033	0,0294	0,0981	0,0493	0,0720	0,0458	0,0244	0,0247	0,0204
1,6	0,0870	0,0703	0,0363	0,0469	0,0654	0,0801	0,0638	0,0786	0,0260	0,0763	0,0420	0,0588	0,0396	0,0244	0,0209	0,0194
1,8	0,0610	0,0507	0,0255	0,0351	0,0459	0,0570	0,0468	0,0556	0,0205	0,0548	0,0322	0,0438	0,0307	0,0182	0,0160	0,0162
2,0	0,0398	0,0337	0,0166	0,0241	0,0299	0,0377	0,0316	0,0366	0,0145	0,0365	0,0224	0,0300	0,0216	0,0132	0,0112	0,0121
2,2	0,0243	0,0207	0,0102	0,0150	0,0183	0,0232	0,0197	0,0225	0,0093	0,0226	0,0142	0,0188	0,0138	0,0086	0,0072	0,0080
2,4	0,0143	0,0123	0,0060	0,0091	0,0108	0,0137	0,0118	0,0133	0,0058	0,0134	0,0087	0,0114	0,0085	0,0054	0,0045	0,0051
2,6	0,0083	0,0072	0,0035	0,0054	0,0063	0,0080	0,0070	0,0078	0,0035	0,0079	0,0052	0,0068	0,0051	0,0033	0,0028	0,0032
2,8	0,0048	0,0042	0,0020	0,0032	0,0036	0,0047	0,0041	0,0045	0,0021	0,0046	0,0031	0,0040	0,0030	0,0020	0,0017	0,0019
3,0	0,0028	0,0025	0,0012	0,0019	0,0021	0,0027	0,0024	0,0026	0,0013	0,0027	0,0018	0,0023	0,0018	0,0012	0,0010	0,0012
3,2	0,0016	0,0015	0,0007	0,0011	0,0012	0,0016	0,0014	0,0015	0,0008	0,0016	0,0011	0,0014	0,0011	0,0007	0,0006	0,0007
3,4	0,0011	0,0010	0,0004	0,0007	0,0008	0,0010	0,0009	0,0010	0,0005	0,0007	0,0007	0,0009	0,0007	0,0005	0,0004	0,0005
3,6	0,0007	0,0006	0,0002	0,0004	0,0005	0,0005	0,0006	0,0006	0,0003	0,0006	0,0004	0,0006	0,0004	0,0003	0,0002	0,0003
3,8	0,0004	0,0004	0,0001	0,0003	0,0003	0,0003	0,0004	0,0004	0,0002	0,0004	0,0003	0,0004	0,0003	0,0003	0,0001	0,0002
4,0	0,0002	0,0002	0,0001	0,0002	0,0002	0,0002	0,0002	0,0002	0,0001	0,0002	0,0002	0,0002	0,0002	0,0002	0,0001	0,0001
4,5	0,0001	0,0001	0,0001	0,0	0,0001	0,0001	0,0001	0,0	0,0001	0,0001	0,0001	0,0001	0,0	0,0	0,0	0,0
5,0	0,0	0,0	0,0	0,0	0,0	0,0	0,0	0,0	0,0	0,0	0,0	0,0	0,0	0,0	0,0	0,0

(continued on page 13)

E, MeV	E _g , MeV										σ _{n, cont.} , b	σ _n , b
	0,568	0,753	0,809	0,835	0,875	0,931	0,967	0,994	1,009	1,009		
0,75	0,0003	0,0	0,0	0,0	0,0	0,0	0,0	0,0	0,0	0,0	0,0	1,3410
0,80	0,0004	0,0052	0,0	0,0	0,0	0,0	0,0	0,0	0,0	0,0	0,0	1,3820
0,85	0,0007	0,0116	0,0082	0,0035	0,0	0,0	0,0	0,0	0,0	0,0	0,0	1,4205
0,90	0,0010	0,0170	0,0194	0,0173	0,0047	0,0	0,0	0,0	0,0	0,0	0,0	1,4582
0,95	0,0012	0,0214	0,0293	0,0308	0,0166	0,0018	0,0	0,0	0,0	0,0	0,0	1,5080
1,0	0,0015	0,0240	0,0361	0,0408	0,0272	0,0090	0,0022	0,0001	0,0	0,0	0,0	1,5080
1,1	0,0019	0,0286	0,0465	0,0545	0,0415	0,0210	0,0079	0,0063	0,0114	0,0142	0,0136	0,5419
1,2	0,0024	0,0288	0,0485	0,0584	0,0479	0,0285	0,0108	0,0119	0,0184	0,0228	0,0753	1,5640
1,4	0,0033	0,0266	0,0459	0,0561	0,0493	0,0337	0,0124	0,0176	0,0224	0,0277	0,3218	1,6630
1,6	0,0035	0,0221	0,0381	0,0467	0,0425	0,0312	0,0110	0,0181	0,0199	0,0245	0,8666	1,7580
1,8	0,0032	0,0168	0,0289	0,0355	0,0332	0,0255	0,0086	0,0158	0,0154	0,0190	1,0371	1,8490
2,0	0,0026	0,0118	0,0204	0,0251	0,0240	0,0191	0,0061	0,0125	0,0109	0,0134	1,3676	1,9250
2,2	0,0018	0,0077	0,0134	0,0165	0,0160	0,0130	0,0041	0,0088	0,0072	0,0088	1,5933	1,9470
2,4	0,0013	0,0048	0,0083	0,0103	0,0101	0,0084	0,0026	0,0059	0,0045	0,0056	1,7391	1,9550
2,6	0,0008	0,0029	0,0051	0,0063	0,0062	0,0053	0,0016	0,0038	0,0028	0,0035	1,8304	1,9600
2,8	0,0006	0,0017	0,0030	0,0038	0,0038	0,0033	0,0010	0,0024	0,0017	0,0021	1,8851	1,9620
3,0	0,0004	0,0010	0,0018	0,0023	0,0023	0,0020	0,0006	0,0015	0,0010	0,0013	1,9023	1,9480
3,2	0,0002	0,0006	0,0011	0,0014	0,0014	0,0012	0,0004	0,0009	0,0006	0,0008	1,9190	1,9462
3,4	0,0001	0,0004	0,0007	0,0009	0,0009	0,0008	0,0002	0,0006	0,0004	0,0005	1,9290	1,9463
3,6	0,0	0,0002	0,0003	0,0004	0,0005	0,0004	0,0001	0,0003	0,0002	0,0003	1,9365	1,9464
3,8	0,0	0,0001	0,0001	0,0003	0,0003	0,0003	0,0001	0,0002	0,0001	0,0002	1,9448	1,9508
4,0	0,0	0,0001	0,0001	0,0002	0,0002	0,0002	0,0001	0,0001	0,0001	0,0001	1,9501	1,9540
4,5	0,0	0,0	0,0	0,0001	0,0001	0,0001	0,0	0,0	0,0	0,0	1,9341	1,9354
5,0	0,0	0,0	0,0	0,0	0,0	0,0	0,0	0,0	0,0	0,0	1,9056	1,9056

It is difficult to assess the error of the data obtained for σ_{n^*} . It seems possible to attribute an error of $\sim 20\%$ to the data on σ_{n^*} in the region up to 5 MeV, but above the threshold of the processes (n, n^*x) in the 5-10 MeV region, the accuracy is poorer, being $\sim 50\%$. Above 10 MeV the cross-section for the reactions (n, n^*) is determined mainly by the pre-equilibrium processes. Taking into account the accuracy of measurement of these processes for other nuclei, the accuracy of the evaluated σ_{n^*} in this region is put at $\sim 30\%$.

1.5. The energy distribution of inelastically-scattered neutrons

For the resolved levels of the target nucleus, the energy distribution of inelastically-scattered neutrons is determined uniquely by the incident neutron energy E , the level excitation energy E_q , the angle of emission ϑ and the ratio of the nuclear mass to the neutron mass M . It can be described in the following form [18]:

$$P(E, E', E_q) = \sum_{n=1}^N P_n \delta[E - E'_n(E, \vartheta, E_q)], \quad (1.19)$$

where

$$E'_n(E, \vartheta, E_q) = \frac{E}{(M+1)^2} \left\{ 2\mu_L^2 + M \left(1 - \frac{M+1}{M} \frac{E_q}{E} \right) \pm 2\mu_L \sqrt{\mu_L^2 + M \left(1 - \frac{M+1}{M} \frac{E_q}{E} \right)^2} \right\} \quad (1.20)$$

($\mu_L = \cos \vartheta$ is the cosine of the scattering angle in the L system). If $\frac{M+1}{M} E_q < E < \frac{M}{M-1} E_q$, then both values of E'_n are possible, and in expression (1.18) $N = 2$. In this case

$$P_1 = \frac{1}{2} f(\mu_{c1}) \quad \text{u} \quad P_2 = \frac{1}{2} f(\mu_{c2}), \quad (1.21)$$

where μ_{c1} and μ_{c2} are the roots of the equation linking the cosine of the scattering angle μ_c in the C system with μ_L ; $\frac{1}{2} f(\mu_c)$ is the angular distribution in the C system.

If $\mu_{c1} > \mu_{c2}$, a plus sign is assigned to E'_1 and a minus sign to E'_2 in formula (1.20). At higher energies, i.e. at $E > \frac{M}{M-1} E_q$, only the value E'_1 ("+" sign) is taken, and $N = 1$, $P_1 = 1$ and $P_2 = 0$.

In the present paper the angular distribution of inelastically scattered neutrons for processes involving compound nucleus formation was assumed to be isotropic in the C system.

In the overlapping levels region of the target nucleus (from 1.009 MeV to the threshold of the reaction (n,2n) at 5.241 MeV) the following evaporation spectrum was assumed for the energy distribution of inelastically-scattered neutrons with excitation of a continuous spectrum:

$$P(E, E') \approx \frac{E'}{T^2} e^{-\frac{E'}{T}}, \quad 1.009 \text{ MeV} < E' < E, \quad (1.22)$$

where E' is the energy of the emitted neutron;

T is the nuclear temperature.

Because of the absence of any experimental data for the ^{241}Pu nucleus, the energy dependence of the temperature T was based on our evaluation [19] for ^{239}Pu , and in the 1 MeV region this fits closely the data from the mean energies of inelastically scattered neutrons obtained from the excitation cross-sections of the levels evaluated here.

The evaluated data for T are presented in Table 1.4 and Fig. 1.6.

Table 1.4.

Dependence of nuclear temperature on incident neutron energy

$E, \text{ MeV}$	$T, \text{ MeV}$	$E, \text{ MeV}$	$T, \text{ MeV}$
1,2	0,387	3,6	0,498
1,4	0,403	3,8	0,502
1,6	0,418	4,0	0,505
1,8	0,432	4,5	0,511
2,0	0,443	5,0	0,516
2,2	0,453	5,5	0,520
2,4	0,462	6,0	0,523
2,6	0,470	6,5	0,525
2,8	0,477	7,0	0,527
3,0	0,484	7,5	0,529
3,2	0,490	8,0	0,530
3,4	0,494	8,0-15,0	0,530

In the neutron energy range above 5 MeV, allowance must be made for the possible occurrence of the pre-equilibrium mechanism of neutron emission which leads to hardening of the spectrum. The following expression was adopted for this part of the spectrum:

$$P_{\text{pre}}(E, E') \sim \sum_{n=3}^{\bar{n}} \left(\frac{E-E'}{E+B_n} \right)^{n-2} (n+1)^2 (n-1); \quad E' < E, \quad (1.23)$$

where $\bar{n} = \sqrt{g(E + B_n)}$ is the average number of excitations; g is the one-particle density of the nuclear states, equal to σ_a/π^2 .

The contributions of both parts of the spectrum are determined by the contribution of the process mechanisms to the spectrum of the first neutron emitted (see Fig. 1.7). A detailed description of the pre-equilibrium mechanism contribution is given in section 2, and the inelastically-scattered neutron spectrum for the continuous spectrum of the levels is also presented in that section.

1.6. Angular distributions of inelastically-scattered neutrons

There is no experimental information on the angular distributions of inelastically-scattered neutrons. If we make the usual assumption that inelastic scattering involving compound nucleus formation is isotropic in the centre-of-mass system, all anisotropy will be produced by direct processes. In this case the angular distribution can be calculated by the coupled-channel method [21]. As the parameters needed for this calculation are not known accurately enough, only the mean cosine of the inelastic scattering angle is given here, as in Ref. [19]. Scattering was assumed to be isotropic in the region up to 100 keV. In the region above 100 keV it was assumed that the anisotropy of the angular distribution was caused solely by direct excitation of the first level. The "effective" direct excitation cross-sections necessary for taking the inelastic scattering anisotropy into account are given in Table 1.5. The mean scattering cosine at this level is given in Table 1.6.

Table 1.5.

"Effective" first level direct excitation cross-sections
necessary for taking inelastic scattering and anisotropy into account

E , MeV	$\sigma_{n',np}$, b	E , MeV	$\sigma_{n',np}$, b
0,2	0,018	6,0	0,100
0,4	0,059	7,0	0,096
0,6	0,077	8,0	0,092
0,8	0,090	9,0	0,088
1,0	0,094	10,0	0,083
1,4	0,102	11,0	0,080
2,0	0,106	12,0	0,078
3,0	0,107	13,0	0,076
4,0	0,104	14,0	0,073
5,0	0,103	15,0	0,0708

Table 1.6.

The mean neutron inelastic scattering cosine for first level excitation

$E, \text{ MeV}$	$\overline{\text{Cos } \theta}$	$E, \text{ MeV}$	$\overline{\text{Cos } \theta}$
0,2	0,009	6,0	0,225
0,4	0,026	7,0	0,238
0,6	0,044	8,0	0,251
0,8	0,061	9,0	0,264
1,0	0,079	10,0	0,275
1,4	0,105	11,0	0,285
2,0	0,135	12,0	0,295
3,0	0,169	13,0	0,302
4,0	0,191	14,0	0,306
5,0	0,210	15,0	0,307

2. EVALUATION OF THE CROSS-SECTIONS FOR THE REACTIONS
 (n,2n), (n,3n), (n,n'f) AND (n,2n'f)
 AND THE NEUTRON SPECTRA ACCOMPANYING
 THESE REACTIONS

There is no experimental information at all on the above reactions in a ^{241}Pu nucleus. An evaluation can thus be performed only by means of calculations based on the model proposed by us, which employs experimental information for nuclei occurring in successive decay stages [22]. This model was refined as follows.

It was assumed that a proportion of the neutrons is emitted from the nucleus until statistical equilibrium is attained therein. The spectrum of these neutrons was assumed to have the form [20]:

$$I'_{np}(E,E') = \beta \frac{2s+1}{2\pi^2 \hbar^3} \frac{\epsilon G_{abc}(E) G_c(E,E')}{|M^2| g^*(E+B_n)^3} \sum_{n=n_0, n_0+2}^{\bar{n}} \left(\frac{E-E'}{E+B_n}\right)^{n-2} (n+1)(n-1), \quad (2.1)$$

*/

where $\sigma_{abc}(E)$ is the cross-section for neutron absorption by the nucleus;

$|M^2|$ is the mean matrix element of the interaction between states with n and $n+2$ excitons;

n_0 is the initial number of excitons, assumed by us here to be

$$3, \bar{n} = \sqrt{g(E+B_n)};$$

$\sigma_c(E,E')$ is the cross-section for the reaction inverse to neutron emission; $\beta = 2/3$.

It was also assumed that statistical equilibrium is established in the nucleus after the emission of the first neutron, and the second and third neutrons are emitted from the nucleus in the equilibrium state. The spectrum of the first neutron emitted from the equilibrium nucleus was taken as [23]

*/ Translator's note: the subscript "Hp" apparently means "non-equilibrium" and "p" (see below, e.g. Eq. (2.3)) means "equilibrium". This may be confirmed by reference to Ref. [20], which, however, was not available in the Library at the time of translation.

$$I'_p(E, E') = E' G_p(E, E') \rho(E - B_n - E'). \quad (2.2)$$

If we consider that $\left[\frac{M^2}{g^4} \right] = \alpha A$, where $\alpha = 3.3 \times 10^{-4} \text{ MeV}^{-2}$ [20, 24], then the spectrum (2.1) gives the absolute value of the pre-equilibrium neutron emission cross-section as a function of the incident neutron energy (Table 2.1).

Table 2.1

Dependence of the pre-equilibrium contribution to the inelastic interaction cross-section for ^{241}Pu on incident neutron energy

Energy, MeV	7	9	12	15
Contribution, %	0.06	0.10	0.15	0.19

The spectra of the first neutrons emitted determine the excitation spectra of the residual nuclei after the emission of the first neutron $\chi'_{np}(E)$.

It is not difficult to obtain the nuclear excitation probability distribution after the emission of the second and third neutrons respectively:

$$\chi'_{np}{}^{n+1}(E) = \int_{E-B_n}^{E_{max}} \chi'^n(E') S(E', E) dE', \quad (2.3)$$

where $S(E', E)$ is the probability that the nucleus A with an excitation E' will emit a neutron with an energy $E_n = E' - E - B_n$ and be transformed into the nucleus A-1 with an energy E.

The probability $S(E', E)$ is normalized by the condition

$$\int_{E-B_n}^{E_{max}} S(E, E') dE' = \Gamma_n(E) / \Gamma(E), \quad (2.4)$$

where $\Gamma_n(E)^0$ and $\Gamma(E)$ are the neutron and total widths respectively.

The probability $S(E', E)$ is identical for nuclei with the first neutron emitted both in the equilibrium and pre-equilibrium states, as in our assumptions the nucleus changes to the equilibrium state after the first neutron is emitted. Formula (2.2) defines $S(E', E)$ to within the accuracy of normalization

$$S(E;E) = f(E') \sigma_c(E' - B_n - E) (E' - B_n - E) \rho(E), \quad (2.5)$$

where $f(E')$ is determined from the normalization condition (2.4)

$$f(E') \int_{E' - B_n}^{E' - B_n} \sigma_c(E' - B_n - E) (E' - B_n - E) \rho(E) dE = \frac{f_n(E)}{f(E)}.$$

These expressions were obtained taking into account that $\sigma_c(E, E') = \sigma_c(E')$.

Then

$$\chi_{HP}^2(E) = \rho(E) \int_{E - B_{nA}}^{E_{max}} \chi_{HP}^1(E') f(E') \sigma_c(E' - B_{nA} - E) (E' - B_{nA} - E) dE'; \quad (2.6)$$

$$\chi_{HP}^3(E) = \rho(E) \int_{E - B_{nA,1}}^{E_{max}} \chi_{HP}^2(E') f(E') \sigma_c(E' - B_{nA,1} - E) (E' - B_{nA,1} - E) dE'. \quad (2.7)$$

The distributions χ_{HP}^2 were used for averaging the emission probabilities of successive particles.

The final formulae for calculating the cross-sections for the reactions $(n, 2n)$, $(n, 3n)$, (n, n^*f) and $(n, 2n^*f)$ take the form:

$$\begin{aligned} \sigma_{n,2n}(E_n) &= \sigma_{n,n^*f}(E_n) \int_{B_{nA}}^{E_n} \left(\frac{\sigma_{n,n^*f}}{\sigma_{ne} - \sigma_{np}} \right)_{A-1, E-B_{nA}} \chi_{HP}^1(E) dE \\ &+ \int_0^{E_n - B_{nA}} \left(\frac{\sigma_{n,n^*f}}{\sigma_{ne} - \sigma_{np}} \right)_{A-2, E-B_{nA}} \chi_{HP}^2(E) dE + \sigma_{HP}(E_n) \int_{B_{nA}}^{E_n} \left(\frac{\sigma_{n,n^*f}}{\sigma_{ne} - \sigma_{np}} \right) \chi_{HP}^1(E) dE \end{aligned} \quad (2.8)$$

$$\begin{aligned} &+ \int_0^{E_n - B_{nA}} \left(\frac{\sigma_{n,n^*f}}{\sigma_{ne} - \sigma_{np}} \right)_{A-2, E-B_{nA}} \chi_{HP}^2(E) dE; \\ \sigma_{n,3n}(E_n) &= \sigma_{n,n^*f}(E_n) \int_{B_{nA}}^{E_n} \left(\frac{\sigma_{n,n^*f}}{\sigma_{ne} - \sigma_{np}} \right)_{A-1, E-B_{nA}} \chi_{HP}^1(E) dE \\ &+ \int_{B_{nA,1}}^{E_n - B_{nA}} \left(\frac{\sigma_{n,n^*f}}{\sigma_{ne} - \sigma_{np}} \right)_{A-2, E-B_{nA,1}} \chi_{HP}^2(E) dE \int_{B_{nA,1}}^{E_n - B_{nA} - B_{nA,1}} \left(\frac{\sigma_{n,n^*f}}{\sigma_{ne} - \sigma_{np}} \right)_{A-3, E-B_{nA,1}} \chi_{HP}^3(E) dE + \\ &+ \sigma_{HP}(E_n) \int_{B_{nA}}^{E_n} \left(\frac{\sigma_{n,n^*f}}{\sigma_{ne} - \sigma_{np}} \right)_{A-1, E-B_{nA}} \chi_{HP}^1(E) dE \int_{B_{nA,1}}^{E_n - B_{nA}} \left(\frac{\sigma_{n,n^*f}}{\sigma_{ne} - \sigma_{np}} \right)_{A-2, E-B_{nA,1}} \chi_{HP}^2(E) dE + \\ &+ \int_0^{E_n - B_{nA} - B_{nA,1}} \left(\frac{\sigma_{n,n^*f}}{\sigma_{ne} - \sigma_{np}} \right)_{A-3, E-B_{nA,1}} \chi_{HP}^3(E) dE; \end{aligned} \quad (2.9)$$

$$\begin{aligned} \sigma_{n,n'y}(E_n) &= \sigma_{n,n'x}(E_n) \int_0^{E_n} \left(\frac{\sigma_{nf}}{\sigma_{ne} - \sigma_{Hp,A,1,E-D_{nA}}} \right) \chi_p^1(E) dE + \\ &+ \sigma_{Hp}(E_n) \int_0^{E_n} \left(\frac{\sigma_{nf}}{\sigma_{ne} - \sigma_{Hp,A,1,E-D_{nA}}} \right) \chi_{Hp}^1(E) dE; \end{aligned} \quad (2.10)$$

$$\begin{aligned} \sigma_{n,2n'y}(E_n) &= \sigma_{n,n'x}(E_n) \int_0^{E_n} \left(\frac{\sigma_{n,2n'y}}{\sigma_{ne} - \sigma_{Hp,A,1,E-D_{nA}}} \right) \chi_p^1(E) dE \int_0^{E_1-D_{nA}} \left(\frac{\sigma_{nf}}{\sigma_{ne} - \sigma_{Hp,A,2,E-D_{nA,1}}} \right) \chi_p^2(E) dE + \\ &+ \sigma_{Hp}(E_n) \int_0^{E_n} \left(\frac{\sigma_{n,2n'y}}{\sigma_{ne} - \sigma_{Hp,A,1,E-D_{nA}}} \right) \chi_{Hp}^1(E) dE \int_0^{E_1-D_{nA}} \left(\frac{\sigma_{nf}}{\sigma_{ne} - \sigma_{Hp,A,2,E-D_{nA,1}}} \right) \chi_{Hp}^2(E) dE. \end{aligned} \quad (2.11)$$

Here $\sigma_{n,n'x} = \sigma_{ne} - \sigma_{nf} - \sigma_{ny} - \sigma_{Hp}$, and σ_{Hp} is the cross-section for the pre-equilibrium emission of a neutron in accordance with Table 2.1.

The unmeasured cross-section σ_{nF} is also needed for the calculations, as well as its first partial fission contribution σ_{nf} which is defined by the relation $\sigma_{nF} = \sigma_{nf} + \sigma_{n,n'f} + \sigma_{n,2n'f}$. It is obtained as follows: $\sigma_{n,n'f}$ is calculated for the assumed value of σ_{nf} which is then derived from the condition $\sigma_{nF} = \sigma_{nf} + \sigma_{n,n'f}$. Above the threshold of the reaction $(n,2n'f)$ it is necessary to perform precisely the same adjustment for the nucleus A-1 in advance.

The level density was expressed, as before, as $\rho(U) = \exp\sqrt{(4aU)}/U^{3/2}$. All the constants and cross-sections needed for the calculations were taken from our own evaluations for ^{240}Pu [25], ^{239}Pu [19] and the present evaluation for ^{241}Pu .

The evaluated cross-sections for the reactions $(n,2n)$ and $(n,3n)$ are given in Table 2.2 and Fig. 2.1.

Table 2.2

Evaluated cross-sections for the reactions (n,2n) and (n,3n) for ^{241}Pu

E, MeV	$\sigma_{n,2n}$, b	$\sigma_{n,3n}$, b	E, MeV	$\sigma_{n,2n}$, b	$\sigma_{n,3n}$, b
1	2	3	4	5	6
5,5	0,0300	0,0	10,5	0,7917	0,0
6,0	0,8200	0,0	11,0	0,7510	0,0
6,5	0,9850	0,0	11,5	0,7027	0,0
7,0	1,0200	0,0	12,0	0,6799	0,010
7,5	1,0150	0,0	12,5	0,5772	0,050
8,0	1,0035	0,0	13,0	0,4273	0,120
8,5	1,0033	0,0	13,5	0,3436	0,160
9,0	1,0026	0,0	14,0	0,2626	0,178
9,5	0,9738	0,0	14,5	0,2347	0,190
10,0	0,8830	0,0	15,0	0,2340	0,195

The spectrum of the first neutron in the reaction (n,n^{*}x) is defined by formulae (2.1) and (2.2).

The spectrum of the second neutron in the reaction (n,2n^{*}x) is defined by the following formula:

$$I^1(E,E') = \int_{B_{n,1}+E'}^E \chi^1(\epsilon) S(\epsilon, \epsilon - B_{n,1} - E') d\epsilon; \quad (2.12)$$

and that of the third neutron by:

$$I^3(E,E') = \int_{B_{n,1}+E}^{E-B_{n,1}} \chi^2(\epsilon) S(\epsilon, \epsilon - B_{n,1} - E') d\epsilon. \quad (2.13)$$

The neutron spectrum of the reaction (n,n^{*}γ) is defined by the formula:

$$I_{n,n'}^4(E,E') = I^1(E,E') \frac{\Gamma_{n,n'}(E-E')}{\Gamma_n(E-E')}. \quad (2.14)$$

The spectrum of the first neutron in the reaction (n,2n) is defined by the formula

$$I'_{n,2n}(E, E') = I'(E, E') \cdot P_1(E, E - E'), \quad (2.15)$$

where

$$P_1(E, E - E') = \begin{cases} 0 & ; E' > E - B_{nA} \\ \int_0^{E - E' - B_{nA}} S(E - E', \epsilon) \frac{\Gamma_{nA,1}(\epsilon)}{\Gamma_{A-1}(\epsilon)} d\epsilon & ; E' < E - B_{nA} \end{cases}$$

The spectrum of the first neutron in the reaction (n,3n) is defined by the formula

$$I'_{n,3n}(E, E') = I'(E, E') P_2(E, E - E'), \quad (2.16)$$

where

$$P_2(E, E - E') = \begin{cases} 0 & ; E' > E - B_{nA} - B_{nA-1} \\ \int_{B_{nA-1}}^{E - B_{nA} - E'} S(E - E', \epsilon) \frac{\Gamma_{nA,1}(\epsilon)}{\Gamma_{A-1}(\epsilon)} d\epsilon & ; E' < E - B_{nA} - B_{nA-1} \end{cases}$$

The spectrum of the second neutron in the reaction (n,2n) is defined by the formula

$$I^2_{n,2n}(E, E') = \int_{E' - B_{nA}}^E \chi'(\epsilon) S(\epsilon, \epsilon - B_{nA} - E') \frac{\Gamma_{nA,1}(\epsilon - B_{nA} - E')}{\Gamma(\epsilon - B_{nA} - E')} d\epsilon. \quad (2.17)$$

The spectrum of the second neutron in the reaction (n,3n) is defined by formula (2.1)

$$I^2_{n,3n}(E, E') = \int_{E' + B_{nA} + B_{nA-1}}^E \chi'(\epsilon) S(\epsilon, \epsilon - B_{nA} - E') \frac{\Gamma_{nA,1}(\epsilon - B_{nA} - E')}{\Gamma(\epsilon - B_{nA} - E')} d\epsilon. \quad (2.18)$$

The evaluated spectra of the reactions (n,2n), (n,3n) and (n,n') are given in Table 2.3.

Table 2.3

Spectra of the reactions (n,n') , $(n,2n)$ and $(n,3n)$

E _n MeV	Type of re- action	Energy of secondary neutrons, MeV																
		1	2	3	4	5	6	7	8	9	10	11	12	13	14	15	16	17
1.5	(n,n')	0.05	0.1	0.2	0.3	0.4	0.5	0.6	0.7	0.8	0.9	1.0	1.1	1.2	1.3	1.4		
		2.0	2.2	2.1	1.6	1.2	0.82	0.55	0.33	0.21	0.11	0.059	0.032	0.013	0.005	0.0015		
2.0	(n,n')	0.05	0.1	0.2	0.3	0.4	0.5	0.6	0.7	0.8	0.9	1.0	1.2	1.4	1.6	1.8		
		1.4	1.9	1.55	1.55	1.17	0.91	0.65	0.46	0.32	0.21	0.12	0.052	0.017	0.0045	0.001		
3.0	(n,n')	0.1	0.2	0.3	0.4	0.6	0.8	1.0	1.2	1.4	1.6	1.8	2.0	2.2	2.4			
		1.45	1.50	1.35	1.20	0.75	0.47	0.25	0.13	0.071	0.032	0.014	0.006	0.002	0.001			
4.0	(n,n')	0.1	0.2	0.4	0.6	0.8	1.0	1.2	1.4	1.6	1.8	2.0	2.2	2.4	2.6	2.8		
		1.00	1.30	1.05	0.79	0.52	0.33	0.20	0.12	0.066	0.037	0.020	0.010	0.004	0.002	0.001		
5.0	(n,n')	0.1	0.2	0.3	0.4	0.6	0.8	1.0	1.2	1.6	2.0	2.5	3.0	3.2				
		0.95	1.10	1.13	0.91	0.66	0.55	0.38	0.24	0.10	0.027	0.010	0.002	0.001				
	(n,n')	0.1	0.3	0.6	0.9	1.2	1.5	1.8	2.1	2.4	2.7	3.0	3.5	4.0	5.0	5.5		
		0.35	0.99	0.75	0.48	0.29	0.17	0.09	0.036	0.033	0.021	0.015	0.010	0.007	0.003	0.001		
6.0	$(n,2n)$ 1st neutron	0.06	0.1	0.3	0.6	0.7	-	-	-	-	-	-	-	-	-	-	-	-
		1.20	1.30	1.50	1.20	0.8	-	-	-	-	-	-	-	-	-	-	-	-
	$(n,2n)$ 2nd neutron	0.04	0.08	0.12	0.16	0.20	0.24	0.28	0.32	0.36	0.40	0.44	0.48	0.52	0.56	0.64		
		0.38	1.15	1.92	2.51	2.37	2.93	2.81	2.54	2.16	1.77	1.36	0.99	0.69	0.44	0.14		
(n,n')	0.1	0.2	0.5	0.8	0.9	1.0	1.6	2.0	2.6	3.0	4.0	5.0	6.0	6.8				
	0.50	0.60	0.55	0.75	0.66	0.58	0.22	0.11	0.05	0.03	0.015	0.009	0.005	0.001				
7.0	$(n,2n)$ 1st neutron	0.1	0.2	0.3	0.5	0.9	1.5	1.75	-	-	-	-	-	-	-	-	-	-
		0.80	0.95	1.00	0.88	0.53	0.20	0.14	-	-	-	-	-	-	-	-	-	-
	$(n,2n)$ 2nd neutron	0.04	0.08	0.12	0.16	0.20	0.28	0.44	0.52	0.60	0.68	0.92	1.2	1.3	1.4	1.6		
		0.082	0.28	0.53	0.78	1.00	1.40	1.60	1.40	1.20	1.00	0.44	0.10	0.045	0.020	0.002		
(n,n')	0.1	0.5	1.0	1.5	2.0	2.5	3.0	3.5	4.0	5.0	6.0	7.0	8.0	8.5				
	0.60	0.67	0.42	0.22	0.10	0.055	0.060	0.042	0.019	0.020	0.013	0.0085	0.0045	0.001				

I	2	3	4	5	6	7	8	9	10	11	12	13	14	15	16	17
9,0	$(n,2n)$															
	1st neutron	0,1	0,3	0,5	1,0	1,5	2,0	2,5	3,0	3,5	-	-	-	-	-	-
	2nd neutron	0,04	0,08	0,12	0,2	0,3	0,4	0,5	0,6	0,9	1,2	1,6	1,9	2,3	2,5	3,0
11,0	$(n,2n)$															
	1st neutron	0,1	0,3	0,5	1,0	1,5	2,0	2,5	3,0	3,5	4,0	5,0	5,5	-	-	-
	2nd neutron	0,021	0,076	0,15	0,33	0,55	0,75	0,86	0,92	0,79	0,53	0,22	0,10	0,022	0,010	0,001
13,0	(n,n')															
	1st neutron	0,1	0,3	0,9	1,2	1,9	2,5	3,0	4,0	5,0	6,0	7,0	8,0	9,0	10,0	10,5
	2nd neutron	0,30	0,44	0,43	0,37	0,20	0,10	0,07	0,03	0,035	0,030	0,022	0,014	0,010	0,004	0,001
15,0	$(n,2n)$															
	1st neutron	0,1	0,3	0,5	1,0	1,5	2,0	2,5	3,0	3,5	4,0	5,0	5,5	-	-	-
	2nd neutron	0,04	0,12	0,2	0,3	0,5	0,7	0,9	1,2	-	1,6	2,0	2,5	3,0	3,5	4,0
15,0	(n,n')															
	1st neutron	0,4	0,7	1,2	2,0	3,0	4,0	5,0	6,0	7,0	8,0	9,0	10,0	11,0	12,9	-
	2nd neutron	0,27	0,29	0,23	0,18	0,12	0,069	0,047	0,036	0,054	0,041	0,031	0,023	0,015	0,001	-
15,0	$(n,2n)$															
	1st neutron	0,4	0,7	1,2	2,0	3,0	4,0	5,0	6,0	7,0	-	-	-	-	-	-
	2nd neutron	0,24	0,30	0,43	0,29	0,11	0,049	0,030	0,022	0,016	-	-	-	-	-	-
15,0	$(n,2n)$															
	1st neutron	0,34	0,06	0,12	0,2	0,3	0,5	0,7	1,0	1,5	2,0	3,0	4,0	5,0	-	-
	2nd neutron	0,005	0,019	0,039	0,10	0,17	0,32	0,45	0,51	0,46	0,33	0,076	0,008	0,001	-	-
15,0	(n,n')															
	1st neutron	0,5	1,0	2,0	3,0	4,0	5,0	6,0	7,0	8,0	9,0	10,0	11,0	13,0	14,0	14,9
	2nd neutron	0,19	0,17	0,11	0,075	0,066	0,072	0,066	0,057	0,044	0,076	0,058	0,045	0,021	0,010	0,001
15,0	$(n,2n)$															
	1st neutron	0,5	1,0	2,0	3,0	4,0	5,0	6,0	7,0	8,0	9,0	9,8	-	-	-	-
	2nd neutron	0,03	0,06	0,12	0,22	0,20	0,13	0,087	0,067	0,053	0,040	0,035	-	-	-	-
15,0	$(n,2n)$															
	1st neutron	0,04	0,08	0,12	0,3	0,4	0,5	0,6	0,7	1,0	1,4	1,8	3,0	4,0	5,0	5,6
	2nd neutron	0,004	0,016	0,034	0,151	0,233	0,30	0,37	0,41	0,49	0,48	0,37	0,10	0,032	0,005	0,001
15,0	$(n,3n)$															
	1st neutron	0,15	0,5	1,0	1,5	2,0	2,25	-	-	-	-	-	-	-	-	-
	2nd neutron	1,50	1,00	0,20	0,04	0,005	0,001	-	-	-	-	-	-	-	-	-
15,0	$(n,3n)$															
	1st neutron	0,04	0,08	0,12	0,2	0,3	0,4	0,6	0,8	1,0	1,4	1,6	1,7	-	-	-
	2nd neutron	0,039	0,14	0,26	0,56	0,87	1,1	1,1	0,94	0,56	0,19	0,066	0,041	-	-	-
15,0	$(n,3n)$															
	1st neutron	0,4	0,08	0,2	0,3	0,4	0,5	0,6	0,8	1,0	1,5	2,0	-	-	-	-
	2nd neutron	1,30	1,60	1,70	1,50	1,20	0,95	0,72	0,39	0,20	0,025	0,002	-	-	-	-

3. ANGULAR DISTRIBUTIONS OF ELASTICALLY SCATTERED NEUTRONS

No experimental values whatsoever exist for the angular distributions of elastically scattered neutrons for the ^{241}Pu nucleus. Since the angular distributions are defined principally by the potential scattering which is only weakly dependent on the properties of the nucleus, the angular distributions for the ^{235}U nucleus [26] were used as evaluated data. This nucleus was chosen because comparatively good measurements exist for it. The angular distributions are presented in the form of the expansion:

$$\frac{d\sigma}{d\Omega} = \frac{\bar{\sigma}_n}{4\pi} \left[1 + \sum_{\ell=1}^N a_{\ell}(E) P_{\ell}(\cos\theta) \right], \quad (3.1)$$

where $P_{\ell}(\cos\theta)$ is a Legendre polynomial, and the coefficients a_{ℓ} are given in Table 3.1.

The values of the coefficients a_{ℓ} enable the angular distributions in the energy range 0.1-15 MeV to be calculated. In the energy range below 0.1 MeV the angular distribution is considered to be isotropic in the centre of mass system.

Table 3.1

Expansion coefficients a_l of the angular distributions of elastically scattered neutrons for ^{241}Pu

E, MeV	σ_n, b	a_1	a_2	a_3	a_4	a_5	a_6	a_7	a_8	a_9	a_{10}	a_{11}	a_{12}	a_{13}	a_{14}
0,1	10,569	0,260000	0,025000	0,098000	0	0	0	0	0	0	0	0	0	0	0
0,2	8,862	0,512000	0,150000	0,050000	0	0	0	0	0	0	0	0	0	0	0
0,4	6,805	0,819666	0,539000	0,135000	0	0	0	0	0	0	0	0	0	0	0
0,6	5,497	1,136800	0,816000	0,329000	0,019600	0,004600	0	0	0	0	0	0	0	0	0
0,8	4,564	1,253660	1,041660	0,666333	0,133600	0,021600	0	0	0	0	0	0	0	0	0
1,0	4,033	1,267000	1,138000	0,519000	0,344500	0,080250	0	0	0	0	0	0	0	0	0
1,2	3,771	1,360500	1,224000	1,203330	0,499000	0,114633	0	0	0	0	0	0	0	0	0
1,5	3,472	1,435509	1,425680	1,813550	1,240916	0,301875	0	0	0	0	0	0	0	0	0
2,0	3,296	1,654733	1,884355	2,140139	1,759702	0,792190	0,2038102	0,0289893	0	0	0	0	0	0	0
2,5	4,172	2,065425	2,373784	2,667598	2,536690	1,547614	0,6254454	0,1512705	0	0	0	0	0	0	0
3,0	4,496	2,155640	2,525543	2,630681	2,470130	1,648876	0,7016294	0,1588083	0	0	0	0	0	0	0
3,5	4,714	2,276122	2,780413	2,780413	2,633214	1,818172	0,8777380	0,2453365	0,0163554	0	0	0	0	0	0
4,0	4,790	2,364664	3,101904	3,302078	3,069287	2,173974	1,1058630	0,4676767	0,1748377	0,0437942	0	0	0	0	0
4,5	4,675	2,418113	3,307022	3,677836	3,653867	2,920698	1,9211360	1,1384320	0,5346770	0,0481476	0	0	0	0	0
5,0	4,539	2,438787	3,359526	3,836232	3,810287	3,238319	2,1880030	1,3735180	0,8223245	0,3578867	0,0759573	0	0	0	0
5,5	4,338	2,460411	3,409912	3,905463	3,852715	3,301809	2,2583960	1,4408820	0,9098089	0,4539343	0,1331014	0	0	0	0
6,0	4,091	2,457095	3,333445	3,923151	4,070323	3,836704	3,2262640	2,2300580	1,1996630	0,4914448	0,1464750	0,0251939	0	0	0
7,0	3,616	2,504444	3,403467	4,018247	4,320263	4,185540	3,7543810	2,9681780	1,9050880	0,9368784	0,3276277	0,0644719	0	0	0
8,0	3,270	2,537760	3,519016	4,145319	4,574554	4,583560	4,2416100	3,6435490	2,7170790	1,6455810	0,7731540	0,2635800	0,0530664	0	0
9,0	3,074	2,532933	3,538986	4,147563	4,601106	4,761234	4,5251520	4,0141830	3,2664220	2,2438360	1,2006670	0,4693062	0,1072832	0	0
10,0	2,983	2,565787	3,628595	4,307180	4,768872	5,054234	4,9220690	4,4850700	3,8624450	2,9714440	1,9044910	0,9586593	0,3536017	0,0758701	0
11,0	2,965	2,447645	3,240619	3,622697	3,831917	4,087413	4,2705530	4,3599610	4,3484060	3,9569300	3,0033920	1,7679880	0,7457630	0,1752026	0
12,0	2,970	2,412038	3,104848	3,418013	3,545832	3,758765	3,9841260	4,0964080	4,1701930	4,0197010	3,3241600	2,1579540	0,9837086	0,2404101	0
13,0	3,056	2,486820	3,288875	3,707874	3,900516	4,092870	4,3512520	4,4920420	4,5511990	4,4942920	4,0475840	3,0570080	1,8209110	0,7712680	0,1773042
14,0	3,180	2,450417	3,191698	3,521943	3,699214	3,809976	4,0627390	4,2513690	4,3251970	4,3562090	4,1047980	3,3476610	2,1825980	1,0148050	0,2619896
15,0	3,284	2,365747	2,980194	3,145254	3,222019	3,237232	3,4134450	3,6739110	3,7844310	3,8915100	3,8490180	3,3866840	2,4125960	1,2325260	0,3584035

4. THE FISSION NEUTRON SPECTRUM

Only one paper [27] exists on the measurement of the fission neutron spectrum for ^{241}Pu . Measurements were carried out for thermal neutrons using two methods - the proton-recoil method ($E_n = 1.6-7.0$ MeV) and the time-of-flight method ($E_n = 0.3-6.0$ MeV). In the former case target purity was responsible for over 90% of the fission from ^{241}Pu , and in the latter case isotopic purity accounted for more than 96%. To check the results, measurements of the fission neutron spectrum of ^{235}U were performed under the same conditions. The results of the measurements were well approximated by the Maxwellian distribution

$$N_M = \frac{2}{\sqrt{x}} \frac{1}{T_M^{3/2}} \sqrt{E} e^{-\frac{E}{T_M}}, \quad (4.1)$$

the mean energy \bar{E} of which is linked with T_M by the relation $\bar{E} = \frac{3}{2} T_M$. The values of T_M and \bar{E} obtained in Ref. [27] are 1.335 ± 0.034 and 2.002 ± 0.051 MeV respectively.

In order to make allowance for the variation in the fission neutron spectrum with the incident neutron energy, it is possible to use the link between the mean energy of the fission spectrum (\bar{E}) and the mean number of neutrons per fission ($\bar{\nu}$), disregarding the neutrons emitted during processes which preceded fission. The following dependences for T_M , based on systematics, were proposed in Ref. [28]:

$$T_M = 0,353 + 0,510 [1 + \bar{\nu}(E)]^{1/2} \quad (4.2)$$

and

$$T_M = 0,997 + 0,125 \bar{\nu}(E).$$

The dependence (4.2) and the data on $\bar{\nu}(E)$ evaluated in Part 4 of the preprint were used in the present paper. Calculation of T_M at the thermal point gives a value of 1.36 MeV which agrees with the measured value in Ref. [27].

5. EVALUATION OF THE SPECTRA OF GAMMA RAYS
ACCOMPANYING THE INELASTIC PROCESSES

No experimentally measured spectra of the gamma rays accompanying inelastic processes exist for ^{241}Pu . The gamma-ray spectra from the processes (n,n') , $(n,2n)$ and $(n,3n)$ were evaluated using the statistical model in the same way as for the ^{240}Pu nucleus [25]. The discrete lines of the gamma rays were not calculated. For the spectrum of gamma rays accompanying fission we used the spectrum of gamma rays accompanying thermal fission of a ^{235}U nucleus [29].

Tables 5.1-5.5 show the spectra of gamma rays accompanying the processes (n,n') , (n,F) , $(n,2n)$, $(n,3n)$ and (n,γ) respectively.

Table 5.1

Spectra of gamma rays accompanying reactions (n,n')

E_n , MeV	E_γ , MeV															
	0,05	0,1	0,2	0,3	0,4	0,6	0,8	1	1,5	2	2,5	3	4	5	6	7
15	0,004	0,027	0,17	0,41	0,75	1,53	2,39	3,22	3,10	2,37	1,62	0,99	0,41	0,15	0,05	0,012
12	0,004	0,025	0,16	0,39	0,70	1,43	2,24	3,00	2,82	2,03	1,34	0,75	0,24	0,06	0,02	0,003
9	0,003	0,024	0,15	0,37	0,69	1,37	2,12	2,81	2,48	1,65	0,91	0,47	0,11	0,02	0,003	0,0
6	0,003	0,022	0,143	0,35	0,67	1,20	1,71	2,29	1,78	1,01	0,47	0,19	0,02	0,002	-	-
3	0,002	0,017	0,13	0,32	0,54	1,01	1,31	1,25	0,83	0,45	0,2	0,0	-	-	-	-
1	0,001	0,002	0,011	0,043	0,13	0,51	0,71	0,0	-	-	-	-	-	-	-	-

Table 5.2

Spectra of fission gamma rays

E_n , MeV	E_γ , MeV															
	0,1	0,2	0,3	0,5	0,7	1,0	1,5	2,0	2,5	3,0	4,0	5,0	6,0	8,0	10,0	
0,0 - 15,0	1,0	5,2	6,3	6,2	5,0	3,2	1,2	0,65	0,40	0,22	0,089	0,027	0,014	0,001	0,0	

Table 5.3

Spectra of gamma rays accompanying reactions (n,γ)

E_n , MeV	E_γ , MeV														
	0,05	0,1	0,2	0,4	0,6	0,8	1,0	1,5	2	3	4	5	6	8	10
15	0,008	0,059	0,35	2,01	3,05	3,54	3,72	3,35	2,75	1,56	0,77	0,34	0,14	0,02	0,002
12	0,008	0,058	0,34	1,91	3,00	3,47	3,62	3,22	2,45	1,32	0,61	0,23	0,08	0,009	0,0
9	0,008	0,056	0,32	1,90	2,96	3,39	3,52	3,02	2,25	1,07	0,42	0,14	0,05	0,003	0,0
6	0,008	0,054	0,32	1,80	2,91	3,29	3,35	2,70	1,95	0,79	0,24	0,07	0,02	0,0	-
3	0,008	0,053	0,31	1,80	2,81	3,11	3,16	2,45	1,52	0,47	0,10	0,02	0,003	0,0	-
1	0,008	0,052	0,30	1,79	2,73	2,95	2,91	2,05	1,16	0,25	0,004	0,0	-	-	-

Table 5.4

Spectra of gamma rays accompanying reactions (n,2n)

E_n , MeV	E_γ , MeV													
	0,05	0,1	0,2	0,3	0,5	0,8	1,2	1,6	2,0	2,5	3	4	5	6
8	0,004	0,02	0,12	0,30	0,72	0,85	0,51	0	-	-	-	-	-	-
11	0,003	0,01	0,09	0,24	0,69	0,98	0,98	0,75	0,48	0,22	0,08	0,005	-	-
15	0,006	0,04	0,20	0,59	1,67	2,16	2,04	1,63	1,15	0,70	0,39	0,09	0,02	0,004

Table 5.5

Spectra of gamma rays accompanying reactions (n,3n)

E_n , MeV	E_γ , MeV													
	0,05	0,1	0,2	0,3	0,5	0,7	0,9	1,1	1,3	1,5	1,8	2,1	2,4	
15	0,001	0,004	0,03	0,062	0,16	0,27	0,31	0,33	0,29	0,24	0,15	0,09	0,04	

6. CONCLUSION

The present paper contains the results of an evaluation of nuclear data performed with a view to establishing a complete ^{241}Pu file in our national evaluated nuclear data library. The mean group constants obtained on the basis of the evaluated data are shown in Table 6.1.

Table 6.1

Mean group constants for the ^{241}Pu nucleus

No.	E_i, E_{i+1}	σ_t	σ_f	σ_{γ}	σ_n	σ_{in}	ν_t	μ_t	ξ
1	2	3	4	5	6	7	8	9	10
	MeV								
1	6,5 - 10,5	6,708	1,914	0,006	3,451	1,337	4,015	0,8396	0,00133
2	4,0 - 6,5	7,852	1,419	0,007	4,527	1,829	3,606	0,8097	0,00158
3	2,5 - 4,0	7,926	1,508	0,011	4,525	1,952	3,358	0,7940	0,00221
4	1,4 - 2,5	7,412	1,691	0,058	3,930	1,853	3,134	0,5496	0,00374
5	0,8 - 1,4	7,215	1,597	0,098	3,265	1,525	3,070	0,4273	0,00475
6	0,4 - 0,8	7,454	1,511	0,076	5,691	1,156	3,000	0,3667	0,00526
7	0,2 - 0,4	10,340	1,734	0,116	7,859	0,631	2,763	0,2331	0,00636
8	0,1 - 0,2	12,248	2,009	0,227	9,729	0,277	2,944	0,1273	0,00724
	кэВ								
9	46,5 - 100	13,750	2,261	0,412	10,042	0,175	2,734	0,0552	0,00774
10	21,5 - 46,5	14,919	2,675	0,539	11,703	0,002	2,929	0,0274	0,00812
11	10,0 - 21,5	16,332	3,143	0,697	12,232	0,000	2,926	0,0100	0,00822
12	4,65 - 10	18,277	4,498	1,079	12,750	0,000	2,924	0,0056	0,00925
13	2,15 - 4,65	21,145	6,437	1,606	13,102	0,000	2,924	0,0038	0,00927
14	1,0 - 2,15	24,867	8,875	2,614	13,372	0,000	2,924	0,0030	0,00927
	эВ								
15	465 - 1000	30,284	12,218	3,920	13,596	0,000	2,924	0,0028	0,00927
16	215 - 465	43,264	22,744	6,773	13,767	0,070	2,924	0,0028	0,00927
17	100 - 215	46,747	26,006	6,872	13,869	0,000	2,924	0,0028	0,00927
18	46,5 - 100	64,250	39,340	10,020	14,930	0,000	2,924	0,0028	0,00927
19	21,5 - 46,5	90,540	61,930	10,000	18,460	0,000	2,924	0,0028	0,00927
20	10,0 - 21,5	198,140	138,550	43,110	16,480	0,000	2,924	0,0028	0,00927
21	4,65 - 10,0	289,070	239,330	26,480	17,210	0,000	2,924	0,0028	0,00927
22	2,15 - 4,65	180,300	116,360	54,200	9,740	0,300	2,924	0,0029	0,00927
23	1,0 - 2,15	41,070	26,270	2,300	11,900	0,000	2,924	0,0028	0,00927
24	0,465 - 1,0	82,520	52,930	15,210	14,330	0,000	2,924	0,0028	0,00927
25	0,215 - 0,465	1196,470	784,340	328,860	13,270	0,000	2,924	0,0028	0,00927
26	0,0253	1389,000	1015,000	362,000	11,200	0,300	2,924	0,0028	0,00927

In conclusion, here is a list of measurements that need to be carried out most, in order to refine the nuclear data for ^{241}Pu :

- (a) The unresolved resonance energy range (measurements of G_t for energies 0.1-100 keV);
- (b) The resonance energy range (measurements of G_γ);
- (c) The thermal range (measurements of α in the 0.1-1.0 eV range);
- (d) The fast range (measurements of G_t up to 15 MeV and measurements of $\frac{dG_n}{d\Omega}$, G_{nx} and G_n).

The authors would like to thank Academician A.K. Krasin of the BSSR Academy of Sciences for his support of the work on the evaluation of nuclear constants, and senior technician A.I. Furs for his assistance with the numerical calculations.

FIGURES

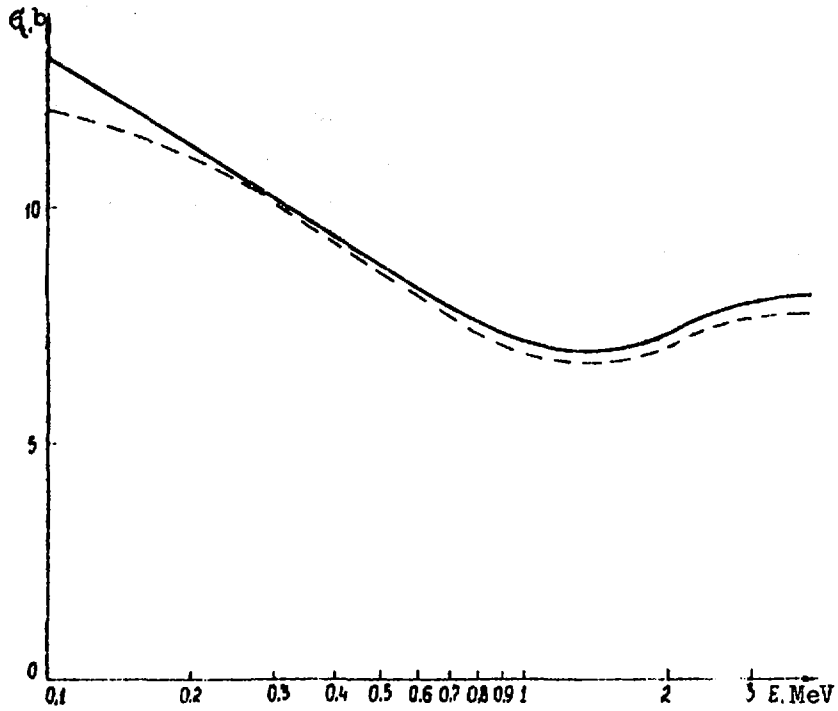


Fig. 1.1. Comparison of the data on $\sigma_t(^{241}\text{Pu})$:
— = evaluated; - - - = calculated
using the optical model.

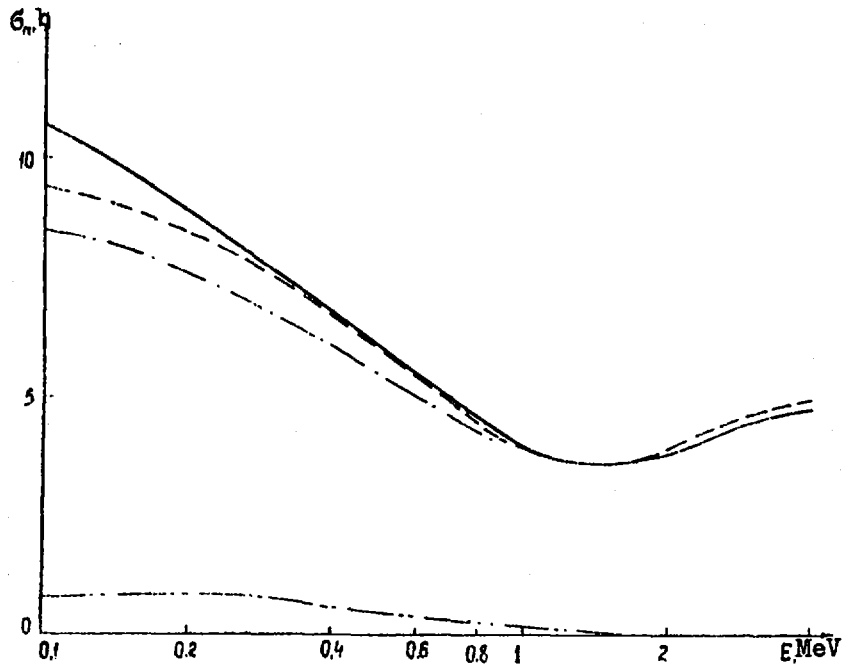


Fig. 1.2. Comparison of the data on $\sigma_n(^{241}\text{Pu})$:

———— = evaluated; - - - - = calculated

using the optical model: - · - · - = the poten-

tial scattering contribution; · · · · · =

the compound scattering contribution.

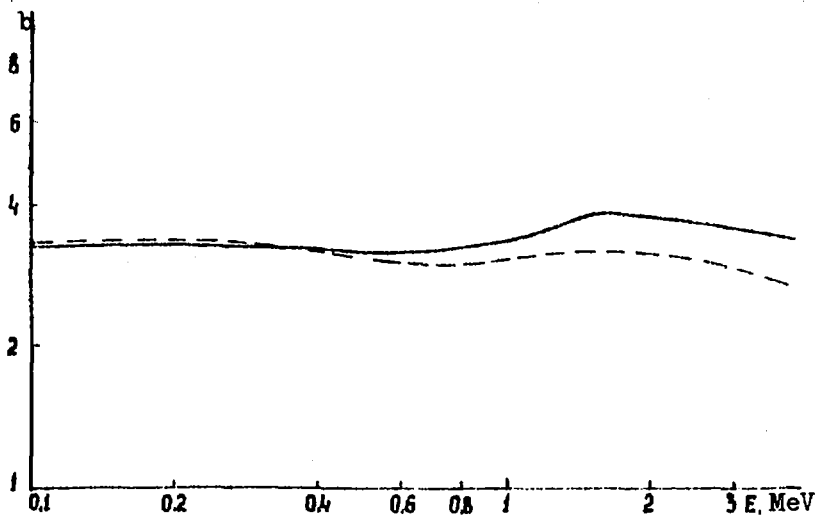


Fig. 1.3. Comparison of the data on $\sigma_c(^{241}\text{Pu})$:

———— = the sum of the evaluated cross-section σ_{nx}

and the compound elastic scattering cross-section:

- - - - = calculated with the optical model.

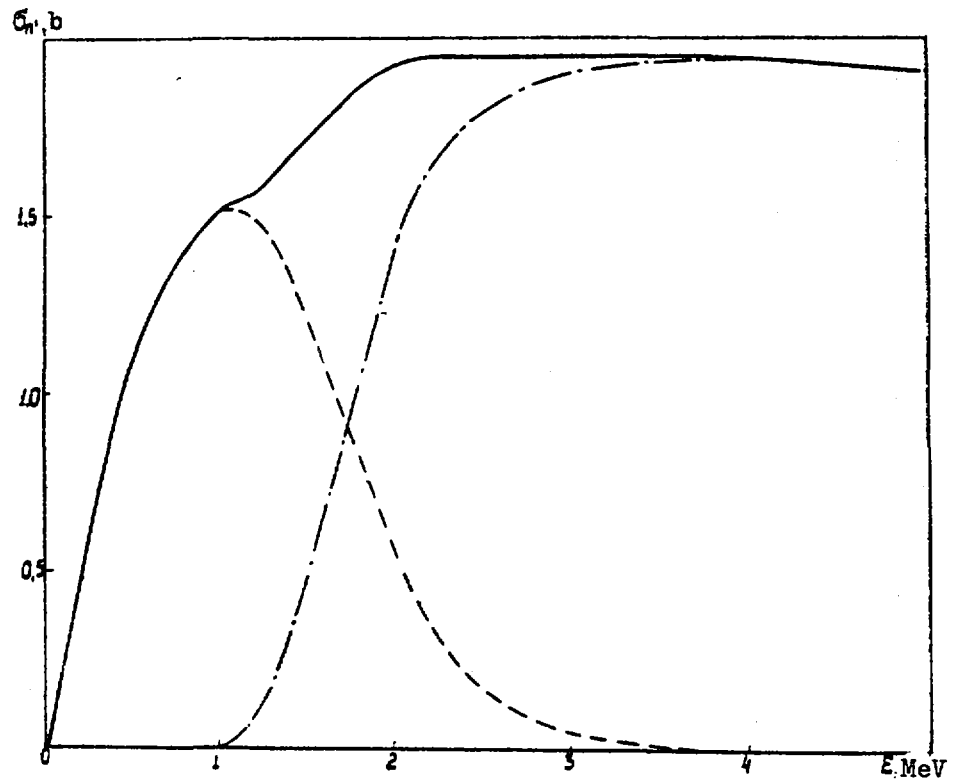


Fig. 1.4. The evaluated cross-section $\sigma_{n,b}({}^{241}\text{Pu})$ in the energy range up to 5 MeV: - - - - = the excitation cross-section of the discrete spectrum: - . - . - . = the excitation cross-section of the continuous spectrum.

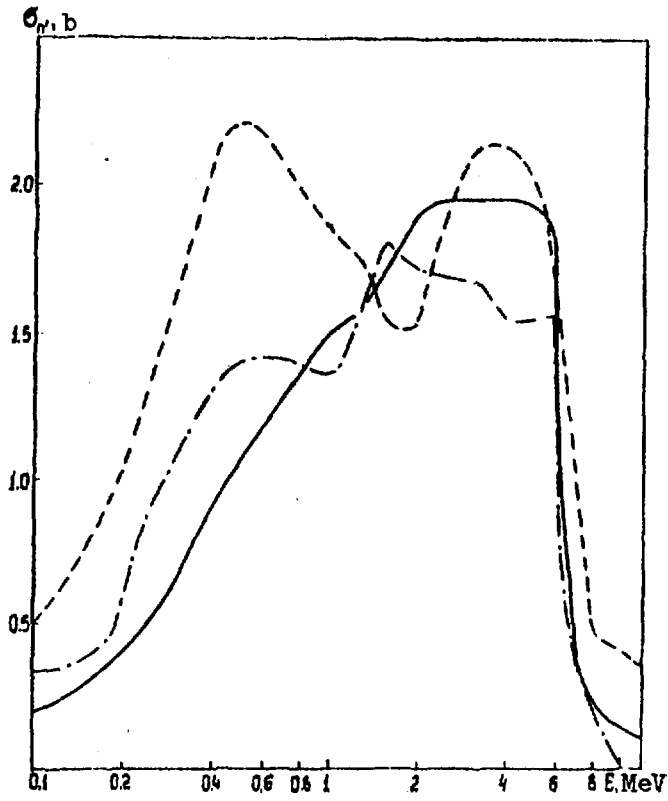


Fig. 1.5. Comparison of the results of the present evaluation of σ_n with the data of other authors: — = the present evaluation; - - - = the data of Prince; - · - · - = the data of Kaner and Yiftah.

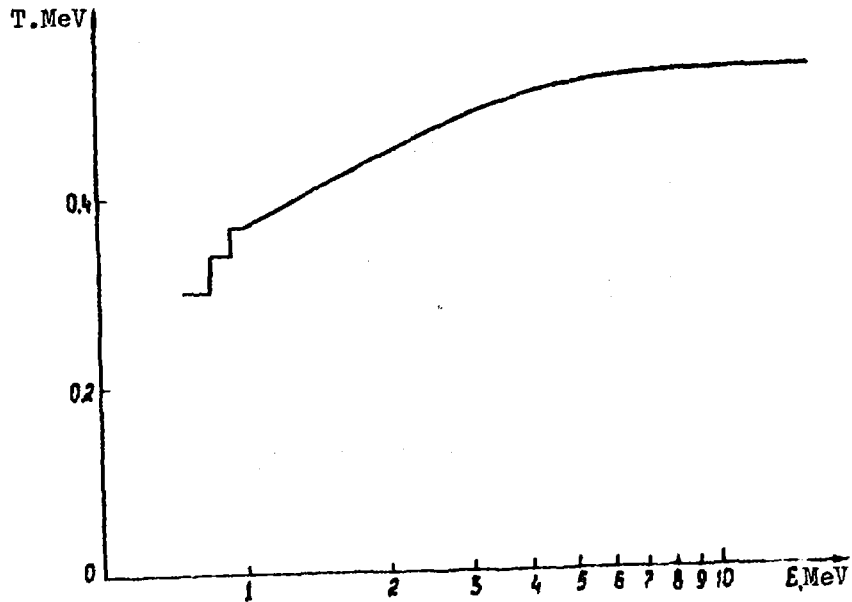


Fig. 1.6. Dependence of nuclear temperature T on incident neutron energy.

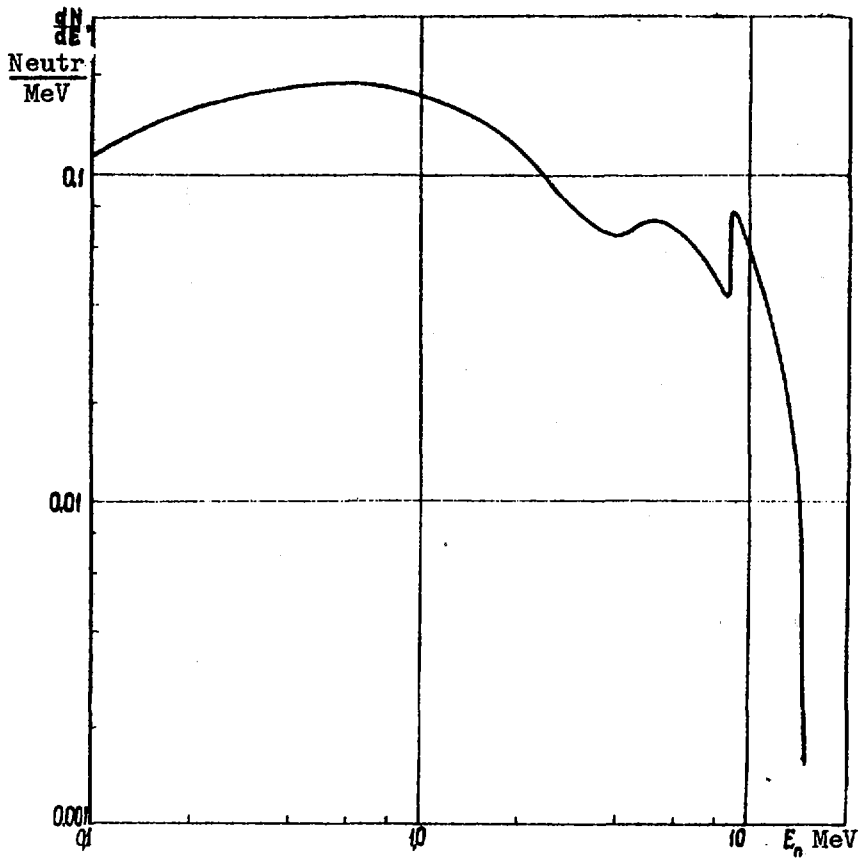


Fig. 1.7. 15 MeV neutron inelastic scattering spectrum for ^{241}Pu . The minima in the spectrum at energies ~ 4 and 8.5 MeV are caused by the competition of the processes $(n,3n)$, $(n,2n'f)$ and $(n,2n)(n,n'f)$ respectively with inelastic scattering.

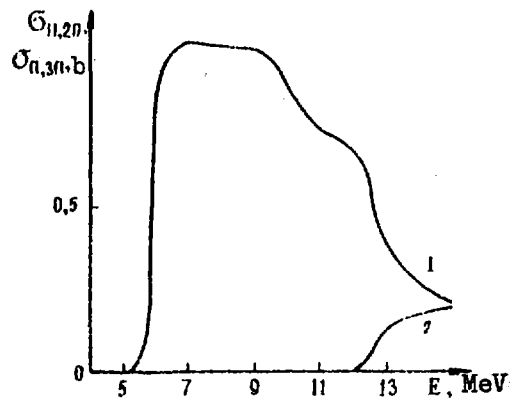


Fig. 2.1. Evaluated cross-sections for reactions: 1 = $(n,2n)$; 2 = $(n,3n)$.

REFERENCES

- l. Phys. Rev., C, vol.3, 1971, p.234
- INSKIJ, V.M., Yad. Fiz. 22 (1975) 670.
- , C, vol.1, 1970, p.275.
- tnost' urovnej i struktura atomnykh yader.
structure of atomic nuclei), M., Atomizdat (1969).
- sy atomov i ehnergii svyazi yader.
nuclear binding energies), M., Atomizdat (1974).
- ik Yu.V. J. Nucl. Phys., vol.39, 1962, p.551.
- [1] ANTSILOV, G.V., KON'SHIN, V.A., SUKHOVITSKIJ, E.Sh., Trudy III Vsesoyuznoj konferentsii po nejtronnoj fizike. (Proceedings of the 3rd All-Union Conference on Neutron Physics), Kiev, 2 (1976) 21.
- [8] BLOKHIN, A.I., IGNATYUK, A.V., Trudy III Vsesoyuznoj konferentsii po nejtronnoj fizike. (Proceedings of the 3rd All-Union Conference on Neutron Physics), Kiev, 3 (1976) 3.
- [9] Bohr N. Nature, vol.137, 1936, p.344.
- [10] Hauser W., Feshbach H. Phys. Rev., vol.87, 1952, p.366.
- [11] Bohr N., Wheller J. Phys. Rev., vol.54, 1939, p.426.
- [12] Hill R., Wheller J. Phys. Rev., vol.89, 1953, p.1102.
- [13] Lynn J.E. AERE-R-7468, 1974.
- [14] Lynn J.E. Theory of Neutron Resonance Reactions, Clarendon Press, Oxford, 1968, p.396.
- [15] Lambropoulos P. Nucl. Sci. Eng., vol.46, 1971, p.356.
- [16] Kaner M., Yiftah S. IA-1276, 1973.
- [17] Prince A. Proc. of the IAEA Conf. on Nuclear Data for Reactors, Helsinki, vol.2, 1970, p.825.
- [18] KOLESOV, V.E., NIKOLAEV, M.N., Yadernye konstanty. (Nuclear constants) issue 8, part 4 (1972) 53.
- [19] KON'SHIN, V.A. et al., Yadernye konstanty. (Nuclear constants) issue 16 (1974) 329.
- [20] Braga-Mar Caszan G.M., Milazzo-Colli L. Phys. Rev., C, vol.6, 1972, p.1398.
- [21] Tamura T. Rev. Mod. Phys., vol.37, 1965, p.679.

- [22] SUKHOVITSKIJ, E.Sh., KON'SHIN, V.A., Vestsi Akad. Navuk BSSR, Ser. Fiz.-Ehnerg. Navuk, No. 3 (1974) 23.
- [23] BLATT, J., WEISKOPF, V., Teoreticheskaya yadernaya fizika. (Theoretical nuclear physics), M., Izdat. inostr. lit. (1954).
- [24] BIRYUKOV, N.S. et al. Trudy III Vsesoyuznoj konferentsii po nejtronnoj fizike. (Proceedings of the 3rd All-Union Conference on Neutron Physics), Kiev, 4 (1976) 113.
- [25] ANTSIPOV, G.V. et al. Trudy III Vsesoyuznoj konferentsii po nejtronnoj fizike. (Proceedings of the 3rd All-Union Conference on Neutron Physics), Kiev, 2 (1976) 34.
- [26] SUKHOVITSKIJ, E.Sh., BENDERSKIJ, A.R., KON'SHIN, V.A. Trudy III Vsesoyuznoj konferentsii po nejtronnoj fizike. (Proceedings of the 3rd All-Union Conference on Neutron Physics), Kiev, 2 (1976) 38.
- [27] Smith A.B., Syoblom R.K., Roberts J.H. Phys. Rev., vol.123, 1961, p.2140.
- [28] Howerton R.J., Doyas R.J. Nucl. Sci. Eng., vol.46, 1971, p.414.
- [29] Verbinski V.V., Veber K., Sund R.E. Phys. Rev., vol.7,1973,p.1173.

Part 6

Representation of the Complete Pu-241
Evaluated Nuclear Data File in the
ENDF/B Format

Abstract

This publication contains a printout of the full file of evaluated nuclear data for ^{241}Pu in the ENDF/B format.

The printout includes resonance parameters, neutron cross-sections, angular and energy distributions of secondary neutrons and average number of neutrons per fission event $\bar{\nu}$. The resolved resonance region is shown in Reich-Moore parameters and parameters of modified Adler-Adler formalism. In the region of unresolved resonances, apart from cross-sections average resonance parameters are given. The data were recorded on magnetic tape and transmitted to the Nuclear Data Centre of the USSR State Committee on the Utilization of Atomic Energy.

79-7974
Translated from Russian

Byelorussian SSR Academy of Sciences

A.V. Lykov Institute of Heat and Mass Transfer

PRINTOUT OF EVALUATED NUCLEAR DATA
OF THE COMPLETE ^{241}Pu FILE

Preprint No. 7

Minsk 1979

9.42410+04	2.38986+02	1	1	0	12024	1451	1
0.00000+00	0.00000+00	0	0	0	02024	1451	2
0.00000+00	0.00000+00	0	0	207	73024	1451	3
94-PJ-241 ITMO	EVAL-FEB/79	KON'SHIN,	SUKHOVITSKII,	ANTSIPOV	2024	1451	4
	DIST-MAY/79	REV-		12MA79	2024	1451	5
PRINCIPAL EVALUATORS-	G.V.ANTSIPOV,	V.A.KON'SHIN,	E.S.SUKHOVITSKII,		2024	1451	6
	J.V.PORODZINSKII,	G.B.MOROGOVSKII,			2024	1451	7
	L.A.BAKHANOVICH,	A.B.KLEPATSKII,			2024	1451	8
					2024	1451	9
					2024	1451	10
					2024	1451	11
					2024	1451	12
					2024	1451	13
					2024	1451	14
					2024	1451	15
					2024	1451	16
					2024	1451	17
					2024	1451	18
					2024	1451	19
					2024	1451	20
					2024	1451	21
					2024	1451	22
					2024	1451	23
					2024	1451	24
					2024	1451	25
					2024	1451	26
					2024	1451	27
					2024	1451	28
					2024	1451	29
					2024	1451	30
					2024	1451	31
					2024	1451	32
					2024	1451	33
					2024	1451	34
					2024	1451	35
					2024	1451	36
					2024	1451	37
					2024	1451	38
					2024	1451	39
					2024	1451	40
					2024	1451	41
					2024	1451	42
					2024	1451	43
					2024	1451	44
					2024	1451	45
					2024	1451	46
					2024	1451	47

THE LEAST SQUARES METHOD WAS APPLIED TO THE DATA FROM (25,26,27) RENORMALIZED TO THE CF-252 NU-VALUE (1) TO OBTAIN THE EVALUATED NU-VALUE,

MF = 2 RESONANCE PARAMETERS

IN THE RESOLVED RESONANCE ENERGY REGION THE RESONANCE PARAMETERS WERE OBTAINED BY PARAMETRIZATION OF THE EXPERIMENTAL DATA BOTH FOR THE SIGMA TOTAL (2) AND THE SIGMA FISSION (3) BY THE MODIFIED ADLER-ADLER FORMALISM

$SIGMA(E) = A/SORT(E)*SUM(K)(G(K)*PSI + H(K)*HI)$

WHERE SIGMA(E) - CROSS SECTION,
 G(K),H(K) - PARAMETERS OF THE K-RESONANCE,
 PSI, HI - DOPPLER FUNCTIONS,
 SUM(K) - SUMMATION FROM 1 TO N,
 N - NUMBER OF RESONANCES TAKEN INTO CONSIDERATION,
 A = 2.6*10**6 (B/EV**0.5),
 OUR MODIFIED ADLER-ADLER PARAMETERS ARE NOT WIDELY USED, THEREFORE WE RECOMMEND ALSO REICH-MOORE RESOLVED RESONANCE PARAMETERS GIVEN BY J. BLONS AND H. DERRIEN (JOURN. DE PHYS., 37, 659, 1976)
 THE LATTER PARAMETERS ARE GIVEN BELOW,

ER	AJ	GN	GG	GF1	GF2	
2.60000-01	3.00000+00	4.37142-05	4.00000-02	7.50000-02	0.00000+00	2024 1451 37
4.26000+00	3.00000+00	6.17714-04	4.00000-02	2.00000-02	0.00000+00	2024 1451 38
4.58000+00	2.00000+00	4.50000-04	4.00000-02	-2.40000-02	1.00000-01	2024 1451 39
5.45000+00	2.00000+00	3.55700-03	4.00000-02	-1.29200+00	1.60000-02	2024 1451 40
6.93000+00	5.00000+00	7.09714-04	4.00000-02	-8.90000-02	0.00000+00	2024 1451 41
8.61000+00	3.00000+00	8.70000-04	4.00000-02	4.10000-02	0.00000+00	2024 1451 42
9.62000+00	2.00000+00	4.70400-04	4.00000-02	1.02000-01	3.10000-02	2024 1451 43
9.98000+00	2.00000+00	2.22000-03	4.00000-02	3.92000-01	6.18000-01	2024 1451 44
1.27700+01	2.00000+00	9.36000-04	4.00000-02	-2.33000-01	0.00000+00	2024 1451 45
1.34200+01	3.00000+00	2.19771-03	4.00000-02	0.00000+00	2.90000-02	2024 1451 46
1.39000+01	2.50000+00	2.60000-05	4.00000-02	5.30000-02	0.00000+00	2024 1451 47

1,47000+01	2,00000+00	6,48880-03	4,00000-02	1,00000+01	1,70000+02	2024	1451	48
1,57600+01	2,00000+00	1,82040+03	4,00000-02	-4,00000+01	5,30000+02	2024	1451	49
1,66700+01	3,00000+00	1,16226-03	4,00000-02	1,84000+01	0,00000+00	2024	1451	50
1,78300+01	3,00000+00	3,49771-03	4,00000-02	0,00000+00	0,00000+00	2024	1451	51
1,82000+01	3,00000+00	1,60285-04	4,00000-02	2,70000+02	0,00000+00	2024	1451	52
2,07000+01	3,00000+00	3,57428-04	4,00000-02	5,00000+02	3,00000+03	2024	1451	53
2,18700+01	3,00000+00	4,88571-03	4,00000-02	0,00000+00	3,30000+02	2024	1451	54
2,19500+01	3,00000+00	9,03571-03	4,00000-02	1,80000+02	0,00000+00	2024	1451	55
2,29300+01	3,00000+00	6,61428-04	4,00000-02	2,11000+01	7,00000+02	2024	1451	56
2,37600+01	2,00000+00	3,38800-04	4,00000-02	2,00000+01	-5,00000+02	2024	1451	57
2,40700+01	3,00000+00	1,00971-03	4,00000-02	1,50000+02	0,30000+00	2024	1451	58
2,44100+01	2,00000+00	3,60000+04	4,00000-02	6,40000-02	0,00000+00	2024	1451	59
2,64800+01	2,00000+00	5,44560-03	4,00000-02	2,57000+01	-7,00000+03	2024	1451	60
2,75000+01	3,00000+00	2,57142-03	4,00000-02	0,00000+00	2,20000+02	2024	1451	61
2,77200+01	2,00000+00	6,50400-04	4,00000-02	-9,00000+01	0,00000+00	2024	1451	62
2,87200+01	2,00000+00	4,71040-03	4,00000-02	5,43000+01	5,20000+02	2024	1451	63
2,90000+01	2,00000+00	3,50000-04	4,00000-02	-1,23000+01	-7,80000+02	2024	1451	64
3,01000+01	2,50000+00	3,50000+03	4,00000-02	3,20000+02	0,00000+00	2024	1451	65
3,07000+01	3,00000+00	2,18828-03	4,00000-02	0,00000+00	-2,12000+01	2024	1451	66
3,33000+01	3,00000+00	1,50837-04	4,00000-02	6,00000+02	5,00000+02	2024	1451	67
3,37400+01	3,00000+00	2,80285-04	4,00000-02	0,00000+00	6,20000+02	2024	1451	68
3,47700+01	2,00000+00	2,60040-03	4,00000-02	-1,16900+00	1,23000+01	2024	1451	69
3,49800+01	3,00000+00	3,45428-04	4,00000-02	1,00000+02	6,00000+03	2024	1451	70
3,61900+01	3,00000+00	6,00000+03	4,00000-02	5,00000+03	3,10000+02	2024	1451	71
3,71700+01	2,00000+00	4,70000-04	4,00000-02	3,14000+01	6,26000+01	2024	1451	72
3,81000+01	3,00000+00	3,16285-04	4,00000-02	-2,50000+02	3,40000+02	2024	1451	73
3,84000+01	3,00000+00	3,00000-03	4,00000-02	0,00000+00	1,00000+00	2024	1451	74
3,93200+01	3,00000+00	1,27628-03	4,00000-02	4,60000-02	1,20000+01	2024	1451	75
3,98300+01	3,00000+00	1,36628-03	4,00000-02	6,10000-02	0,00000+00	2024	1451	76
4,07200+01	2,00000+00	2,56200-03	4,00000-02	-1,06300+00	-5,00000+02	2024	1451	77
4,27000+01	3,00000+00	2,59714-04	4,00000-02	2,20000+01	0,00000+00	2024	1451	78
4,33900+01	3,00000+00	2,50285-04	4,00000-02	0,00000+00	2,20000+02	2024	1451	79
4,65100+01	3,00000+00	1,37571-03	4,00000-02	0,00000+00	-2,45000+01	2024	1451	80
4,71000+01	2,50000+00	1,20000-04	4,00000-02	2,27000+01	0,00000+00	2024	1451	81
4,83400+01	2,00000+00	6,93840-03	4,00000-02	-2,91000+01	1,42000+01	2024	1451	82
5,05100+01	3,00000+00	5,7428-06	4,00000-02	6,00000+03	4,35000+01	2024	1451	83
5,21300+01	2,50000+00	1,00600-04	4,00000-02	3,20000+02	0,00000+00	2024	1451	84
5,77600+01	2,50000+00	1,80000-04	4,00000-02	1,50000+01	0,00000+00	2024	1451	85
5,81200+01	2,00000+00	1,40040-03	4,00000-02	8,00000+02	3,76000+01	2024	1451	86
5,92200+01	2,00000+00	2,44560-03	4,00000-02	-4,52000+01	4,20000+02	2024	1451	87
6,04400+01	3,00000+00	3,70028-03	4,00000-02	7,20000+02	-6,50000+02	2024	1451	88
6,06400+01	2,00000+00	7,17600-04	4,00000-02	-1,65000+01	2,56000+01	2024	1451	89
6,21200+01	2,00000+00	6,17680-03	4,00000-02	-5,53000+01	3,70000+02	2024	1451	90
6,30300+01	3,00000+00	2,15837-04	4,00000-02	0,00000+00	2,00000+02	2024	1451	91
6,43800+01	3,00000+00	8,57142-03	4,00000-02	0,00000+00	3,10000+02	2024	1451	92
6,55900+01	3,00000+00	4,47514-03	4,00000-02	2,56000+01	6,00000+03	2024	1451	93
6,64800+01	3,00000+00	3,34028-03	4,00000-02	-1,20000+02	2,00000+02	2024	1451	94

6,78300+01	3,00000+00	1,20685+03	4,00000-02	4,70000+02	0,00000+00	2024	1451	95
6,92700+01	3,00000+00	1,00000-03	4,00000-02	0,00000+00	1,10000+02	2024	1451	96
7,17700+01	2,50000+00	1,00000-04	4,00000-02	4,70000+02	0,00000+00	2024	1451	97
7,23400+01	2,00000+00	1,84200-03	4,00000-02	2,12000+01	1,17000+01	2024	1451	98
7,39600+01	3,00000+00	4,92000-04	4,00000-02	1,70000+02	0,00000+00	2024	1451	99
7,59000+01	3,00000+00	4,22571-03	4,00000-02	8,10000+02	0,00000+00	2024	1451	100
7,71600+01	3,00000+00	3,73028-03	4,00000-02	0,00000+00	-1,70000+02	2024	1451	101
7,82100+01	2,00000+00	4,181080-03	4,00000-02	1,48400+00	2,00000+02	2024	1451	102
8,02500+01	3,00000+00	4,17342-03	4,00000-02	0,00000+00	5,10000+02	2024	1451	103
8,09000+01	2,00000+00	1,87080-03	4,00000-02	2,31000+00	0,00000+00	2024	1451	104
8,15500+01	2,00000+00	1,36704-02	4,00000-02	3,09000+01	-1,86000+01	2024	1451	105
8,32700+01	2,00000+00	5,13240-03	4,00000-02	7,00000-03	4,70000+02	2024	1451	106
8,54600+01	3,00000+00	2,10000-03	4,00000-02	0,00000+00	9,00000+02	2024	1451	107
8,57300+01	3,00000+00	2,96828-03	4,00000-02	1,68830+01	0,00000+00	2024	1451	108
8,61200+01	2,00000+00	1,50000-03	4,00000-02	-4,17000+01	-1,50000+01	2024	1451	109
8,70400+01	3,00000+00	5,70171-03	4,00000-02	0,00000+00	4,80000+02	2024	1451	110
8,80400+01	2,00000+00	2,61120-03	4,00000-02	2,56000+01	6,40000+02	2024	1451	111
8,91500+01	2,00000+00	2,50320-03	4,00000-02	-6,00000+01	2,81000+01	2024	1451	112
8,96600+01	3,00000+00	2,10857-04	4,00000-02	0,00000+00	-1,68000+01	2024	1451	113
9,07600+01	3,00000+00	1,85571-03	4,00000-02	3,00000+03	-1,29000+01	2024	1451	114
9,14000+01	2,50000+00	7,30000-05	4,00000-02	2,10000+02	0,00000+00	2024	1451	115
9,18600+01	2,50000+00	1,00000-04	4,00000-02	2,50000+02	0,00000+00	2024	1451	116
9,39400+01	3,00000+00	2,62837-04	4,00000-02	9,00000+02	0,00000+00	2024	1451	117
9,44700+01	2,50000+00	1,40000-04	4,00000-02	7,30000+02	0,00000+00	2024	1451	118
9,54200+01	2,00000+00	1,11120-03	4,00000-02	5,90000+02	2,80000+01	2024	1451	119
9,61200+01	2,00000+00	4,70400-04	4,00000-02	-1,90000+02	-6,90000+02	2024	1451	120
9,65500+01	2,00000+00	6,50600-04	4,00000-02	3,55000+01	5,30000+03	2024	1451	121
9,75800+01	3,00000+00	5,29714-04	4,00000-02	0,00000+00	2,71000+01	2024	1451	122
9,84100+01	3,00000+00	5,54771-03	4,00000-02	1,71000+01	-1,80000+02	2024	1451	123
9,97800+01	3,00000+00	2,42742-03	4,00000-02	3,87000+01	7,40000+02	2024	1451	124
1,00700+02	2,50000+00	4,00000-04	4,00000-02	3,32000+01	0,00000+00	2024	1451	125
1,01610+02	3,00000+00	8,75142-04	4,00000-02	-4,20000+02	-5,00000+03	2024	1451	126
1,02580+02	2,00000+00	1,82280-03	4,00000-02	8,76000+01	0,00000+00	2024	1451	127
1,03660+02	3,00000+00	1,09971-03	4,00000-02	0,00000+00	2,10000+02	2024	1451	128

THE AVERAGE RESONANCE PARAMETERS IN THE REGION 0.1 KEV TO 100 KEV ARE OBTAINED BY SELF-CONSISTENT ANALYSIS (9) OF THE AVERAGE PARAMETERS FROM THE RESOLVED RESONANCE ENERGY REGION, THE EVALUATED FISSION CROSS SECTION AND THE EXPERIMENTAL ALPHA VALUE OF REF. 4, THE EVALUATED FISSION CROSS SECTION IS BASED ON THE FISSION CROSS SECTION RATIO MEASUREMENTS BY FURSUW ET AL, (5), BEHRENS AND CARLSON (6), KAPPELER ET AL, (7), WHITE ET AL, (8),

MF = 3 SMOOTH CROSS SECTIONS

EVALUATION OF TOTAL AND FISSION CROSS SECTIONS IN THE

2024	1451	129
2024	1451	130
2024	1451	131
2024	1451	132
2024	1451	133
2024	1451	136
2024	1451	135
2024	1451	136
2024	1451	137
2024	1451	138
2024	1451	139
2024	1451	140
2024	1451	141

THERMAL ENERGY REGION IS BASED ON EXPERIMENTAL DATA OF REF. (10, 11, 12, 13) AND REF. (14 THROUGH 21) RESPECTIVELY, THE DATA WERE RENORMALIZED TO THE 2200 M/SEC EVALUATED DATA OF LEMMEL TO OBTAIN ELASTIC AND INELASTIC SCATTERING CROSS SECTION IN THE REGION 0.1 TO 100 KEV THE AVERAGE RESONANCE PARAMETERS WERE USED, EVALUATED CAPTURE CROSS SECTION IN THIS ENERGY REGION WAS EXTRACTED FROM DATA ON ALPHA(4), EXPERIMENTAL DATA FROM REFERENCES 5, 6, 8, 22 WERE USED AS BASIC IN FISSION CROSS SECTION EVALUATION IN THE REGION 0.1 KEV TO 15.0 MEV, EVALUATED TOTAL AND ELASTIC SCATTERING CROSS SECTIONS FOR PU-239 (23) IN THE REGION 0.1 TO 15.0 MEV WERE USED FOR OBTAINING PU-241 DATA, CAPTURE, INELASTIC SCATTERING, (N,2N), (N,3N) - CROSS SECTIONS WERE OBTAINED BY OPTICAL AND STATISTICAL MODELS WITH CAREFULLY ADJUSTED PARAMETERS TAKING INTO ACCOUNT (N, GAMMA FISSION)-REACTION.

MF = 4 NEUTRON ANGULAR DISTRIBUTIONS

ELASTICALLY SCATTERED NEUTRON ANGULAR DISTRIBUTIONS IDENTICAL TO THAT OF U-235 (24) WERE ACCEPTED,

MF = 5 ENERGY DISTRIBUTION OF SECONDARY NEUTRONS

MT=4 TO REPRODUCE THE ENERGY DISTRIBUTIONS IN THE REGION BELOW 5 MEV THE EVAPORATION MODEL SPECTRUM WAS USED, ABOVE 5 MEV THE CONTRIBUTION OF PREEQUILIBRIUM NEUTRONS WAS INCLUDED, CALCULATIONS OF (N,2N) AND (N,3N) NEUTRON SPECTRA WERE MADE TAKING INTO ACCOUNT THE PREEQUILIBRIUM EMISSION OF THE FIRST NEUTRON,

REFERENCES

1.	LEMMEL H.D., WASHINGTON CONF., V.1, P.286, (1975)	2024	1451	142
2.	ROLAR W., CARRARO G., KNOXVILLE CONF., V.2, P.707 (1971)	2024	1451	143
3.	BLONS J. ET AL., KNOXVILLE CONF., V.2, P.836 (1971)	2024	1451	144
4.	WESTON L.W., TODD J.H., ORNL-4800, P.4 (1972)	2024	1451	145
5.	FURSOV B.I. ET AL., KIEV CONF., V.6, P.3 (1976)	2024	1451	146
6.	BEHRENS J.W., CARLSON G.W., UCID-16878 (1975)	2024	1451	147
7.	KAPPELER F. ET AL., IAEA CONF. ON NUCLEAR DATA FOR REACTORS, V.2, P.77 (1970)	2024	1451	148
8.	WHITE P.H. ET AL., PROC. OF SYMPOSIUM OF PHYSICS AND CHEMISTRY OF FISSION, SALZBURG, V.1, P.219, (1965)	2024	1451	149
9.	ANTISIPOV G.V. ET AL., YADERNYE KONSTANTY, 25 (1977)	2024	1451	150
		2024	1451	151
		2024	1451	152
		2024	1451	153
		2024	1451	154
		2024	1451	155
		2024	1451	156
		2024	1451	157
		2024	1451	158
		2024	1451	159
		2024	1451	160
		2024	1451	161
		2024	1451	162
		2024	1451	163
		2024	1451	164
		2024	1451	165
		2024	1451	166
		2024	1451	167
		2024	1451	168
		2024	1451	169
		2024	1451	170
		2024	1451	171
		2024	1451	172
		2024	1451	173
		2024	1451	174
		2024	1451	175
		2024	1451	176
		2024	1451	177
		2024	1451	178
		2024	1451	179
		2024	1451	180
		2024	1451	181
		2024	1451	182
		2024	1451	183
		2024	1451	184
		2024	1451	185
		2024	1451	186
		2024	1451	187
		2024	1451	188

10.	CRAIG D.S., WESTCOTT C.H., AECL-1948 (1964) AND CAN. J. PHYS., V.42, P.2384 (1968)	2024	1451	189
11.	SIMPSON F.B. ET AL., BULL. AM. PHYS. SOC., V.3, P.176 (1958)	2024	1451	190
12.	SMITH J.R., WASH-1124, P.64 (1968), WASH-1093, P.60 (1968)	2024	1451	191
13.	SMITH J.R., YOUNG T.E., WASH-1136, P.43 (1969)	2024	1451	192
14.	WATANABE T., IN-1012 (1966)	2024	1451	193
15.	WATANABE T. ET AL., PHYS. REV., B, V.133, P.390 (1964), IDO-16995 (1964)	2024	1451	194
16.	SEPPI E.J., PRIVATE COMMUNICATION (1958)	2024	1451	195
17.	JAMES G.D., AERE-R-4597 (1964), NUCL. PHYS., V.65, P.353 (1965)	2024	1451	196
18.	ADAMCHUK YU. V. ET AL., GENEVA CONF., V.4, P.259 (1955)	2024	1451	197
19.	SEPPI E.J. ET AL., HW-55879, P.50 (1958)	2024	1451	198
20.	WHITE P.H. ET AL., PARIS CONF., V.2, P.29 (1967)	2024	1451	199
21.	DE SAUSSURE G. ET AL., NUCL. SCI. ENG., V.5, P.49 (1959)	2024	1451	200
22.	KAPPELER F. ET AL., NUCL. SCI. ENG., V.51, P.124 (1973)	2024	1451	201
23.	KONSHIN V.A. ET AL., YADERNYE KONSTANTY, 16, P.329 (1974)	2024	1451	202
24.	SUKHOVITSKII E.S. ET AL., KIEV CONF., V.2, P.38 (1976)	2024	1451	203
25.	CUNDE H. ET AL., J. NUCL. ENERGY, V.22, P.53 (1968)	2024	1451	204
26.	FREHAUT J. ET AL., CEA-R-4626 (1974)	2024	1451	205
27.	DYACHENKO N.P. ET AL., ATOMNAYA ENERGIYA, 4, V.36 (1974)	2024	1451	206

0.00000+00	0.00000+00	1	451	283	12024	1451	210
0.00000+00	0.00000+00	1	452	14	12024	1451	211
0.00000+00	0.00000+00	2	151	442	12024	1451	212
0.00000+00	0.00000+00	3	1	73	12024	1451	213
0.00000+00	0.00000+00	3	2	36	12024	1451	214
0.00000+00	0.00000+00	3	3	35	12024	1451	215
0.00000+00	0.00000+00	3	4	29	12024	1451	216
0.00000+00	0.00000+00	3	16	10	12024	1451	217
0.00000+00	0.00000+00	3	17	6	12024	1451	218
0.00000+00	0.00000+00	3	18	87	12024	1451	219
0.00000+00	0.00000+00	3	51	23	12024	1451	220
0.00000+00	0.00000+00	3	52	21	12024	1451	221
0.00000+00	0.00000+00	3	53	19	12024	1451	222
0.00000+00	0.00000+00	3	54	19	12024	1451	223
0.00000+00	0.00000+00	3	55	19	12024	1451	224
0.00000+00	0.00000+00	3	56	19	12024	1451	225
0.00000+00	0.00000+00	3	57	18	12024	1451	226
0.00000+00	0.00000+00	3	58	18	12024	1451	227
0.00000+00	0.00000+00	3	59	18	12024	1451	228
0.00000+00	0.00000+00	3	60	18	12024	1451	229
0.00000+00	0.00000+00	3	61	17	12024	1451	230
0.00000+00	0.00000+00	3	62	16	12024	1451	231
0.00000+00	0.00000+00	3	63	15	12024	1451	232
0.00000+00	0.00000+00	3	64	15	12024	1451	233
0.00000+00	0.00000+00	3	64	15	12024	1451	234
0.00000+00	0.00000+00	3	65	14	12024	1451	235

0.00000+00	0.00000+00	3	66	13	12024	1451	236
0.00000+00	0.00000+00	3	67	11	12024	1451	237
0.00000+00	0.00000+00	3	68	11	12024	1451	238
0.00000+00	0.00000+00	3	69	11	12024	1451	239
0.00000+00	0.00000+00	3	70	11	12024	1451	240
0.00000+00	0.00000+00	3	71	11	12024	1451	241
0.00000+00	0.00000+00	3	72	11	12024	1451	242
0.00000+00	0.00000+00	3	73	10	12024	1451	243
0.00000+00	0.00000+00	3	74	10	12024	1451	244
0.00000+00	0.00000+00	3	75	10	12024	1451	245
0.00000+00	0.00000+00	3	76	10	12024	1451	246
0.00000+00	0.00000+00	3	77	10	12024	1451	247
0.00000+00	0.00000+00	3	78	16	12024	1451	248
0.00000+00	0.00000+00	3	79	82	12024	1451	249
0.00000+00	0.00000+00	4	2	90	12024	1451	250
0.00000+00	0.00000+00	4	16	2	12024	1451	251
0.00000+00	0.00000+00	4	17	2	12024	1451	252
0.00000+00	0.00000+00	4	18	2	12024	1451	253
0.00000+00	0.00000+00	4	19	2	12024	1451	254
0.00000+00	0.00000+00	4	51	606	12024	1451	255
0.00000+00	0.00000+00	4	52	N	12024	1451	256
0.00000+00	0.00000+00	4	53	N	12024	1451	257
0.00000+00	0.00000+00	4	54	N	12024	1451	258
0.00000+00	0.00000+00	4	55	N	12024	1451	259
0.00000+00	0.00000+00	4	56	N	12024	1451	260
0.00000+00	0.00000+00	4	57	N	12024	1451	261
0.00000+00	0.00000+00	4	58	N	12024	1451	262
0.00000+00	0.00000+00	4	59	N	12024	1451	263
0.00000+00	0.00000+00	4	60	N	12024	1451	264
0.00000+00	0.00000+00	4	61	N	12024	1451	265
0.00000+00	0.00000+00	4	62	N	12024	1451	266
0.00000+00	0.00000+00	4	63	N	12024	1451	267
0.00000+00	0.00000+00	4	64	N	12024	1451	268
0.00000+00	0.00000+00	4	65	N	12024	1451	269
0.00000+00	0.00000+00	4	66	N	12024	1451	270
0.00000+00	0.00000+00	4	67	N	12024	1451	271
0.00000+00	0.00000+00	4	68	N	12024	1451	272
0.00000+00	0.00000+00	4	69	N	12024	1451	273
0.00000+00	0.00000+00	4	70	N	12024	1451	274
0.00000+00	0.00000+00	4	71	N	12024	1451	275
0.00000+00	0.00000+00	4	72	N	12024	1451	276
0.00000+00	0.00000+00	4	73	N	12024	1451	277
0.00000+00	0.00000+00	4	74	N	12024	1451	278
0.00000+00	0.00000+00	4	75	N	12024	1451	279
0.00000+00	0.00000+00	4	76	N	12024	1451	280
0.00000+00	0.00000+00	4	77	N	12024	1451	281
0.00000+00	0.00000+00	4	78	N	12024	1451	282
0.00000+00	0.00000+00	5	16	8	12024	1451	283
0.00000+00	0.00000+00	5	17	12	12024	1451	284
0.00000+00	0.00000+00	5	18	16	12024	1451	285

0.00000+00	0.00000+00	5	91	84	12024	1451	283
0.00000+00	0.00000+00	0	0	0	12024	1451	284
9.42410+04	2.38986+02	0	2	0	12024	1452	285
0.00000+00	0.00000+00	0	0	1	332024	1452	286
53	2	2	2	2	12024	1452	287
2.55000-02	2.92440+00	1.00000+04	2.92569+00	2.00000+04	2.92704+00	1452	288
4.00000+04	2.92974+00	6.00000+04	2.93243+00	8.00000+04	2.93313+00	1452	289
1.00000+03	2.93783+00	2.00000+05	2.95133+00	4.00000+05	2.97841+00	1452	290
6.00000+05	3.00557+00	8.00000+05	3.03283+00	1.00000+06	3.06018+00	1452	291
1.50000+06	3.12894+00	2.00000+06	3.19826+00	2.50000+06	3.26815+00	1452	292
3.00000+06	3.33859+00	3.50000+06	3.40959+00	4.00000+06	3.48118+00	1452	293
4.50000+06	3.55330+00	5.00000+06	3.62600+00	5.50000+06	3.69928+00	1452	294
6.00000+06	3.77310+00	6.50000+06	3.84748+00	7.00000+06	3.92243+00	1452	295
7.50000+06	3.99794+00	8.00000+06	4.07402+00	9.00000+06	4.22285+00	1452	296
1.00000+07	4.38394+00	1.10000+07	4.54227+00	1.20000+07	4.70285+00	1452	297
1.50000+07	4.86569+00	1.40000+07	5.03077+00	1.50000+07	5.19810+00	1452	298
0.00000+00	0.00000+00	0	0	0	0	0	299
0.00000+00	0.00000+00	0	0	0	0	0	300
9.42410+04	2.38986+02	0	0	1	0	0	301
9.42410+04	1.00000+00	0	0	1	2	0	302
-2.50000-01	1.45000+02	1	4	0	0	0	303
-2.50000-01	8.45439-01	0	0	1	0	0	304
2.38986+02	0.00000+00	7	0	18	0	0	305
0.00000+00	0.00000+00	0.00000+00	0.00000+00	0.00000+00	0.00000+00	0.00000+00	306
0.00000+00	0.00000+00	0.00000+00	0.00000+00	0.00000+00	0.00000+00	0.00000+00	307
0.00000+00	0.00000+00	0.00000+00	0.00000+00	0.00000+00	0.00000+00	0.00000+00	308
0.00000+00	0.00000+00	0	0	1	0	0	309
0.00000+00	0.00000+00	0	0	0	1344	1122024	310
-2.50000-01	1.50000-01	6.97594+05	4.05487-05	-2.50000-01	1.50000-01	12024	311
4.85062-07	4.38284-05	-2.50000-01	1.50000-01	6.92887-05	-3.27970+06	12024	312
-1.00000-02	5.00000-03	6.65017+03	0.00000+00	-1.00000-02	5.00000-03	12024	313
-13.27508-05	0.00000+00	-1.00000-02	3.00000-03	9.92515-05	0.00000+00	12024	314
2.58000-01	5.00000-02	4.46036-04	-2.12161-05	2.58000-01	5.00000-02	12024	315
2.92985-04	-2.81410-05	2.58000-01	3.00000-02	1.52269-04	8.61079+06	12024	316
4.28000+03	3.45000-02	2.12666-05	3.66759-05	4.28000+03	3.45000-02	12024	317
1.07607-03	3.53000-05	4.28000+00	3.45000-02	1.05116-05	-1.41654-05	12024	318
4.50000+00	8.20000+02	4.03662-04	-3.36676-05	4.50000+00	8.20000+02	12024	319
3.56555-04	-4.77597-05	4.50000+00	8.20000+02	9.74631-05	-7.06521-06	12024	320
6.00000+00	6.45000-01	4.15135+04	1.86498-05	6.00000+00	6.45000-01	12024	321
3.93765-04	1.96527-05	6.00000+00	6.45000-01	1.51293-05	1.06149+06	12024	322
9.95000+00	6.45000-02	9.66821+04	5.70281-03	6.93000+00	6.45000-02	12024	323
7.66167-04	6.06721-05	6.93000+00	6.45000-02	1.92832-04	-3.12771-06	12024	324
8.62000+00	9.75000-02	1.56766+03	-7.7621-05	8.62000+00	9.75000-02	12024	325
1.00612-05	-3.29613-05	8.02000+00	4.75000-02	4.01624-04	-1.57944-05	12024	326
9.58000+00	9.65000-02	1.05861+04	-4.50658-05	9.58000+00	9.65000-02	12024	327
7.70485-05	-7.42824+05	9.58000+00	9.65000-02	1.86192-05	-1.14238+05	12024	328
1.00100+01	5.11500-01	2.63457+04	-1.68508-05	1.00100+01	5.11500-01	12024	329

2,62311-04-2	6,5541-05	1,00100-01	3,11500-01	1,36876-05	1,63155-06	2024	2151	330
1,27900-01	1,36500-01	3,08710-04	3,66733-06	1,27900-01	1,36500-01	2024	2151	331
3,68590-04	1,05935-05	1,27900-01	1,36500-01	2,08575-05	4,60096-06	2024	2151	332
1,34200-01	3,60000-02	4,63125-03	2,04718-04	1,34200-01	3,60000-02	2024	2151	333
2,05830-03	1,09600-02	1,34200-01	3,60000-02	1,74446-03	7,25393-05	2024	2151	334
1,47500-01	7,65909-02	4,54734-03	3,39520-05	1,47500-01	7,65909-02	2024	2151	335
4,10443-03	2,38651-04	1,47500-01	7,65909-02	8,65169-04	7,17039-05	2024	2151	336
1,60200-01	2,75000-01	2,93844-04	3,67339-05	1,60200-01	2,75000-01	2024	2151	337
3,68232-04	3,03538-03	1,60200-01	2,75000-01	2,07341-03	1,16875-05	2024	2151	338
1,66700-01	1,12500-01	6,68735-04	3,15047-05	1,66700-01	1,12500-01	2024	2151	339
3,46208-04	1,46600-05	1,66700-01	1,12500-01	9,68788-03	7,03958-06	2024	2151	340
1,78400-01	2,85000-02	5,67290-03	1,35253-04	1,78400-01	2,85000-02	2024	2151	341
1,72503-03	1,98093-04	1,78400-01	2,85000-02	2,39791-03	1,02812-04	2024	2151	342
1,82400-01	3,20000-02	3,91154-04	7,70065-05	1,82400-01	3,20000-02	2024	2151	343
5,16309-05	6,51361-06	1,82400-01	3,20000-02	2,05335-04	2,45935-05	2024	2151	344
2,07100-01	8,40000-02	3,95732-04	2,83701-05	2,07100-01	8,40000-02	2024	2151	345
1,40537-04	2,06832-05	2,07100-01	8,40000-02	6,86727-05	3,05493-06	2024	2151	346
2,14300-01	5,20430-02	2,16163-04	1,33864-05	2,14300-01	5,20430-02	2024	2151	347
4,56659-05	7,00644-07	2,19300-01	5,20430-02	6,18606-05	3,40678-06	2024	2151	348
2,30000-01	1,71222-03	3,24230-04	1,31971-05	2,30000-01	1,71222-03	2024	2151	349
2,87723-04	1,92203-03	2,30000-01	1,31971-05	3,76927-03	1,18801-06	2024	2151	350
3,68806-01	2,28800-01	1,40803-04	4,52040-06	3,68806-01	2,28800-01	2024	2151	351
3,85221-05	1,48334-05	2,36800-01	2,28800-01	1,28321-05	2,43118-06	2024	2151	352
2,40800-01	7,68205-02	8,87626-04	1,70348-05	2,40800-01	7,68205-02	2024	2151	353
5,76872-04	8,33578-05	2,40800-01	7,68205-02	1,63699-04	1,58996-05	2024	2151	354
2,40100-01	4,60000-01	8,61785-06	7,00286-06	2,40100-01	4,60000-01	2024	2151	355
3,26748-05	1,25914-05	2,46100-01	4,80000-01	2,30380-07	5,12194-06	2024	2151	356
2,04200-01	1,56738-01	1,31725-03	3,99173-05	2,64200-01	1,56738-01	2024	2151	357
1,14516-03	4,83136-05	2,64200-01	1,56738-01	1,34697-04	1,18476-06	2024	2151	358
2,76200-01	6,75050-01	4,64298-03	3,71439-07	2,76200-01	6,75050-01	2024	2151	359
2,75117-06	2,20694-06	7,67700-01	6,75050-01	6,82633-10	5,30103-07	2024	2151	360
2,88600-01	2,96414-01	6,50822-04	2,96414-01	2,88600-01	2,96414-01	2024	2151	361
2,21282-04	2,63698-03	2,88800-01	2,96414-01	4,57336-05	3,96928-07	2024	2151	362
2,94200-01	1,17000-01	3,36821-04	1,60917-05	2,94200-01	1,17000-01	2024	2151	363
2,77940-04	3,7370-03	2,94200-01	1,17000-01	3,68615-05	4,86447-06	2024	2151	364
3,10300-01	1,7244-01	6,45699-04	2,96414-01	3,10300-01	1,7244-01	2024	2151	365
6,16875-04	2,93940-05	3,10300-01	1,7244-01	7,84965-05	4,34579-07	2024	2151	366
3,33000-01	1,10250-01	6,3615-03	1,10038-05	3,33000-01	1,10250-01	2024	2151	367
7,50121-05	1,20031-05	3,33000-01	1,10250-01	8,37482-07	2,21090-07	2024	2151	368
3,37800-01	6,90050-02	1,71119-04	2,66759-05	3,37800-01	6,90050-02	2024	2151	369
1,26406-04	8,63668-06	3,37800-01	2,66759-05	3,17220-05	5,84306-06	2024	2151	370
3,49000-01	1,32600-01	1,23141-04	2,59953-05	3,49000-01	1,32600-01	2024	2151	371
1,22582-04	5,18783-03	3,49000-01	1,23141-04	3,52831-06	8,47367-06	2024	2151	372
3,50000-01	4,40000-02	3,65746-04	3,87254-05	3,50000-01	4,40000-02	2024	2151	373
1,20835-04	6,75272-06	3,50000-01	4,40000-02	1,40846-04	1,12490-06	2024	2151	374
3,61700-01	3,80000-02	1,25304-04	3,61438-05	3,61700-01	3,80000-02	2024	2151	375
6,70367-08	5,36243-08	3,61700-01	3,80000-02	5,41733-05	1,06644-05	2024	2151	376

3,75000+01	4,28500-01	3,02149-07	2,41719-07	3,75000+01	4,28500+01	2024	2151	377
3,44030-06	2,75224-06	3,75000+01	4,28500-01	9,98040-09	7,64593-07	2024	2151	378
3,81400+01	7,75000-02	3,75000+01	4,28500-01	3,81400+01	7,75000-02	2024	2151	379
1,31216-04	4,79809-06	3,81400+01	7,75000-02	7,85401-05	1,03688-06	2024	2151	380
3,93500+01	1,55250-01	3,89248-04	9,52660-05	3,93500+01	1,55250-01	2024	2151	381
3,86107-04	8,79485-06	3,93500+01	1,55250-01	3,99509-05	3,03069-05	2024	2151	382
3,98900+01	7,65000-02	7,80895-04	7,76546-05	3,98900+01	7,65000-02	2024	2151	383
4,72072-04	4,60564-05	3,98900+01	7,65000-02	1,67700-04	3,45003-05	2024	2151	384
4,09000+01	7,04400-01	1,78205-04	7,97641-06	4,09000+01	7,04400-01	2024	2151	385
1,35260-04	1,82795-06	4,09000+01	7,04400-01	6,36405-06	1,37985-06	2024	2151	386
4,27500+01	1,41878-01	4,27500+01	1,41878-01	4,27500+01	1,41878-01	2024	2151	387
6,89429-05	1,55725-05	4,27500+01	1,41878-01	1,62021-05	5,37338-06	2024	2151	388
4,54500+01	2,50000-02	5,33186-04	8,39279-05	4,54500+01	2,50000-02	2024	2151	389
1,38709+04	6,59443-05	4,34500+01	2,50000-02	2,22054-04	1,51538-05	2024	2151	390
4,65700+01	1,47500-01	3,58240-04	4,83253-05	4,65700+01	1,47500-01	2024	2151	391
3,41819-04	3,14215-05	4,65700+01	1,47500-01	3,01262-05	2,30486-05	2024	2151	392
4,81000+01	2,65306-01	8,73078-04	4,19852-05	6,81000+01	2,65306-01	2024	2151	393
7,98974-04	5,04808-05	4,81000+01	2,65306-01	7,80657-05	4,61860-05	2024	2151	394
5,03500+01	3,88500-01	1,36727-04	3,86765-05	5,03500+01	3,88500-01	2024	2151	395
6,24516-05	4,48871-06	5,03500+01	3,86765-05	9,41827-06	1,35978-05	2024	2151	396
5,22400+01	8,00000-02	1,47431-04	1,85744-05	5,22400+01	8,00000-02	2024	2151	397
8,23945-06	6,67696-06	5,22400+01	1,85744-05	3,52270-05	8,14454-06	2024	2151	398
5,81700+01	2,96500+01	7,30538-05	1,08922-05	5,83700+01	2,96500+01	2024	2151	399
1,27782-04	9,54177-06	5,83700+01	2,96500+01	4,65773-06	7,35182-06	2024	2151	400
5,92700+01	5,10000-01	2,28860-04	1,02905-04	5,92700+01	5,10000-01	2024	2151	401
2,01957-04	4,76668-06	5,92700+01	1,02905-04	3,93682-06	3,71117-04	2024	2151	402
6,05100+01	1,00000-01	1,44018-03	9,10081-05	6,05100+01	1,00000-01	2024	2151	403
9,39703-04	1,86169-04	6,05100+01	1,00000-01	2,85264-04	8,95157-05	2024	2151	404
6,22500+01	2,70408-01	6,04089-04	2,9822-05	6,22500+01	2,70408-01	2024	2151	405
4,21426-04	6,49580-05	6,22500+01	2,70408-01	6,19457-05	3,51758-05	2024	2151	406
6,50000+01	9,67500-01	1,57370-04	4,14298-05	6,50000+01	9,67500-01	2024	2151	407
4,34356-09	2,27140-05	6,50000+01	9,67500-01	4,51022-06	2,16851-05	2024	2151	408
6,45400+01	3,10000-02	1,76584-04	1,14344-04	6,45400+01	3,10000-02	2024	2151	409
5,90856-05	9,63597-06	6,45400+01	3,10000-02	7,62885-05	4,37785-05	2024	2151	410
6,57300+01	1,62000-01	1,09490-03	1,26334-05	6,57300+01	1,62000-01	2024	2151	411
6,50669-04	2,50456-06	6,57300+01	1,26334-05	1,87409-04	3,72405-06	2024	2151	412
6,66200+01	8,65000-02	2,19040-03	1,98696-04	6,66200+01	8,65000-02	2024	2151	413
6,97449-04	4,53090-05	6,66200+01	1,98696-04	5,01549-04	8,45133-05	2024	2151	414
7,56000+01	7,45000-02	1,10194-09	8,81557-16	7,56000+01	7,45000-02	2024	2151	415
5,73636-05	4,44474-06	6,73600+01	7,45000-02	1,80284-10	1,36167-06	2024	2151	416
5,42600+01	2,98000-02	9,29418-04	3,92216-05	6,82700+01	2,98000-02	2024	2151	417
6,84659-04	6,30200-05	6,82700+01	2,98000-02	2,71811-04	1,75084-06	2024	2151	418
6,92400+01	2,32000-02	1,15115-03	1,03484-04	6,92400+01	2,32000-02	2024	2151	419
4,31987-04	1,54439-05	6,92400+01	2,32000-02	4,61404-04	4,15186-05	2024	2151	420
7,22500+01	1,33644-01	2,71333-04	2,33080-05	7,22500+01	1,33644-01	2024	2151	421
2,87638-04	6,30607-06	7,22500+01	2,33080-05	3,92897-05	1,05827-05	2024	2151	422
7,59100+01	1,05900-02	1,05900+01	3,80000-02	7,59100+01	1,05900-02	2024	2151	423

4.49344-04-2	7.77304-06	7.39100+01	1.05000-02	4.41646+04	1.39041+06	2024	2151	424
7.58600+01	3.04000-02	3.51468-03	7.85852-05	7.58600+01	3.04000-02	2024	2151	425
2.57683+03	2.08327-04	7.58600+01	3.04000-02	9.50551-04-7	5.23011-05	2024	2151	426
7.71400+01	2.67288-02	4.14762-03	8.75681-05	7.71400+01	2.67288-02	2024	2151	427
9.48501-04-5	5.1704+03	7.71400+01	2.67288-02	1.91964+03	4.36933+05	2024	2151	428
7.77000+01	1.27500+00	1.02287-07	8.18203+08	7.77000+01	1.27500+00	2024	2151	429
6.28103+03	2.05420-05	7.77000+01	1.27500+00	1.33658+09	4.76841-06	2024	2151	430
8.02100+01	3.20000-02	7.65666-03	2.29117-04	8.02100+01	3.20000-02	2024	2151	431
2.21819-03	5.11228-03	8.02100+01	3.20000-02	1.05307-03-9	2.1839+05	2024	2151	432
8.14600+01	6.30000+02	2.23918+03	1.95831+04	8.14600+01	6.30000+02	2024	2151	433
1.61343-03	7.69109+03	0.14600+01	6.30000+02	5.26645+04	4.66193+05	2024	2151	434
8.20700+01	5.00000-03	1.55966+04	7.68283-05	8.20700+01	5.00000-03	2024	2151	435
2.71177-04-6	8.80000+05	8.20700+01	5.00000-03	5.13302-06-7	9.5910+06	2024	2151	436
8.31400+01	5.80000+02	2.38576-03	5.06806+05	8.31400+01	5.80000+02	2024	2151	437
1.32980-03	6.21071+03	8.31400+01	5.80000+02	8.43637+04	8.07274+07	2024	2151	438
8.54200+01	1.00000-01	1.00443-03	1.31251-04	8.54200+01	1.00000-01	2024	2151	439
8.32600-04	7.95482-05	8.34200+01	1.00000-01	1.91949+04	2.37636+05	2024	2151	440
8.57000+01	1.50000+01	4.38872-04	2.09114-04	8.57000+01	1.50000+01	2024	2151	441
5.19202-04	6.39708-03	8.57000+01	1.50000+01	1.84953-05	5.46249-05	2024	2151	442
8.62000+01	2.40000-01	1.03808-08	8.30466-09	8.62000+01	2.40000-01	2024	2151	443
5.31909-03	1.06210-03	8.62000+01	2.40000-01	7.11739+10	2.83033+06	2024	2151	444
8.70100+01	5.20815-02	3.28886-03	4.60902-05	8.70100+01	5.20815-02	2024	2151	445
1.83348-03	1.35014-03	8.70100+01	5.20815-02	9.71955+04-1	8.7327-05	2024	2151	446
8.79500+01	1.95000-01	2.78078-04	1.98783-05	8.79500+01	1.95000-01	2024	2151	447
2.88773-04-7	7.20632-05	8.79500+01	1.95000-01	3.81326+05	2.60383-05	2024	2151	448
8.92000+01	4.00000-01	1.14401-04	0.21864+05	8.92000+01	4.00000-01	2024	2151	449
1.86761-04-1	1.90443+05	8.92000+01	4.00000-01	4.70632-06-1	6.2389-05	2024	2151	450
9.06800+01	6.25000-02	6.25101-04	2.44183-04	9.06800+01	6.25000-02	2024	2151	451
3.57181-03	8.80648-03	9.06800+01	6.25000-02	2.19547+04	9.85500+05	2024	2151	452
4.13500+01	2.40000-01	1.98600+10	1.58889-10	9.13500+01	2.40000-01	2024	2151	453
4.69357-03-1	1.08555-05	9.13500+01	2.40000-01	3.63962+11	6.71558+06	2024	2151	454
9.18100+01	6.00000-02	4.13923-11	5.31138-11	9.18100+01	6.00000-02	2024	2151	455
5.40551-03	1.08021+03	9.18100+01	6.00000-02	2.16722-11-6	6.8243+06	2024	2151	456
9.38800+01	1.48000+01	2.92033-03	7.72460-06	9.38800+01	1.48000+01	2024	2151	457
8.13586+03	4.86476+06	9.38800+01	1.48000+01	6.19920+06	4.06822-06	2024	2151	458
9.53600+01	7.12500-02	5.73667-05	4.62933-05	9.53600+01	7.12500-02	2024	2151	459
1.85016-04-1	1.54933-05	9.53600+01	7.12500-02	2.55141+05	5.20016+05	2024	2151	460
9.61000+01	2.76764+01	6.32637-05	2.00055-05	9.61000+01	2.76764+01	2024	2151	461
1.00982+04-5	1.4288-06	9.61000+01	2.76764+01	1.00533+04-1	5.1489-05	2024	2151	462
9.75000+01	2.96632-01	1.21181-07-9	6.9449-08	9.75000+01	2.96632-01	2024	2151	463
1.11495-04	1.97000-03	9.75000+01	2.96632-01	1.79573-08-1	2.3253-05	2024	2151	464
9.83700+01	9.70000-02	1.57836-03-1	8.0166-04	9.83700+01	9.70000-02	2024	2151	465
1.50077-03-2	0.3143+06	9.83700+01	9.70000-02	8.13638-04-1	6.3823-04	2024	2151	466
9.97800+01	1.75000-01	3.31036-04	3.91033-05	9.97800+01	1.75000-01	2024	2151	467
2.89171-04	3.46001-05	9.97800+01	1.75000-01	1.35193+04	1.44796-05	2024	2151	468
1.00700+02	3.80000-01	2.14291-05-1	7.1433-05	1.00700+02	3.80000-01	2024	2151	469
4.73687-03-1	6.9287-05	1.00700+02	3.80000-01	3.21446+05-7	8.6200-07	2024	2151	470

1.01520+02	7.12815-02	5.22765+04	5.42854-05	1.01520+02	7.12815-02	2024	2151	471
1.93472-04	5.39864-06	1.01520+02	7.12815-02	4.85225-04	3.44736-05	2024	2151	472
1.02400+02	2.26000-01	8.73348-03	3.45141-05	1.02400+02	2.26000-01	2024	2151	473
7.40062-03-1	2.6354-03	1.02400+02	2.26000-01	3.57948-05	2.63770-05	2024	2151	474
1.03630+02	1.15500-01	3.69994-04	4.48086-05	1.03630+02	1.15500-01	2024	2151	475
1.33231-04-6	1.8362-06	1.03630+02	1.15500-01	2.11946+04-4	4.60627-05	2024	2151	476
1.07540+02	7.15000-02	9.42809-05	8.73555-05	1.07540+02	7.15000-02	2024	2151	477
5.61740-07-4	4.49392-07	1.07540+02	7.15000-02	8.72431-05-1	1.03315-04	2024	2151	478
1.07990+02	4.20000-02	7.52000-04-1	2.2734-04	1.07990+02	4.20000-02	2024	2151	479
3.06008-04-3	1.17958-05	1.07990+02	4.20000-02	9.00053-04-1	1.08990-04	2024	2151	480
1.09170+02	2.33000-01	2.27149-04	1.41981-05	1.09170+02	2.33000-01	2024	2151	481
1.54513-04-4	1.34876-06	1.09170+02	2.33000-01	8.95334-06	2.18866-03	2024	2151	482
1.10500+02	4.00000-01	2.53145-10	1.86517-10	1.10500+02	4.00000-01	2024	2151	483
3.87037-06-3	0.96330-06	1.10500+02	4.00000-01	4.11476+11	2.60652-06	2024	2151	484
1.13240+02	2.00000-02	4.18356-04-8	0.3893-05	1.13240+02	2.00000-02	2024	2151	485
3.01630-04	1.20910-03	1.13240+02	2.00000-02	8.07659+04-1	1.28411-04	2024	2151	486
1.15400+02	1.20000+00	1.86605-07-1	4.8833+07	1.15400+02	1.20000+00	2024	2151	487
3.76681-05-3	0.1343-05	1.15400+02	1.20000+00	1.09456-08	2.51492+05	2024	2151	488
1.17200+02	1.40000-01	3.49932-04-6	2.26411-05	1.17200+02	1.40000-01	2024	2151	489
4.69894-04-5	3.6366-05	1.17200+02	1.40000-01	2.23020-03-6	1.4557-03	2024	2151	490
1.20330+02	3.00000-01	1.20330+02	3.00000-01	1.20330+02	3.00000-01	2024	2151	491
7.32366-05	7.92434-06	1.20330+02	3.00000-01	2.47516-03	4.57403-05	2024	2151	492
1.22250+02	2.40000-01	5.48544+04-1	3.1842+04	1.22250+02	2.40000-01	2024	2151	493
6.74020-04-1	1.58378-05	1.22250+02	2.40000-01	2.25454-04-1	1.50664+04	2024	2151	494
1.23380+02	4.73372-02	1.65608-03	8.36304+05	1.23380+02	4.73372-02	2024	2151	495
6.77111-04	1.59011-03	1.23380+02	4.73372-02	2.06093+03	9.45473-05	2024	2151	496
1.24080+02	2.29592-03	3.05507-06	2.44403-06	1.24080+02	2.29592-03	2024	2151	497
5.33105-03	1.67586-05	1.24080+02	2.44403-06	8.08030-07-1	1.14343-05	2024	2151	498
1.25346+02	3.50000-01	2.11973+03	1.68359+05	1.25346+02	3.50000-01	2024	2151	499
1.99714-05	4.24976-06	1.25346+02	3.50000-01	5.95087+06	1.76783-05	2024	2151	500
1.26150+02	6.00000-02	3.44034-06	6.17526+06	1.26150+02	6.00000-02	2024	2151	501
6.26516+05	1.65332-05	1.26150+02	6.00000-02	6.10194+06-5	5.76391-06	2024	2151	502
1.27930+02	3.52769-01	1.26225+07-3	0.1801-08	1.27930+02	3.52769+01	2024	2151	503
1.16398-04	1.26104-03	1.27930+02	3.52769+01	2.06956-08-1	1.0522-03	2024	2151	504
1.28580+02	2.25060-02	3.67536-03-4	0.7464+04	1.28580+02	2.25060-02	2024	2151	505
2.03131-03	1.78376-04	1.28580+02	2.25060-02	4.58612-03-6	7.0093+04	2024	2151	506
1.30080+02	2.92505-01	4.15500-09-3	3.25001-02	1.30080+02	2.92505-01	2024	2151	507
2.04632-04	2.34143-05	1.30080+02	2.92505-01	6.74631+10-2	0.9182+05	2024	2151	508
1.30800+02	2.40000-02	1.02236-02-1	0.3243-03	1.30800+02	2.40000-02	2024	2151	509
3.71928-03	2.92249-04	1.30800+02	2.40000-02	8.20913-03-1	1.28244+03	2024	2151	510
1.33080+02	4.80000+01	4.03081-07-3	2.4063-07	1.33080+02	4.80000+01	2024	2151	511
1.67984-04	1.20543-05	1.33080+02	2.4063-07	4.00744-08-1	1.0903+05	2024	2151	512
1.33740+02	3.30608-02	4.13667+03-3	3.98013-04	1.33740+02	3.30608-02	2024	2151	513
1.40233-03	4.14618-05	1.33740+02	3.30608-02	4.30019+03	3.75836+04	2024	2151	514
1.34730+02	6.74673-01	4.26765-05	1.02829-05	1.34730+02	6.74673-01	2024	2151	515
7.40172-05	2.67072-05	1.34730+02	1.02829-05	1.06010-05-1	1.56766+05	2024	2151	516
1.59650+02	5.00000-03	4.47887-03	3.76030-04	1.59650+02	5.00000-03	2024	2151	517

1,31038-03	2,55192-04	1,36650+02	5,00000-03	4,91605-03	1,43163-04	20224	2151	518
1,38380+02	1,50601-01	5,75755+04	-4,35546-05	1,38380+02	1,50601-01	02024	2151	519
3,90160-04	3,55176-05	1,38330+02	1,50601-01	2,95042-04	7,48125-05	02024	2151	520
1,40250+02	4,08580-02	3,12373-03	1,30133-04	1,40250+02	4,08580-02	02024	2151	521
1,33334-03	1,05617-04	1,40230+02	4,08580-02	2,38644-03	2,45180-03	02024	2151	522
1,13330+02	1,53586-01	3,30666-04	-2,04533-09	1,41330+02	1,53586-01	02024	2151	523
6,34847-05	6,87637+00	1,41330+02	1,53586-01	1,03343-04	6,85030-06	02024	2151	524
1,42200+02	6,73883-02	4,56949-03	-3,56283-02	1,42200+02	6,73883-02	02024	2151	525
2,03241-03	1,13705-04	1,42200+02	6,73883-02	3,64611-03	4,69990-04	02024	2151	526
1,45140+02	4,42560-02	1,10193-04	-8,81543-05	1,45140+02	4,42560-02	02024	2151	527
2,67331-04	2,60932+05	1,45140+02	4,42560-02	8,53669+05	1,14248-04	02024	2151	528
1,46200+02	9,48812-02	1,60915-03	-6,71141-05	1,46200+02	9,48812-02	02024	2151	529
9,30844-04	2,47444-05	1,46200+02	9,48812-02	9,44891-04	-9,18585-05	02024	2151	530
1,47000+02	1,20000-01	2,17007-00	-1,73654-06	1,47000+02	1,20000-01	02024	2151	531
7,74596-05	1,11541-05	1,47000+02	1,20000-01	6,20191-07	-1,28900-05	02024	2151	532
1,48920+02	3,52330-02	1,22815-03	-2,00074-05	1,48920+02	3,52330-02	02024	2151	533
6,42199-04	5,20913-05	1,48920+02	3,52330-02	9,50394+04	-7,21637-05	02024	2151	534
1,00000+02	1,00000+05	2	0	2	0	02024	2151	535
2,50000+00	8,45439-01	0	0	2	0	02024	2151	536
2,38986+02	0,00000+00	0	0	2	0	02024	2151	537
2,00000+00	0,00000+00	0	0	198	322024	02024	2151	538
0,00000+00	0,00000+00	1,00000+00	1,00000+00	0,00000+00	2,00000+00	02024	2151	539
1,00000+02	3,08910+00	0,00000+00	3,58330-04	4,30000+02	7,40410-01	02024	2151	540
1,50000+02	3,08880+00	0,00000+00	3,58303-04	4,30000+02	7,40410-01	02024	2151	541
2,00000+02	3,08850+00	0,00000+00	3,58270-04	4,30000+02	7,40390-01	02024	2151	542
3,00000+02	3,08790+00	0,00000+00	3,58200-04	4,30000+02	7,40390-01	02024	2151	543
4,00000+02	3,08730+00	0,00000+00	3,58130-04	4,30000+02	7,40370-01	02024	2151	544
5,00000+02	3,08630+00	0,00000+00	3,58066-04	4,30000+02	7,40380-01	02024	2151	545
6,00000+02	3,08620+00	0,00000+00	3,57997-04	4,30000+02	7,40370-01	02024	2151	546
7,00000+02	3,08560+00	0,00000+00	3,57929-04	4,30000+02	7,40360-01	02024	2151	547
8,00000+02	3,08500+00	0,00000+00	3,57863-04	4,30000+02	7,40360-01	02024	2151	548
9,00000+02	3,08440+00	0,00000+00	3,57797-04	4,30000+02	7,40350-01	02024	2151	549
1,00000+03	3,08390+00	0,00000+00	3,57726-04	4,30000+02	7,40340-01	02024	2151	550
1,50000+03	3,08100+00	0,00000+00	3,57591-04	4,30000+02	7,40300-01	02024	2151	551
2,00000+03	3,07810+00	0,00000+00	3,57053-04	4,30000+02	7,40260-01	02024	2151	552
3,00000+03	3,07230+00	0,00000+00	3,56385-04	4,30000+02	7,40180-01	02024	2151	553
4,00000+03	3,06650+00	0,00000+00	3,55712-04	4,30000+02	7,40100-01	02024	2151	554
5,00000+03	3,06070+00	0,00000+00	3,55042-04	4,30000+02	7,40010-01	02024	2151	555
6,00000+03	3,05490+00	0,00000+00	3,54374-04	4,30000+02	7,39920-01	02024	2151	556
7,00000+03	3,04920+00	0,00000+00	3,53708-04	4,30000+02	7,39830-01	02024	2151	557
8,00000+03	3,04350+00	0,00000+00	3,53042-04	4,30000+02	7,39740-01	02024	2151	558
9,00000+03	3,03770+00	0,00000+00	3,52378-04	4,30000+02	7,39650-01	02024	2151	559
1,00000+04	3,03200+00	0,00000+00	3,51715-04	4,30000+02	7,39560-01	02024	2151	560
1,50000+04	3,02620+00	0,00000+00	3,51052-04	4,30000+02	7,39020-01	02024	2151	561
2,00000+04	2,97550+00	0,00000+00	3,45157-04	4,30000+02	7,38430-01	02024	2151	562
3,00000+04	2,92000+00	0,00000+00	3,38725-04	4,30000+02	7,37010-01	02024	2151	563
4,00000+04	2,86570+00	0,00000+00	3,32418-04	4,30000+02	7,35250-01	02024	2151	564

4,40000+04	2,84420+00	0,00000+00	3,29930-04	4,30000+02	7,34440-01	02024	2151	565
5,00000+04	2,81240+00	0,00000+00	3,26234-04	4,30000+02	7,33110-01	02024	2151	566
6,00000+04	2,76010+00	0,00000+00	3,20170-04	4,30000+02	7,30560-01	02024	2151	567
7,00000+04	2,70880+00	0,00000+00	3,14222-04	4,30000+02	7,27590-01	02024	2151	568
8,00000+04	2,65830+00	0,00000+00	3,08359-04	4,30000+02	7,24190-01	02024	2151	569
9,00000+04	2,60920+00	0,00000+00	3,02669-04	4,30000+02	7,20350-01	02024	2151	570
1,00000+05	2,56090+00	0,00000+00	2,97059+04	4,30000+02	7,16090-01	02024	2151	571
3,00000+00	0,00000+00	3	0	198	322024	02024	2151	572
0,00000+00	0,00000+00	1,00000+00	1,00000+00	0,00000+00	1,00000+00	02024	2151	573
1,00000+02	2,37320+00	0,00000+00	2,75291+04	4,30000+02	3,38340-01	02024	2151	574
1,50000+02	2,37300+00	0,00000+00	2,75250+04	4,30000+02	3,38330-01	02024	2151	575
2,00000+02	2,37280+00	0,00000+00	2,75241+04	4,30000+02	3,38310-01	02024	2151	576
3,00000+02	2,37230+00	0,00000+00	2,75180-04	4,30000+02	3,38290-01	02024	2151	577
4,00000+02	2,37190+00	0,00000+00	2,75140-04	4,30000+02	3,38270-01	02024	2151	578
5,00000+02	2,37140+00	0,00000+00	2,75080-04	4,30000+02	3,38240-01	02024	2151	579
6,00000+02	2,37100+00	0,00000+00	2,75033-04	4,30000+02	3,38220-01	02024	2151	580
7,00000+02	2,37050+00	0,00000+00	2,74984-04	4,30000+02	3,38200-01	02024	2151	581
8,00000+02	2,37010+00	0,00000+00	2,74930-04	4,30000+02	3,38170-01	02024	2151	582
9,00000+02	2,36960+00	0,00000+00	2,74880-04	4,30000+02	3,38150-01	02024	2151	583
1,00000+03	2,36920+00	0,00000+00	2,74827-04	4,30000+02	3,38130-01	02024	2151	584
1,50000+03	2,36700+00	0,00000+00	2,74666-04	4,30000+02	3,38010-01	02024	2151	585
2,00000+03	2,36470+00	0,00000+00	2,74507-04	4,30000+02	3,37890-01	02024	2151	586
3,00000+03	2,36030+00	0,00000+00	2,73790-04	4,30000+02	3,37650-01	02024	2151	587
4,00000+03	2,35580+00	0,00000+00	2,72756-04	4,30000+02	3,37400-01	02024	2151	588
5,00000+03	2,35130+00	0,00000+00	2,72556-04	4,30000+02	3,37160-01	02024	2151	589
6,00000+03	2,34690+00	0,00000+00	2,72261-04	4,30000+02	3,36910-01	02024	2151	590
7,00000+03	2,34250+00	0,00000+00	2,71727-04	4,30000+02	3,36650-01	02024	2151	591
8,00000+03	2,33800+00	0,00000+00	2,71216-04	4,30000+02	3,36400-01	02024	2151	592
9,00000+03	2,33360+00	0,00000+00	2,70702-04	4,30000+02	3,36140-01	02024	2151	593
1,00000+04	2,32920+00	0,00000+00	2,70190-04	4,30000+02	3,35880-01	02024	2151	594
1,50000+04	2,32070+00	0,00000+00	2,69650-04	4,30000+02	3,35520-01	02024	2151	595
2,00000+04	2,28560+00	0,00000+00	2,65134-04	4,30000+02	3,33110-01	02024	2151	596
3,00000+04	2,24290+00	0,00000+00	2,60175-04	4,30000+02	3,30090-01	02024	2151	597
4,00000+04	2,20190+00	0,00000+00	2,55315-04	4,30000+02	3,26860-01	02024	2151	598
5,00000+04	2,16450+00	1,66202-02	2,50397-04	4,30000+02	3,25520-01	02024	2151	599
6,00000+04	2,15990+00	2,50546-02	2,50397-04	4,30000+02	3,23450-01	02024	2151	600
7,00000+04	2,11960+00	3,47717-02	2,45868-04	4,30000+02	3,19880-01	02024	2151	601
8,00000+04	2,08010+00	4,17926-02	2,41290-04	4,30000+02	3,16190-01	02024	2151	602
9,00000+04	2,04130+00	4,73569-02	2,36794-04	4,30000+02	3,12400-01	02024	2151	603
1,00000+05	2,00330+00	5,19632-02	2,32337-04	4,30000+02	3,08540-01	02024	2151	604
1,00000+05	1,96610+00	5,58641-02	2,28064-04	4,30000+02	3,04620-01	02024	2151	605
2,38986+02	0,00000+00	1	0	6	0	02024	2151	606
1,00000+00	0,00000+00	0,00000+00	1	0	198	322024	2151	607
0,00000+00	0,00000+00	1,00000+00	1,00000+00	0,00000+00	2,00000+00	02024	2151	608
1,00000+02	4,90440+00	0,00000+00	9,80880-04	4,30000+02	1,46616-03	02024	2151	609
1,50000+02	4,90400+00	0,00000+00	9,80850-04	4,30000+02	1,46606-03	02024	2151	610
2,00000+02	4,90350+00	0,00000+00	9,80700-04	4,30000+02	1,46597-03	02024	2151	611

3,00000+02	4,90260+00	0,00000+00	9,80520-04	4,30000+02	1,46379-03	20224	2151	612
4,00000+02	4,90170+00	0,00000+00	9,80340-04	4,30000+02	1,46361-03	20224	2151	613
5,00000+02	4,90070+00	0,00000+00	9,80160-04	4,30000+02	1,46342-03	20224	2151	614
6,00000+02	4,89980+00	0,00000+00	9,79980-04	4,30000+02	1,46324-03	20224	2151	615
7,00000+02	4,89890+00	0,00000+00	9,79780-04	4,30000+02	1,46306-03	20224	2151	616
8,00000+02	4,89800+00	0,00000+00	9,79580-04	4,30000+02	1,46287-03	20224	2151	617
9,00000+02	4,89710+00	0,00000+00	9,79420-04	4,30000+02	1,46269-03	20224	2151	618
1,00000+03	4,89610+00	0,00000+00	9,79220-04	4,30000+02	1,46250-03	20224	2151	619
2,00000+03	4,89510+00	0,00000+00	9,78300-04	4,30000+02	1,46158-03	20224	2151	620
3,00000+03	4,88690+00	0,00000+00	9,77380-04	4,30000+02	1,46066-03	20224	2151	621
4,00000+03	4,87780+00	0,00000+00	9,75560-04	4,30000+02	1,45817-03	20224	2151	622
5,00000+03	4,86860+00	0,00000+00	9,73720-04	4,30000+02	1,45696-03	20224	2151	623
6,00000+03	4,85950+00	0,00000+00	9,71900-04	4,30000+02	1,45511-03	20224	2151	624
7,00000+03	4,85030+00	0,00000+00	9,70060-04	4,30000+02	1,45324-03	20224	2151	625
8,00000+03	4,84120+00	0,00000+00	9,68240-04	4,30000+02	1,45138-03	20224	2151	626
9,00000+03	4,83220+00	0,00000+00	9,66420-04	4,30000+02	1,44950-03	20224	2151	627
1,00000+04	4,82310+00	0,00000+00	9,64620-04	4,30000+02	1,44762-03	20224	2151	628
2,00000+04	4,81400+00	0,00000+00	9,62880-04	4,30000+02	1,44574-03	20224	2151	629
3,00000+04	4,76900+00	0,00000+00	9,53800-04	4,30000+02	1,43622-03	20224	2151	630
4,00000+04	4,72450+00	0,00000+00	9,44900-04	4,30000+02	1,42665-03	20224	2151	631
5,00000+04	4,63670+00	0,00000+00	9,27340-04	4,30000+02	1,40715-03	20224	2151	632
6,00000+04	4,55060+00	0,00000+00	9,10120-04	4,30000+02	1,38732-03	20224	2151	633
7,00000+04	4,51660+00	0,00000+00	9,03320-04	4,30000+02	1,37931-03	20224	2151	634
8,00000+04	4,46610+00	0,00000+00	8,93220-04	4,30000+02	1,36722-03	20224	2151	635
9,00000+04	4,38330+00	0,00000+00	8,76660-04	4,30000+02	1,34693-03	20224	2151	636
1,00000+05	4,30200+00	0,00000+00	8,60400-04	4,30000+02	1,32651-03	20224	2151	637
2,00000+05	4,22240+00	0,00000+00	8,44480-04	4,30000+02	1,30600-03	20224	2151	638
3,00000+05	4,14420+00	0,00000+00	8,28840-04	4,30000+02	1,28546-03	20224	2151	639
4,00000+05	4,06760+00	0,00000+00	8,13520-04	4,30000+02	1,26494-03	20224	2151	640
5,00000+05	4,00000+00	0,00000+00	8,00000+00	4,30000+02	1,24442-03	20224	2151	641
6,00000+05	3,93330+00	1,00000+00	7,86660+00	4,30000+02	1,22390-03	20224	2151	642
7,00000+05	3,86660+00	0,00000+00	7,73330+00	4,30000+02	1,20338-03	20224	2151	643
8,00000+05	3,80000+00	0,00000+00	7,60000+00	4,30000+02	1,18286-03	20224	2151	644
9,00000+05	3,73330+00	0,00000+00	7,46660+00	4,30000+02	1,16234-03	20224	2151	645
1,00000+06	3,66660+00	0,00000+00	7,33330+00	4,30000+02	1,14182-03	20224	2151	646
2,00000+06	3,60000+00	0,00000+00	7,20000+00	4,30000+02	1,12130-03	20224	2151	647
3,00000+06	3,53330+00	0,00000+00	7,06660+00	4,30000+02	1,10078-03	20224	2151	648
4,00000+06	3,46660+00	0,00000+00	6,93330+00	4,30000+02	1,08026-03	20224	2151	649
5,00000+06	3,40000+00	0,00000+00	6,80000+00	4,30000+02	1,05974-03	20224	2151	650
6,00000+06	3,33330+00	0,00000+00	6,66660+00	4,30000+02	1,03922-03	20224	2151	651
7,00000+06	3,26660+00	0,00000+00	6,53330+00	4,30000+02	1,01870-03	20224	2151	652
8,00000+06	3,20000+00	0,00000+00	6,40000+00	4,30000+02	99818-03	20224	2151	653
9,00000+06	3,13330+00	0,00000+00	6,26660+00	4,30000+02	97766-03	20224	2151	654
1,00000+07	3,06660+00	0,00000+00	6,13330+00	4,30000+02	95714-03	20224	2151	655
2,00000+07	3,00000+00	0,00000+00	6,00000+00	4,30000+02	93662-03	20224	2151	656
3,00000+07	2,93330+00	0,00000+00	5,86660+00	4,30000+02	91610-03	20224	2151	657
4,00000+07	2,86660+00	0,00000+00	5,73330+00	4,30000+02	89558-03	20224	2151	658
5,00000+07	2,80000+00	0,00000+00	5,60000+00	4,30000+02	87506-03	20224	2151	659

6,00000+03	3,05490+00	0,00000+00	6,10980-04	4,30000+02	6,86670-01	20224	2151	659
7,00000+03	3,04920+00	0,00000+00	6,09840-04	4,30000+02	6,87120-01	20224	2151	660
8,00000+03	3,04350+00	0,00000+00	6,08700-04	4,30000+02	6,87560-01	20224	2151	661
9,00000+03	3,03770+00	0,00000+00	6,07540-04	4,30000+02	6,87990-01	20224	2151	662
1,00000+04	3,03200+00	0,00000+00	6,06400-04	4,30000+02	6,88410-01	20224	2151	663
2,00000+04	3,00360+00	0,00000+00	6,00720-04	4,30000+02	6,90400-01	20224	2151	664
3,00000+04	2,99750+00	0,00000+00	5,95100-04	4,30000+02	6,92180-01	20224	2151	665
4,00000+04	2,92000+00	0,00000+00	5,84000-04	4,30000+02	6,95110-01	20224	2151	666
5,00000+04	2,86570+00	0,00000+00	5,73140-04	4,30000+02	6,97190-01	20224	2151	667
6,00000+04	2,84420+00	0,00000+00	5,68840-04	4,30000+02	6,97790-01	20224	2151	668
7,00000+04	2,81240+00	1,86060-03	5,62600-04	4,30000+02	6,98430-01	20224	2151	669
8,00000+04	2,76010+00	4,99930-03	5,52020-04	4,30000+02	6,98450-01	20224	2151	670
9,00000+04	2,70880+00	8,73430-03	5,41760-04	4,30000+02	6,98450-01	20224	2151	671
1,00000+05	2,65850+00	1,28006-02	5,31700-04	4,30000+02	6,97270-01	20224	2151	672
2,00000+05	2,60920+00	1,70446-02	5,21640-04	4,30000+02	6,95530-01	20224	2151	673
3,00000+05	2,56090+00	2,13662-02	5,12180-04	4,30000+02	6,92660-01	20224	2151	674
4,00000+05	2,50000+00	0,00000+00	5,00000+00	4,30000+02	6,89220-01	20224	2151	675
5,00000+05	2,40000+00	2,00000+00	4,80000+00	4,30000+02	6,85440-01	20224	2151	676
6,00000+05	2,37320+00	0,00000+00	4,74600-04	4,30000+02	6,87530-01	20224	2151	677
7,00000+05	2,37280+00	0,00000+00	4,74560-04	4,30000+02	6,87510-01	20224	2151	678
8,00000+05	2,37230+00	0,00000+00	4,74460-04	4,30000+02	6,87490-01	20224	2151	679
9,00000+05	2,37190+00	0,00000+00	4,74360-04	4,30000+02	6,87460-01	20224	2151	680
1,00000+06	2,37140+00	0,00000+00	4,74260-04	4,30000+02	6,87440-01	20224	2151	681
2,00000+06	2,37100+00	0,00000+00	4,74200-04	4,30000+02	6,87410-01	20224	2151	682
3,00000+06	2,37050+00	0,00000+00	4,74100-04	4,30000+02	6,87380-01	20224	2151	683
4,00000+06	2,37010+00	0,00000+00	4,74020-04	4,30000+02	6,87360-01	20224	2151	684
5,00000+06	2,36960+00	0,00000+00	4,73920-04	4,30000+02	6,87330-01	20224	2151	685
6,00000+06	2,36920+00	0,00000+00	4,73840-04	4,30000+02	6,87300-01	20224	2151	686
7,00000+06	2,36870+00	0,00000+00	4,73740-04	4,30000+02	6,87270-01	20224	2151	687
8,00000+06	2,36830+00	0,00000+00	4,73660-04	4,30000+02	6,87240-01	20224	2151	688
9,00000+06	2,36780+00	0,00000+00	4,73560-04	4,30000+02	6,87210-01	20224	2151	689
1,00000+07	2,36740+00	0,00000+00	4,73460-04	4,30000+02	6,87180-01	20224	2151	690
2,00000+07	2,36700+00	0,00000+00	4,73360-04	4,30000+02	6,87150-01	20224	2151	691
3,00000+07	2,36650+00	0,00000+00	4,73260-04	4,30000+02	6,87120-01	20224	2151	692
4,00000+07	2,36610+00	0,00000+00	4,73160-04	4,30000+02	6,87090-01	20224	2151	693
5,00000+07	2,36560+00	0,00000+00	4,73060-04	4,30000+02	6,87060-01	20224	2151	694
6,00000+07	2,36520+00	0,00000+00	4,72960-04	4,30000+02	6,87030-01	20224	2151	695
7,00000+07	2,36470+00	0,00000+00	4,72860-04	4,30000+02	6,87000-01	20224	2151	696
8,00000+07	2,36430+00	0,00000+00	4,72760-04	4,30000+02	6,86970-01	20224	2151	697
9,00000+07	2,36380+00	0,00000+00	4,72660-04	4,30000+02	6,86940-01	20224	2151	698
1,00000+08	2,36340+00	0,00000+00	4,72560-04	4,30000+02	6,86910-01	20224	2151	699
2,00000+08	2,36290+00	0,00000+00	4,72460-04	4,30000+02	6,86880-01	20224	2151	700
3,00000+08	2,36250+00	0,00000+00	4,72360-04	4,30000+02	6,86850-01	20224	2151	701
4,00000+08	2,36210+00	0,00000+00	4,72260-04	4,30000+02	6,86820-01	20224	2151	702
5,00000+08	2,36160+00	0,00000+00	4,72160-04	4,30000+02	6,86790-01	20224	2151	703
6,00000+08	2,36120+00	0,00000+00	4,72060-04	4,30000+02	6,86760-01	20224	2151	704
7,00000+08	2,36070+00	0,00000+00	4,71960-04	4,30000+02	6,86730-01	20224	2151	705

8.000000+04	2.041330+00	1.965777-02	4.082260-04	4.300000+02	8.583400-01	202024	2151	706
9.000000+04	2.005330+00	2.617354-02	4.000680-04	4.300000+02	8.510200-01	202024	2151	707
1.000000+03	1.966110+00	3.280744-02	3.932220-04	4.300000+02	8.432400-01	202024	2151	708
4.000000+00	0.000000+00	0.000000+00	0.000000+00	0.000000+00	0.000000+00	202024	2151	709
5.000000+00	0.000000+00	2.000000+00	1.000000+00	0.000000+00	2.000000+00	202024	2151	710
1.000000+02	2.031130+00	0.000000+00	4.068220-04	4.300000+02	4.503380-01	202024	2151	711
1.500000+02	2.033700+00	0.000000+00	4.067800-04	4.300000+02	4.504000-01	202024	2151	712
2.000000+02	2.033700+00	0.000000+00	4.067400-04	4.300000+02	4.504200-01	202024	2151	713
3.000000+02	2.033430+00	0.000000+00	4.066800-04	4.300000+02	4.504500-01	202024	2151	714
4.000000+02	2.033300+00	0.000000+00	4.066600-04	4.300000+02	4.504800-01	202024	2151	715
5.000000+02	2.033260+00	0.000000+00	4.066200-04	4.300000+02	4.505100-01	202024	2151	716
6.000000+02	2.033220+00	0.000000+00	4.066400-04	4.300000+02	4.505400-01	202024	2151	717
7.000000+02	2.033180+00	0.000000+00	4.066300-04	4.300000+02	4.505800-01	202024	2151	718
8.000000+02	2.033140+00	0.000000+00	4.066200-04	4.300000+02	4.506100-01	202024	2151	719
9.000000+02	2.033100+00	0.000000+00	4.066200-04	4.300000+02	4.506400-01	202024	2151	720
1.000000+03	2.033000+00	0.000000+00	4.066140-04	4.300000+02	4.506700-01	202024	2151	721
1.500000+03	2.028700+00	0.000000+00	4.057400-04	4.300000+02	4.508300-01	202024	2151	722
2.000000+03	2.028800+00	0.000000+00	4.053600-04	4.300000+02	4.509900-01	202024	2151	723
3.000000+03	2.023300+00	0.000000+00	4.036600-04	4.300000+02	4.513000-01	202024	2151	724
4.000000+03	2.019100+00	0.000000+00	4.038200-04	4.300000+02	4.516000-01	202024	2151	725
5.000000+03	2.015500+00	0.000000+00	4.030600-04	4.300000+02	4.519000-01	202024	2151	726
6.000000+03	2.011900+00	0.000000+00	4.023000-04	4.300000+02	4.522000-01	202024	2151	727
7.000000+03	2.008300+00	0.000000+00	4.015200-04	4.300000+02	4.524900-01	202024	2151	728
8.000000+03	2.004700+00	0.000000+00	4.007600-04	4.300000+02	4.527700-01	202024	2151	729
9.000000+03	2.001100+00	0.000000+00	4.000000-04	4.300000+02	4.530500-01	202024	2151	730
1.000000+04	1.997500+00	0.000000+00	3.992400-04	4.300000+02	4.533200-01	202024	2151	731
1.500000+04	1.977400+00	0.000000+00	3.954800-04	4.300000+02	4.536000-01	202024	2151	732
2.000000+04	1.958700+00	0.000000+00	3.917400-04	4.300000+02	4.538800-01	202024	2151	733
3.000000+04	1.921900+00	0.000000+00	3.873800-04	4.300000+02	4.542700-01	202024	2151	734
4.000000+04	1.885800+00	0.000000+00	3.821600-04	4.300000+02	4.548900-01	202024	2151	735
5.000000+04	1.871600+00	6.392000-03	3.743200-04	4.300000+02	4.559270-01	202024	2151	736
6.000000+04	1.850000+00	3.771600-03	3.700800-04	4.300000+02	4.566600-01	202024	2151	737
7.000000+04	1.815000+00	6.577400-03	3.731400-04	4.300000+02	4.598600-01	202024	2151	738
8.000000+04	1.781000+00	1.149010-02	3.563400-04	4.300000+02	4.595500-01	202024	2151	739
9.000000+04	1.748400+00	1.683860-02	3.496800-04	4.300000+02	4.587100-01	202024	2151	740
1.000000+05	1.715000+00	2.241530-02	3.431400-04	4.300000+02	4.573700-01	202024	2151	741
1.000000+03	1.683600+00	2.809420-02	3.367200-04	4.300000+02	4.555600-01	202024	2151	742
3.000000+00	0.000000+00	0.000000+00	0.000000+00	0.000000+00	0.000000+00	202024	2151	743
9.000000+00	0.000000+00	0.000000+00	0.000000+00	0.000000+00	0.000000+00	202024	2151	744
9.424100+04	2.389860+02	0.000000+00	0.000000+00	99	0.000000+00	202024	2151	745
2.930000+02	0.000000+00	0.000000+00	0.000000+00	2	210	202024	2151	746
1.000000-04	2.362600+04	2.000000-04	1.670480+04	4.000000-04	1.180700+04	202024	2151	748
8.000000-04	8.341800+03	1.000000-03	7.457450+03	2.000000-03	5.254420+03	202024	2151	749
3.000000-03	4.281520+03	4.500000-03	3.480140+03	6.500000-03	2.878460+03	202024	2151	750
8.500000-03	2.500020+03	1.050000-02	2.234620+03	1.450000-02	1.877220+03	202024	2151	751
2.000000-02	1.576660+03	2.500000-02	1.398660+03	2.530000-02	1.390030+03	202024	2151	752

3.000000-02	1.270997+03	3.500000-02	1.775130+03	4.000000-02	1.100750+03	202024	2151	753
4.500000-02	2.641920+03	5.500000-02	9.940800+03	5.500000-02	9.545200+03	202024	2151	754
6.500000-02	2.117000+02	5.500000-02	8.934700+02	7.700000-02	8.702100+02	202024	2151	755
7.500000-02	5.148000+02	8.000000-02	8.359600+02	8.500000-02	8.233600+02	202024	2151	756
9.000000-02	1.140000+02	5.500000-02	8.075400+02	1.000000-01	8.051000+02	202024	2151	757
1.000000-01	2.083300+02	1.100000-01	8.082900+02	1.150000-01	8.140000+02	202024	2151	758
1.100000-01	5.201200+02	1.250000-01	8.302600+02	1.300000-01	8.421100+02	202024	2151	759
1.350000-01	6.066100+02	1.400000-01	8.808700+02	1.450000-01	9.028900+02	202024	2151	760
1.500000-01	2.817000+02	1.550000-01	9.591700+02	1.600000-01	9.930000+02	202024	2151	761
1.850000-01	1.032200+03	1.700000-01	1.073820+03	1.750000-01	1.118780+03	202024	2151	762
1.850000-01	1.168226+03	1.850000-01	1.230771+03	1.900000-01	1.296666+03	202024	2151	763
1.950000-01	1.377530+03	2.000000-01	1.469477+03	2.000000-01	1.255916+03	202024	2151	764
2.100000-01	1.062338+03	2.150000-01	1.778190+03	2.200000-01	1.555919+03	202024	2151	765
2.500000-01	0.000000+03	2.300000-01	2.111040+03	2.250000-01	1.693771+03	202024	2151	766
2.500000-01	2.277850+03	2.350000-01	3.343397+03	2.300000-01	2.201131+03	202024	2151	767
3.000000-01	1.888910+03	2.500000-01	2.371390+03	2.350000-01	2.380341+03	202024	2151	768
3.500000-01	2.261910+03	2.700000-01	3.132330+03	2.400000-01	3.335551+03	202024	2151	769
3.850000-01	1.843996+03	2.850000-01	1.701530+03	2.450000-01	1.906631+03	202024	2151	770
3.900000-01	1.414782+03	3.000000-01	1.274070+03	2.500000-01	1.549931+03	202024	2151	771
3.950000-01	1.033255+03	3.050000-01	9.433950+02	2.550000-01	1.150700+03	202024	2151	772
3.950000-01	7.936160+02	3.350000-01	7.169920+02	2.600000-01	8.680100+02	202024	2151	773
3.950000-01	5.988600+02	3.500000-01	5.458000+02	2.650000-01	6.551200+02	202024	2151	774
3.950000-01	3.552200+02	3.650000-01	4.226500+02	2.700000-01	4.987300+02	202024	2151	775
3.950000-01	3.638600+02	3.800000-01	3.352660+02	2.750000-01	3.905500+02	202024	2151	776
3.950000-01	2.968800+02	3.950000-01	2.788300+02	2.800000-01	3.169900+02	202024	2151	777
4.050000-01	2.505000+02	4.100000-01	3.370400+02	2.850000-01	2.633900+02	202024	2151	778
4.200000-01	2.136660+02	4.250000-01	2.033580+02	2.900000-01	2.243900+02	202024	2151	779
4.300000-01	1.855700+02	4.400000-01	1.773400+02	2.950000-01	1.942400+02	202024	2151	780
4.300000-01	1.633350+02	4.550000-01	1.504450+02	3.000000-01	1.706470+02	202024	2151	781
4.300000-01	1.284500+02	4.700000-01	1.185400+02	3.050000-01	1.390910+02	202024	2151	782
5.300000-01	1.631140+02	4.850000-01	9.711600+01	3.100000-01	1.109930+02	202024	2151	783
5.300000-01	7.754000+01	5.000000-01	8.481000+01	3.150000-01	9.218000+01	202024	2151	784
5.300000-01	7.982000+01	5.050000-01	7.799000+01	3.200000-01	8.234600+01	202024	2151	785
6.000000-01	7.522800+01	6.000000-01	7.412000+01	3.250000-01	7.649000+01	202024	2151	786
6.300000-01	7.231000+01	6.400000-01	7.148000+01	3.300000-01	7.316000+01	202024	2151	787
6.600000-01	6.909800+01	6.700000-01	6.928300+01	3.350000-01	7.072000+01	202024	2151	788
6.600000-01	6.799800+01	6.750000-01	6.738000+01	3.400000-01	6.863300+01	202024	2151	789
7.000000-01	6.513000+01	7.000000-01	6.410000+01	3.450000-01	6.623300+01	202024	2151	790
8.000000-01	6.216000+01	7.800000-01	6.126000+01	3.500000-01	6.310000+01	202024	2151	791
8.000000-01	5.958000+01	8.200000-01	5.879000+01	3.550000-01	6.060000+01	202024	2151	792
9.200000-01	5.729000+01	8.500000-01	5.657000+01	3.600000-01	5.802000+01	202024	2151	793
9.800000-01	5.523000+01	1.000000+00	5.468000+01	3.650000-01	5.580000+01	202024	2151	794
1.000000+00	1.309970+01	1.000000+00	1.268200+01	3.700000+00	5.400000+00	202024	2151	795
1.000000+00	1.191930+01	1.100000+00	1.159000+01	3.750000+00	1.229000+00	202024	2151	796
2.000000+00	1.104220+01	2.000000+00	1.088400+01	3.800000+00	1.133000+00	202024	2151	797
2.000000+00	1.033600+01	2.400000+00	1.016200+01	3.850000+00	1.058400+00	202024	2151	798
3.000000+00	9.821000+00	3.000000+00	9.668000+00	3.900000+00	9.985000+00	202024	2151	799

4.01074+04	0.00000+00	4.50000+04	7.00000-02	5.50000+04	1.06000-01	2024	3	4	874
6.50000+04	1.24000-01	7.50000+04	1.48000-01	8.50000+04	1.05000-01	2024	3	4	875
9.50000+04	1.01000-01	1.00000+05	1.71000-01	1.20000+05	2.31000-01	2024	3	4	877
1.40000+05	2.05000-01	1.00000+05	5.00000-01	1.80000+05	5.47000-01	2024	3	4	878
2.00000+05	3.98000-01	2.20000+05	1.52000-01	2.40000+05	5.02000-01	2024	3	4	879
2.60000+05	5.52000-01	2.80000+05	0.30000-01	3.00000+05	6.00000-01	2024	3	4	900
3.20000+05	7.17000-01	3.40000+05	7.71000-01	3.60000+05	8.22000-01	2024	3	4	901
3.80000+05	8.72000-01	4.00000+05	9.16000-01	4.20000+05	9.50000-01	2024	3	4	902
4.40000+05	9.85000-01	4.60000+05	1.01700-00	4.80000+05	1.05300+00	2024	3	4	903
5.00000+05	1.08200+00	5.20000+05	1.15180+00	5.40000+05	1.19600+00	2024	3	4	904
5.60000+05	1.24000+00	5.80000+05	1.29200+00	6.00000+05	1.34100+00	2024	3	4	905
6.20000+05	1.38200+00	6.40000+05	1.42050+00	6.60000+05	1.48320+00	2024	3	4	906
6.80000+05	1.50800+00	7.00000+05	1.53800+00	7.20000+05	1.61900+00	2024	3	4	907
7.40000+05	1.62400+00	7.60000+05	1.64600+00	7.80000+05	1.75800+00	2024	3	4	908
8.00000+05	1.73400+00	8.20000+05	1.74500+00	8.40000+05	1.89700+00	2024	3	4	909
8.60000+05	1.83800+00	8.80000+05	1.83500+00	9.00000+05	2.03600+00	2024	3	4	910
9.20000+05	1.93800+00	9.40000+05	1.91600+00	9.60000+05	2.17500+00	2024	3	4	911
9.80000+05	2.03400+00	1.00000+06	1.98500+00	1.00000+06	2.31400+00	2024	3	4	912
1.00000+06	2.12600+00	1.00000+06	2.05400+00	1.00000+06	2.45300+00	2024	3	4	913
1.10000+06	2.21400+00	1.00000+06	2.12300+00	1.00000+06	2.59200+00	2024	3	4	914
1.20000+06	2.29800+00	1.00000+06	2.19200+00	1.00000+06	2.73100+00	2024	3	4	915
1.30000+06	2.37800+00	1.00000+06	2.26100+00	1.00000+06	2.87000+00	2024	3	4	916
1.40000+06	2.45400+00	1.00000+06	2.33000+00	1.00000+06	3.00900+00	2024	3	4	917
1.50000+06	2.52600+00	1.00000+06	2.39900+00	1.00000+06	3.14800+00	2024	3	4	918
1.60000+06	2.59400+00	1.00000+06	2.46800+00	1.00000+06	3.28700+00	2024	3	4	919
1.70000+06	2.65800+00	1.00000+06	2.53700+00	1.00000+06	3.42600+00	2024	3	4	920
1.80000+06	2.71800+00	1.00000+06	2.60600+00	1.00000+06	3.56500+00	2024	3	4	921
1.90000+06	2.77400+00	1.00000+06	2.67500+00	1.00000+06	3.70400+00	2024	3	4	922
2.00000+06	2.82600+00	1.00000+06	2.74400+00	1.00000+06	3.84300+00	2024	3	4	923
2.10000+06	2.87400+00	1.00000+06	2.81300+00	1.00000+06	3.98200+00	2024	3	4	924
2.20000+06	2.91800+00	1.00000+06	2.88200+00	1.00000+06	4.12100+00	2024	3	4	925
2.30000+06	2.95800+00	1.00000+06	2.95100+00	1.00000+06	4.26000+00	2024	3	4	926
2.40000+06	3.00000+00	1.00000+06	3.02000+00	1.00000+06	4.39900+00	2024	3	4	927
2.50000+06	3.03800+00	1.00000+06	3.08900+00	1.00000+06	4.53800+00	2024	3	4	928
2.60000+06	3.07200+00	1.00000+06	3.15800+00	1.00000+06	4.67700+00	2024	3	4	929
2.70000+06	3.10200+00	1.00000+06	3.22700+00	1.00000+06	4.81600+00	2024	3	4	930
2.80000+06	3.12800+00	1.00000+06	3.29600+00	1.00000+06	4.95500+00	2024	3	4	931
2.90000+06	3.15000+00	1.00000+06	3.36500+00	1.00000+06	5.09400+00	2024	3	4	932
3.00000+06	3.16800+00	1.00000+06	3.43400+00	1.00000+06	5.23300+00	2024	3	4	933
3.10000+06	3.18200+00	1.00000+06	3.50300+00	1.00000+06	5.37200+00	2024	3	4	934
3.20000+06	3.19200+00	1.00000+06	3.57200+00	1.00000+06	5.51100+00	2024	3	4	935
3.30000+06	3.19800+00	1.00000+06	3.64100+00	1.00000+06	5.65000+00	2024	3	4	936
3.40000+06	3.20000+00	1.00000+06	3.71000+00	1.00000+06	5.78900+00	2024	3	4	937
3.50000+06	3.19800+00	1.00000+06	3.77900+00	1.00000+06	5.92800+00	2024	3	4	938
3.60000+06	3.19200+00	1.00000+06	3.84800+00	1.00000+06	6.06700+00	2024	3	4	939
3.70000+06	3.18200+00	1.00000+06	3.91700+00	1.00000+06	6.20600+00	2024	3	4	940
3.80000+06	3.16800+00	1.00000+06	3.98600+00	1.00000+06	6.34500+00	2024	3	4	941
3.90000+06	3.15000+00	1.00000+06	4.05500+00	1.00000+06	6.48400+00	2024	3	4	942
4.00000+06	3.12800+00	1.00000+06	4.12400+00	1.00000+06	6.62300+00	2024	3	4	943
4.10000+06	3.10200+00	1.00000+06	4.19300+00	1.00000+06	6.76200+00	2024	3	4	944
4.20000+06	3.07200+00	1.00000+06	4.26200+00	1.00000+06	6.90100+00	2024	3	4	945
4.30000+06	3.03800+00	1.00000+06	4.33100+00	1.00000+06	7.04000+00	2024	3	4	946
4.40000+06	3.00000+00	1.00000+06	4.40000+00	1.00000+06	7.17900+00	2024	3	4	947
4.50000+06	2.95800+00	1.00000+06	4.46900+00	1.00000+06	7.31800+00	2024	3	4	948
4.60000+06	2.91200+00	1.00000+06	4.53800+00	1.00000+06	7.45700+00	2024	3	4	949
4.70000+06	2.86200+00	1.00000+06	4.60700+00	1.00000+06	7.59600+00	2024	3	4	950
4.80000+06	2.80800+00	1.00000+06	4.67600+00	1.00000+06	7.73500+00	2024	3	4	951
4.90000+06	2.75000+00	1.00000+06	4.74500+00	1.00000+06	7.87400+00	2024	3	4	952
5.00000+06	2.68800+00	1.00000+06	4.81400+00	1.00000+06	8.01300+00	2024	3	4	953
5.10000+06	2.62200+00	1.00000+06	4.88300+00	1.00000+06	8.15200+00	2024	3	4	954
5.20000+06	2.55200+00	1.00000+06	4.95200+00	1.00000+06	8.29100+00	2024	3	4	955
5.30000+06	2.47800+00	1.00000+06	5.02100+00	1.00000+06	8.43000+00	2024	3	4	956
5.40000+06	2.40000+00	1.00000+06	5.09000+00	1.00000+06	8.56900+00	2024	3	4	957
5.50000+06	2.31800+00	1.00000+06	5.15900+00	1.00000+06	8.70800+00	2024	3	4	958
5.60000+06	2.23200+00	1.00000+06	5.22800+00	1.00000+06	8.84700+00	2024	3	4	959
5.70000+06	2.14200+00	1.00000+06	5.29700+00	1.00000+06	8.98600+00	2024	3	4	960
5.80000+06	2.04800+00	1.00000+06	5.36600+00	1.00000+06	9.12500+00	2024	3	4	961
5.90000+06	1.95000+00	1.00000+06	5.43500+00	1.00000+06	9.26400+00	2024	3	4	962
6.00000+06	1.84800+00	1.00000+06	5.50400+00	1.00000+06	9.40300+00	2024	3	4	963
6.10000+06	1.74200+00	1.00000+06	5.57300+00	1.00000+06	9.54200+00	2024	3	4	964
6.20000+06	1.63200+00	1.00000+06	5.64200+00	1.00000+06	9.68100+00	2024	3	4	965
6.30000+06	1.51800+00	1.00000+06	5.71100+00	1.00000+06	9.82000+00	2024	3	4	966
6.40000+06	1.40000+00	1.00000+06	5.78000+00	1.00000+06	9.95900+00	2024	3	4	967
6.50000+06	1.27800+00	1.00000+06	5.84900+00	1.00000+06	10.09800+00	2024	3	4	968
6.60000+06	1.15200+00	1.00000+06	5.91800+00	1.00000+06	10.23700+00	2024	3	4	969
6.70000+06	1.02200+00	1.00000+06	5.98700+00	1.00000+06	10.37600+00	2024	3	4	970
6.80000+06	88800+00	1.00000+06	6.05600+00	1.00000+06	10.51500+00	2024	3	4	971
6.90000+06	75400+00	1.00000+06	6.12500+00	1.00000+06	10.65400+00	2024	3	4	972
7.00000+06	61800+00	1.00000+06	6.19400+00	1.00000+06	10.79300+00	2024	3	4	973
7.10000+06	48000+00	1.00000+06	6.26300+00	1.00000+06	10.93200+00	2024	3	4	974
7.20000+06	34000+00	1.00000+06	6.33200+00	1.00000+06	11.07100+00	2024	3	4	975
7.30000+06	20000+00	1.00000+06	6.40100+00	1.00000+06	11.21000+00	2024	3	4	976
7.40000+06	6000+00	1.00000+06	6.47000+00	1.00000+06	11.34900+00	2024	3	4	977
7.50000+06	0+00	1.00000+06	6.53900+00	1.00000+06	11.48800+00	2024	3	4	978
7.60000+06	0+00	1.00000+06	6.60800+00	1.00000+06	11.62700+00	2024	3	4	979
7.70000+06	0+00	1.00000+06	6.67700+00	1.00000+06	11.76600+00	2024	3	4	980
7.80000+06	0+00	1.00000+06	6.74600+00	1.00000+06	11.90500+00	2024	3	4	981
7.90000+06	0+00	1.00000+06	6.81500+00	1.00000+06	12.04400+00	2024	3	4	982
8.00000+06	0+00	1.00000+06	6.88400+00	1.00000+06	12.18300+00	2024	3	4	983
8.10000+06	0+00	1.00000+06	6.95300+00	1.00000+06	12.32200+00	2024	3	4	984
8.20000+06	0+00	1.00000+06	7.02200+00	1.00000+06	12.46100+00	2024	3	4	985
8.30000+06	0+00	1.00000+06	7.09100+00	1.00000+06	12.60000+00	2024	3	4	986
8.40000+06	0+00	1.00000+06	7.16000+00	1.00000+06	12.73900+00	2024	3	4	987
8.50000+06	0+00	1.00000+06	7.22900+00	1.00000+06	12.87800+00	2024	3	4	988
8.60000+06	0+00	1.00000+06	7.29800+00	1.00000+06	13.01700+00	2024	3	4	989
8.70000+06	0+00	1.00000+06	7.36700+00	1.00000+06	13.15600+00	2024	3	4	990
8.80000+06	0+00	1.00000+06	7.43600+00	1.00000+06	13.29500+00	2024	3	4	991
8.90000+06	0+00	1.00000+06	7.50500+00	1.00000+06	13.43400+00	2024	3	4	992
9.00000+06	0+00	1.00000+06	7.57400+00	1.00000+06	13.57300+00	2024	3	4	993
9.10000+06	0+00	1.00000+06	7.64300+00	1.00000+06	13.71200+00	2024	3	4	994

4.60000+05	5.92000-02	4.80000+05	6.10000-02	5.00000+05	6.23000-02	2024	3	53	1082
5.50000+05	6.56000-02	6.00000+05	6.72000-02	6.50000+05	6.89000-02	2024	3	53	1083
7.00000+05	7.00000-02	7.00000+05	7.24000-02	7.00000+05	7.30000-02	2024	3	53	1084
8.50000+05	7.25000-02	8.00000+05	7.11000-02	8.50000+05	8.01000-02	2024	3	53	1085
1.00000+06	8.09000-02	1.10000+06	8.60000-02	1.20000+06	8.91000-02	2024	3	53	1086
1.40000+06	4.79000-02	1.60000+06	3.63000-02	1.80000+06	2.55000-02	2024	3	53	1087
2.00000+06	1.66000-02	2.20000+06	1.02000-02	2.40000+06	6.00000-03	2024	3	53	1088
2.60000+06	3.50000-03	2.80000+06	2.00000-03	3.00000+06	1.20000-03	2024	3	53	1089
3.20000+06	7.00000-04	3.40000+06	4.00000-04	3.60000+06	2.00000-04	2024	3	53	1090
3.80000+06	1.00000-04	4.00000+06	1.00000-04	4.50000+06	1.00000-04	2024	3	53	1091
4.50000+06	0.00000+00	1.50000+07	0.00000+00	0.00000+00	0.00000+00	2024	3	53	1092
0.00000+00	0.00000+00	0.00000+00	0.00000+00	0.00000+00	0.00000+00	2024	3	54	1093
9.42410+04	2.38986+02	0	0	0	0	2024	3	54	1094
2.95000+02	-1.67000+05	0	0	1	462024	2024	3	54	1095
1.67694+05	0.00000+00	1.80000+05	2.70000-03	2.00000+05	7.50000-03	2024	3	54	1096
2.20000+05	1.20000-02	2.40000+05	1.59000-02	1.60000+05	1.83000-02	2024	3	54	1098
2.80000+05	2.03000-02	3.00000+05	2.24000-02	3.20000+05	2.43000-02	2024	3	54	1099
3.40000+05	2.62000-02	3.60000+05	2.77000-02	3.80000+05	2.92000-02	2024	3	54	1100
4.00000+05	3.05000-02	4.20000+05	3.15000-02	4.40000+05	3.27000-02	2024	3	54	1101
4.60000+05	3.37000-02	4.80000+05	3.51000-02	5.00000+05	3.63000-02	2024	3	54	1102
5.20000+05	3.95000-02	6.00000+05	4.22000-02	6.50000+05	4.54000-02	2024	3	54	1103
7.00000+05	4.91000-02	7.50000+05	3.31000-02	8.00000+05	3.68000-02	2024	3	54	1104
8.50000+05	6.00000-02	9.00000+05	6.20000-02	9.50000+05	6.52000-02	2024	3	54	1105
1.00000+06	6.55000-02	1.10000+06	1.10000-02	1.20000+06	6.08000-02	2024	3	54	1106
1.40000+06	5.64000-02	1.60000+06	4.69000-02	1.80000+06	3.51000-02	2024	3	54	1107
2.00000+06	2.41000-02	2.20000+06	1.50000-02	2.40000+06	9.10000-03	2024	3	54	1108
2.60000+06	5.40000-03	2.80000+06	3.20000-03	3.00000+06	1.90000-03	2024	3	54	1109
3.20000+06	1.10000-03	3.40000+06	7.00000-04	3.60000+06	4.00000-04	2024	3	54	1110
3.80000+06	3.00000-04	4.00000+06	2.00000-04	4.00000+06	0.00000-04	2024	3	54	1111
1.50000+07	0.00000+00	0.00000+00	0.00000+00	0.00000+00	0.00000+00	2024	3	54	1112
0.00000+00	0.00000+00	0.00000+00	0.00000+00	0.00000+00	0.00000+00	2024	3	54	1113
9.42410+04	2.38986+02	0	0	0	0	2024	3	55	1114
2.95000+02	-1.09000+05	0	0	1	472024	2024	3	55	1115
1.69767+05	0.00000+00	1.80000+05	1.19000-02	2.00000+05	2.99000-02	2024	3	55	1116
2.20000+05	4.65000-02	2.40000+05	5.98000-02	2.60000+05	6.80000-02	2024	3	55	1118
2.80000+05	7.49000-02	3.00000+05	8.20000-02	3.20000+05	8.87000-02	2024	3	55	1119
3.40000+05	9.47000-02	3.60000+05	1.00000-01	3.80000+05	1.04900-01	2024	3	55	1120
4.00000+05	1.09000-01	4.20000+05	1.12000-01	4.40000+05	1.15200-01	2024	3	55	1121
4.60000+05	1.17800-01	4.80000+05	1.21000-01	5.00000+05	1.23300-01	2024	3	55	1122
5.20000+05	1.28700-01	6.00000+05	1.13000-01	6.50000+05	1.33300-01	2024	3	55	1123
7.00000+05	1.36200-01	7.50000+05	1.38500-01	8.00000+05	1.38700-01	2024	3	55	1124
8.50000+05	1.37200-01	9.00000+05	1.33900-01	9.50000+05	1.31400-01	2024	3	55	1125
1.00000+06	1.24900-01	1.10000+06	1.20700-01	1.20000+06	1.07300-01	2024	3	55	1126
1.40000+06	8.67000-02	1.60000+06	6.54000-02	1.80000+06	4.59000-02	2024	3	55	1127
2.00000+06	2.99000-02	2.20000+06	1.85000-02	2.40000+06	1.08000-02	2024	3	55	1128

2.60000+06	6.30000-03	2.80000+06	3.60000-03	3.00000+06	2.10000+03	2024	3	55	1129
3.20000+06	1.20000-03	3.40000+06	8.00000-04	3.60000+06	5.00000+04	2024	3	55	1130
3.80000+06	3.00000-04	4.00000+06	2.00000-04	4.50000+06	1.00000+04	2024	3	55	1131
4.50000+06	0.00000+00	1.50000+07	0.00000+00	0.00000+00	0.00000+00	2024	3	55	1132
0.00000+00	0.00000+00	0.00000+00	0.00000+00	0.00000+00	0.00000+00	2024	3	55	1133
9.42410+04	2.38986+02	0	0	0	0	2024	3	56	1134
2.95000+02	-1.72000+05	0	0	1	482024	2024	3	56	1135
1.72720+05	0.00000+00	1.80000+05	1.33000-02	2.00000+05	3.63000-02	2024	3	56	1136
2.20000+05	5.74000-02	2.40000+05	7.42000-02	2.60000+05	8.41000-02	2024	3	56	1137
2.80000+05	9.25000-02	3.00000+05	1.01100-01	3.20000+05	1.09000-01	2024	3	56	1138
3.40000+05	1.15900-01	3.60000+05	1.21700-01	3.80000+05	1.26900-01	2024	3	56	1139
4.00000+05	1.31100-01	4.20000+05	1.33800-01	4.40000+05	1.46000-01	2024	3	56	1140
4.60000+05	1.59400-01	4.80000+05	1.42400-01	5.00000+05	1.44600-01	2024	3	56	1141
5.20000+05	1.49600-01	6.00000+05	1.51500-01	6.50000+05	1.53500-01	2024	3	56	1142
7.00000+05	1.50600-01	7.50000+05	1.59200-01	8.00000+05	1.60200-01	2024	3	56	1143
8.50000+05	1.59700-01	9.00000+05	1.57000-01	9.50000+05	1.55200-01	2024	3	56	1144
1.00000+06	1.48200-01	1.10000+06	1.38500-01	1.20000+06	1.26000-01	2024	3	56	1145
1.40000+06	1.04100-01	1.60000+06	8.01000-02	1.80000+06	5.17000-02	2024	3	56	1146
2.00000+06	5.77000-02	2.20000+06	2.32000-02	2.40000+06	1.37000-02	2024	3	56	1147
2.60000+06	8.00000-03	2.80000+06	4.70000-03	3.00000+06	2.70000-03	2024	3	56	1148
3.20000+06	1.60000-03	3.40000+06	1.00000-03	3.60000+06	5.00000-04	2024	3	56	1149
3.80000+06	3.00000-04	4.00000+06	2.00000-04	4.50000+06	1.00000-04	2024	3	56	1150
5.00000+06	0.00000+00	5.00000+06	0.00000+00	1.50000+07	0.00000+00	2024	3	56	1151
0.00000+00	0.00000+00	0.00000+00	0.00000+00	0.00000+00	0.00000+00	2024	3	56	1152
9.42410+04	2.38986+02	0	0	0	0	2024	3	57	1153
2.95000+02	-2.50000+05	0	0	1	452024	2024	3	57	1154
2.50962+05	0.00000+00	2.40000+05	3.40000-03	2.60000+05	1.18000-02	2024	3	57	1155
2.80000+05	2.02000-02	3.00000+05	8.10000-02	3.20000+05	3.24000-02	2024	3	57	1156
3.40000+05	4.19000-02	3.60000+05	4.76000-02	3.80000+05	5.26000-02	2024	3	57	1157
4.00000+05	5.09000-02	4.20000+05	5.04300-02	4.40000+05	6.37000-02	2024	3	57	1158
4.60000+05	6.67000-02	4.80000+05	6.98000-02	5.00000+05	7.24000-02	2024	3	57	1159
5.00000+05	7.85000-02	6.00000+05	8.26000-02	6.50000+05	8.68000-02	2024	3	57	1160
7.00000+05	9.14000-02	7.50000+05	7.39000-02	8.00000+05	9.94000-02	2024	3	57	1161
8.50000+05	1.01900-01	9.00000+05	1.03300-01	9.50000+05	1.04400-01	2024	3	57	1162
1.00000+06	1.06100-01	1.10000+06	1.10000-01	1.20000+06	9.07000-02	2024	3	57	1163
1.40000+06	7.95000-02	1.60000+06	3.38000-02	1.80000+06	4.68000-02	2024	3	57	1164
2.00000+06	3.16000-02	2.20000+06	1.97000-02	2.40000+06	1.18000-02	2024	3	57	1165
2.60000+06	7.00000-03	2.80000+06	4.10000-03	3.00000+06	2.40000-03	2024	3	57	1166
3.20000+06	1.40000-03	3.40000+06	9.00000-04	3.60000+06	6.00000-04	2024	3	57	1167
3.80000+06	4.00000-04	4.00000+06	2.00000-04	4.50000+06	1.00000-04	2024	3	57	1168
5.00000+06	0.00000+00	5.00000+06	0.00000+00	1.50000+07	0.00000+00	2024	3	57	1169
0.00000+00	0.00000+00	0.00000+00	0.00000+00	0.00000+00	0.00000+00	2024	3	57	1170
9.42410+04	2.38986+02	0	0	0	0	2024	3	57	1171
2.95000+02	-2.35000+05	0	0	1	432024	2024	3	58	1172
2.50962+05	0.00000+00	2.40000+05	3.40000-03	2.60000+05	1.18000-02	2024	3	58	1173
2.80000+05	2.02000-02	3.00000+05	8.10000-02	3.20000+05	3.24000-02	2024	3	58	1174
3.40000+05	4.19000-02	3.60000+05	4.76000-02	3.80000+05	5.26000-02	2024	3	58	1175

2,35983+05	0,00000+00	2,40000+05	7,60000-03	2,60000+05	2,61000-02	2024	3	58	1176	
2,80000+05	4,25000-02	3,00000+05	3,77000-02	3,20000+05	7,15000-02	2024	3	58	1177	
3,40000+05	8,50000-02	3,00000+05	7,46000-02	3,80000+05	1,04300-01	2024	3	58	1178	
4,00000+05	1,12400-01	4,20000+05	1,16800-01	4,40000+05	1,24700-01	2024	3	58	1179	
4,60000+05	1,30100-01	4,80000+05	1,55500-01	5,00000+05	1,39700-01	2024	3	58	1180	
5,20000+05	1,48800-01	6,00000+05	1,53200-01	6,50000+05	1,57100-01	2024	3	58	1181	
5,80000+05	1,61100-01	7,50000+05	1,64100-01	8,00000+05	1,65100-01	2024	3	58	1182	
6,40000+05	1,63800-01	9,00000+05	1,60200-01	9,50000+05	1,57600-01	2024	3	58	1183	
7,00000+05	1,40600-01	1,10000+06	1,42200-01	1,20000+06	1,27600-01	2024	3	58	1184	
7,60000+06	1,03500-01	1,60000+06	7,86000-02	1,80000+06	5,56000-02	2024	3	58	1185	
8,20000+06	3,66000-02	2,20000+06	2,25000-02	2,40000+06	1,33000-02	2024	3	58	1186	
8,80000+06	7,80000-03	2,80000+06	4,50000-03	3,00000+06	2,60000-03	2024	3	58	1187	
9,40000+06	1,50000-03	3,40000+06	1,00000-03	3,60000+06	6,00000-04	2024	3	58	1188	
1,00000+07	4,00000-04	4,00000+06	2,00000-04	4,00000+06	0,00000+00	2024	3	58	1189	
0,00000+00	0,00000+00		0		0	2024	3	59	1191	
9,42410+04	2,38986+02		0		0	2024	3	59	1192	
2,93000+02	2,35100+05		0		1	432024	3	59	1193	
	43					2024	3	59	1194	
2,36084+05	0,00000+00	2,60000+05	2,00000-04	2,80000+05	4,00000-04	2024	3	59	1195	
3,00000+05	7,00000-04	3,20000+05	1,10000-03	3,40000+05	1,50000-03	2024	3	59	1196	
3,60000+05	2,00000-03	3,80000+05	2,50000-03	4,00000+05	3,00000-03	2024	3	59	1197	
4,20000+05	3,50000-03	4,40000+05	4,10000-03	4,60000+05	4,60000-03	2024	3	59	1198	
4,80000+05	5,30000-03	5,00000+05	6,00000-03	5,50000+05	7,80000-03	2024	3	59	1199	
6,00000+05	9,70000-03	6,50000+05	1,18000-02	7,00000+05	1,42000-02	2024	3	59	1200	
7,50000+05	1,68000-02	8,00000+05	1,94000-02	8,50000+05	2,20000-02	2024	3	59	1201	
9,00000+05	2,43000-02	9,50000+05	2,67000-02	1,00000+06	2,81000-02	2024	3	59	1202	
1,10000+06	2,73000-02	1,20000+06	2,88000-02	1,40000+06	2,94000-02	2024	3	59	1203	
1,60000+06	2,60000-02	1,80000+06	2,05000-02	2,00000+06	1,45000-02	2024	3	59	1204	
2,20000+06	9,50000-03	2,40000+06	3,80000-03	2,60000+06	3,50000-03	2024	3	59	1205	
2,80000+06	2,10300-03	3,00000+06	1,30000-03	3,20000+06	8,00000-04	2024	3	59	1206	
3,40000+06	5,00000-04	3,60000+06	3,00000-04	3,80000+06	2,00000-04	2024	3	59	1207	
4,00000+06	1,00000-04	4,50000+06	1,00000-04	4,50000+06	0,00000+00	2024	3	59	1208	
1,50000+07	0,00000+00		0		0	2024	3	59	1209	
0,00000+00	0,00000+00		0		0	2024	3	60	1210	
9,42410+04	2,38986+02		0		10	0	3	60	1211	
2,93000+02	2,44000+05		0		0	1	432024	3	60	1212
	43						2024	3	60	1213
2,45020+05	0,00000+00	2,60000+05	1,53000-02	2,80000+05	2,76000-02	2024	3	60	1214	
3,00000+05	4,14000-02	3,20000+05	5,41000-02	3,40000+05	6,55000-02	2024	3	60	1215	
3,60000+05	7,55000-02	3,80000+05	8,44000-02	4,00000+05	9,20000-02	2024	3	60	1216	
4,20000+05	9,81000-02	4,40000+05	1,03800-01	4,60000+05	1,08600-01	2024	3	60	1217	
4,80000+05	1,15600-01	5,00000+05	1,17600-01	5,50000+05	1,26300-01	2024	3	60	1218	
6,00000+05	1,31100-01	6,50000+05	1,35400-01	7,00000+05	1,39900-01	2024	3	60	1219	
7,50000+05	1,43700-01	8,00000+05	1,45800-01	8,50000+05	1,46600-01	2024	3	60	1220	
9,00000+05	1,64300-01	9,50000+05	1,43200-01	1,00000+06	1,37300-01	2024	3	60	1221	
1,10000+06	1,28800-01	1,20000+06	1,17800-01	1,40000+06	9,81000-02	2024	3	60	1222	

1,60000+06	7,63000-02	1,80000+06	5,48000-02	2,00000+06	3,65000-02	2024	3	60	1223	
2,20000+06	2,26000-02	2,40000+06	1,54000-02	2,60000+06	7,90000-03	2024	3	60	1224	
2,80000+06	4,60000-03	3,00000+06	2,70000-03	3,20000+06	1,60000-03	2024	3	60	1225	
3,40000+06	7,00000-04	3,60000+06	6,00000-04	3,80000+06	4,00000-04	2024	3	60	1226	
4,00000+06	2,00000-04	4,50000+06	1,00000-04	4,50000+06	0,00000+00	2024	3	60	1227	
1,50000+07	0,00000+00		0		0	2024	3	60	1228	
0,00000+00	0,00000+00		0		0	2024	3	60	1229	
9,42410+04	2,38986+02		0		0	0	0	61	1230	
2,93000+02	2,96000+05		0		11	0	0	61	1231	
	40				0	1	402024	3	61	1232
	2						2024	3	61	1233
2,97258+05	0,00000+00	3,00000+05	4,00000-04	3,20000+05	2,80000-03	2024	3	61	1234	
3,40000+05	5,50000-03	3,60000+05	8,20000-03	3,80000+05	1,08000-02	2024	3	61	1235	
4,00000+05	1,32000-02	4,20000+05	1,53000-02	4,40000+05	1,73000-02	2024	3	61	1236	
4,60000+05	1,91000-02	4,80000+05	2,10000-02	5,00000+05	2,27000-02	2024	3	61	1237	
5,20000+05	2,68000-02	6,00000+05	3,02000-02	6,50000+05	3,37000-02	2024	3	61	1238	
7,00000+05	3,75000-02	7,50000+05	4,13000-02	8,00000+05	4,49000-02	2024	3	61	1239	
8,50000+05	4,61000-02	9,00000+05	5,08000-02	9,50000+05	5,43000-02	2024	3	61	1240	
1,00000+06	5,41000-02	1,10000+06	5,14000-02	1,20000+06	5,16000-02	2024	3	61	1241	
1,40000+06	4,93000-02	1,60000+06	4,20000-02	1,80000+06	3,22000-02	2024	3	61	1242	
2,00000+06	2,24000-02	2,20000+06	1,42000-02	2,40000+06	8,70000-03	2024	3	61	1243	
2,60000+06	5,20000-03	2,80000+06	3,10000-03	3,00000+06	1,80000-03	2024	3	61	1244	
3,20000+06	1,10000-03	3,40000+06	7,00000-04	3,60000+06	4,00000-04	2024	3	61	1245	
3,80000+06	3,00000-04	4,00000+06	2,00000-04	4,50000+06	1,00000-04	2024	3	61	1246	
4,50000+06	0,00000+00	1,50000+07	0,00000+00			2024	3	61	1247	
0,00000+00	0,00000+00		0		0	0	0	61	1248	
9,42410+04	2,38986+02		0		12	0	0	62	1249	
2,93000+02	3,34000+05		0		0	1	392024	3	62	1250
	39						2024	3	62	1251
3,55983+05	0,00000+00	3,40000+05	1,30000-02	3,60000+05	6,80000-03	2024	3	62	1252	
4,00000+05	1,32000-02	4,00000+05	1,96000-02	4,20000+05	2,55000-02	2024	3	62	1253	
4,40000+05	3,11000-02	4,60000+05	3,61000-02	4,80000+05	4,10000-02	2024	3	62	1254	
5,00000+05	4,53000-02	5,50000+05	5,48000-02	6,00000+05	6,18000-02	2024	3	62	1255	
6,50000+05	6,80000-02	7,50000+05	7,40000-02	7,50000+05	7,94000-02	2024	3	62	1256	
8,00000+05	8,58000-02	8,50000+05	8,70000-02	9,00000+05	8,88000-02	2024	3	62	1257	
9,50000+05	9,08000-02	1,00000+06	8,93000-02	1,10000+06	8,44000-02	2024	3	62	1258	
1,20000+06	8,06000-02	1,40000+06	7,20000-02	1,60000+06	3,88000-02	2024	3	62	1259	
1,80000+06	4,38000-02	2,00000+06	5,00000-02	2,20000+06	1,38000-02	2024	3	62	1260	
2,40000+06	1,14000-02	2,60000+06	6,80000-03	2,80000+06	4,00000-03	2024	3	62	1261	
3,00000+06	2,30000-03	3,20000+06	1,40000-03	3,40000+06	9,00000-04	2024	3	62	1262	
3,60000+06	6,00000-04	3,80000+06	4,00000-04	4,00000+06	2,00000-04	2024	3	62	1263	
4,50000+06	1,00000-04	4,50000+06	3,00000-04	1,50000+07	0,00000+00	2024	3	62	1264	
0,00000+00	0,00000+00		0		0	0	0	63	1265	
9,42410+04	2,38986+02		0		13	0	0	63	1266	
2,93000+02	3,61000+05		0		0	1	362024	3	63	1267
	36						2024	3	63	1268
3,62510+05	0,00000+00	3,80000+05	1,80000-03	4,00000+05	4,10000-03	2024	3	63	1269	
4,20000+05	6,40000-03	4,40000+05	8,80000-03	4,60000+05	1,10000-02	2024	3	63	1270	

4,20000+05	1,32000-02	5,00000+05	1,52000-02	5,50000+05	2,00000+02	2024	3	63	1276
6,00000+03	2,40000-02	6,50000+03	2,70000-02	7,00000+03	3,18000+02	2024	3	63	1271
7,50000+03	3,58000-02	8,00000+03	3,94000-02	8,50000+03	4,26000+02	2024	3	63	1272
9,00000+03	4,53000-02	9,50000+03	4,50000-02	1,00000+06	4,89000+02	2024	3	63	1273
1,10000+06	4,67000-02	1,20000+06	4,72000-02	1,40000+06	4,58000+02	2024	3	63	1274
1,60000+06	3,96000-02	1,80000+06	3,07000-02	2,00000+06	2,16000+02	2024	3	63	1275
2,20000+06	1,38000-02	2,40000+06	8,50000+03	3,60000+06	5,10000+02	2024	3	63	1276
2,80000+06	3,00000-03	3,00000+06	1,80000-03	3,20000+06	1,10000+02	2024	3	63	1277
3,40000+06	7,00000-04	3,60000+06	4,00000-04	3,80000+06	3,00000+02	2024	3	63	1278
4,00000+06	2,00000-04	4,00000+06	0,00000+00	1,50000+07	0,00000+00	2024	3	63	1279
0,00000+00	0,00000+00	0	0	0	0	02024	3	0	1280
9,42410+04	2,38986+02	0	0	14	0	02024	3	64	1281
2,93000+02	4,78000+05	0	0	0	1	352024	3	64	1282
	35	2				2024	3	64	1283
3,79582+05	0,00000+00	4,00000+05	2,00000-04	4,20000+05	5,00000-04	2024	3	64	1284
4,40000+05	9,00000-04	4,60000+05	1,30000-03	4,80000+05	1,80000-03	2024	3	64	1285
5,00000+05	2,40000-03	5,50000+05	3,90000-03	6,00000+05	5,50000+03	2024	3	64	1286
6,50000+05	7,20000-03	7,00000+05	7,00000-03	7,50000+05	1,14000+02	2024	3	64	1287
8,00000+05	1,37000-02	8,50000+05	1,59000-02	9,00000+05	1,79000+02	2024	3	64	1288
9,50000+05	2,01000-02	1,00000+06	2,14000-02	1,10000+06	2,11000+02	2024	3	64	1289
1,20000+06	2,23000-02	1,40000+06	2,44000-02	1,60000+06	2,24000+02	2024	3	64	1290
1,80000+06	1,82000-02	2,00000+06	1,32000-02	2,20000+06	4,60000-03	2024	3	64	1291
2,40000+06	5,40000-03	2,60000+06	5,30000-03	2,80000+06	2,00000-03	2024	3	64	1292
3,00000+06	1,20000-03	3,20000+06	7,00000-04	3,40000+06	5,00000+04	2024	3	64	1293
3,60000+06	3,00000-04	3,80000+06	2,00000-04	4,00000+06	1,00000+04	2024	3	64	1294
4,00000+06	0,00000+00	1,50000+07	0,00000+00	0	0	2024	3	64	1295
0,00000+00	0,00000+00	0	0	0	0	02024	3	0	1296
9,42410+04	2,38986+02	0	0	15	0	02024	3	65	1297
2,93000+02	4,44000+05	0	0	0	1	322024	3	65	1298
	32	2				2024	3	65	1299
4,45858+05	0,00000+00	4,60000+05	8,00000-04	4,80000+05	1,90000-03	2024	3	65	1300
5,00000+05	3,00000-03	5,50000+05	6,10000-03	6,00000+05	8,90000-03	2024	3	65	1301
6,50000+05	1,16000-02	7,00000+05	1,42000-02	7,50000+05	1,67000-02	2024	3	65	1302
8,00000+05	1,89000-02	8,50000+05	2,08000-02	9,00000+05	2,24000-02	2024	3	65	1303
9,50000+05	2,39000-02	1,00000+06	2,45000-02	1,10000+06	2,52000-02	2024	3	65	1304
1,20000+06	2,58000-02	1,40000+06	2,47000-02	1,60000+06	2,09000-02	2024	3	65	1305
1,80000+06	1,60000-02	2,00000+06	1,12000-02	2,20000+06	7,20000-03	2024	3	65	1306
2,40000+06	4,50000-03	2,60000+06	2,80000-03	2,80000+06	1,70000-03	2024	3	65	1307
3,00000+06	1,00000-03	3,20000+06	6,00000-04	3,40000+06	4,00000-04	2024	3	65	1308
3,60000+06	2,00000-04	3,80000+06	1,00000-04	4,00000+06	1,00000-04	2024	3	65	1309
4,00000+06	0,00000+00	1,50000+07	0,00000+00	0	0	2024	3	65	1310
0,00000+00	0,00000+00	0	0	0	0	02024	3	0	1311
9,42410+04	2,38986+02	0	0	16	0	02024	3	66	1312
2,93000+02	4,99000+05	0	0	0	1	292024	3	66	1313
	29	2				2024	3	66	1314
5,01088+05	0,00000+00	5,50000+05	8,00000-04	6,00000+05	2,10000-03	2024	3	66	1315
6,50000+05	3,70000-03	7,00000+05	5,50000-03	7,50000+05	7,50000-03	2024	3	66	1316

8,00000+05	9,50000-03	8,50000+05	1,15000-02	9,00000+05	1,34000-02	2024	3	66	1317
9,50000+05	1,53000-02	1,00000+06	1,67000-02	1,10000+06	1,67000-02	2024	3	66	1318
1,20000+06	1,84000-02	1,40000+06	2,04000-02	1,60000+06	1,94000-02	2024	3	66	1319
1,80000+06	1,62000-02	2,00000+06	1,21000-02	2,20000+06	8,00000-03	2024	3	66	1320
2,40000+06	5,10000-03	2,60000+06	5,20000-03	2,80000+06	1,90000-03	2024	3	66	1321
3,00000+06	1,20000-03	3,20000+06	7,00000-04	3,40000+06	5,00000-04	2024	3	66	1322
3,60000+06	3,00000-04	3,80000+06	2,00000-04	4,00000+06	1,00000-04	2024	3	66	1323
4,00000+06	0,00000+00	1,50000+07	0,00000+00	0	0	2024	3	66	1324
0,00000+00	0,00000+00	0	0	0	0	02024	3	0	1325
9,42410+04	2,38986+02	0	0	17	0	02024	3	67	1326
2,93000+02	5,68000+05	0	0	0	1	242024	3	67	1327
	24	2				2024	3	67	1328
5,70377+05	0,00000+00	7,00000+05	1,00000-04	7,50000+05	3,00000-04	2024	3	67	1329
8,00000+05	4,00000-04	8,50000+05	7,00000-04	9,00000+05	1,00000-03	2024	3	67	1330
9,50000+05	1,20000-03	1,00000+06	1,50000-03	1,10000+06	1,90000-03	2024	3	67	1331
1,20000+06	2,40000-03	1,40000+06	5,30000-03	1,60000+06	3,50000-03	2024	3	67	1332
1,80000+06	3,20000-03	2,00000+06	2,60000-03	2,20000+06	1,80000-03	2024	3	67	1333
2,40000+06	1,50000-03	2,60000+06	8,00000-04	2,80000+06	6,00000-04	2024	3	67	1334
3,00000+06	4,00000-04	3,20000+06	2,00000-04	3,40000+06	1,00000-04	2024	3	67	1335
3,60000+06	0,00000+00	3,80000+06	0,00000+00	4,00000+06	0,00000+00	2024	3	67	1336
4,00000+06	0,00000+00	0	0	0	0	02024	3	0	1337
9,42410+04	2,38986+02	0	0	18	0	02024	3	68	1338
2,93000+02	7,53000+05	0	0	0	1	242024	3	68	1339
	24	2				2024	3	68	1340
7,56151+05	0,00000+00	8,00000+05	5,20000-03	8,50000+05	1,16000-02	2024	3	68	1341
9,00000+05	1,70000-02	9,50000+05	2,14000-02	1,00000+06	2,40000-02	2024	3	68	1342
1,10000+06	2,66000-02	1,20000+06	2,88000-02	1,40000+06	2,66000-02	2024	3	68	1343
1,60000+06	2,21000-02	1,80000+06	1,68000-02	2,00000+06	1,18000-02	2024	3	68	1344
2,20000+06	7,70000-03	2,40000+06	4,80000-03	2,60000+06	2,90000-03	2024	3	68	1345
2,80000+06	1,70000-03	3,00000+06	1,60000-03	3,20000+06	6,00000-04	2024	3	68	1346
3,40000+06	4,00000-04	3,60000+06	2,00000-04	3,80000+06	1,00000-04	2024	3	68	1347
4,00000+06	1,00000-04	4,00000+06	0,00000+00	1,50000+07	0,00000+00	2024	3	68	1348
0,00000+00	0,00000+00	0	0	0	0	02024	3	0	1349
9,42410+04	2,38986+02	0	0	19	0	02024	3	69	1350
2,93000+02	8,09000+05	0	0	0	1	232024	3	69	1351
	23	2				2024	3	69	1352
8,12385+05	0,00000+00	8,50000+05	8,20000-03	9,00000+05	1,94000-02	2024	3	69	1353
9,50000+05	2,93000-02	1,00000+06	3,61000-02	1,10000+06	4,65000-02	2024	3	68	1354
1,20000+06	4,85000-02	1,40000+06	4,59000-02	1,60000+06	3,81000-02	2024	3	69	1355
1,80000+06	2,89000-02	2,00000+06	2,04000-02	2,20000+06	1,36000-02	2024	3	69	1356
2,40000+06	8,30000-03	2,60000+06	5,10000-03	2,80000+06	3,00000-03	2024	3	69	1357
3,00000+06	1,80000-03	3,20000+06	1,10000-03	3,40000+06	7,00000-04	2024	3	69	1358
3,60000+06	3,00000-04	3,80000+06	1,00000-04	4,00000+06	1,00000-04	2024	3	69	1359
4,00000+06	0,00000+00	1,50000+07	0,00000+00	0	0	2024	3	69	1360
0,00000+00	0,00000+00	0	0	0	0	02024	3	0	1361
9,42410+04	2,38986+02	0	0	20	0	02024	3	70	1362
2,93000+02	8,35000+05	0	0	0	1	242024	3	70	1363

8,38494+05	24	0,00000+00	2	8,50000+05	3,50000-03	9,00000+05	1,73000-02	2024	3	70	1364
9,50000+05	3,80000-02	1,00000+06	4,00000-02	1,00000+06	4,00000-02	1,10000+06	2,45000-02	2024	3	70	1365
1,20000+06	3,84000-02	1,40000+06	2,51000-02	1,40000+06	2,51000-02	1,60000+06	4,67000-02	2024	3	70	1366
1,80000+06	3,55000-02	2,00000+06	2,51000-02	2,00000+06	2,51000-02	2,20000+06	1,65000-02	2024	3	70	1367
2,40000+06	1,03000-02	2,60000+06	6,30000-03	2,60000+06	6,30000-03	2,80000+06	3,80000-03	2024	3	70	1368
3,00000+06	2,30000-03	3,20000+06	1,40000-04	3,20000+06	1,40000-04	3,40000+06	9,00000-04	2024	3	70	1369
3,60000+06	4,00000-04	3,80000+06	3,00000-04	3,80000+06	3,00000-04	4,00000+06	2,00000-04	2024	3	70	1370
4,20000+06	1,00000-04	4,50000+06	0,00000+00	4,50000+06	0,00000+00	5,00000+07	0,00000+00	2024	3	70	1371
0,00000+00	0,00000+00	0	0	0	0	0	0	2024	3	0	1372
9,42410+04	2,38986+02	0	21	0	0	0	0	02024	3	71	1373
2,93000+02	-8,75000+05	0	0	0	0	1	0	232024	3	71	1374
								2024	3	71	1375
								2024	3	71	1376
8,78615+05	0,00000+00	9,00000+05	4,70000-03	9,50000+05	1,66000-02	9,50000+05	1,66000-02	2024	3	71	1377
1,00000+06	2,72000-02	1,10000+06	4,15000-02	1,20000+06	4,79000-02	1,20000+06	4,79000-02	2024	3	71	1378
1,40000+06	4,93000-02	1,60000+06	4,25000-02	1,60000+06	3,32000-02	1,60000+06	3,32000-02	2024	3	71	1379
2,00000+06	2,40000-02	2,20000+06	1,60000-02	2,40000+06	1,01000-02	2,40000+06	1,01000-02	2024	3	71	1380
2,60000+06	6,20000-03	2,80000+06	3,20000-03	3,00000+06	2,30000-03	3,00000+06	2,30000-03	2024	3	71	1381
3,20000+06	1,40000-03	3,40000+06	9,00000-04	3,60000+06	5,00000-04	3,60000+06	5,00000-04	2024	3	71	1382
3,80000+06	3,00000-04	4,00000+06	2,00000-04	4,20000+06	1,00000-04	4,20000+06	1,00000-04	2024	3	71	1383
4,40000+06	0,00000+00	4,50000+07	0,00000+00	4,50000+07	0,00000+00	0	0	2024	3	71	1384
0,00000+00	0,00000+00	0	0	0	0	0	0	02024	3	0	1385
9,42410+04	2,38986+02	0	22	0	0	0	0	02024	3	72	1386
2,93000+02	-9,31000+05	0	0	0	0	1	0	222024	3	72	1387
								2024	3	72	1388
9,34896+05	0,00000+00	9,50000+05	1,80000-03	1,00000+06	9,00000-03	9,00000+05	3,37000-02	2024	3	72	1389
1,10000+06	2,10000-02	1,20000+06	2,85000-02	1,40000+06	3,37000-02	1,40000+06	3,37000-02	2024	3	72	1390
1,60000+06	3,12000-02	1,80000+06	2,55000-02	2,00000+06	1,91000-02	2,00000+06	1,91000-02	2024	3	72	1391
2,20000+06	1,30000-02	2,40000+06	3,40000-03	2,60000+06	5,30000-03	2,60000+06	5,30000-03	2024	3	72	1392
2,80000+06	3,30000-03	3,00000+06	2,00000-03	3,20000+06	1,20000-03	3,20000+06	1,20000-03	2024	3	72	1393
3,40000+06	8,00000-04	3,60000+06	4,00000-04	3,80000+06	5,00000-04	3,80000+06	5,00000-04	2024	3	72	1394
4,00000+06	2,00000-04	4,20000+06	1,00000-04	4,40000+06	0,00000-04	4,40000+06	0,00000-04	2024	3	72	1395
1,50000+07	0,00000+00	0	0	0	0	0	0	2024	3	72	1396
0,00000+00	0,00000+00	0	0	0	0	0	0	02024	3	0	1397
9,42410+04	2,38986+02	0	23	0	0	0	0	02024	3	73	1398
2,93000+02	-9,07000+05	0	0	0	0	1	0	202024	3	73	1399
								2024	3	73	1400
9,71046+05	0,00000+00	1,00000+06	2,20000-03	1,10000+06	7,90000-03	7,90000+05	0,00000-04	2024	3	73	1401
1,20000+06	1,08000-02	1,40000+06	1,24000-02	1,60000+06	1,10000-02	1,60000+06	1,10000-02	2024	3	73	1402
1,80000+06	8,60000-03	2,00000+06	6,10000-03	2,20000+06	4,10000-03	2,20000+06	4,10000-03	2024	3	73	1403
2,40000+06	2,60000-03	2,60000+06	1,60000-03	2,80000+06	1,00000-03	2,80000+06	1,00000-03	2024	3	73	1404
3,00000+06	6,00000-04	3,20000+06	4,00000-04	3,40000+06	2,00000-04	3,40000+06	2,00000-04	2024	3	73	1405
3,60000+06	1,00000-04	3,80000+06	1,00000-04	4,00000+06	1,00000-04	4,00000+06	1,00000-04	2024	3	73	1406
4,20000+06	0,00000+00	4,00000+07	0,00000+00	0	0	0	0	2024	3	73	1407
0,00000+00	0,00000+00	0	0	0	0	0	0	02024	3	0	1408
9,42410+04	2,38986+02	0	24	0	0	0	0	02024	3	74	1409
2,93000+02	-9,94000+05	0	0	0	0	1	0	202024	3	74	1410

9,98139+05	25	0,00000+00	2	1,00000+06	1,00000-04	1,10000+06	6,30000-03	2024	3	74	1411
1,20000+06	1,79000-02	1,40000+06	1,76000-02	1,60000+06	1,81100-02	1,60000+06	1,81100-02	2024	3	74	1412
1,80000+06	1,55000-02	2,00000+06	1,25000-02	2,20000+06	8,80000-03	2,20000+06	8,80000-03	2024	3	74	1413
2,40000+06	3,90000-03	2,60000+06	3,80000-03	2,80000+06	2,40000-03	2,80000+06	2,40000-03	2024	3	74	1414
3,00000+06	1,50000-03	3,20000+06	9,00000-04	3,40000+06	6,00000-04	3,40000+06	6,00000-04	2024	3	74	1415
3,60000+06	3,00000-04	3,80000+06	2,00000-04	4,00000+06	1,00000-04	4,00000+06	1,00000-04	2024	3	74	1416
4,20000+06	0,00000+00	4,00000+07	0,00000+00	0	0	0	0	2024	3	74	1417
0,00000+00	0,00000+00	0	0	0	0	0	0	02024	3	0	1418
9,42410+04	2,38986+02	0	25	0	0	0	0	02024	3	75	1419
2,93000+02	-1,00900+06	0	0	0	0	1	0	192024	3	75	1420
								2024	3	75	1421
								2024	3	75	1422
1,01322+06	0,00000+00	1,10000+06	1,14000-02	1,20000+06	1,84000-02	1,20000+06	1,84000-02	2024	3	75	1423
1,40000+06	2,24000-02	1,60000+06	1,99000-02	1,80000+06	1,54000-02	1,80000+06	1,54000-02	2024	3	75	1424
2,00000+06	1,09000-02	2,20000+06	1,20000-02	2,40000+06	4,50000-03	2,40000+06	4,50000-03	2024	3	75	1425
2,60000+06	2,80000-03	2,80000+06	1,70000-03	3,00000+06	1,00000-03	3,00000+06	1,00000-03	2024	3	75	1426
3,20000+06	6,00000-04	3,40000+06	1,00000-04	3,60000+06	2,00000-04	3,60000+06	2,00000-04	2024	3	75	1427
3,80000+06	1,00000-04	4,00000+06	1,00000-04	4,20000+06	0,00000-04	4,20000+06	0,00000-04	2024	3	75	1428
4,40000+06	0,00000+00	0	0	0	0	0	0	2024	3	75	1429
0,00000+00	0,00000+00	0	0	0	0	0	0	02024	3	0	1430
9,42410+04	2,38986+02	0	26	0	0	0	0	02024	3	76	1431
2,93000+02	-1,60700+06	0	0	0	0	1	0	192024	3	76	1432
								2024	3	76	1433
1,01322+06	0,00000+00	1,10000+06	1,42000-02	1,20000+06	2,28000-02	1,20000+06	2,28000-02	2024	3	76	1434
1,40000+06	2,77000-02	1,60000+06	2,95000-02	1,80000+06	1,90000-02	1,80000+06	1,90000-02	2024	3	76	1435
2,00000+06	1,54000-02	2,20000+06	4,80000-03	2,40000+06	5,60000-03	2,40000+06	5,60000-03	2024	3	76	1436
2,60000+06	3,50000-03	2,80000+06	2,10000-03	3,00000+06	1,50000-03	3,00000+06	1,50000-03	2024	3	76	1437
3,20000+06	8,00000-04	3,40000+06	3,60000-04	3,60000+06	3,00000-04	3,60000+06	3,00000-04	2024	3	76	1438
3,80000+06	2,00000-04	4,00000+06	1,00000-04	4,20000+06	0,00000-04	4,20000+06	0,00000-04	2024	3	76	1439
4,40000+06	0,00000+00	0	0	0	0	0	0	2024	3	76	1440
0,00000+00	0,00000+00	0	0	0	0	0	0	02024	3	0	1441
9,42410+04	2,38986+02	0	27	0	0	0	0	02024	3	91	1442
2,93000+02	-1,60700+06	0	0	0	0	1	0	392024	3	91	1443
								2024	3	91	1444
1,01423+06	0,00000+00	1,10000+06	1,36000-02	1,20000+06	7,53000-02	1,20000+06	7,53000-02	2024	3	91	1445
1,40000+06	3,21800-02	1,60000+06	0,00000-02	1,80000+06	1,03710-02	1,80000+06	1,03710-02	2024	3	91	1446
2,00000+06	1,36700-02	2,20000+06	1,54330-02	2,40000+06	1,73910+00	2,40000+06	1,73910+00	2024	3	91	1447
2,60000+06	1,85040-03	2,80000+06	1,85510+02	3,00000+06	1,96230+00	3,00000+06	1,96230+00	2024	3	91	1448
3,20000+06	1,91900+00	3,40000+06	1,92900+00	3,60000+06	1,93650+00	3,60000+06	1,93650+00	2024	3	91	1449
3,80000+06	1,94480+00	4,00000+06	1,85000+00	4,20000+06	1,93610+00	4,20000+06	1,93610+00	2024	3	91	1450
4,40000+06	1,90560+00	5,00000+06	1,85970+00	6,00000+06	9,73860-01	6,00000+06	9,73860-01	2024	3	91	1451
6,00000+06	2,75800-01	7,00000+06	1,59900+00	7,80000+06	2,78000-01	7,80000+06	2,78000-01	2024	3	91	1452
8,00000+06	6,27700-01	8,50000+06	1,35150-01	9,00000+06	1,71300-01	9,00000+06	1,71300-01	2024	3	91	1453
9,50000+06	1,52000-01	1,00000+07	1,35000-01	1,00000+07	1,20500-01	1,00000+07	1,20500-01	2024	3	91	1454
1,00000+07	1,09500-01	1,10000+07	1,01000-01	1,20000+07	9,20000-02	1,20000+07	9,20000-02	2024	3	91	1455
1,20000+07	8,59000-02	1,30000+07	4,00000-02	1,35000+07	7,00000-02	1,35000+07	7,000				

0.00000+00						2024	4	2	1552
0.00000+00	1.00000+02	0	0	1		02024	4	2	1553
0.00000+00						2024	4	2	1554
0.00000+00	1.00000+04	0	0	1		02024	4	2	1555
0.00000+00						2024	4	2	1556
0.00000+00	1.00000+05	0	0	3		02024	4	2	1557
2.60000-01	2.50000-02	8.00000-03	0	0		2024	4	2	1558
0.00000+00	2.00000+05	0	0	3		02024	4	2	1559
5.12000-01	1.50000-01	5.00000-02	0	0		2024	4	2	1560
0.00000+00	4.00000+05	0	0	3		02024	4	2	1561
8.89666-01	5.39000-01	1.35000-01	0	0		2024	4	2	1562
0.00000+00	6.00000+05	0	0	3		02024	4	2	1563
1.13680+00	8.16000-01	3.29400-01	1.96000-02	3.60000-03		2024	4	2	1564
0.00000+00	8.00000+05	0	0	3		02024	4	2	1565
1.23366+00	1.04166+00	6.66333-01	1.35666+00	2.16000-02		2024	4	2	1566
0.00000+00	1.00000+06	0	0	3		02024	4	2	1567
1.26700+00	1.13800+00	9.28000+01	3.44500+00	8.02500-02		2024	4	2	1568
0.00000+00	1.20000+06	0	0	3		02024	4	2	1569
1.26050+00	1.22400+00	1.20833+00	4.98000-01	1.14833+00		2024	4	2	1570
0.00000+00	1.50000+06	0	0	3		02024	4	2	1571
1.43551+00	1.42568+00	1.81355+00	1.24092+00	3.01875+00		2024	4	2	1572
0.00000+00	2.00000+06	0	0	3		02024	4	2	1573
1.65473+00	1.88430+00	2.14014+00	1.75970+00	7.92190+00	2.05810+00	2024	4	2	1574
2.49893-02						2024	4	2	1575
0.00000+00	2.50000+06	0	0	7		2024	4	2	1576
2.06542+00	1.37378+00	2.66760+00	2.53669+00	1.54761+00	6.25445+00	2024	4	2	1577
1.51270-01						2024	4	2	1578
0.00000+00	3.00000+06	0	0	7		02024	4	2	1579
2.15564+00	1.52554+00	2.63068+00	2.47013+00	1.64888+00	7.01629+00	2024	4	2	1580
1.58808-01						2024	4	2	1581
0.00000+00	3.50000+06	0	0	8		02024	4	2	1582
2.27612+00	2.78041+00	2.78041+00	2.63321+00	1.81817+00	8.17736-01	2024	4	2	1583
2.45350-01	1.63554-02					2024	4	2	1584
0.00000+00	4.00000+06	0	0	9		02024	4	2	1585
2.36466+00	3.10190+00	3.30208+00	3.06929+00	2.17397+00	1.10586+00	2024	4	2	1586
2.67677-01	1.74838+01	4.37942-02				2024	4	2	1587
0.00000+00	4.50000+06	0	0	9		02024	4	2	1588
2.41811+00	3.30702+00	3.67784+00	3.65387+00	2.92070+00	1.92114+00	2024	4	2	1589
1.13843+00	5.34677-01	1.48148-01				2024	4	2	1590
0.00000+00	5.00000+06	0	0	10		02024	4	2	1591
2.43879+00	3.35953+00	3.83623+00	3.81028+00	3.23832+00	2.18860+00	2024	4	2	1592
1.37552+00	8.22324-01	3.57887-01	1.59573-02			2024	4	2	1593
0.00000+00	5.50000+06	0	0	10		02024	4	2	1594
2.46041+00	3.40941+00	3.90546+00	3.85272+00	3.30181+00	2.25840+00	2024	4	2	1595
1.44088+00	9.09809-01	4.53954-01	1.33101-01			2024	4	2	1596
0.00000+00	6.00000+06	0	0	11		02024	4	2	1597
2.45770+00	3.33344+00	3.92315+00	4.07032+00	3.83620+00	3.22626+00	2024	4	2	1598

2.23606+00	1.19986+00	4.91445-01	1.46473-01	2.51939-02		2024	4	2	1599
0.00000+00	7.00000+06	0	0	11		02024	4	2	1600
2.50644+00	3.40347+00	4.01825+00	4.32026+00	4.18554+00	3.75438+00	2024	4	2	1601
2.96818+00	1.90507+00	9.36878-01	3.27628-01	6.44719-02		2024	4	2	1602
0.00000+00	8.00000+06	0	0	12		02024	4	2	1603
2.53776+00	3.19022+00	4.14532+00	4.57453+00	4.58356+00	4.24161+00	2024	4	2	1604
3.64355+00	2.71708+00	1.64558+00	7.73154-01	2.63580-01	5.30664+00	2024	4	2	1605
0.00000+00	9.00000+06	0	0	12		02024	4	2	1606
2.55243+00	3.33897+00	4.14756+00	4.60111+00	4.76123+00	4.52515+00	2024	4	2	1607
4.01418+00	3.26642+00	2.24364+00	1.20067+00	4.69306-01	1.07280-01	2024	4	2	1608
0.00000+00	1.00000+07	0	0	13		02024	4	2	1609
2.56577+00	3.62660+00	4.30718+00	4.76887+00	4.05423+00	4.92207+00	2024	4	2	1610
4.43557+00	3.86244+00	2.97144+00	1.90444+00	9.58659-01	3.53602-01	2024	4	2	1611
7.58791-02						2024	4	2	1612
0.00000+00	1.10000+07	0	0	13		02024	4	2	1613
2.44764+00	3.24082+00	3.62270+00	3.83192+00	4.08741+00	4.27055+00	2024	4	2	1614
4.35976+00	4.34661+00	3.95698+00	3.00339+00	1.76799+00	7.45763-01	2024	4	2	1615
1.75203-01						2024	4	2	1616
0.00000+00	1.20000+07	0	0	13		02024	4	2	1617
2.41204+00	3.70463+00	3.41807+00	3.54583+00	3.57876+00	3.98413+00	2024	4	2	1618
4.09641+00	4.17017+00	4.01970+00	3.32418+00	2.15745+00	9.89709-01	2024	4	2	1619
2.40416-01						2024	4	2	1620
0.00000+00	1.30000+07	0	0	14		02024	4	2	1621
2.43632+00	3.28883+00	3.70787+00	3.90052+00	4.09287+00	4.55125+00	2024	4	2	1622
4.49294+00	3.55120+00	4.49429+00	3.03758+00	3.05701+00	1.82091+00	2024	4	2	1623
7.71266-01	1.77303-01					2024	4	2	1624
0.00000+00	1.40000+07	0	0	14		02024	4	2	1625
2.45642+00	3.19170+00	3.52174+00	3.16224+00	3.30998+00	4.06280+00	2024	4	2	1626
4.25237+00	4.32520+00	4.35621+00	4.10480+00	3.34766+00	2.18260+00	2024	4	2	1627
1.01480+00	2.61940-01					2024	4	2	1628
0.00000+00	1.50000+07	0	0	14		02024	4	2	1629
2.36575+00	2.99019+00	3.14525+00	3.22802+00	2.23723+00	3.41344+00	2024	4	2	1630
3.67391+00	4.78443+00	3.89151+00	3.84902+00	3.38668+00	2.41270+00	2024	4	2	1631
1.23253+00	3.58406-01					2024	4	2	1632
0.00000+00	0.00000+00	0	0	0		02024	4	0	1633
9.42410+04	2.38986+02	0	0	0		02024	4	16	1634
0.00000+00	2.38986+02	1	2	0		02024	4	16	1635
0.00000+00	0.00000+00	0	0	0		02024	4	0	1636
9.42410+04	2.38986+02	0	0	0		02024	4	17	1637
0.00000+00	2.38986+02	1	2	0		02024	4	17	1638
0.00000+00	0.00000+00	0	0	0		02024	4	0	1639
9.42410+04	2.38986+02	0	0	0		02024	4	18	1640
0.00000+00	2.38986+02	1	2	0		02024	4	18	1641
0.00000+00	0.00000+00	0	0	0		02024	4	0	1642
9.42410+04	2.38986+02	0	2	0		02024	4	51	1643
0.00000+00	2.38986+02	0	2	0		02024	4	51	1644
0.00000+00	0.00000+00	0	0	1		672024	4	51	1645

8,66,000+01	5,16000+01	9,39700+01	5,18000+01	9,84800+01	5,20000+01	2024	4	51	1834
1,00000+00	5,21000+01					2024	4	51	1835
0,00000+00	6,50000+05	0	0	1		192024	4	51	1836
	19					2024	4	51	1837
-1,00000+00	4,53000+01	-9,84800+01	4,53000+01	-9,39700+01	4,53000+01	2024	4	51	1838
-8,66000+01	4,54000+01	-7,66000+01	4,58000+01	-6,42800+01	4,66000+01	2024	4	51	1839
-5,00000+01	4,75000+01	-3,42000+01	4,85000+01	-1,73600+01	4,93000+01	2024	4	51	1840
0,00000+00	4,99000+01	1,73600+01	5,02000+01	3,42000+01	5,05000+01	2024	4	51	1841
5,00000+01	5,08000+01	6,42800+01	5,10000+01	7,66000+01	5,14000+01	2024	4	51	1842
8,66000+01	5,18000+01	9,39700+01	5,21000+01	9,84800+01	5,24000+01	2024	4	51	1843
1,00000+00	5,25000+01					2024	4	51	1844
0,00000+00	7,00000+05	0	0	1		192024	4	51	1845
	19					2024	4	51	1846
-1,00000+00	4,49000+01	-9,84800+01	4,48000+01	-9,39700+01	4,47000+01	2024	4	51	1847
-8,66000+01	4,49000+01	-7,66000+01	4,53000+01	-6,42800+01	4,62000+01	2024	4	51	1848
-5,00000+01	4,72000+01	-3,42000+01	4,84000+01	-1,73600+01	4,92000+01	2024	4	51	1849
0,00000+00	4,98000+01	1,73600+01	5,01000+01	3,42000+01	5,04000+01	2024	4	51	1850
5,00000+01	5,07000+01	6,42800+01	5,10000+01	7,66000+01	5,15000+01	2024	4	51	1851
8,66000+01	5,20000+01	9,39700+01	5,25000+01	9,84800+01	5,28000+01	2024	4	51	1852
1,00000+00	5,29000+01					2024	4	51	1853
0,00000+00	7,50000+05	0	0	1		192024	4	51	1854
	19					2024	4	51	1855
-1,00000+00	4,44000+01	-9,84800+01	4,44000+01	-9,39700+01	4,43000+01	2024	4	51	1856
-8,66000+01	4,44000+01	-7,66000+01	4,56000+01	-6,42800+01	4,60000+01	2024	4	51	1857
-5,00000+01	4,72000+01	-3,42000+01	4,84000+01	-1,73600+01	4,93000+01	2024	4	51	1858
0,00000+00	4,98000+01	1,73600+01	5,01000+01	3,42000+01	5,02000+01	2024	4	51	1859
5,00000+01	5,03000+01	6,42800+01	5,07000+01	7,66000+01	5,09000+01	2024	4	51	1860
8,66000+01	5,16000+01	9,39700+01	5,25000+01	9,84800+01	5,21000+01	2024	4	51	1861
1,00000+00	5,28000+01					2024	4	51	1862
0,00000+00	8,00000+05	0	0	1		192024	4	51	1863
	19					2024	4	51	1864
-1,00000+00	4,44000+01	-9,84800+01	4,32000+01	-9,39700+01	4,40000+01	2024	4	51	1865
-8,66000+01	4,41000+01	-7,66000+01	4,48000+01	-6,42800+01	4,59000+01	2024	4	51	1866
-5,00000+01	4,73000+01	-3,42000+01	4,85000+01	-1,73600+01	4,96000+01	2024	4	51	1867
0,00000+00	5,00000+01	1,73600+01	5,01000+01	3,42000+01	5,00000+01	2024	4	51	1868
5,00000+01	4,97000+01	6,42800+01	5,00000+01	7,66000+01	5,00000+01	2024	4	51	1869
8,66000+01	5,06000+01	9,39700+01	5,08000+01	9,84800+01	5,12000+01	2024	4	51	1870
1,00000+00	5,19000+01					2024	4	51	1871
0,00000+00	8,50000+05	0	0	1		192024	4	51	1872
	19					2024	4	51	1873
-1,00000+00	4,33000+01	-9,84800+01	4,33000+01	-9,39700+01	4,34000+01	2024	4	51	1874
-8,66000+01	4,36000+01	-7,66000+01	4,44000+01	-6,42800+01	4,58000+01	2024	4	51	1875
-5,00000+01	4,74000+01	-3,42000+01	4,88000+01	-1,73600+01	5,00000+01	2024	4	51	1876
0,00000+00	5,02000+01	1,73600+01	5,01000+01	3,42000+01	4,98000+01	2024	4	51	1877
5,00000+01	4,92000+01	6,42800+01	4,90000+01	7,66000+01	4,89000+01	2024	4	51	1878
8,66000+01	4,95000+01	9,39700+01	5,09000+01	9,84800+01	5,07000+01	2024	4	51	1879
1,00000+00	5,08000+01					2024	4	51	1880
0,00000+00	9,00000+05	0	0	1		192024	4	51	1881
	19					2024	4	51	1882
-1,00000+00	4,25000+01	-9,84800+01	4,26000+01	-9,39700+01	4,27000+01	2024	4	51	1883
-8,66000+01	4,30000+01	-7,66000+01	4,40000+01	-6,42800+01	4,57000+01	2024	4	51	1884
-5,00000+01	4,76000+01	-3,42000+01	4,91000+01	-1,73600+01	5,04000+01	2024	4	51	1885
0,00000+00	5,06000+01	1,73600+01	5,01000+01	3,42000+01	4,95000+01	2024	4	51	1886
5,00000+01	4,87000+01	6,42800+01	4,83000+01	7,66000+01	4,90000+01	2024	4	51	1887
8,66000+01	4,96000+01	9,39700+01	4,94000+01	9,84800+01	4,96000+01	2024	4	51	1888
1,00000+00	5,00000+01					2024	4	51	1889
0,00000+00	9,50000+05	0	0	1		192024	4	51	1890
	19					2024	4	51	1891
-1,00000+00	4,17000+01	-9,84800+01	4,17000+01	-9,39700+01	4,18000+01	2024	4	51	1892
-8,66000+01	4,23000+01	-7,66000+01	4,36000+01	-6,42800+01	4,56000+01	2024	4	51	1893
-5,00000+01	4,78000+01	-3,42000+01	4,97000+01	-1,73600+01	5,08000+01	2024	4	51	1894
0,00000+00	5,08000+01	1,73600+01	5,01000+01	3,42000+01	4,92000+01	2024	4	51	1895
5,00000+01	4,81000+01	6,42800+01	4,75000+01	7,66000+01	4,73000+01	2024	4	51	1896
8,66000+01	4,78000+01	9,39700+01	4,87000+01	9,84800+01	4,92000+01	2024	4	51	1897
1,00000+00	4,96000+01					2024	4	51	1898
0,00000+00	1,00000+06	0	0	1		192024	4	51	1899
	19					2024	4	51	1900
-1,00000+00	4,08000+01	-9,84800+01	4,09000+01	-9,39700+01	4,09000+01	2024	4	51	1901
-8,66000+01	4,16000+01	-7,66000+01	4,32000+01	-6,42800+01	4,54000+01	2024	4	51	1902
-5,00000+01	4,79000+01	-3,42000+01	4,99000+01	-1,73600+01	5,10000+01	2024	4	51	1903
0,00000+00	5,10000+01	1,73600+01	5,01000+01	3,42000+01	4,89000+01	2024	4	51	1904
5,00000+01	4,77000+01	6,42800+01	4,69000+01	7,66000+01	4,68000+01	2024	4	51	1905
8,66000+01	4,73000+01	9,39700+01	4,82000+01	9,84800+01	4,90000+01	2024	4	51	1906
1,00000+00	4,93000+01					2024	4	51	1907
0,00000+00	1,10000+06	0	0	1		192024	4	51	1908
	19					2024	4	51	1909
-1,00000+00	3,98000+01	-9,84800+01	3,99000+01	-9,39700+01	3,99000+01	2024	4	51	1910
-8,66000+01	4,07000+01	-7,66000+01	4,26000+01	-6,42800+01	4,52000+01	2024	4	51	1911
-5,00000+01	4,79000+01	-3,42000+01	5,00000+01	-1,73600+01	5,10000+01	2024	4	51	1912
0,00000+00	5,10000+01	1,73600+01	5,00000+01	3,42000+01	4,83000+01	2024	4	51	1913
5,00000+01	4,10000+01	6,42800+01	4,66000+01	7,66000+01	4,66000+01	2024	4	51	1914
8,66000+01	4,75000+01	9,39700+01	4,84000+01	9,84800+01	4,93000+01	2024	4	51	1915
1,00000+00	4,98000+01					2024	4	51	1916
0,00000+00	1,20000+06	0	0	1		192024	4	51	1917
	19					2024	4	51	1918
-1,00000+00	3,88000+01	-9,84800+01	3,89000+01	-9,39700+01	3,88000+01	2024	4	51	1919
-8,66000+01	3,97000+01	-7,66000+01	4,20000+01	-6,42800+01	4,49000+01	2024	4	51	1920
-5,00000+01	4,78000+01	-3,42000+01	5,01000+01	-1,73600+01	5,08000+01	2024	4	51	1921
0,00000+00	5,08000+01	1,73600+01	4,98000+01	3,42000+01	4,78000+01	2024	4	51	1922
5,00000+01	4,67000+01	6,42800+01	4,63000+01	7,66000+01	4,67000+01	2024	4	51	1923
8,66000+01	4,78000+01	9,39700+01	4,92000+01	9,84800+01	5,06000+01	2024	4	51	1924
1,00000+00	5,18000+01					2024	4	51	1925
0,00000+00	1,40000+06	0	0	1		192024	4	51	1926
	19					2024	4	51	1927

-1,00000+00	3,74000+01	9,84800-01	3,72000-01	9,39700-01	3,68000-01	2024	4	51	1928
-8,66000-01	3,79000-01	7,66000-01	4,07000-01	6,42800-01	4,42000-01	2024	4	51	1929
-5,00000-01	4,74000-01	3,42000-01	4,98000-01	1,73600-01	5,02000-01	2024	4	51	1930
0,00000+00	5,00000+01	1,73600-01	4,88000-01	3,42000-01	4,68000-01	2024	4	51	1931
5,00000+01	4,58000-01	6,42800-01	4,59000-01	7,66000-01	4,74000-01	2024	4	51	1932
8,66000-01	4,94000-01	9,39700-01	5,26000-01	9,84800-01	5,52000-01	2024	4	51	1933
1,00000+00	5,73000-01					2024	4	51	1934
0,00000+00	1,60000+06	0	0	1		192024	4	51	1935
	19	2				2024	4	51	1936
-1,00000+00	3,59000-01	9,84800-01	5,54000-01	9,39700-01	3,45000-01	2024	4	51	1937
-8,66000-01	3,57000-01	7,66000-01	3,92000-01	6,42800-01	4,34000-01	2024	4	51	1938
-5,00000-01	4,69000-01	3,42000-01	4,94000-01	1,73600-01	4,93000-01	2024	4	51	1939
0,00000+00	4,88000+01	1,73600-01	4,76000-01	3,42000-01	4,56000-01	2024	4	51	1940
5,00000+01	4,49000-01	6,42800-01	4,56000-01	7,66000-01	4,86000-01	2024	4	51	1941
8,66000-01	5,24000-01	9,39700-01	5,80000-01	9,84800-01	6,17000-01	2024	4	51	1942
1,00000+00	6,50000-01					2024	4	51	1943
0,00000+00	1,80000+06	0	0	1		192024	4	51	1944
	19	2				2024	4	51	1945
-1,00000+00	3,46000-01	9,84800-01	3,35000-01	9,39700-01	3,22000-01	2024	4	51	1946
-8,66000-01	3,37000-01	7,66000-01	3,71000-01	6,42800-01	4,27000-01	2024	4	51	1947
-5,00000-01	4,64000-01	3,42000-01	4,85000-01	1,73600-01	4,89000-01	2024	4	51	1948
0,00000+00	4,63000-01	1,73600-01	4,59000-01	3,42000-01	4,44000-01	2024	4	51	1949
5,00000+01	4,39000-01	6,42800-01	4,56000-01	7,66000-01	5,00000-01	2024	4	51	1950
8,66000-01	5,64000-01	9,39700-01	6,46000-01	9,84800-01	6,95000-01	2024	4	51	1951
1,00000+00	7,34000-01					2024	4	51	1952
0,00000+00	2,00000+06	0	0	1		192024	4	51	1953
	19	2				2024	4	51	1954
-1,00000+00	3,35000-01	9,84800-01	3,16000-01	9,39700-01	3,07000-01	2024	4	51	1955
-8,66000-01	3,42000-01	7,66000-01	3,71000-01	6,42800-01	4,25000-01	2024	4	51	1956
-5,00000-01	4,60000-01	3,42000-01	4,67000-01	1,73600-01	4,61000-01	2024	4	51	1957
0,00000+00	4,53000-01	1,73600-01	4,45000-01	3,42000-01	4,36000-01	2024	4	51	1958
5,00000+01	4,35000-01	6,42800-01	4,58000-01	7,66000-01	5,14000-01	2024	4	51	1959
8,66000-01	6,00000-01	9,39700-01	6,95000-01	9,84800-01	7,69000-01	2024	4	51	1960
1,00000+00	7,97000-01					2024	4	51	1961
0,00000+00	2,20000+06	0	0	1		192024	4	51	1962
	19	2				2024	4	51	1963
-1,00000+00	3,06000-01	9,84800-01	2,91000-01	9,39700-01	2,92000-01	2024	4	51	1964
-8,66000-01	3,23000-01	7,66000-01	3,92000-01	6,42800-01	4,32000-01	2024	4	51	1965
-5,00000-01	4,53000-01	3,42000-01	4,50000-01	1,73600-01	4,40000-01	2024	4	51	1966
0,00000+00	4,36000-01	1,73600-01	4,45000-01	3,42000-01	4,41000-01	2024	4	51	1967
5,00000+01	4,43000-01	6,42800-01	4,68000-01	7,66000-01	5,23000-01	2024	4	51	1968
8,66000-01	6,11000-01	9,39700-01	7,16000-01	9,84800-01	8,30000-01	2024	4	51	1969
1,00000+00	8,38000-01					2024	4	51	1970
0,00000+00	2,40000+06	0	0	1		192024	4	51	1971
	19	2				2024	4	51	1972
-1,00000+00	2,62000-01	9,84800-01	2,62000-01	9,39700-01	2,97000-01	2024	4	51	1973
-8,66000-01	3,38000-01	7,66000-01	4,17000-01	6,42800-01	6,47000-01	2024	4	51	1974

-5,00000-01	4,45000-01	3,42000-01	4,25000-01	1,73600-01	4,13000-01	2024	4	51	1975
0,00000+00	4,19000-01	1,73600-01	4,44000-01	3,42000-01	4,58000-01	2024	4	51	1976
5,00000+01	4,62000-01	6,42800-01	4,83000-01	7,66000-01	5,32000-01	2024	4	51	1977
8,66000-01	6,15000-01	9,39700-01	7,30000-01	9,84800-01	8,63000-01	2024	4	51	1978
1,00000+00	8,77000-01					2024	4	51	1979
0,00000+00	2,60000+06	0	0	1		192024	4	51	1980
	19	2				2024	4	51	1981
-1,00000+00	2,08000-01	9,84800-01	2,31000-01	9,39700-01	2,67000-01	2024	4	51	1982
-8,66000-01	3,56000-01	7,66000-01	4,66000-01	6,42800-01	4,58000-01	2024	4	51	1983
-5,00000-01	4,38000-01	3,42000-01	3,96000-01	1,73600-01	3,84000-01	2024	4	51	1984
0,00000+00	4,03000-01	1,73600-01	4,56000-01	3,42000-01	4,85000-01	2024	4	51	1985
5,00000+01	4,91000-01	6,42800-01	4,50000-01	7,66000-01	5,42000-01	2024	4	51	1986
8,66000-01	6,16000-01	9,39700-01	7,37000-01	9,84800-01	8,81000-01	2024	4	51	1987
1,00000+00	9,13000-01					2024	4	51	1988
0,00000+00	2,80000+06	0	0	1		192024	4	51	1989
	19	2				2024	4	51	1990
-1,00000+00	1,65000-01	9,84800-01	1,93000-01	9,39700-01	2,59000-01	2024	4	51	1991
-8,66000-01	3,81000-01	7,66000-01	4,81000-01	6,42800-01	4,88000-01	2024	4	51	1992
-5,00000-01	4,30000-01	3,42000-01	3,64000-01	1,73600-01	3,52000-01	2024	4	51	1993
0,00000+00	3,90000-01	1,73600-01	4,66000-01	3,42000-01	5,20000-01	2024	4	51	1994
5,00000+01	5,35000-01	6,42800-01	5,20000-01	7,66000-01	5,49000-01	2024	4	51	1995
8,66000-01	6,16000-01	9,39700-01	7,33000-01	9,84800-01	8,84000-01	2024	4	51	1996
1,00000+00	9,47000-01					2024	4	51	1997
0,00000+00	3,00000+06	0	0	1		192024	4	51	1998
	19	2				2024	4	51	1999
-1,00000+00	1,55000-01	9,84800-01	1,69000-01	9,39700-01	2,53000-01	2024	4	51	2000
-8,66000-01	3,89000-01	7,66000-01	4,99000-01	6,42800-01	5,05000-01	2024	4	51	2001
-5,00000-01	4,22000-01	3,42000-01	3,34000-01	1,73600-01	3,15000-01	2024	4	51	2002
0,00000+00	3,78000-01	1,73600-01	4,82000-01	3,42000-01	5,63000-01	2024	4	51	2003
5,00000+01	5,85000-01	6,42800-01	5,60000-01	7,66000-01	5,57000-01	2024	4	51	2004
8,66000-01	6,09000-01	9,39700-01	7,42000-01	9,84800-01	8,99000-01	2024	4	51	2005
1,00000+00	9,71000-01					2024	4	51	2006
0,00000+00	3,20000+06	0	0	1		192024	4	51	2007
	19	2				2024	4	51	2008
-1,00000+00	1,07000-01	9,84800-01	1,46000-01	9,39700-01	2,47000-01	2024	4	51	2009
-8,66000-01	3,82000-01	7,66000-01	4,97000-01	6,42800-01	5,04000-01	2024	4	51	2010
-5,00000-01	4,14000-01	3,42000-01	3,17000-01	1,73600-01	3,07000-01	2024	4	51	2011
0,00000+00	3,73000-01	1,73600-01	4,82000-01	3,42000-01	5,67000-01	2024	4	51	2012
5,00000+01	5,93000-01	6,42800-01	5,72000-01	7,66000-01	5,67000-01	2024	4	51	2013
8,66000-01	6,17000-01	9,39700-01	7,53000-01	9,84800-01	9,11000-01	2024	4	51	2014
1,00000+00	9,83000-01					2024	4	51	2015
0,00000+00	3,40000+06	0	0	1		192024	4	51	2016
	19	2				2024	4	51	2017
-1,00000+00	8,60000-02	9,84800-01	1,31000-01	9,39700-01	2,45000-01	2024	4	51	2018
-8,66000-01	3,74000-01	7,66000-01	4,88000-01	6,42800-01	5,06000-01	2024	4	51	2019
-5,00000-01	4,07000-01	3,42000-01	3,07000-01	1,73600-01	3,01000-01	2024	4	51	2020
0,00000+00	3,69000-01	1,73600-01	4,80000-01	3,42000-01	5,70000-01	2024	4	51	2021

5,00000+01	6,02000+01	6,42800+01	5,80000-01	7,66000+01	5,75000+01	2024	4	51	2022
8,66000+01	6,32000+01	9,39700+01	7,63000+01	9,84800+01	9,14000+01	2024	4	51	2023
1,00000+00	9,85000+01					2024	4	51	2024
0,00000+00	3,60000+06	0	0	1	18	2024	4	51	2025
	18					2024	4	51	2026
41,00000+00	7,30000+02	9,84800+01	1,15000-01	8,66000+01	3,66000+01	2024	4	51	2027
47,66000+01	4,77000+01	6,42800+01	4,93000-01	5,00000+01	3,98000+01	2024	4	51	2028
43,42000+01	2,96000+01	7,73600+01	2,94000-01	0,00000+00	3,65000+01	2024	4	51	2029
1,73600+01	4,80000+01	3,42000+01	5,74000+01	5,00000+01	6,10000+01	2024	4	51	2030
6,42800+01	5,85000+01	7,66000+01	5,87000+01	8,66000+01	6,52000+01	2024	4	51	2031
9,39700+01	7,78000+01	9,84800+01	9,16000+01	1,00000+00	9,86000+01	2024	4	51	2032
0,00000+00	3,80000+06	0	0	1	14	2024	4	51	2033
	19					2024	4	51	2034
41,00000+00	5,80000+02	9,84800+01	1,05000-01	9,39700+01	2,37000+01	2024	4	51	2035
18,66000+01	3,58000+01	7,66000+01	4,62000-01	6,42800+01	4,86000+01	2024	4	51	2036
15,00000+01	3,91000+01	3,42000+01	2,89000-01	1,73600+01	2,94000+01	2024	4	51	2037
0,00000+00	3,62000+01	1,73600+01	4,79000-01	3,42000+01	5,77000+01	2024	4	51	2038
5,00000+01	6,16000+01	6,42800+01	5,91000+01	7,66000+01	6,02000+01	2024	4	51	2039
8,66000+01	6,75000+01	9,39700+01	7,97000+01	9,84800+01	9,16000+01	2024	4	51	2040
1,00000+00	9,80000+01					2024	4	51	2041
0,00000+00	4,00000+06	0	0	1	19	2024	4	51	2042
	19					2024	4	51	2043
41,00000+00	5,20000+02	9,84800+01	9,60000-02	9,39700+01	2,39000+01	2024	4	51	2044
18,66000+01	3,52000+01	7,66000+01	4,44000-01	6,42800+01	4,76000+01	2024	4	51	2045
15,00000+01	3,85000+01	3,42000+01	2,85000-01	1,73600+01	2,99000+01	2024	4	51	2046
0,00000+00	3,67000+01	1,73600+01	4,79000-01	3,42000+01	5,79000+01	2024	4	51	2047
5,00000+01	6,21000+01	6,42800+01	5,93000+01	7,66000+01	6,13000+01	2024	4	51	2048
8,66000+01	6,99000+01	9,39700+01	8,09000+01	9,84800+01	9,14000+01	2024	4	51	2049
1,00000+00	9,66000+01					2024	4	51	2050
0,00000+00	4,50000+06	0	0	1	19	2024	4	51	2051
	19					2024	4	51	2052
1,00000+00	4,10000+02	9,84800+01	8,70000-02	9,39700+01	2,42000+01	2024	4	51	2053
18,66000+01	3,37000+01	7,66000+01	4,08000-01	6,42800+01	4,46000+01	2024	4	51	2054
15,00000+01	3,74000+01	3,42000+01	2,78000-01	1,73600+01	3,11000+01	2024	4	51	2055
0,00000+00	3,83000+01	1,73600+01	4,78000-01	3,42000+01	5,82000+01	2024	4	51	2056
5,00000+01	6,28000+01	6,42800+01	5,94000+01	7,66000+01	6,47000+01	2024	4	51	2057
8,66000+01	7,68000+01	9,39700+01	8,39000+01	9,84800+01	8,83000+01	2024	4	51	2058
1,00000+00	9,21000+01					2024	4	51	2059
0,00000+00	5,00000+06	0	0	1	19	2024	4	51	2060
	19					2024	4	51	2061
1,00000+00	3,80000+02	9,84800+01	8,60000-02	9,39700+01	2,50000+01	2024	4	51	2062
18,66000+01	3,25000+01	7,66000+01	3,62000-01	6,42800+01	4,10000+01	2024	4	51	2063
15,00000+01	3,64000+01	3,42000+01	2,77000-01	1,73600+01	3,25000+01	2024	4	51	2064
0,00000+00	4,00000+01	1,73600+01	4,79000-01	3,42000+01	5,84000+01	2024	4	51	2065
5,00000+01	6,32000+01	6,42800+01	5,93000+01	7,66000+01	6,78000+01	2024	4	51	2066
8,66000+01	8,41000+01	9,39700+01	8,70000+01	9,84800+01	8,50000+01	2024	4	51	2067
1,00000+00	8,56000+01					2024	4	51	2068

0,00000+00	5,50000+06	0	0	1	19	2024	4	51	2069
	19					2024	4	51	2070
1,00000+00	3,90000+02	9,84800+01	8,60000-02	9,39700+01	2,57000+01	2024	4	51	2071
18,66000+01	3,15000+01	7,66000+01	3,17000-01	6,42800+01	3,78000+01	2024	4	51	2072
15,00000+01	3,56000+01	3,42000+01	2,79000-01	1,73600+01	3,40000+01	2024	4	51	2073
0,00000+00	4,16000+01	1,73600+01	4,79000-01	3,42000+01	5,65000+01	2024	4	51	2074
5,00000+01	6,35000+01	6,42800+01	5,91000+01	7,66000+01	7,16000+01	2024	4	51	2075
8,66000+01	7,74000+01	9,39700+01	8,12000+01	9,84800+01	8,12000+01	2024	4	51	2076
1,00000+00	9,74000+01					2024	4	51	2077
0,00000+00	6,00000+06	0	0	1	19	2024	4	51	2078
	19					2024	4	51	2079
1,00000+00	4,00000+02	9,84800+01	8,90000-02	9,39700+01	2,62000+01	2024	4	51	2080
18,66000+01	3,02000+01	7,66000+01	2,75000-01	6,42800+01	3,46000+01	2024	4	51	2081
15,00000+01	3,49000+01	3,42000+01	2,83000-01	1,73600+01	3,52000+01	2024	4	51	2082
0,00000+00	4,37000+01	1,73600+01	4,79000-01	3,42000+01	5,85000+01	2024	4	51	2083
5,00000+01	6,38000+01	6,42800+01	5,92000+01	7,66000+01	7,51000+01	2024	4	51	2084
8,66000+01	9,97000+01	9,39700+01	9,58000+01	9,84800+01	9,17000+01	2024	4	51	2085
1,00000+00	6,90000+01					2024	4	51	2086
0,00000+00	6,50000+06	0	0	1	19	2024	4	51	2087
	19					2024	4	51	2088
1,00000+00	4,00000+02	9,84800+01	9,40000-02	9,39700+01	2,67000+01	2024	4	51	2089
18,66000+01	2,37000+01	7,66000+01	2,38000-01	6,42800+01	3,21000+01	2024	4	51	2090
15,00000+01	3,44000+01	3,42000+01	2,86000-01	1,73600+01	3,62000+01	2024	4	51	2091
0,00000+00	4,47000+01	1,73600+01	4,79000-01	3,42000+01	5,86000+01	2024	4	51	2092
5,00000+01	6,47000+01	6,42800+01	5,93000+01	7,66000+01	7,88000+01	2024	4	51	2093
8,66000+01	1,07500+00	9,39700+01	1,00700+00	9,84800+01	7,46000+01	2024	4	51	2094
1,00000+00	6,12000+01					2024	4	51	2095
0,00000+00	7,00000+06	0	0	1	9	2024	4	51	2096
	19					2024	4	51	2097
1,00000+00	4,50000+02	9,84800+01	1,02000-01	9,39700+01	2,73000+01	2024	4	51	2098
18,66000+01	2,76000+01	7,66000+01	2,07000-01	6,42800+01	2,95000+01	2024	4	51	2099
15,00000+01	3,41000+01	3,42000+01	2,93000-01	1,73600+01	3,68000+01	2024	4	51	2100
0,00000+00	4,50000+01	1,73600+01	4,80000-01	3,42000+01	5,87000+01	2024	4	51	2101
5,00000+01	6,46000+01	6,42800+01	5,94000+01	7,66000+01	8,122000+01	2024	4	51	2102
8,66000+01	1,16100+00	9,39700+01	1,05700+00	9,84800+01	7,21000+01	2024	4	51	2103
1,00000+00	5,50000+01					2024	4	51	2104
0,00000+00	7,50000+06	0	0	1	19	2024	4	51	2105
	19					2024	4	51	2106
1,00000+00	4,70000+02	9,84800+01	1,11000-01	9,39700+01	2,76000+01	2024	4	51	2107
18,66000+01	2,74000+01	7,66000+01	1,87000-01	6,42800+01	2,75000+01	2024	4	51	2108
15,00000+01	3,40000+01	3,42000+01	2,98000-01	1,73600+01	3,74000+01	2024	4	51	2109
0,00000+00	4,65000+01	1,73600+01	4,80000-01	3,42000+01	5,89000+01	2024	4	51	2110
5,00000+01	6,53000+01	6,42800+01	5,98000+01	7,66000+01	8,60000+01	2024	4	51	2111
8,66000+01	1,26600+00	9,39700+01	1,11500+00	9,84800+01	6,97000+01	2024	4	51	2112
1,00000+00	5,02000+01					2024	4	51	2113
0,00000+00	8,00000+06	0	0	1	19	2024	4	51	2114
	19					2024	4	51	2115

-1,000000+00	5,000000-02	-9,848000-01	1,200000-01	-9,397000+01	2,810000-01	12024	4	51	2116
-8,660000-01	2,730000+01	-7,660000-01	1,820000-01	-6,428000-01	2,580000+01	12024	4	51	2117
-5,000000-01	3,400000+01	-3,420000-01	3,090000-01	-1,736000-01	3,810000-01	12024	4	51	2118
0,000000+00	4,710000-01	1,736000-01	4,800000-01	3,420000-01	5,910000-01	12024	4	51	2119
5,000000-01	6,510000-01	6,428000-01	6,080000-01	7,660000+01	8,890000-01	12024	4	51	2120
8,660000-01	1,323000+00	9,397000+01	1,183000+00	9,848000-01	6,860000-01	12024	4	51	2121
1,000000+00	4,780000-01					192024	4	51	2122
0,000000+00	8,560000+06	0	0	1		192024	4	51	2123
-1,000000+00	5,200000-02	-9,848000-01	1,340000-01	-9,397000+01	2,970000-01	12024	4	51	2124
-8,660000-01	2,820000-01	-7,660000-01	1,750000-01	-6,428000-01	2,510000-01	12024	4	51	2125
-5,000000-01	3,430000+01	-3,420000-01	3,160000-01	-1,736000-01	3,810000-01	12024	4	51	2126
0,000000+00	4,730000-01	1,736000-01	4,630000-01	3,420000-01	5,970000-01	12024	4	51	2127
5,000000-01	6,740000-01	6,428000-01	6,240000-01	7,660000+01	9,080000-01	12024	4	51	2128
8,660000-01	1,407000+00	9,397000-01	1,270000+00	9,848000-01	7,020000-01	12024	4	51	2129
1,000000+00	4,860000-01					192024	4	51	2130
0,000000+00	9,000000+06	0	0	1		192024	4	51	2131
-1,000000+00	5,600000-02	-9,848000-01	1,480000-01	-9,397000+01	3,120000-01	12024	4	51	2132
-8,660000-01	2,900000-01	-7,660000-01	1,700000-01	-6,428000-01	2,490000-01	12024	4	51	2133
-5,000000-01	3,460000+01	-3,420000-01	3,310000-01	-1,736000-01	3,820000-01	12024	4	51	2134
0,000000+00	4,730000-01	1,736000-01	4,900000-01	3,420000-01	6,150000-01	12024	4	51	2135
5,000000-01	6,940000-01	6,428000-01	6,450000-01	7,660000+01	9,230000-01	12024	4	51	2136
8,660000-01	1,476000+00	9,397000-01	1,357000+00	9,848000-01	7,460000-01	12024	4	51	2137
1,000000+00	5,180000-01					192024	4	51	2138
0,000000+00	9,500000+06	0	0	1		192024	4	51	2139
-1,000000+00	6,200000-02	-9,848000-01	1,720000-01	-9,397000+01	3,300000-01	12024	4	51	2140
-8,660000-01	3,010000-01	-7,660000-01	1,680000-01	-6,428000-01	2,470000-01	12024	4	51	2141
-5,000000-01	3,480000+01	-3,420000-01	3,450000-01	-1,736000-01	3,820000-01	12024	4	51	2142
0,000000+00	4,720000-01	1,736000-01	4,960000-01	3,420000-01	6,310000-01	12024	4	51	2143
5,000000-01	7,190000-01	6,428000-01	7,400000-01	7,660000+01	9,360000-01	12024	4	51	2144
8,660000-01	1,546000+00	9,397000-01	1,442000+00	9,848000-01	8,030000-01	12024	4	51	2145
1,000000+00	5,600000+07					192024	4	51	2146
0,000000+00	1,000000+07	0	0	1		192024	4	51	2147
-1,000000+00	7,200000-02	-9,848000-01	1,890000-01	-9,397000+01	3,560000-01	12024	4	51	2148
-8,660000-01	3,130000-01	-7,660000-01	1,660000-01	-6,428000-01	2,460000-01	12024	4	51	2149
-5,000000-01	3,500000+01	-3,420000-01	3,590000-01	-1,736000-01	3,830000-01	12024	4	51	2150
0,000000+00	4,710000-01	1,736000-01	5,030000-01	3,420000-01	6,900000-01	12024	4	51	2151
5,000000-01	7,490000-01	6,428000-01	7,000000-01	7,660000+01	9,460000-01	12024	4	51	2152
8,660000-01	1,607000+00	9,397000-01	1,537000+00	9,848000-01	8,570000-01	12024	4	51	2153
1,000000+00	6,190000-01					192024	4	51	2154
0,000000+00	1,050000+07	0	0	1		192024	4	51	2155
-1,000000+00	8,000000-02	-9,848000-01	2,100000-01	-9,397000+01	3,800000-01	12024	4	51	2156
-8,660000-01	3,250000-01	-7,660000-01	1,650000-01	-6,428000-01	2,450000-01	12024	4	51	2157

-5,000000-01	3,560000-01	-3,420000-01	3,740000-01	-1,736000-01	3,840000-01	12024	4	51	2163
0,000000+00	4,700000-01	1,736000-01	5,080000-01	3,420000-01	6,740000-01	12024	4	51	2164
5,000000-01	7,800000-01	6,428000-01	7,260000-01	7,660000+01	9,540000-01	12024	4	51	2165
8,660000-01	1,666000+00	9,397000-01	1,624000+00	9,848000-01	9,270000-01	12024	4	51	2166
1,000000+00	6,800000-01					192024	4	51	2167
0,000000+00	1,100000+07	0	0	1		192024	4	51	2168
-1,000000+00	8,800000-02	-9,848000-01	2,320000-01	-9,397000+01	4,100000-01	12024	4	51	2169
-8,660000-01	3,360000-01	-7,660000-01	1,630000-01	-6,428000-01	2,440000-01	12024	4	51	2170
-5,000000-01	3,610000+01	-3,420000-01	3,400000-01	-1,736000-01	3,850000-01	12024	4	51	2171
0,000000+00	4,690000-01	1,736000-01	5,140000-01	3,420000-01	6,960000-01	12024	4	51	2172
5,000000-01	8,150000-01	6,428000-01	7,520000-01	7,660000+01	9,620000-01	12024	4	51	2173
8,660000-01	1,723000+00	9,397000-01	1,720000+00	9,848000-01	9,980000-01	12024	4	51	2174
1,000000+00	7,370000-01					192024	4	51	2175
0,000000+00	1,150000+07	0	0	1		192024	4	51	2176
-1,000000+00	1,000000-01	-9,848000-01	2,580000-01	-9,397000+01	4,350000-01	12024	4	51	2177
-8,660000-01	3,440000-01	-7,660000-01	1,600000-01	-6,428000-01	2,430000-01	12024	4	51	2178
-5,000000-01	3,660000+01	-3,420000-01	3,400000-01	-1,736000-01	3,860000-01	12024	4	51	2179
0,000000+00	4,660000-01	1,736000-01	5,190000-01	3,420000-01	7,200000-01	12024	4	51	2180
5,000000-01	8,540000-01	6,428000-01	7,840000-01	7,660000+01	9,700000-01	12024	4	51	2181
8,660000-01	1,781000+00	9,397000-01	1,820000+00	9,848000-01	1,072000+00	12024	4	51	2182
1,000000+00	7,960000-01					192024	4	51	2183
0,000000+00	1,200000+07	0	0	1		192024	4	51	2184
-1,000000+00	1,100000-01	-9,848000-01	2,870000-01	-9,397000+01	4,610000-01	12024	4	51	2185
-8,660000-01	3,600000-01	-7,660000-01	1,580000-01	-6,428000-01	2,410000-01	12024	4	51	2186
-5,000000-01	3,710000+01	-3,420000-01	3,300000-01	-1,736000-01	3,870000-01	12024	4	51	2187
0,000000+00	4,570000-01	1,736000-01	5,230000-01	3,420000-01	7,410000-01	12024	4	51	2188
5,000000-01	8,900000-01	6,428000-01	8,080000-01	7,660000+01	9,720000-01	12024	4	51	2189
8,660000-01	1,833000+00	9,397000-01	1,930000+00	9,848000-01	1,145000+00	12024	4	51	2190
1,000000+00	8,660000-01					192024	4	51	2191
0,000000+00	1,250000+07	0	0	1		192024	4	51	2192
-1,000000+00	1,200000-01	-9,848000-01	3,180000-01	-9,397000+01	4,910000-01	12024	4	51	2193
-8,660000-01	3,730000-01	-7,660000-01	1,550000-01	-6,428000-01	2,390000-01	12024	4	51	2194
-5,000000-01	3,750000+01	-3,420000-01	4,410000-01	-1,736000-01	3,880000-01	12024	4	51	2195
0,000000+00	4,500000-01	1,736000-01	5,270000-01	3,420000-01	7,630000-01	12024	4	51	2196
5,000000-01	9,260000-01	6,428000-01	8,350000-01	7,660000+01	9,750000-01	12024	4	51	2197
8,660000-01	1,886000+00	9,397000-01	2,047000+00	9,848000-01	1,222000+00	12024	4	51	2198
1,000000+00	9,340000-01					192024	4	51	2199
0,000000+00	1,300000+07	0	0	1		192024	4	51	2200
-1,000000+00	1,300000-01	-9,397000-01	3,490000-01	-9,397000+01	5,220000-01	12024	4	51	2201
-8,660000-01	3,860000-01	-7,660000-01	1,550000-01	-6,428000-01	2,360000-01	12024	4	51	2202
-5,000000-01	3,810000+01	-3,420000-01	4,600000-01	-1,736000-01	3,880000-01	12024	4	51	2203
0,000000+00	4,400000-01	1,736000-01	5,330000-01	3,420000-01	7,860000-01	12024	4	51	2204

5,000000+01	9,620000+01	6,428000+01	8,590000+01	7,660000+01	9,780000+01	2024	4	51	2210
8,600000+01	1,930000+00	9,397000+01	2,165000+00	9,848000+01	1,290000+00	2024	4	51	2211
1,000000+00	1,000000+00					2024	4	51	2212
0,000000+00	1,350000+07	0	0	1	192024	4	51	2213	
	19	2			2024	4	51	2214	
-1,000000+00	1,400000+01	9,848000+01	3,820000+01	9,397000+01	5,500000+01	2024	4	51	2215
-8,600000+01	4,010000+01	7,660000+01	1,530000+01	6,428000+01	2,350000+01	2024	4	51	2216
-5,000000+01	3,860000+01	3,420000+01	4,800000+01	1,736000+01	3,900000+01	2024	4	51	2217
0,000000+00	4,280000+01	1,736000+01	5,400000+01	3,420000+01	6,160000+01	2024	4	51	2218
5,000000+01	1,004000+00	6,428000+01	8,820000+01	7,660000+01	9,790000+01	2024	4	51	2219
8,660000+01	1,970000+00	9,397000+01	2,275000+00	9,848000+01	1,564000+00	2024	4	51	2220
1,000000+00	1,076000+00					2024	4	51	2221
0,000000+00	1,400000+07	0	0	1	192024	4	51	2222	
	19	2			2024	4	51	2223	
-1,000000+00	1,500000+01	9,848000+01	4,150000+01	9,397000+01	5,910000+01	2024	4	51	2224
-8,660000+01	4,130000+01	7,660000+01	1,500000+01	6,428000+01	2,340000+01	2024	4	51	2225
-5,000000+01	3,890000+01	3,420000+01	4,980000+01	1,736000+01	3,910000+01	2024	4	51	2226
0,000000+00	4,130000+01	1,736000+01	5,460000+01	3,420000+01	8,420000+01	2024	4	51	2227
5,000000+01	1,044000+00	6,428000+01	9,040000+01	7,660000+01	9,800000+01	2024	4	51	2228
8,660000+01	2,010000+00	9,397000+01	2,390000+00	9,848000+01	1,430000+00	2024	4	51	2229
1,000000+00	1,143000+00					2024	4	51	2230
0,000000+00	1,450000+07	0	0	1	192024	4	51	2231	
	19	2			2024	4	51	2232	
-1,000000+00	1,620000+01	9,848000+01	4,450000+01	9,397000+01	6,240000+01	2024	4	51	2233
-8,660000+01	4,270000+01	7,660000+01	1,490000+01	6,428000+01	2,330000+01	2024	4	51	2234
-5,000000+01	3,940000+01	3,420000+01	5,190000+01	1,736000+01	3,920000+01	2024	4	51	2235
0,000000+00	3,940000+01	1,736000+01	5,520000+01	3,420000+01	8,700000+01	2024	4	51	2236
5,000000+01	1,087000+00	6,428000+01	9,300000+01	7,660000+01	9,810000+01	2024	4	51	2237
8,660000+01	2,047000+00	9,397000+01	2,510000+00	9,848000+01	1,503000+00	2024	4	51	2238
1,000000+00	1,207000+00					2024	4	51	2239
0,000000+00	1,500000+07	0	0	1	192024	4	51	2240	
	19	2			2024	4	51	2241	
-1,000000+00	1,800000+01	9,848000+01	4,800000+01	9,397000+01	6,620000+01	2024	4	51	2242
-8,660000+01	4,400000+01	7,660000+01	1,470000+01	6,428000+01	2,332000+01	2024	4	51	2243
-5,000000+01	3,980000+01	3,420000+01	3,380000+01	1,736000+01	3,910000+01	2024	4	51	2244
0,000000+00	3,750000+01	1,736000+01	3,590000+01	3,420000+01	9,100000+01	2024	4	51	2245
5,000000+01	1,137000+00	6,428000+01	9,460000+01	7,660000+01	9,820000+01	2024	4	51	2246
8,660000+01	2,077000+00	9,397000+01	2,620000+00	9,848000+01	1,583000+00	2024	4	51	2247
1,000000+00	1,280000+00					2024	4	51	2248
0,000000+00	0,000000+00	0	0	0	0	2024	4	51	2249
9,42410+04	2,38986+02	0	0	0	0	02024	4	52	2250
0,000000+00	2,38986+02	0	0	0	0	02024	4	52	2251
0,000000+00	0,000000+00	0	0	0	0	02024	4	52	2252
9,42410+04	2,38986+02	0	0	0	0	02024	4	53	2253
0,000000+00	2,38986+02	0	0	0	0	02024	4	53	2254
0,000000+00	0,000000+00	0	0	0	0	02024	4	53	2255
9,42410+04	2,38986+02	0	0	0	0	02024	4	54	2256

0,000000+00	2,38986+02	1				02024	4	54	2257
0,000000+00	0,000000+00	0				02024	4	54	2258
9,42410+04	2,38986+02	0				02024	4	55	2259
0,000000+00	0,000000+00	0				02024	4	55	2260
9,42410+04	2,38986+02	0				02024	4	56	2261
0,000000+00	0,000000+00	0				02024	4	56	2262
9,42410+04	2,38986+02	0				02024	4	56	2263
0,000000+00	0,000000+00	0				02024	4	57	2264
9,42410+04	2,38986+02	0				02024	4	57	2265
0,000000+00	0,000000+00	0				02024	4	57	2266
9,42410+04	2,38986+02	0				02024	4	58	2267
0,000000+00	0,000000+00	0				02024	4	58	2268
9,42410+04	2,38986+02	0				02024	4	58	2269
0,000000+00	0,000000+00	0				02024	4	59	2270
9,42410+04	2,38986+02	0				02024	4	59	2271
0,000000+00	0,000000+00	0				02024	4	59	2272
9,42410+04	2,38986+02	0				02024	4	60	2273
0,000000+00	0,000000+00	0				02024	4	60	2274
9,42410+04	2,38986+02	0				02024	4	60	2275
0,000000+00	0,000000+00	0				02024	4	60	2276
9,42410+04	2,38986+02	0				02024	4	61	2277
0,000000+00	0,000000+00	0				02024	4	61	2278
9,42410+04	2,38986+02	0				02024	4	61	2279
0,000000+00	0,000000+00	0				02024	4	62	2280
9,42410+04	2,38986+02	0				02024	4	62	2281
0,000000+00	0,000000+00	0				02024	4	62	2282
9,42410+04	2,38986+02	0				02024	4	63	2283
0,000000+00	0,000000+00	0				02024	4	63	2284
9,42410+04	2,38986+02	0				02024	4	63	2285
0,000000+00	0,000000+00	0				02024	4	64	2286
9,42410+04	2,38986+02	0				02024	4	64	2287
0,000000+00	0,000000+00	0				02024	4	64	2288
9,42410+04	2,38986+02	0				02024	4	65	2289
0,000000+00	0,000000+00	0				02024	4	65	2290
9,42410+04	2,38986+02	0				02024	4	65	2291
0,000000+00	0,000000+00	0				02024	4	66	2292
9,42410+04	2,38986+02	0				02024	4	66	2293
0,000000+00	0,000000+00	0				02024	4	67	2294
9,42410+04	2,38986+02	0				02024	4	67	2295
0,000000+00	0,000000+00	0				02024	4	67	2296
9,42410+04	2,38986+02	0				02024	4	68	2297
0,000000+00	0,000000+00	0				02024	4	68	2298
9,42410+04	2,38986+02	0				02024	4	68	2299
0,000000+00	0,000000+00	0				02024	4	69	2300
9,42410+04	2,38986+02	0				02024	4	69	2301
0,000000+00	0,000000+00	0				02024	4	69	2302
9,42410+04	2,38986+02	0				02024	4	69	2303

9,42410+04	2,38986+02	0	0	0	0	02024	4	70	2304
0,00000+00	2,38986+02	1	2	0	0	02024	4	70	2305
0,00000+00	0,00000+00	0	0	0	0	02024	4	0	2306
9,42410+04	2,38986+02	0	0	0	0	02024	4	71	2307
0,00000+00	2,38986+02	1	0	0	0	02024	4	71	2308
0,00000+00	0,00000+00	0	0	0	0	02024	4	0	2309
9,42410+04	2,38986+02	0	0	0	0	02024	4	72	2310
0,00000+00	2,38986+02	1	0	0	0	02024	4	72	2311
0,00000+00	0,00000+00	0	0	0	0	02024	4	0	2312
9,42410+04	2,38986+02	0	0	0	0	02024	4	73	2313
0,00000+00	2,38986+02	1	0	0	0	02024	4	73	2314
0,00000+00	0,00000+00	0	0	0	0	02024	4	0	2315
9,42410+04	2,38986+02	0	0	0	0	02024	4	74	2316
0,00000+00	2,38986+02	1	0	0	0	02024	4	74	2317
0,00000+00	0,00000+00	0	0	0	0	02024	4	0	2318
9,42410+04	2,38986+02	0	0	0	0	02024	4	75	2319
0,00000+00	2,38986+02	1	0	0	0	02024	4	75	2320
0,00000+00	0,00000+00	0	0	0	0	02024	4	0	2321
9,42410+04	2,38986+02	0	0	0	0	02024	4	76	2322
0,00000+00	2,38986+02	1	0	0	0	02024	4	76	2323
0,00000+00	0,00000+00	0	0	0	0	02024	4	0	2324
9,42410+04	2,38986+02	0	0	0	0	02024	4	91	2325
0,00000+00	2,38986+02	1	0	0	0	02024	4	91	2326
0,00000+00	0,00000+00	0	0	0	0	02024	4	0	2327
9,42410+04	2,38986+02	0	0	0	0	02024	0	0	2328
0,00000+00	2,38986+02	1	0	2	0	02024	5	16	2329
9,42410+04	0,00000+00	0	1	1	0	22024	5	16	2330
0,00000+00	2,38986+02	1	0	0	0	2024	5	16	2331
6,00000+06	5,00000-01	1,50000+07	5,00000-01	0	0	2024	5	16	2332
0,00000+00	0,00000+00	0	0	0	1	62024	5	16	2333
0,00000+00	6,00000+06	0	0	0	1	2024	5	16	2334
0,00000+00	0,00000+00	0	0	0	1	52024	5	16	2335
6,00000+04	1,20000+00	1,00000+05	1,30000+00	3,00000+05	1,60000+00	2024	5	16	2336
6,00000+05	1,20000+00	7,00000+05	8,00000-01	0	0	2024	5	16	2337
0,00000+00	7,00000+06	0	0	0	1	72024	5	16	2338
1,00000+05	8,00000-01	1,20000+05	4,50000-01	3,00000+05	1,00000+00	2024	5	16	2339
5,00000+05	8,00000-01	9,00000+05	5,30000-01	1,50000+06	2,00000-01	2024	5	16	2340
1,75000+06	1,40000-01	0	0	0	0	2024	5	16	2341
0,00000+00	9,00000+06	0	0	0	1	92024	5	16	2342
1,00000+05	6,00000-01	3,00000+05	8,00000-01	5,00000+05	7,30000-01	2024	5	16	2343
1,00000+06	4,50000-01	1,50000+06	2,20000-01	2,00000+06	1,20000-01	2024	5	16	2344
2,50000+06	6,00000-02	5,00000+06	3,00000-02	3,50000+06	2,00000-02	2024	5	16	2345
0,00000+00	1,10000+07	0	0	0	1	122024	5	16	2346
	12	2				2024	5	16	2347

1,00000+05	5,20000-01	3,00000+05	7,00000-01	5,00000+05	6,60000-01	2024	5	16	2351
1,00000+06	4,50000-01	1,80000+06	2,20000-01	2,00000+06	1,20000-01	2024	5	16	2352
2,50000+06	7,60000-02	3,00000+06	4,80000-02	3,50000+06	2,80000-02	2024	5	16	2353
4,00000+06	2,00000-02	5,00000+06	1,30000-02	5,50000+06	1,00000-02	2024	5	16	2354
0,00000+00	1,50000+07	0	0	0	1	92024	5	16	2355
4,00000+05	2,40000-01	7,00000+05	3,00000-01	1,20000+06	4,30000-01	2024	5	16	2356
2,60000+06	2,90000-01	3,00000+06	1,10000-01	4,00000+06	4,90000-02	2024	5	16	2357
5,00000+06	3,00000-02	6,00000+06	2,20000-02	7,00000+06	1,60000-02	2024	5	16	2358
0,00000+00	1,50000+07	0	0	0	1	112024	5	16	2359
5,00000+05	3,00000-02	1,00000+06	0,00000-02	2,00000+06	1,20000-01	2024	5	16	2360
3,00000+06	2,20000-01	4,00000+06	2,00000-01	5,00000+06	1,30000-01	2024	5	16	2361
6,00000+06	8,70000-02	7,00000+06	6,70000-02	8,00000+06	5,30000-02	2024	5	16	2362
7,00000+06	4,00000-02	9,80000+06	3,50000-02	0	0	2024	5	16	2363
0,00000+00	0,00000+00	0	0	1	1	22024	5	16	2364
6,00000+06	5,00000+01	1,50000+07	5,00000-01	0	0	2024	5	16	2365
0,00000+00	0,00000+00	0	0	0	1	62024	5	16	2366
0,00000+00	6,00000+05	0	0	0	1	2024	5	16	2367
4,00000+04	3,80000-01	8,00000+04	1,15000+00	1,20000+05	1,42000+00	2024	5	16	2368
1,60000+05	2,51000+00	2,00000+05	2,87000+00	2,40000+05	2,93000+00	2024	5	16	2369
2,80000+05	2,61000+00	3,20000+05	2,54000+00	3,60000+05	2,16000+00	2024	5	16	2370
4,00000+05	1,77000+00	4,40000+05	1,36000+00	4,80000+05	9,40000-01	2024	5	16	2371
5,20000+05	6,90000-01	5,60000+05	4,40000-01	6,00000+05	2,40000-01	2024	5	16	2372
6,40000+05	1,40000-01	0	0	0	0	2024	5	16	2373
0,00000+00	7,00000+06	0	0	1	1	162024	5	16	2374
4,00000+04	8,30000-02	8,00000+04	2,80000-01	1,20000+05	5,30000-01	2024	5	16	2375
1,00000+05	7,60000-01	2,00000+05	1,00000+00	2,80000-05	1,40000+00	2024	5	16	2376
3,60000+05	1,50000+00	4,40000+05	1,60000+00	5,20000+05	1,40000+00	2024	5	16	2377
6,00000+05	1,20000+00	6,50000+05	1,00000+00	9,20000+05	4,40000-01	2024	5	16	2378
1,20000+06	1,00000-01	1,30000+06	4,50000-02	1,40000+06	2,00000-02	2024	5	16	2379
1,60000+06	2,00000-03	0	0	0	0	2024	5	16	2380
0,00000+00	9,00000+06	0	0	1	1	172024	5	16	2381
4,00000+04	2,10000-02	8,00000+04	7,60000-02	1,20000+05	1,50000-01	2024	5	16	2382
2,00000+05	3,30000-01	3,00000+05	5,50000-01	4,00000+05	7,50000-01	2024	5	16	2383
5,00000+05	8,60000-01	6,00000+05	5,20000-01	7,00000+05	9,20000-01	2024	5	16	2384
9,00000+05	7,90000-01	1,20000+06	5,30000-01	1,40000+06	3,50000-01	2024	5	16	2385
1,60000+06	2,20000-01	1,90000+06	1,00000-01	2,30000+06	2,20000-02	2024	5	16	2386
2,50000+06	1,00000-02	3,00000+06	1,00000-03	0	0	2024	5	16	2387
0,00000+00	1,10000+07	0	0	1	1	142024	5	16	2388
4,00000+04	1,00000-02	1,20000+05	8,00000-02	2,00000+05	1,80000-01	2024	5	16	2389

3,00000+05	3,20000+01	5,00000+05	6,00000-01	7,00000+05	7,00000+01	2024	5	16	2398
7,00000+05	7,10000-01	1,20000+06	6,00000-01	1,60000+06	3,00000+01	2024	5	16	2399
2,00000+06	1,80000+01	2,30000+06	6,60000-02	3,00000+06	2,00000+02	2024	5	16	2400
3,50000+06	4,50000-03	4,00000+06	1,00000-05			2024	5	16	2401
0,00000+00	1,30000+07	0	0	1	13	2024	5	16	2402
	13					2024	5	16	2403
4,00000+04	5,00000-03	8,00000+04	1,90000-02	1,20000+05	3,90000+02	2024	5	16	2404
2,00000+05	1,00000-01	3,00000+05	1,70000-02	5,00000+05	5,20000-01	2024	5	16	2405
7,00000+05	4,50000-01	1,00000+06	5,10000-01	1,50000+06	4,60000+01	2024	5	16	2406
2,00000+06	3,30000-01	3,00000+06	7,60000-02	4,00000+06	8,00000+03	2024	5	16	2407
5,00000+06	1,00000-03					2024	5	16	2408
0,00000+00	1,50000+07	0	0	1	16	2024	5	16	2409
	16					2024	5	16	2410
4,00000+04	4,00000-03	8,00000+04	1,60000-02	1,20000+05	3,40000-02	2024	5	16	2411
3,00000+05	1,51000-01	4,00000+05	2,33000-01	5,00000+05	3,00000-01	2024	5	16	2412
6,00000+05	3,70000-01	7,00000+05	4,10000-01	1,00000+06	4,90000+01	2024	5	16	2413
1,40000+06	4,80000-01	1,80000+06	3,70000-01	2,20000+06	2,60000+01	2024	5	16	2414
3,00000+06	1,00000-01	4,00000+06	3,20000-02	5,00000+06	5,00000-03	2024	5	16	2415
5,60000+06	1,00000-05					2024	5	16	2416
0,00000+00	0,00000+00	0	0	0	0	2024	5	16	2417
9,42410+04	2,38986+02	0	0	0	0	2024	5	17	2418
0,00000+00	0,00000+00	0	1	1	1	2024	5	17	2419
	1					2024	5	17	2420
1,50000+07	3,33300+01					2024	5	17	2421
0,00000+00	0,00000+00	0	0	1	1	2024	5	17	2422
	1					2024	5	17	2423
0,00000+00	1,50000+07	0	0	1	1	2024	5	17	2424
	6					2024	5	17	2425
1,50000+05	1,50000+00	5,00000+05	1,00000+00	1,00000+06	2,00000-01	2024	5	17	2426
1,50000+06	4,00000-02	2,00000+06	5,00000-03	2,50000+06	1,00000-03	2024	5	17	2427
9,00000+00	0,00000+00	0	1	1	1	2024	5	17	2428
	1					2024	5	17	2429
1,50000+07	3,33300+01					2024	5	17	2430
0,00000+00	0,00000+00	0	0	1	1	2024	5	17	2431
	1					2024	5	17	2432
0,00000+00	1,50000+07	0	0	1	1	2024	5	17	2433
	12					2024	5	17	2434
4,00000+04	3,90000-02	8,00000+04	1,40000-01	1,20000+05	2,60000-01	2024	5	17	2435
2,00000+05	5,60000-01	3,00000+05	8,70000-01	4,00000+05	1,10000+00	2024	5	17	2436
6,00000+05	1,10000+00	8,00000+05	9,40000-01	1,00000+06	5,60000-01	2024	5	17	2437
1,40000+06	1,90000-01	1,60000+06	6,60000-02	1,70000+06	4,10000-02	2024	5	17	2438
0,00000+00	0,00000+00	0	1	1	1	2024	5	17	2439
	1					2024	5	17	2440
1,50000+07	3,33300+01					2024	5	17	2441
0,00000+00	0,00000+00	0	0	1	1	2024	5	17	2442
	1					2024	5	17	2443
0,00000+00	1,50000+07	0	0	1	1	2024	5	17	2444

	11	2				2024	5	17	2445
4,00000+04	1,30000+00	8,00000+04	1,60000+00	2,00000+05	1,70000+00	2024	5	17	2446
3,00000+05	1,50000+00	4,00000+05	1,20000+00	5,00000+05	9,50000-01	2024	5	17	2447
6,00000+05	7,20000-01	8,00000+05	5,90000+01	1,00000+06	2,00000-01	2024	5	17	2448
1,30000+06	2,50000-02	2,00000+06	2,00000-03			2024	5	17	2449
0,00000+00	0,00000+00	0	0	0	0	2024	5	17	2450
9,42410+04	2,38986+02	0	0	1	1	2024	5	18	2451
-1,00000+10	0,00000+00	0	7	1	1	2024	5	18	2452
	1					2024	5	18	2453
1,00000-05	1,00000+00	1,50000+07	1,00000+00			2024	5	18	2454
0,00000+00	0,00000+00	0	0	1	1	2024	5	18	2455
	33					2024	5	18	2456
2,33000-02	1,36000+06	1,00000+04	1,36100+06	4,00000+04	1,36200+06	2024	5	18	2457
1,00000+05	1,36300+06	2,00000+05	1,36500+06	4,00000+05	1,36800+06	2024	5	18	2458
6,00000+05	1,37200+06	8,00000+05	1,37500+06	1,00000+06	1,37800+06	2024	5	18	2459
1,30000+06	1,38700+06	2,00000+06	1,39600+06	2,50000+06	1,40300+06	2024	5	18	2460
3,00000+06	1,41300+06	5,50000+06	1,42200+06	4,00000+06	1,43100+06	2024	5	18	2461
4,50000+06	1,43900+06	5,00000+06	1,44800+06	5,50000+06	1,45300+06	2024	5	18	2462
6,00000+06	1,46500+06	6,50000+06	1,47400+06	7,00000+06	1,48300+06	2024	5	18	2463
7,50000+06	1,49100+06	8,00000+06	1,50000+06	9,00000+06	1,51700+06	2024	5	18	2464
1,00000+07	1,53500+06	1,10000+07	1,55200+06	1,20000+07	1,56900+06	2024	5	18	2465
1,30000+07	1,59200+06	1,40000+07	1,60300+06	1,50000+07	1,62100+06	2024	5	18	2466
0,00000+00	0,00000+00	0	0	0	0	2024	5	18	2467
9,42410+04	2,38986+02	0	0	1	1	2024	5	18	2468
0,00000+00	0,00000+00	0	1	1	1	2024	5	18	2469
	1					2024	5	18	2470
1,50000+06	1,00000+00	1,50000+07	1,00000+00			2024	5	18	2471
0,00000+00	0,00000+00	0	0	1	1	2024	5	18	2472
	11					2024	5	18	2473
0,00000+00	1,50000+06	0	0	1	1	2024	5	18	2474
	15					2024	5	18	2475
5,00000+04	2,00000+00	1,00000+05	2,20000+00	2,00000+05	2,10000+00	2024	5	18	2476
3,00000+05	1,60000+00	4,00000+05	1,20000+00	5,00000+05	8,10000-01	2024	5	18	2477
6,00000+05	5,50000-01	7,00000+05	3,30000-01	8,00000+05	2,10000-01	2024	5	18	2478
9,00000+05	1,10000-01	1,00000+06	3,90000-02	1,10000+06	3,20000-02	2024	5	18	2479
1,20000+06	1,30000-02	1,50000+06	5,00000-03	1,40000+06	1,50000-03	2024	5	18	2480
0,00000+00	2,00000+06	0	0	1	1	2024	5	18	2481
	15					2024	5	18	2482
5,00000+04	1,40000+00	1,00000+05	1,90000+00	2,00000+05	1,85000+00	2024	5	18	2483
3,00000+05	1,55000+00	4,00000+05	1,17000+00	5,00000+05	9,10000-01	2024	5	18	2484
6,00000+05	6,50000-01	7,00000+05	4,60000-01	8,00000+05	3,20000-01	2024	5	18	2485
9,00000+05	2,10000-01	1,00000+06	1,20000-01	1,20000+06	5,10000-02	2024	5	18	2486
1,40000+06	1,70000-02	1,60000+06	4,50000-03	1,80000+06	1,00000-03	2024	5	18	2487
0,00000+00	3,00000+06	0	0	1	1	2024	5	18	2488
	14					2024	5	18	2489
1,00000+05	1,45000+00	2,00000+05	1,50000+00	3,00000+05	1,35000+00	2024	5	18	2490
4,00000+05	1,20000+00	6,00000+05	7,50000+00	8,00000+05	4,70000+00	2024	5	18	2491

1,000000+06	2,500000-01	1,200000+06	1,300000-01	1,400000+06	7,100000+02	2024	5	91	2492
1,600000+06	3,200000+02	1,800000+06	1,400000-02	2,000000+06	6,000000+03	2024	5	91	2493
2,200000+06	2,000000-03	2,300000+06	1,000000-03			2024	5	91	2494
0,000000+00	4,000000+06	0	0	1	15	2024	5	91	2495
1,000000+03	1,000000+00	2,000000+05	1,300000+00	4,000000+05	1,050000+00	2024	5	91	2496
6,000000+05	7,900000-01	8,000000+05	5,200000-01	1,000000+06	3,300000-01	2024	5	91	2498
1,200000+06	2,000000-01	1,400000+06	1,200000-01	1,600000+06	6,800000+02	2024	5	91	2499
1,800000+06	3,700000-02	2,000000+06	2,000000-02	2,200000+06	1,000000-02	2024	5	91	2500
2,400000+06	4,000000-03	2,600000+06	2,000000-03	2,800000+06	1,000000+03	2024	5	91	2501
0,000000+00	5,000000+06	0	0	1	13	2024	5	91	2502
1,000000+05	9,500000-01	2,000000+05	1,100000+00	3,000000+05	1,130000+00	2024	5	91	2504
4,000000+05	9,100000+01	6,000000+05	6,600000-01	8,000000+05	5,500000+01	2024	5	91	2505
1,000000+06	3,800000+01	1,200000+06	2,400000-01	1,600000+06	1,000000+01	2024	5	91	2506
2,000000+06	3,700000+02	2,500000+06	1,000000-02	3,000000+06	2,000000+03	2024	5	91	2507
3,200000+06	1,000000+03	0	0	1	2	2024	5	91	2508
0,000000+00	6,000000+06	0	0	1	15	2024	5	91	2509
1,000000+03	8,500000-01	3,000000+05	9,900000-01	6,000000+05	7,500000+01	2024	5	91	2510
9,000000+05	4,600000-01	1,200000+06	2,900000-01	1,500000+06	1,700000-01	2024	5	91	2512
1,800000+06	9,000000-02	2,100000+06	5,600000-02	2,400000+06	3,300000+02	2024	5	91	2513
2,700000+06	2,100000+02	3,000000+06	1,500000+02	3,500000+06	1,000000+02	2024	5	91	2514
4,000000+06	7,000000+03	5,000000+06	3,000000+03	5,800000+06	1,000000+03	2024	5	91	2515
0,000000+00	7,000000+06	0	0	1	14	2024	5	91	2516
1,000000+05	5,000000-01	2,000000+05	6,000000-01	5,500000+05	5,500000+01	2024	5	91	2518
8,000000+05	7,500000+01	9,000000+05	6,600000-01	1,000000+06	5,800000+01	2024	5	91	2519
1,600000+06	2,200000-01	2,000000+06	1,100000-01	2,600000+06	3,000000+02	2024	5	91	2520
3,000000+06	3,000000-02	4,000000+06	1,500000-02	5,000000+06	9,000000+03	2024	5	91	2521
6,000000+06	5,000000-03	6,800000+06	1,000000-03	0	0	2024	5	91	2522
0,000000+00	9,000000+06	0	0	1	14	2024	5	91	2523
1,000000+06	6,000000-01	5,000000+06	6,700000-01	1,000000+06	4,200000+01	2024	5	91	2524
1,500000+06	2,200000-01	2,000000+06	1,000000-01	2,500000+06	5,500000+02	2024	5	91	2526
3,000000+06	6,000000-02	3,500000+06	4,200000-02	4,000000+06	2,900000+02	2024	5	91	2527
5,000000+06	2,000000-02	6,000000+06	1,300000-02	7,000000+06	8,500000+03	2024	5	91	2528
8,000000+06	4,500000+03	8,500000+06	1,000000-03	0	0	2024	5	91	2529
0,000000+00	1,100000+07	0	0	1	15	2024	5	91	2530
1,000000+05	3,000000+01	3,000000+05	4,400000-01	9,000000+05	4,300000+01	2024	5	91	2531
1,200000+06	3,700000-01	1,900000+06	2,000000-01	2,500000+06	1,000000+01	2024	5	91	2532
3,000000+06	7,000000-02	4,000000+06	3,000000-02	5,000000+06	3,500000+02	2024	5	91	2533
6,000000+06	3,000000+02	7,000000+06	2,200000+02	8,000000+06	1,400000+02	2024	5	91	2534
9,000000+06	1,000000-02	1,000000+07	4,000000-02	1,050000+07	1,000000+03	2024	5	91	2535
0,000000+00	1,300000+07	0	0	1	14	2024	5	91	2537
	2				2024	5	91	2538	

4,000000+05	2,700000-01	7,000000+05	2,900000-01	1,200000+06	2,300000-01	2024	5	91	2539
2,000000+06	1,800000-01	3,000000+06	1,200000-01	4,000000+06	6,900000-02	2024	5	91	2540
5,000000+06	4,700000-02	6,000000+06	3,600000-02	7,000000+06	5,400000-02	2024	5	91	2541
8,000000+06	4,100000-02	9,000000+06	3,100000-02	1,000000+07	2,300000-02	2024	5	91	2542
1,000000-07	1,500000-02	1,200000+07	1,000000-03	0	0	2024	5	91	2543
0,000000+00	1,500000+07	0	0	1	16	2024	5	91	2544
3,600000+05	1,900000-01	1,000000+06	1,700000-01	2,000000+06	1,100000+01	2024	5	91	2546
3,000000+06	7,500000-02	4,000000+06	6,600000-02	5,000000+06	1,200000-02	2024	5	91	2547
6,000000+06	6,600000-02	7,000000+06	5,700000-02	8,000000+06	4,600000-02	2024	5	91	2548
9,000000+06	7,600000-02	1,000000+07	5,800000-02	1,100000+07	4,500000-02	2024	5	91	2549
1,200000+07	3,200000-02	1,300000+07	2,100000-02	1,400000+07	1,000000+02	2024	5	91	2550
1,400000+07	1,000000-03	0	0	0	0	2024	5	91	2551
0,000000+00	0,000000+00	0	0	0	0	2024	5	0	2552
0,000000+00	0,000000+00	0	0	0	0	2026	0	0	2553
0,000000+00	0,000000+00	0	0	0	0	0	0	0	2554

Reproduced by the IAEA in Austria
January 1980
80-886